Department of Experimental Plant Biology
Faculty of Science
Charles University in Prague

Laboratory of Cell Biology
Institute of Experimental Plant Biology
The Czech Academy of Science

Role of exocyst complex in growth and development of moss *Physcomitrella patens*

Anamika Ashok Rawat

A thesis submitted for the degree of
Doctor of Philosophy (PhD)

Prague, 2017

Supervisor:

doc. RNDr. Viktor Žárský, CSc.

Consultant:

doc. RNDr. Fatima Cvrčková, Dr. rer. nat.

Mgr. Lucie Brejšková, Ph.D.

Mgr. Ivan Kulich, Ph.D.

Declaration

I declare that this thesis is the result of my own research except as cited in the references. The thesis has not been accepted for any degree and is not concurrently submitted in candidature of any other degree.

I understand that my work relates to the rights and obligations under the Act No. 121/2000 Coll., the Copyright Act, as amended, in particular the fact that the Charles University in Prague has the right to conclude a license agreement on the use of this work as a school work pursuant to Section 60 paragraph 1 of the Copyright Act.

In Prague, July 2017 Anamika Rawat

Acknowledgements:

First I would like to express my heartiest gratitude to my supervisor doc. Viktor Žárský for giving me the opportunity to be a part of his research team. His insightful leadership and continuous support and encouragement motivated me throughout my studies. I am highly obliged to doc. Fatima Cvrčková whose guidance, support and friendly advices helped me to develop scientific aptitude. I will always remember her kindness and assistance in both personal and lab life, including my first day shopping in Prague! I am enormously thankful to both of them for their extreme help and patience in editing our manuscripts and also this thesis.

I am thankful to Marie Skłodowska- Curie ITN actions "PLANTORIGINS" (FP7- PEOPLE-ITN-2008) who funded this work for initial three years. I feel very fortunate to be part of this project, and would like to thank the whole team of project, esp. to Prof. Liam Dolan, University of Oxford, for a great time in his lab.

I would like to express my gratitude to all the members of Laboratory of Cell Morphogenesis (Charles University) and Laboratory of Cell Biology (IEB) who directly or indirectly have contributed to this work.

I feel very privileged to have nice colleagues around who not only provided a friendly environment in the lab but also outdoors. Lucie and Hanka thank you for all your help at work and for those official and personal translations. Tamara and Denisa, thanks for being wonderful hosts on Christmas eves. Jitka (the baking lady), Klara, Martina and Jana, your lovely smiles, chats and ideas always kept me going, thanks. I am grateful to Nemanja, Lukas, Juraj and 3P's for making cheerful and healthy work environment, and for sharing the ideas. I am thankful to the Kulichs for being friendly and compassionate throughout. I would also appreciate former lab members Michal Grunt, Amparo and Kookie for being amazing friends.

I am thankful to Niketan for his continuous support, motivation and to stand by my side in all times. I also appreciate Cheeku for his super loving company.

Last but not the least, I am grateful to my parents for their inspiration, support and endless love.

Abstract:

During the course of evolution the early land plants gained extensive innovations that can be seen in modern day plants. The polar growth is an ancient feature of eukaryotic cells and is one of preadaptations that helped plants in successful colonization of land. The polar growth in plants regulates not only the direction of cell expansion and structural properties of cell wall but especially also the orientation of cell division, and is governed by various factors, including the exocyst complex. The exocyst is a well conserved vesicle tethering multi-subunit complex involved in tethering of secretory vesicles to the target membrane.

The essential role of the exocyst complex in regulation of various cellular processes in Angiosperms is now well documented. Here I present results of a doctoral project that contributed to phylogenetic analyses of the land plant exocyst complex and especially to uncovering functions of three moss exocyst subunits, namely EXO70 (isoform *PpEXO70.3d*), SEC6 and SEC3 (isoforms *PpSEC3A* and *PpSEC3B*) in the model organism *Physcomitrella patens*.

Various knock-out (KO) mutants in several moss exocyst subunits (*Ppexo70.3d, Ppsec6, Ppsec3a* and *Ppsec3b*) show pleiotropic defects directly or indirectly linked to the cell polarity regulation. Cell elongation and differentiation, cytokinesis, cuticle formation, response to auxin (phytohormone) are impaired in these mutants, resulting in different strength of developmental deviations ranging from inability to develop gametophores to more subtle morphologic deviations linked to different degree of dwarfism in gametophores. Importantly, the exocyst genes are required for completion of the full moss life cycle including sexual reproduction. While a KO mutation in the single-copy subunit PpSEC6 results in lethality, KO mutants of multi-member subunit families are not lethal – *Ppexo70.3d* (one of thirteen *EXO70* paralogs) is sterile due to defective egg cell development, and *Ppsec3* mutants (three *SEC3* paralogs) show partial defects in sporophytes and spore development.

These results show that the exocyst complex function in cellular morphogenesis is not only conserved in moss *P. patens,* and that the exocyst has a crucial role in the moss life cycle, but they also indicate a functional importance of the multiplication of exocyst genes in this representative of basal land plants.

This work was supported by EU Marie Curie Network (No. 238640 PLANTORIGINS), MSMT (NPUI LO1417) and GACR/CSF (15-14886S).

Abstrakt:

První suchozemské rostliny získaly v průběhu svého vývoje rozsáhlá evoluční vylepšení platná i u dnešních moderních rostlin. Polární růst je pradávnou vlastností eukaryotických buněk a jednou z preadaptací, které pomohly rostlinám při úspěšné kolonizaci souše. Polární růst u rostlin určuje nejen směr expanze buněk, strukturní vlastnosti buněčné stěny, ale také orientaci buněčného dělení. Řízení polárního růstu se účastní různé faktory, včetně komplexu exocyst. Exocyst je evolučně konzervovaný poutací komplex, který se skládá z osmi podjednotek, a účastní se poutání (angl. tethering) sekretorických váčků k cílové membráně.

Zásadní role komplexu exocyst v různých buněčných procesech u krytosemenných rostlin je v současnosti dobře dokumentována. V této práci prezentuji výsledky doktorandského projektu, který přispěl k fylogenetické analýze komplexu exocyst u suchozemských rostlin, a zejména k objasnění funkcí tří podjednotek exocystu, konkrétně EXO70 (isoforma *PpEXO70.3d*), SEC6 a SEC3 (isoformy *PpSEC3A* a *PpSEC3B*), u modelového mechu *Physcomitrella patens*.

Několik *knock-out* (KO) mutantů tohoto mechu v různých podjednotkách exocystu (Ppexo70.3d, Ppsec6, Ppsec3a and Ppsec3b) vykazuje pleiotropní defekty, které jsou přímo či nepřímo propojeny s regulací buněčné polarity. Narušen je dlouživý růst a diferenciace buněk, cytokineze, tvorba kutikuly a odpověď na fytohormon auxin, což má za následek různě silné vývojové defekty od neschopnosti vytvářet gametoforů až po malé morfologické odchylky vedoucí k zakrnělému vzrůstu gametoforů. Důležité je, že tyto geny jsou nezbytné pro dokončení životního cyklu mechu, včetně pohlavního rozmnožování. Zatímco KO mutace PpSEC6 (podjednotka kódovaná jediným gene) je letální, KO mutanti podjednotek kódovaných více geny letální nejsou – mutant *Ppexo70.3d* (jeden z třinácti paralogů *EXO70*) je sterilní kvůli defektu při vývoji vaječné buňky a mutanti *Ppsec3* (tři paralogy *SEC3*) vykazují dílčí poruchy ve vývoji sporofytu a spor.

Výsledky uvedené v této práci ukazují, že funkce komplexu exocyst u mechu *P. patens* je konzervována v procesech buněčné morfogeneze, že exocyst hraje klíčovou roli v životním cyklu mechu, ale také naznačují funkční význam znásobení genů kódujících podjednotky exocystu u tohoto zástupce prvních suchozemských rostlin.

Tato práce byla podpořena projekty EU Marie Curie Network (No. 238640 PLANTORIGINS), MŠMT (NPUI LO1417) a GAČR/CSF (15-14886S).

Table of Contents

Introduction 1

1.1. Introduction to model plant *Physcomitrella patens* 1

1.1.1. Evolutionary position of bryophytes 1

1.1.2. *Physcomitrella patens* as a model plant 2

1.1.3. Life cycle 4

1.1.4. Polarized tip growth in moss *P. patens* 5

1.1.5 Presence of hydrophobic wax layer in moss *P. patens* 6

1.2. Exocyst Complex 7

1.2.1. General overview 7

1.2.2. Structure of exocyst complex 8

1.2.3. Function of exocyst complex 10

2. Aims of the project 12

3. Results 13

Paper 1 14

Paper 2 27

Manuscript 3 44

Manuscript 4 80

4. Discussion 101

5. Conclusion 108

6. Literature 109

1. INTRODUCTION

1.1. Introduction to model plant *Physcomitrella patens*

1.1.1 Evolutionary position of bryophytes

Colonization of land by plants took place *approx*. 470-450 million years ago (MYA), and is an event of central importance to life on land. Present day land plants evolved from multicellular algae of fresh water, related to the extant charophyte groups Charales or Coleohaetales. Both charophytes and embryophytes, collectively also known as "streptophytes" form a monophyletic group (Figure 1.1), which is sister to other green algae – chlorophytes. Both these groups share several features, such as cell walls with cellulose, chloroplasts with stacked grana containing chlorophylls a and b, bi- to multiflagellated cells, production of starch, etc., and Zygnematophyceae were suggested to be a sister group to embryophytes (Wodniok *et al*., 2011). According to molecular phylogenies, the three extant bryophyte lineages (liverworts, mosses and hornworts) separated just before the linage ancestral to present day tracheophytes. Liverworts are considered to be the earliest divergent clade, with mosses forming a sister group to clade of hornworts and tracheophytes (Qui *et al.,* 2006). Ligrone *et al.,* (2012), showed that hornworts form a sister group to tracheophytes, and this theory is now widely favored. However, the analyses of plastomes, multigene datasets and morphologies has resolved mosses and liverworts to be monophyletic, but the position of hornworts relative to the mosses + liverworts clade and to tracheophyte is not yet clear. The study conducted by Wicket *et al*., (2014) showed the monophyly of bryophyte lineages, but did not support the hypothesis that (a) liverworts are sister to all other land plants, and (b) the liverworts, mosses and hornworts, respectively, are the successive sister groups to vascular plants. These authors showed a clade with mosses and liverworts as sister to tracheophytes, while hornworts appear to be a sister to all other (non-hornwort) land plants.

After migrating from water to terrestrial environment, the early land plants diverged into different lineages, and underwent several adaptions in order to get acclimatized to various terrestrial habitats. This transition of plants from aquatic to terrestrial environment led to numerous morphological, cellular and physiological changes in plants to adapt to the dry environment. Some of those were development of tough sporopollenin on spores to protect from desiccation and UV-B radiations, formation of waxy layer-cuticle on the plant surfaces, and stomata to regulate rate of water loss from plants (reviewed in Ligrone *et al.,* 2012). Polar development of plants based on polar cell growth would have been yet another factor that allowed plants to develop and flourish on land. Despite several challenges to survive, life on land offered various advantages like abundant sunlight and carbon dioxide to support photosynthesis, Bryophytes were among the first plants to conquer the land *approx*. 475 MYA. The vital land characters

primarily evolved in the bryophyte clade, which hence provides excellent model to understand the early events in evolution of land plants (reviewed in Ligrone *et al.,* 2012).

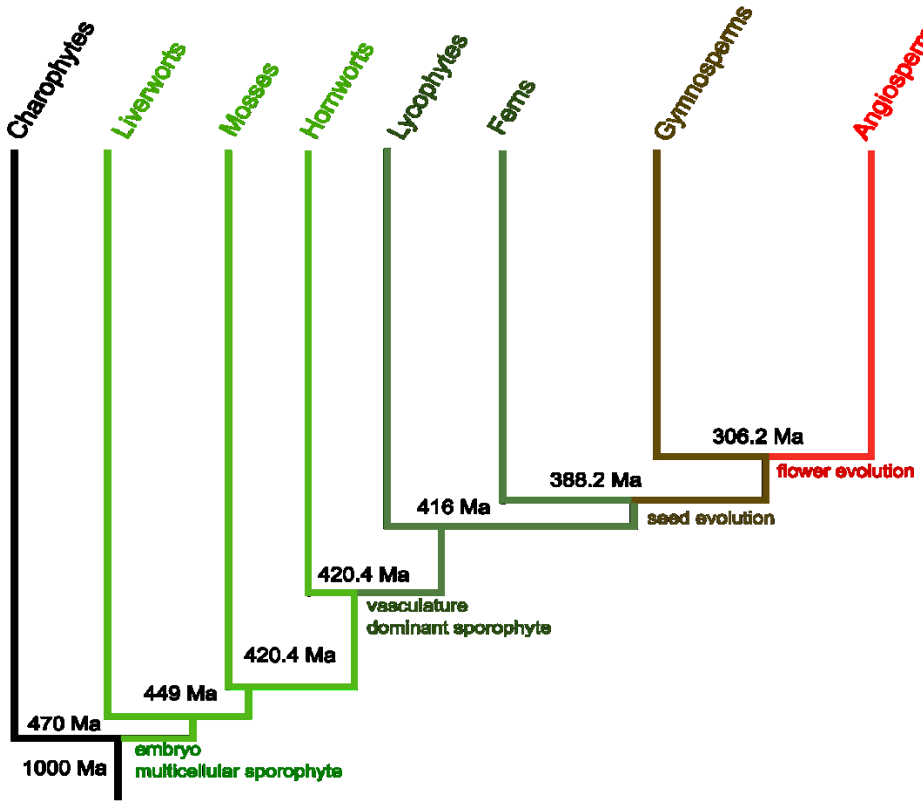

Figure 1.1 Phylogenetic relationships between the major groups of extant plants. Key events that occurred during plant evolution are indicated. The estimated divergence times are indicated in millions of year ago (Ma). Adapted from: Clarke *et al*., 2011; *Pires* & *Dolan,* 2012.

1.1.2. *Physcomitrella patens* as a model plant

Mosses occur in many extreme habitats such as Antarctic tundra to deserts, and also form important components of tropical systems, boreal forests and woodlands in temperate zone. Despite their small size, mosses have huge impact on various ecosystems and are essential contributors to complex biological cycles. Various moss species e.g., *Funaria hygrometrica*, *Physcomitrella patens*, *Ceratodon purpureus*, *Sphagnum,* have been developed as model systems, among which *P. patens* is the most developed and widely used model moss.

Physcomitrella patens (Hedw.) Bruch & Schimp, also known as spreading earthmoss, is a non-vascular land plant belonging to phylum Bryophyta. It is widely distributed in temperate zone, and isolates are available from Europe, N. America, Japan, Africa and Australia (reviewed in Prigge &

Bezanilla, 2010). It is found growing on the exposed banks of ponds, lakes and rivers and finishes its life cycle by producing sexual organs and then sporophytes at lowered temperatures and short days.

For more than two decades, the moss *P.patens* has been employed as an alternative model suitable for plant cell biology studies. It was first established as a laboratory experimental system in the 1920s by Fritz von Wettstein (reviewed in Cove *et al*., 2009). The potential research areas of *P. patens* research include general moss physiology, moss-specific stress resistance mechanism, as well as mechanisms that evolved and are conserved in many land plants i.e. evo-devo studies. From evolutionary perspective, *P. patens* is to the flowering plants as *Drosophilla melanogaster* is to humans! *P. patens* has relatively small genome size of approximately 511 Mbp size, consisting of 27 chromosomes, and is first fully sequenced genome of a bryophyte (Rensing *et al*., 2008). *P. patens* genome is about four times larger than *A. thaliana* (approx. 135 Mbp, consisting of 5 chromosomes only!), but has smaller average gene family size than that in *A. thaliana*, meaning that the moss has a high number of unique genes. Homologues of more than 66% of Arabidopsis thaliana genes are present in *P. patens* gametophytes and >90% of the most closely related homologues of *P. patens* gametophytic transcripts occur in vascular plants, suggesting that gametophytes and sporophytes use similar gene sets (Nishiyama *et al.*, 2003). *P. patens* has many advantages to be used as a model plant. Along with fully sequenced genome, *P. patens* has short generation time (4-8 weeks) and small stature (1-5 mm) with relatively simple body organization and development (see next chapter). It can be easily propagated vegetatively, under controlled conditions in-vitro. The most favorable feature of this moss is the ability to undergo homologous recombination, which allows generating targeted knockout mutants with ease (Kamisugi *et al*., 2005). The dominant haploid phase of *P. patens*, with simple tissue architecture, makes screening of mutants rapid and efficient. Another striking feature is its capacity of regeneration. Even a small piece of any of the moss tissue, be it a detached phyllid, protoplast or a wounded protonema, has ability to undergo re-programing into a meristematic cell and regenerate back into a whole adult moss plant, thus behaving more or less like a germinating spore. Hence, mutants with arrest in any developmental stage can be easily propagated (Cove, *et al*., 2006; Prigge & Bezanilla, 2010). Along with this, performing various molecular techniques, such as RNAi (Bezanilla *et al.,* 2003), Cre-lox-mediated recombination (Schaefer & Zryd, 2001), targeting of multiple genes by CRISPR-Cas9 (Lopez-Obando *et al.,* 2016; Collonnier *et al.,* 2016), is now a routine. *P. patens* has been also established as an expression and purification system for recombinant proteins (Decker & Reski, 2007). These all features make *P. patens* excellent organism for reverse genetic studies, esp. for developmental and physiological process from evolutionary perspective.

1.1.3. Life cycle

P. patens, just like other bryophytes and also higher plants, displays alternation of generations. The main dominant phase of moss life cycle is the haploid gametophyte, which consists of (a) filamentous chloronemata and caulonemata, collectively known as protonemata (b) rhizoids, which develop from the epidermal cells on the gametophore, and (c) a shoot-like structure - gametophore. The diploid phase is represented by a small sporophyte which develops on the apex of the gametophore (Figure 1.2).

The *P. patens* completes its life cycle within 3 months under standard culture conditions. It begins with germination of a haploid spore, which gives rise to a linear array of cells called chloronemata. The chloronemata are slow growing filaments, full of chloroplasts (80-140 in number) and thus perform function of photosynthesis. In chloronemata, the cell plate between two neighboring cells is perpendicular to the axis of cell growth. Subsequent tissue differentiation is phytohormone-, light- and also nutrient-dependent (Johri & Desai, 1973; Ashton *et* al., 1979; Thelander *et* al., 2005; Decker *et al*., 2006). Under the effect of light and auxin, chloronemal filaments give rise to caulonemata (Jang & Dolan, 2011). Caulonemal cells are longer, and contain fewer (50 - 120) chloroplasts. These filaments are easily recognized by their oblique cell walls between two adjacent cells.

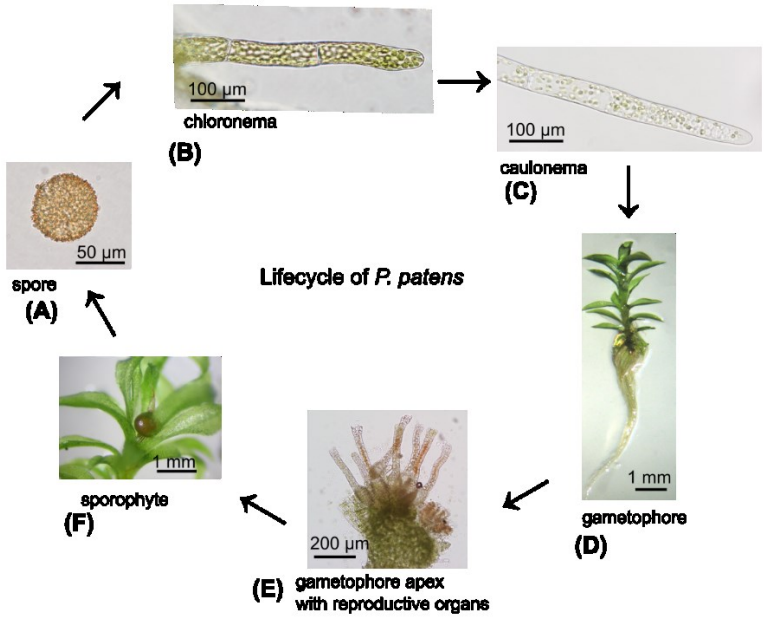

Figure 1.2. *P. patens* life cycle. (A) A haploid spore germinates into (B) chloronemal cells, which continue to grow and differentiate into (C) caulonemal cells. (D) Gametophores, or shoots, emerge off protonemal filaments and are ultimately anchored by rhizoids that grow by tip growth from base of the gametophores. (E) At the apex of the gametophore, both female, archegonia (arrows), and male, antheridia (arrowheads), organs are formed. A motile flagellate sperm fertilizes the egg and the (F) sporophyte develops at the apex of the gametophore.

Both chloronema and caulonema elongate by tip growth (Menand *et al*., 2007). The apical dome in the chloronemal apical cell sometimes is occupied by large organelle e.g. chloroplasts and vacuole. However, the tip region of caulonemal apical cell is rich in cytosol, similar to the cellular organization seen in growing root hairs and pollen tubes of seed plants. Chloronemal tip cell grows at 6 µm/hour, dividing every 24 hours, while caulonema cells grow much faster, 20 µm/h and divides every 7 hour (reviewed in Vidali & Bezanilla, 2012). The side branch initials and bud initials develop on subapical cells of protonemata, giving rise to secondary protonemal filaments and gametophores respectively (Harrison *et al*., 2009).

The second stage of gametophyte development starts with initiation of bud initial. The bud initial, under the effect of cytokinin (Decker *et al.,* 2006), undergoes controlled divisions of the tetrahedral apical cell, to form shoot-like structure called gametophore (Harrison *et al*., 2009). The division of the apical cells forms cells which give rise to leaf-like structures – phyllids. Phyllids are made of single cell layer thick lamina, and have a central midrib. Rhizoids are present at base of gametophores and act to anchor the gametophore on the substrate. Under short day conditions and low temperature, reproductive organs, archegonia and antheridia, are initiated on the apex of gametophore. The development of reproductive organs in *P. patens* has been described in detail in Landberg *et al*. (2013). When mature and in contact with water, the spermatozoids are released from antheridia. Once released, the spermatozoids proceed to fertilize the egg cell located in the archegonial cavity. After 2-3 weeks, the successful fertilization give rise to the sporophyte, which is the only diploid structure in the moss life cycle. The sporophyte, composed of short seta and a spore capsule, can be seen on apex of gametophores. Inside the sporophyte the next generation of haploid spores is generated via meiosis.

1.1.4. Polarized tip growth in moss *P. patens*

In many organisms, such as fungi, animals and plants, polarized growth is essential for proper development and also for survival. Most of the plant cells grow by diffuse growth, while some grow by depositing cell wall material in a highly polarized manner at the tip of the cell. This mode of cell expansion, where a cell grows by precise deposition at the tip, is known as tip growth. Root hairs, pollen tubes, rhizoids, moss protonemata, etc. are a few examples where the cell grows by tip growth. Both gymnosperms and angiosperms rely on tip-growing pollen tubes only for their sexual reproduction, while mosses rely completely on tip growth for their development, starting from spore germination, to protonemata and rhizoid development. Moss protonemata, just like pollen tubes, root hairs and rhizoids, elongate by tip growth mechanism, in which new cell wall material is deposited in a highly polarized manner at the tip of cell, while no growth occurs in rest of the cells (Menand *et al.,* 2007). Actin appears to be central to the process of tip growth in mosses (Vidali *et al*., 2007; Vidali *et al*., 2010). The mutants

in Arabidopsis and maize Arp2/3 subunits have little or no defects in tip growing cells, however analogous mutants show major defect in tip growth of moss protonemal filaments (Harries *et al*., 2005; Perroud & Quatrano, 2006; Finka *et al*., 2008). BRICK1, one of the subunits of the Wave/SCAR complex, is also critical for tip growth in moss. Moss *brk1* mutants show drastic reduction in plant size and delayed cell division. Similar to ARPC4, BRICK1 is present at the apex of tip-growing cells and is required for localization of apically associated factors (Perroud & Quatrano, 2008). Myosins are the motor proteins that transport cargo within the cell along actin filaments. There are several reports showing coordinated action of myosin and actin function at the cell's apex to maintain polarized growth in protonemal cells (Vidali *et al*., 2010; Furt *et al*., 2013)

The exocyst targets the secretory vesicles by coordinating with the actin cytoskeleton cables. EXO70 and SEC3 proteins are associated with plasma membrane (PM) via PI(4,5)P2 and interact with activated RHO GTPases, while the other members of the complex are associated with the secretory vesicles. In yeast SEC15 interacts with myosin V and Rab proteins for targeting of vesicles (reviewed in Wu & Guo, 2015), whereas Exo70 is shown to interact with ARPC1 subunit of Arp2/3 complex (Liu *et al*., 2012). This indicates the interaction of exocyst, actin and GTPases together may mediate the polarized tip growth in mosses as well.

1.1.5 Presence of hydrophobic wax layer in moss *P. patens*

Cuticle is an adaptation acquired by plants early in evolution. The plant cuticle is an insoluble hydrophobic layer that covers the aerial portion of land plant, and protects against UV radiation and also assists in minimizing water loss from cells. Green algae, ancestors of land plants, are aquatic organism and do not need cuticle. Bryophytes are the early land plants and are known to exhibit various adaptations to terrestrial life. Presence of cuticle in mosses has been documented. For example, the cuticle was identified on the calyptra of moss *Funaria hygrometrica* (Budke *et al*., 2011). Buda *et al*., (2013) showed the phyllids of *P. patens* are covered by thin layer of cuticle and this deposition of cuticular waxes is carried out by ATP binding cassette transporter. The mutants in ABC transporter G Δ*ppabcg7* exhibit stunted growth with altered spore wall architecture and reduced cuticular wax deposition on moss phyllids. The ABC transporter gene acts in deposition of cuticle and also prevents organ fusion in Arabidopsis (Luo *et al*., 2007). Early in evolution the spores developed durable spore wall for protection against desiccation and UV radiations. The walls of spores and pollen are made up of intine and exine. The exine is a highly resistant layer made up of sporopollenin, a component secreted from the tapetum layer. In Arabidopsis, the cuticular waxes are deposited on the PM via secretory pathway involving Golgi and TGN (Mcfarlane *et al*., 2014). Recent reports show that components of sporopollenin biosynthetic pathway are conserved between *P. patens* and *Arabidopsis*, and mutation in components of this pathway

causes defective spore development with altered sporopollenin deposition (Morant *et al*., 2007; Li *et al*., 2010; Wallace *et* al., 2015; Daku *et al*., 2016).

1.2. Exocyst Complex

1.2.1. General overview

Membrane compartmentalization is one of the defining characteristics of eukaryotic cells. There is constant exchange of materials between the membrane-bound compartments, and this action is fulfilled by vesicles. Vesicles are small mobile compartments, which function in transporting cargo from one compartment to another. This whole process is performed in four steps. Firstly, the vesicle is formed from the membrane of donor compartment where it also collects its cargo and this process is known as budding. Secondly, the vesicle is transported to its site of delivery. In the third step, the vesicle makes its initial contact with the membrane of target compartment. This process is called tethering, and is precisely regulated by various tethering complexes. In the fourth and final step, the vesicle fuses with the target membrane thus delivering its contents to the target membrane. The vesicle traffic event where the cargo is delivered to the specific sites of the plasma membrane is known as exocytosis.

Exocytosis is the ultimate and fundamental step in polar growth and development of a cell, and the process, both spatially and temporally, is under tight control. Various tethering complexes are responsible for movement of vesicles in plant cell (reviewed in Vukašinović & Žárský, 2016). The complexes GARP and EARP (four subunits), COG and exocyst (eight subunits), and also Dsl1, which comprises three subunits, are all characterized as "CATCHR" complexes. These complexes are evolutionarily related and act in the secretory/biosynthetic pathways. The GARP and COG complexes are involved in retrograde trafficking from endosomes to Golgi and within Golgi, respectively. Another class of tethering complexes are the TRAPP complexes. TRAPP I complex functions in ER-Golgi transport, TRAPP II in *trans*-Golgi-early endosome interface, while TRAPP III is involved in autophogosome formation. The HOPS and CORVET are two homologous, hetero-hexameric tethering complexes, sharing four core subunits, while having two subunits specific to each complex. Both complexes function within endolysosomal pathways, where CORVET functions in endosome-endosome fusion while HOPS bind efficiently to late endosomes and lysosomes. Exocyst is yet another vesicle tethering complex that acts in secretory pathway by tethering secretory vesicles at PM.

Exocyst, also known as the Sec6/8 complex, is an evolutionarily conserved, octameric protein complex consisting of SEC3, SEC5, SEC6, SEC8, SEC10, SEC15, EXO70 and EXO84 subunits (see Heider & Munson, 2012; Wu & Guo, 2015). All of its subunits are known to be conserved, not only in yeast and mammals (Ter-Bush *et* al., 1996; Guo *et* al., 1999) but also in plants (Eliáš *et al.,* 2003). It is a peripheral membrane protein complex, and controls the tethering of endomembrane compartments (here:

secretory vesicles) from donar compartment, in this case TGN, onto the PM. It was first identified during a yeast genetic screen for secretory mutants, where the temperature-sensitive mutants displayed accumulation of vesicles in cytoplasm, which were destined to fuse with the PM (Novick *et al*., 1980; Novick *et al*., 1981). Later the presence of exocyst complex in metazoans and plants was also confirmed (Hsu *et al*., 1998; Eliáš *et al*., 2003).

Proper targeting of the secretory vesicles is essential for fulfillment of various biological processes in plant's life. Cell wall biogenesis, cytokinesis, polar growth, deposition of extracellular material including development of a cell wall, are few examples of the processes carried out by the secretory pathway. The exocyst complex tethers the secretory vesicles, and comes in action before formation of SNARE protein complex takes place. Its activity is directed by action of Rab and Rho GTPases. It has been proposed that exocyst subunit Sec15 interacts with the vesicle via Rab GTPase Sec4 and myosin V, and Sec6 binds to v-SNARE Snc2, whereas Exo70 and Sec3 interacts with Rho GTPases and PI (4,5)P2, and serve as landmarks for cargo delivery (He *et al*., 2007; Zhang *et al*., 2008; Baek *et al*., 2010).

1.2.2. Structure of the exocyst complex

In yeast, exocyst forms a stable, elongated structure, suggesting rod-like architecture of its subunits (Heider *et al*., 2016). The exocyst, along with COG, Dsl and GARP tethering complexes, belongs to the Complex Associated with Tethering Containing Helical Rods (CATCHR) family. The members of this family have low sequence identity but have conserved helical bundle arrangement in secondary and tertiary structure, thus resulting in a rod like conformation of the complex. The molecular weight of complex itself is approximately 750 kDa with its subunits ranging between 70 – 150 kDa (TerBush *et al*., 1996). Crystal structures from quick-freeze EM of fixed exocyst complex have revealed that the rod-like structure of exocyst subunits is due to tandem helical bundles that are tightly packed together in a side by side fashion, giving a 'Y-shaped' or 'T-shaped' appearance to the complex (Hsu *et* al., 1998; reviewed in Heider & Munson, 2012) (Figure 1.3). The structural data suggest that the N and C termini of the helical bundle repeats are positioned at the opposite direction of rod (Sivaram *et al*., 2006). This 'T- or Y-shaped' architecture may be due to the interaction/juxtaposition between members of complex. Such 'Y-shaped' structures linked to the vesicles were seen during cell plate formation in *Arabidopsis thaliana* (Seguí-Simarro *et al*., 2004).

Recently, Picco *et al*., (2017) reconstructed the 3D architecture of yeast exocyst complex *in vivo* and proposed the working model for exocyst complex in vesicle tethering. According to Picco *et al*., (2017), all the subunits except Sec10 are attached to the core of the complex by their N-termini, with C-termini projecting outward, while Sec10 has exactly inverted organization in the complex (Figure 1.4).

They also show that different subunits of the complex are arranged in dimers. Exo70-Sec6 and Sec8-Sec3 subunits form a V-shaped dimer, and these dimers interact at the periphery of the complex by their C-terminal parts. Exo84 and Sec5 subunits are positioned adjacent to both Exo70-Sec6 and Sec8-Sec3 dimers, while Sec10 and Sec15 are located on top of the core and form a dimer that is less interlinked with rest of the complex.

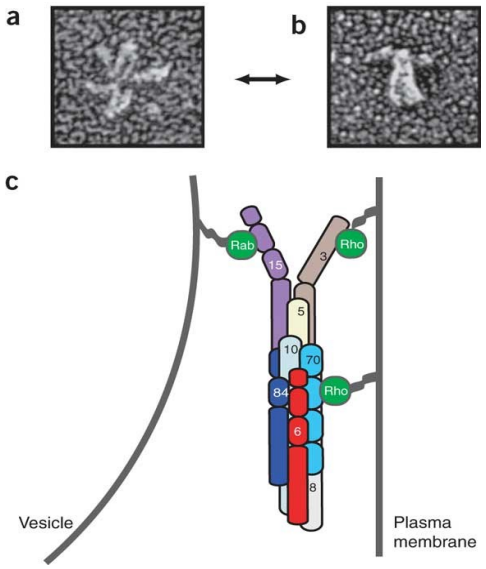

Figure 1.3. A model for the assembled exocyst complex. Quick-freeze EM of purified mammalian brain exocyst complexes either unfixed (a) or fixed with glutaraldehyde (b). (c) Schematic representation of the yeast exocyst complex hypothesizing that each of the exocyst subunits has an elongated helical bundle structure and that they pack together to form a structure similar to that in (b). Taken from: *Munson & Novick*, 2006.

Based on the structure of the complex, the authors propose a model for tethering of secretory vesicles by the exocyst. According to this model, exocyst is positioned at the side of the membrane contact site, thus not interfering with the membrane fusion. The complex binds the vesicle with Sec10-Sec15 dimer and the membrane with Sec3 and Exo70 simultaneously, while the Sec6 by its C-terminus (projecting out of the complex in the empty space between the complex, the vesicle and the PM) interacts with the SNARE complex. The exact number of exocyst complex copies required is not known, however the authors show many exocyst complexes could act in the event of vesicle fusion, and this can be maximum of ~20 complexes at the site of fusion (Figure 1.5).

The Sec3 subunit contains a N-terminally located Pleckstrin Homology domain, which interacts with PI(4,5)P2 and thus the Sec3 gets coupled with the membrane (Baek *et al*., 2010; Bloch *et al*., 2016). Recently, Heider *et al*. (2016) mapped the connectivity between the subunits of the complex showing that there are two stable modules of four subunit each (Sec3-5-6-8 and Sec10-15-Exo70-84) within the complex and that the presence of most of the exocyst subunits are critical for the integrity and stability of the complex.

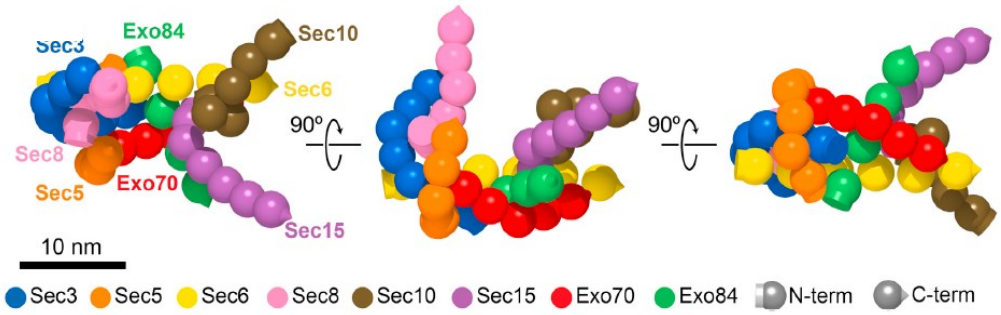

Figure 1.4. The 3D architecture of yeast exocyst complex (Picco *et al*., 2017)

1.2.3. Function of exocyst complex

Membrane trafficking at the polar micro-domains on the plasma membrane (Žárský *et al*., 2009) is a process which is spatially regulated by many factors, and it is essential for effective functioning of several biological processes. The exocyst complex mediates the tethering of secretory vesicle at these highly polarized micro-domains and thus regulates the cell polarity (reviewed in Wu & Guo, 2015). In yeasts, both Sec3 and Exo70 have been shown to interact with membrane phospholipid PI(4,5)P2, thus marking the site of vesicle fusion on the PM (He *et al*., 2007; Zhang *et al*., 2008).

The role of exocyst in polarized exocytosis is well studied in yeast, mammals and plants (reviewed in Wu & Guo, 2015; Vukašinović & Žárský, 2016). In yeast, exocyst is localized near the emerging bud tip, where it delivers the material required for cell wall growth.

In plants exocyst is required for fulfillment of various cellular processes. The pollen germination and pollen tube growth is controlled by the exocyst complex (Cole *et al*., 2005; Hála *et al*., 2008; Bloch *et al*., 2016; Synek *et al*., 2017). The deletion of *SEC3* subunit of the complex causes failure in root hair elongation in maize (Wen *et al*., 2005). The exocyst subunits SEC8 and EXO70A1 are involved in deposition of pectin seed coat in arabidopsis (Kulich *et al*., 2010), while EXO70H4 is required for secondary cell wall formation and callose ring formation in the trichomes of *Arabidopsis* (Kulich *et al*., 2015). Sec6 has been shown to be involved in various processes in Chlamydomonas and Drosophila (Komsic-Buchmann *et al*., 2012; Beronja *et al*., 2006), and in yeast it anchors the exocyst complex at site of active secretion (Songer and Munson, 2009). Sec6 loss of function mutants in *S.cerevisiae* are lethal (Novick *et al*., 1980, 1981). Recent data showing the involvement of exocyst complex in the secondary cell wall deposition in tracheary elements and also Casparian strips formation give new insight in the role of exocyst complex in plants (Vukašinović *et al*., 2016; Lothar *et al.,* 2017). Along with all these functions, the plant exocyst complex also plays an important role in response to pathogens and regulation of autophagy (Pečenková *et al*., 2011; Kulich *et al*., 2013).

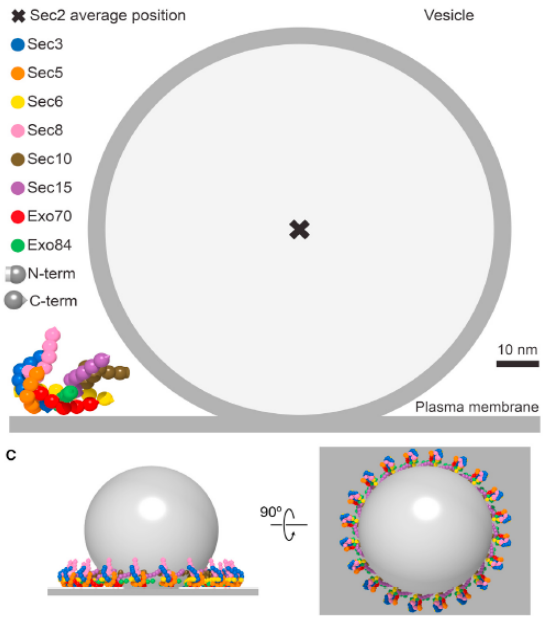

Figure 1.5. Model for the vesicle tethering mediated by exocyst complex (Picco *et al*., 2017)

Auxin is one of the most studied plant hormone, known to be essential for various aspects of plant development. Polar auxin transport is critical component in land plants which controls the polar growth and morphogenesis in plants. PIN proteins are the auxin efflux carriers, and it's the asymmetric distribution of these proteins on PM that controls the transport of auxin in plants. There is need of constitutive recycling of PIN's in the cell and subunits of exocyst complex are known to carry out this recycling of PIN proteins between PM and endosomal compartments (Drdová *et al*., 2013; Tan *et al*., 2016). Thus it can be said that the exocyst complex is involved in polar auxin transport by regulating PIN proteins.

In yeast the exocyst is present at the junction between two future cells and assist in cell abscission. In plants various exocyst subunits have been shown to be localized also at the site of future cell plate (Fendrych *et al*., 2010). During the process of cytokinesis there is high demand of cell wall material to be deposited in between the two daughter cells. Throughout the whole process, right from initiation till maturation of cell plate, the exocyst complex participates intimately in secretory vesicle fusion, and thus plays an important role during cytokinesis in plants (Fendrych *et al*., 2010).

2. AIMS OF THE PROJECT

- To contribute to the reconstruction of the process of evolution of the exocyst complex in plants, with special focus on EXO70 and SEC3 subunits
- To generate and analyze mutants in selected EXO70 paralogs of *P. patens* and find their role in the moss life-cycle
- To characterize the phenotype of *Ppsec6* mutants and study involvement of PpSEC6 in *Physcomitrella patens* cell morphogenesis
- To determine the involvement of SEC3 subunit in polar growth and secretion in moss *P. patens*

3. RESULTS

Paper 1: Evolution of the Land Plant Exocyst Complexes

Paper 2: The *Physcomitrella patens* exocyst subunit EXO70.3d has distinct roles in growth and development, and is essential for completion of the moss life cycle

Manuscript 3: Moss SEC6 exocyst subunit is essential for growth and development

Manuscript 4: The *PpSEC3* genes regulate the sporophyte formation and perispore deposition, giving insight into the spore development in early land plants

Paper 1:

frontiers in
PLANT SCIENCE

ORIGINAL RESEARCH ARTICLE
published: 18 July 2012
doi: 10.3389/fpls.2012.00159

Evolution of the land plant exocyst complexes

Fatima Cvrčková[1]*, Michal Grunt[1], Radek Bezvoda[1], Michal Hála[1,2], Ivan Kulich[1], Anamika Rawat[1] and Viktor Žárský[1,2]

[1] *Department of Experimental Plant Biology, Faculty of Sciences, Charles University, Prague, Czech Republic*
[2] *Institute of Experimental Botany, Academy of Sciences of the Czech Republic, Prague, Czech Republic*

Edited by:
Markus Geisler, University of Fribourg, Switzerland

Reviewed by:
Jürgen Kleine-Vehn, University of Natural Resources and Life Sciences Vienna, Austria
Frantisek Baluska, University of Bonn, Germany

****Correspondence:***
Fatima Cvrčková, Department of Experimental Plant Biology, Faculty of Sciences, Charles University, Viničná 5, CZ 128 44 Praha 2, Czech Republic.
e-mail: fatima.cvrckova@natur.cuni.cz

Exocyst is an evolutionarily conserved vesicle tethering complex functioning especially in the last stage of exocytosis. Homologs of its eight canonical subunits – Sec3, Sec5, Sec6, Sec8, Sec10, Sec15, Exo70, and Exo84 – were found also in higher plants and confirmed to form complexes *in vivo*, and to participate in cell growth including polarized expansion of pollen tubes and root hairs. Here we present results of a phylogenetic study of land plant exocyst subunits encoded by a selection of completely sequenced genomes representing a variety of plant, mostly angiosperm, lineages. According to their evolution histories, plant exocyst subunits can be divided into several groups. The core subunits Sec6, Sec8, and Sec10, together with Sec3 and Sec5, underwent few, if any fixed duplications in the tracheophytes (though they did amplify in the moss *Physcomitrella patens*), while others form larger families, with the number of paralogs ranging typically from two to eight per genome (Sec15, Exo84) to several dozens per genome (Exo70). Most of the diversity, which can be in some cases traced down to the origins of land plants, can be attributed to the peripheral subunits Exo84 and, in particular, Exo70. As predicted previously, early land plants (including possibly also the Rhyniophytes) encoded three ancestral Exo70 paralogs which further diversified in the course of land plant evolution. Our results imply that plants do not have a single "Exocyst complex" – instead, they appear to possess a diversity of exocyst variants unparalleled among other organisms studied so far. This feature might perhaps be directly related to the demands of building and maintenance of the complicated and spatially diverse structures of the endomembranes and cell surfaces in multicellular land plants.

Keywords: exocyst, phylogeny, land plants, co-evolution, gene duplication

INTRODUCTION

Exocyst, or the Sec6/8 complex, is an evolutionarily conserved heterooligomeric protein complex, generally believed to function especially in the last stage of exocytosis – i.e., vesicle tethering, preceding fusion of trans-Golgi network-derived vesicles with the plasmalemma, although additional, also mostly vesicle trafficking-related, exocyst roles have been described (reviewed, e.g., in He and Guo, 2009; Zhang et al., 2010; Heider and Munson, 2012). The eight canonical exocyst subunits, Sec3, Sec5, Sec6, Sec8, Sec10, Sec15, Exo70, and Exo84, were originally identified in yeast (TerBush et al., 1996; Guo et al., 1999). Subsequently, their homologs were found also in metazoans (Guo et al., 1997; Kee et al., 1997) and higher plants (Eliáš et al., 2003). Angiosperm exocyst subunits form complexes *in vivo* (Hála et al., 2008), and participate in exocytosis- or vesicle trafficking-dependent processes, such as cell growth including both tip growth and diffuse surface expansion (Cole et al., 2005; Wen et al., 2005; Synek et al., 2006; Hála et al., 2008), cell division (Fendrych et al., 2010), delivery of materials to the periplasm and cell wall (Wang et al., 2010), biogenesis of specialized cell wall structures such as the myxosperm seed coat (Kulich et al., 2010), pathogen response (Pečenková et al., 2011), and mycorrhiza (Genre et al., 2012). The Exo70 subunit has been also previously implicated in the pollen-stigma interaction in *Brassica* and *Arabidopsis* (Samuel et al., 2009), though its specific role remains controversial (Kitashiba et al., 2011) and the observed phenotypes may be rather due to a generalized secretion defect affecting stigma function (Synek et al., 2006).

Exocyst belongs, together with related COG, GARP, and DSL1 complexes, to the large, evolutionarily ancient family of eukaryotic quatrefoil vesicle tethering complexes (Whyte and Munro, 2002; Koumandou et al., 2007). Structural studies (recently reviewed by Hertzog and Chavrier, 2011) and theoretical sequence-based modeling revealed common structural elements involving rod-like helical bundles in all eight subunits, and a model of exocyst architecture based on aggregation of these bundles has been proposed (Munson and Novick, 2006; Croteau et al., 2009). Electron microscopy observations consistent with this model have been made also in the case of the putative plant exocyst (Seguí-Simmaro et al., 2004). Bundled Sec6, Sec8, Sec10 subunits probably form a core of the complex. At least in the yeast model, Sec6 also participates in its anchoring to the target membrane, and the remaining, more peripherally located subunits mediate interactions with membrane vesicles destined for delivery (as in the case of Sec15, interacting with the vesicle-borne Sec4 GTPase), with the target membrane and associated small GTPases of the Rho family (Sec3 and Exo70), and possibly with other structural or

regulatory proteins (Songer and Munson, 2009). The Exo70 subunit, which can bind to phosphoinositides, is crucial for targeting the complex to the destination membrane also in metazoans (He et al., 2007). Exo84 is also required for proper localization of the exocyst in yeast (Zhang et al., 2005). Surprisingly, the function of these subunits is not restricted to participation in exocytosis, as Exo70 and Exo84 subunits also participate in pre-mRNA splicing (Awashi et al., 2001; Dellago et al., 2011).

While exocyst subunits are encoded by a single gene in yeast or at most a few paralogs in metazoans, a puzzling number of plant isoforms has been identified in particular for the Exo70 subunit, which is encoded by 23 distinct loci in *Arabidopsis thaliana* (Eliáš et al., 2003; Synek et al., 2006). Some other subunits are also encoded by duplicated or triplicated (as in case of *A. thaliana* Exo84) loci. However, the only published phylogenetic studies of the plant exocyst so far are devoted solely to the Exo70 subunit (Eliáš et al., 2003; Synek et al., 2006) or restricted to a very limited species selection (Chong et al., 2010). With growing number of sequenced genomes, and increasing quality of genomic sequence annotations, a broader coverage of plant lineages can now be achieved. Here we present the results of a phylogenetic analysis of the canonical exocyst subunits encoded by 10 land plant genomes representing dicot and monocot angiosperms, a lycophyte (*Selaginella moellendorffii*) and a moss (*Physcomitrella patens*), and propose an evolutionary scenario consistent with our results.

MATERIALS AND METHODS

IDENTIFICATION OF EXOCYST SUBUNIT SEQUENCES

The collection of exocyst subunit sequences has been assembled by exhaustive mining of multiple data sources. For each subunit, a "seed" collection was generated as a non-redundant union of sequences originating from *A. thaliana*, *Arabidopsis lyrata*, *Populus trichocarpa*, *Vitis vinifera*, *Oryza sativa* var. *japonica*, *O. sativa* var. *indica* (omitted in case of Exo70 to keep the project at a manageable scale), *Sorghum bicolor*, *Brachypodium distachyon* and *P. patens*, and identified on the basis of their annotation among (i) components of the exocyst complex as recorded in the COG section of the STRING protein interaction database[1] (Sklarczyk et al., 2011) and (ii) reference sequences from GenBank (Benson et al., 2012). BLAST (McGinnis and Madden, 2004) searches of species-specific portions of the non-redundant section of GenBank and several species-specific resources (see below) have been employed to identify additional sequences from the above listed species, as well as from *S. moellendorffii* and selected members of the genus *Solanum* (see Results).

The additional databases mined included Uniprot (The Uniprot Consortium, 2012), Phytozome[2] (Goodstein et al., 2012), and JGI[3] for multiple species, Solgenomics[4] (Bombarely et al., 2011) and PGSC[5] (Potato Genome Sequencing Consortium, 2011) for *Solanaceae*, The Arabidopsis Information Resource[6] (Lamesch et al., 2012) for *Arabidopsis*, and COSMOSS[7] (Lang et al., 2005) for *Physcomitrella*. Final round of searches was performed between February and May 2012.

Redundancies within the collection were removed on the basis of pairwise BLAST alignments. In case of multiple protein predictions originating from the same locus, protein sequences closest to the most frequent splicing variety were chosen. In some cases, predicted protein sequences were revised based on re-evaluation of the available gene models, taking into account multiple methods of splicing prediction, ESTs, and homologous sequences as described previously (Grunt et al., 2008). The complete collection of sequences including the revised ones is available in the Supplement.

Additional BLAST searches of non-redundant GenBank sequences where performed to identify homologs of outlier sequences as described in Results.

PROTEIN SEQUENCE ALIGNMENTS

For initial estimation of sequence similarity and detection of possible problems with gene structure prediction (i.e., missing or extraneous exons), the interactive MACAW tool (Schuler et al., 1991; Lawrence et al., 1993), or the automated tools ClustalX (Thompson et al., 1997) and KALIGN (Lassmann and Sonnhammer, 2006) have been employed to generate preliminary versions of multiple protein sequence alignments. Final alignments for all subunits except Exo70 have been constructed manually with the aid of BioEdit (Hall, 1999), taking into account the preliminary alignments.

In case of the more numerous and more diverse Exo70 sequences, a similar manual approach has been employed first with a complete collection of *A. thaliana*, *A. lyrata,* and *P. trichocarpa* sequences, resulting in a "skeleton" alignment into which additional sequences in batches of up to 10 have been merged using the "realign selected sequences" feature of ClustalX; the alignments were manually adjusted after each batch using BioEdit with similarity shading for guidance, where considered appropriate.

Because of the admittedly subjective method of alignment construction, we are including the final alignments that have been used for phylogeny reconstruction in the Supplement. We have also performed parallel phylogeny estimations (as described below) with a manually constructed alignment and a KALIGN-constructed one for the Exo84 subunit, producing trees of essentially identical topology (i.e., sharing all significant branches, though differing somewhat in branch length and bootstrap support).

To identify conserved motifs in the divergent Exo70 N-termini, N-terminal sequence portions upstream of the conserved part used in phylogenetic analysis (see below) have been aligned *de novo* using ClustalX. Conserved sequence motifs have been identified visually after removal of obviously non-aligned sequences, manually adjusted in BioEdit and colored using the Dayhoff matrix (as implemented in BioEdit) for presentation.

PHYLOGENETIC ANALYSES

For phylogram construction, alignments except Exo70 were stripped of all columns containing gaps. For Exo70, which is more

[1] http://string-db.org/
[2] http://www.phytozome.net/
[3] http://genome.jgi.doe.gov/
[4] http://solgenomics.net/
[5] http://potatogenomics.plantbiology.msu.edu/
[6] http://www.arabidopsis.org
[7] http://www.cosmoss.org/

divergent than the remaining subunits (especially in its N-terminal part) and where several sequences were C- or N-truncated, only the unreliably aligned N-terminal portion and regions containing gaps in multiple sequences were removed prior to phylogenetic tree calculation.

Trees were computed by the maximum likelihood (ML) method using PHYML v3.0 aLRT (Guindon and Gascuel, 2003; Anisimova and Gascuel, 2006) at Phylogeny.fr (Dereeper et al., 2008) with default settings, using the aLRT test to estimate internal branch reliability. Independently, phylograms were constructed also by the neighbor-joining (NJ) method using ClustalX with 1000 bootstrap samples. Trees were visualized with the aid of the MEGA5 software (Tamura et al., 2011) and manually colored using CorelDraw for presentation.

K_a/K_s ESTIMATIONS

Nucleotide sequences corresponding to selected Exo70 subunits (see Results) have been retrieved from GenBank, and portions corresponding to reliably aligned protein parts have been realigned manually using BioEdit in the "toggle nucleotide to protein" mode to re-create the protein alignment used to calculate the phylogenetic trees. Resulting nucleotide sequence alignments have been analyzed using Selecton (Stern et al., 2007) to obtain codon-specific values of non-synonymous to synonymous mutation rates, providing information on residue-specific selection in the history of the examined sequences.

RESULTS

AN INVENTORY OF EXOCYST SUBUNITS IN 10 PLANT SPECIES

We performed exhaustive searches of sequenced genomes of eight angiosperm and two non-seed plant species with the aim to identify all genes encoding putative exocyst subunits. Among the angiosperms, we included the eudicots *A. thaliana*, *A. lyrata*, poplar (*P. trichocarpa*), and grapevine (*V. vinifera*) as representatives of the rosids. To gain insight also into the asterid lineage, we attempted to find the exocyst subunits in the publicly available tomato (*Solanum lycopersicon*) genome and cDNA sequences, which, however, did not yet cover the complete genome at the time of analysis. In particular, we found no sequences corresponding to Sec5 and Sec8. We therefore located the missing subunits in data from two potato species (*S. phureja* and *S. tuberosum*, respectively); we shall refer to these asterids collectively as *Solanum* sp. From the monocot class, four grass species (rice – *O. sativa*, represented by both *japonica* and *indica* varieties, sorghum – *S. bicolor*, and the model grass *B. distachyon*) have been included. Finally, we also analyzed genome data from one "lower" vascular plant – the lycophyte *S. moellendorffii*, and from the model moss *P. patens*. In total, we have collected 392 distinct protein sequences corresponding to presumed exocyst subunits (**Table 1**).

In agreement with the expected essential character of the exocyst in plants and with previous reports, all genomes encoded at least one copy of each subunit, and most of the subunits were encoded by one or a few loci, except Exo70, which always formed an extensive family of paralogs. Among the remaining subunits, we could upon closer inspection distinguish genuine single-copy or low copy subunits that were never present in more than two versions in the vascular plants (this was the case for Sec3, Sec5, Sec6, Sec8, and Sec10), and intermediate size gene families with more than two and less than eight paralogs in at least one of the species (Sec15 and Exo84). We shall further discuss these three groups separately.

LOW COPY SUBUNITS: SEC3, SEC5, SEC6, SEC8, AND SEC10

The first group of subunits includes Sec3 (in *A. thaliana* encoded by two genes in tandem – AtSEC3A/At1g47550/Arath1_Sec3 and AtSEC3B/At1g47560/Arath2_Sec3), Sec5 (again two *A. thaliana* genes – AtSEC5A/At1g76850/Arath1_Sec5 and AtSEC5B/At1g21170/Arath2_Sec5), Sec6, Sec8, and Sec10 (all encoded by single genes in *A. thaliana* – AtSEC6/At1g71820/Arath_Sec6, AtSEC8/At3g10380/Arath_Sec8 and AtSEC10/At5g12370/Arath_Sec10 – but see comments on possible Sec10 duplication below). Though these subunits are single-copy in some species, each of them is duplicated in at least one angiosperm genome, and all but Sec6 are triplicated in *P. patens*, showing that there is no strict functional requirement on keeping only a single protein version in cells. In fact, multiple splicing variants have been proposed

Table 1 | Numbers of exocyst subunit paralogs encoded by the studied plant genomes.

	Sec3	Sec5	Sec6	Sec8	Sec10	Sec15	Exo70	Exo84
A. thaliana	2	2	1	1	1	2	23	3
A. lyrata	2	2	1	1	1	2	23	3
P. trichocarpa	2	2	2	2	2	5	29	8
Solanum sp.	2[2]	1[3]	1[2]	1[4]	1[2]	2[2]	22[2]	4[2]
V. vinifera	1	1	2	1	1	2	15	3
O. sativa[1]	2(2)	1(1)	1(1)	1(1)	1(1)	4(4)	47	3(3)
S. bicolor	2	1	1	1	1	3	31	3
B. distachyon	2	1	1	1	1	3	27	3
S. moellendorffi	2	1	2	2	2	1	8	2
P. patens	3	3	1	3	3	2	13	7

The complete list of the 392 analyzed genes or proteins including database accession numbers, as well as protein sequences and sequence alignments used in phylogeny calculations, is provided as Supplementary Material.

[1]*japonica variety, with numbers for indica in brackets;* [2]*S. lycopersicon;* [3]*S. phureja;* [4]*S. tuberosum.*

for most *Arabidopsis* subunits in the recent genome annotation (Lamesch et al., 2012).

Tandem duplications affecting angiosperm exocyst genes are apparently not restricted to *Arabidopsis* Sec3. The *A. thaliana* genomic assembly might be problematic in the area around Sec10, since inspection of available GenBank sequences suggests a possible tandem duplication of the Sec10 locus differing by a couple of silent mutations and variant non-coding ends. The duplicated gene appears to be transcribed (see GenBank cDNAs AF479280.1 and AK318699.1 which are in good mutual agreement but differ from the reference genome sequence, though they encode an identical protein). Also in tomato, we found a single possibly functional Sec10 locus and three closely related pseudogenes with multiple stop codons, two of them in tandem (the pseudogenes are not included in the phylogeny; see Supplementary Material for accession numbers).

As a rule, protein sequences of the low copy subunits consist of a single well-defined domain, are well conserved along the whole length (exceptions will be discussed below) and their phylogenetic trees (**Figure 1**) exhibit striking overall mutual similarity. Within the angiosperms, all gene duplications except monocot Sec3 appear to be relatively recent, resulting in within-species paralogs that share at least 80% of identical amino acids in the most distant pair of the *A. thaliana* Sec5 paralogs. Duplicated paralogs cannot be matched among genomes more distant than the two rice varieties, or the two *Arabidopsis* species. The only exception from this pattern of apparently late gene duplications is the Sec3 subunit that has obviously split into two paralogous lineages early in the evolution of monocots or at least grasses.

Rice and *Arabidopsis* versions of any of the low copy subunits share between 59% (Arath1_Sec5 vs. OrysaJ_Sec5) and 81% (Arath_Sec6 vs. OrysaJ_Sec6) of identical amino acids. The Sec6, Sec10, and Sec8 subunits, believed to form the central core of the complex (Munson and Novick, 2006; Croteau et al., 2009), are the best conserved ones. Notably, one of the ancient Sec3 branches (the clade "monocot 1" in **Figure 1**) has considerably diverged from the cluster of dicot sequences and the remaining monocot clade, suggesting a possible release of selection pressure followed by neo- or subfunctionalization. Compared to the degree of conservation found in the angiosperms, the *Physcomitrella* paralogs exhibit major within-genome differences, with the most distant paralogs Phypa1_Sec10 and Phypa3_Sec10 sharing only 51% of identical amino acids.

Two sequences deviate from the standard overall conserved domain structure of the relevant low copy subunits and can be perhaps viewed as "structural outliers" of their corresponding gene families. In the case of the *A. lyrata* Sec3 paralog Araly2_Sec3, the N-terminal part of the conserved domain is replaced by a domain related to a family of RING box/E3 ligases, encoded by a single-exon and flanked at least from one side by a sequence related to Copia-like retroelements, suggesting a very recent retrotransposition-mediated gene fusion. However, this domain combination appears to be unique in the whole of GenBank, and there are no ESTs documenting that this gene is expressed *in planta*; therefore, its functionality and biological significance remains problematic.

The second structural outlier is the *P. patens* Sec10 paralog Phypa2_Sec10, noticed in our previous study (Grunt et al., 2008) because of its unique combination of a N-terminally located Sec10 domain with the formin-specific FH2 domain at the C-end of the protein (see sequence Phypa5 in Grunt et al., 2008). An alternative splicing prediction separates these two domains into two distinct proteins (a short version corresponding to standard Sec10 is included in our phylogeny). The combination of Sec10 and FH2 domains is again unique in GenBank. However, there is a partial cDNA of the formin end (GenBank BY987890.1) indicating gene expression in the moss, albeit it is unclear which splice variants are biologically relevant.

INTERMEDIATE SIZE FAMILIES: SEC15 AND EXO84

The second group of subunits consists of two gene families, Sec15 (with two *A. thaliana* paralogs – AtSEC15A/At3g56640/Arath1_Sec15 and AtSEC15B/At4g02350/Arath2_Sec15) and Exo84 (with three paralogs in *A. thaliana* – AtEXO84a/At5g49830/Arath2_Exo84, AtEXO84b, At1g10385/Arath3_Exo84, and AtEXO84c/At1g10180/Arath1_Exo84). In other studied genomes, Sec15 is encoded by two to five subunits (except *S. moellendorffii*, where only a single protein was found) and Exo84 by three to eight (again except *S. moellendorffii* with only two genes). In both cases the highest number was found in *P. trichocarpa*, and the final poplar subunit count may be even higher, since there is cDNA evidence of additional transcripts encoding proteins identical to the Sec15 paralogs included in our analysis but differing in their non-translated ends, reminiscent of the situation in *A. thaliana* Sec10 (see Supplementary Material).

Phylogenetic trees of both families indicate that at least a part of the observed diversity is ancient, and can be traced back at least to the origins of angiosperms (**Figure 2**). Both gene families can be split into two branches in seed plants, with multiple additional within-branch amplifications. In Sec15, most of these later amplification events (generating two clusters of poplar genes in both branches and a pair of rice genes in the B branch) appear to be fairly recent, reminiscent of those detected for low copy subunits. However, a duplication of the A subunit apparently occurred early in the monocot lineage (no later than at the emergence of grasses), resulting in two monocot- or grass-specific subfamilies, A1 and A2.

In Exo84, the situation is somewhat more complex. Clearly defined A and B branches (named according to the corresponding *A. thaliana* subunits) were found only in the dicots, while related monocot sequences form a rather compact cluster, probably closer to the A branch than to B. The dicot A and B branches and the monocot cluster will be further referred to as the A/B clade (**Figure 2**). Monocot A/B sequences also bear traces of early gene duplication preceding the radiation of grasses, but clearly distinct from the event that produced the A and B branches and followed by little actual sequence divergence (the rice A/B sequences OrysaJ1_Exo84 and OrysaJ2_Exo84 share 78% of identical amino acids). Besides of the A/B clade, a second ancient branch (the C clade) is shared by all examined angiosperms and contains, as a rule, products of single-copy genes with exception of an apparently recent cluster of three poplar sequences. Two mutually related dicot outliers (the CX sequences) are apparently related to the C clade, and proteins similar to them have been predicted also in

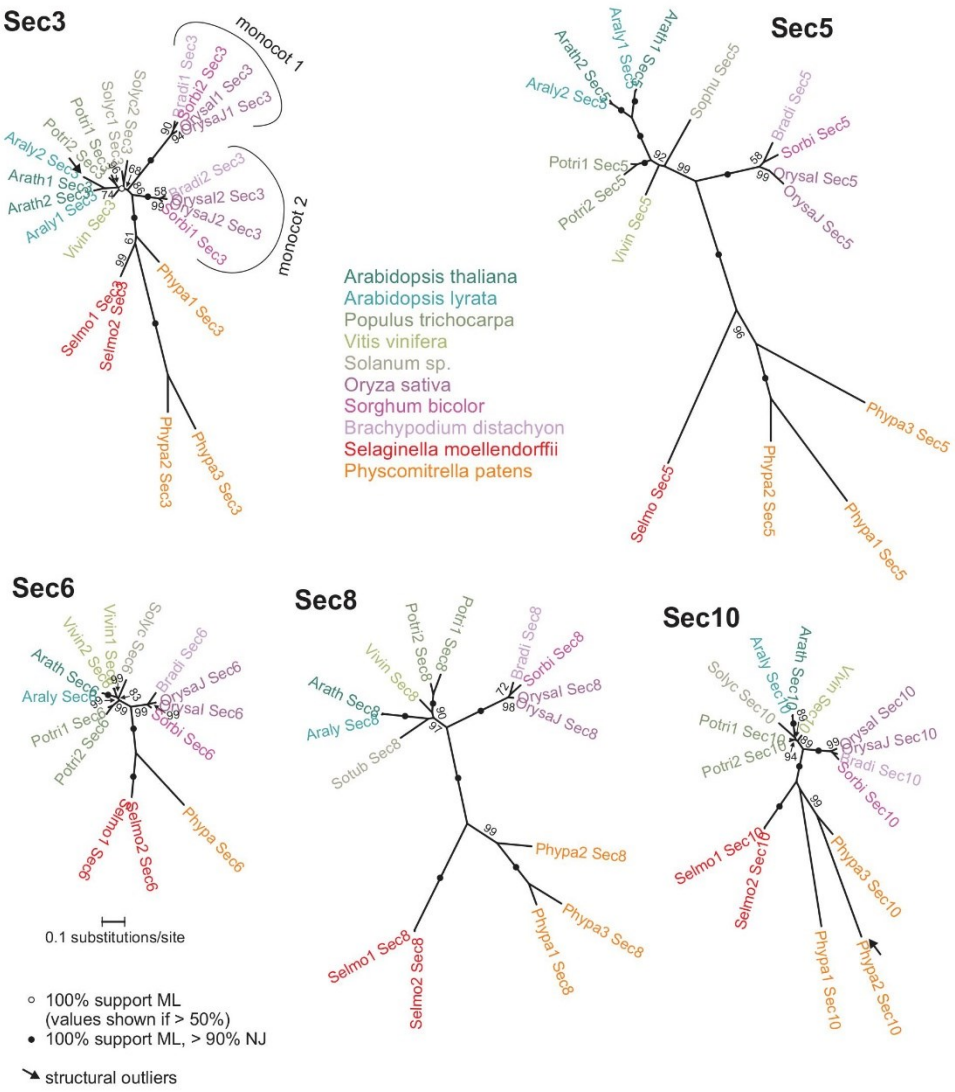

FIGURE 1 | Unrooted maximum likelihood (ML) phylograms of the low copy Exocyst subunits. All SH-like support values above 50% from the aLRT test are shown. Consistent trees were obtained also using the neighbor-joining (NJ) method with 1000 bootstrap samples; nodes with high support by both ML and NJ algorithms are marked by black dots. Arrows denote "structural outliers," i.e., sequences deviating from the standard domain organization of typical representatives of the protein family. All trees are at the same scale.

Ricinus communis (GenBank XM_002526525.1) and *Glycine max* (GenBank XM_003541318.1). A genomic DNA sequence fragment from *V. vinifera* (GenBank AM443616.2) contains patches of a possible ORF similar to the CX sequences in an area annotated as non-coding. While the grapevine genome annotation may require updating, it is also possible that these patches are vestiges of a lost gene that may have had a wider distribution.

In contrast to the angiosperms, the lycophyte and moss Sec15 sequences exhibit only minimum diversification, while Exo84 underwent duplication in *S. moellendorffii* and extensive

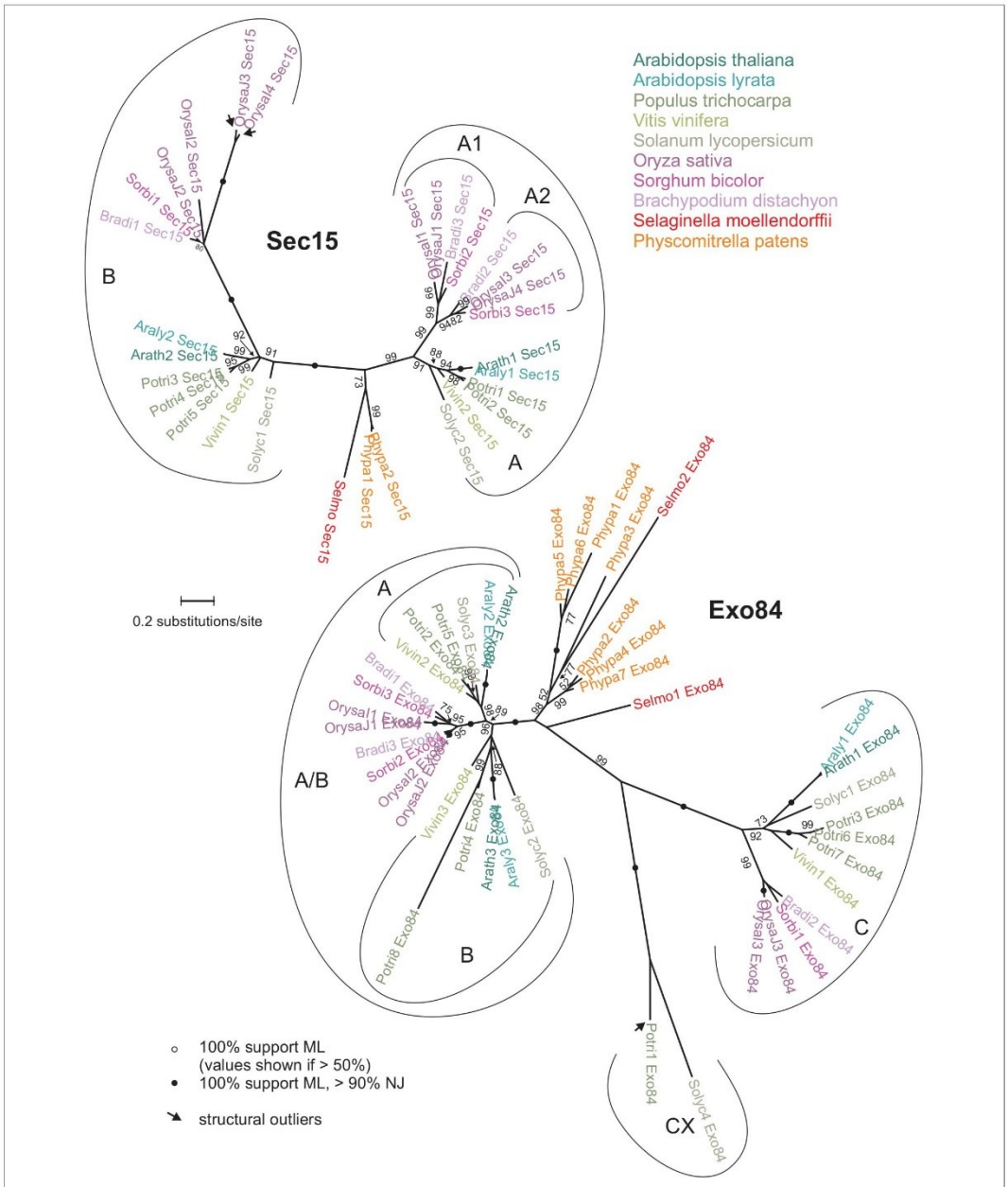

FIGURE 2 | Unrooted maximum likelihood (ML) phylograms of Sec15 and Exo84. All SH-like support values above 50% are shown. Consistent trees were obtained also using the neighbor-joining (NJ) method; nodes with high support by both ML and NJ algorithms are marked by black dots. Arrows denote "structural outliers" (see **Figure 1**). Both trees are at the same scale.

amplification, producing seven rather diversified paralogs, in *P. patens*. While the branching order is not reliable in the non-angiosperm sequences, the resulting tree does not exclude the possibility that the two major Exo84 clades might have appeared already at the base of the vascular plants.

Compared to the low copy subunits, Sec15 and Exo84 sequences exhibit greater diversity, with *Arabidopsis* AtSec15A and AtSec15B sharing 48%, AtExo84A and AtExo84B 59%, and AtExo84B and AtExo84C only 34% of identical amino acids. Nevertheless, the angiosperm branches of the phylogram appear to be rather compact, and the only conspicuously diversified poplar Exo84B paralog, Potri8_Exo84, may not be expressed, as we could not find any corresponding ESTs.

All sequences from each family can be aligned reliably along the whole length, with only three exceptions. The predicted rice Sec15 paralogs OrysaJ3_Sec15 and OrysaI4_Sec15 are missing a C-terminal part of the characteristic Sec15 domain and have instead an unrelated sequence. No homologs with such a gene organization have been found in GenBank, and there are no ESTs matching these genes. Together with the long distance from the rest of B clade Sec15 sequences, indicating relaxed selection, this suggest that these *O. sativa* Sec15 outliers may actually correspond to a pseudogene that has arisen not long before the separation of the *japonica* and *indica* varieties and that is now in the process of decay. The third structural outlier, Potri1_Exo84, one of the outlier CX sequences with a long C-terminal extension, also lacks cDNA or EST support, and it is thus not clear if it is expressed at all.

THE ENORMOUS DIVERSITY OF EXO70 PARALOGS

The large Exo70 family consists of 23 paralogs in *A. thaliana*, representing eight previously identified clades (Synek et al., 2006): AtExo70A1/At5g03540/ArathA1_Exo70, AtExo70A2/At5g52340/ArathA2_Exo70, and AtExo70A3/At5g52350/ArathA3_Exo70 in clade A, AtExo70B1/At5g58430/ArathB1_Exo70 and AtExo70B2/At1g07000/ArathB2_Exo70 in clade B, AtExo70C1/At5g13150/ArathC1_Exo70 and AtExo70C2/At5g13990/ArathC2_Exo70 in clade C, AtExo70D1/At1g72470/ArathD1_Exo70, AtExo70D2/At1g54090/ArathD2_Exo70, and AtExo70D3/At3g14090/ArathD3_Exo70 in clade D, AtExo70E1/At3g29400/ArathE1_Exo70 and AtExo70E2/At5g61010/ArathE2_Exo70 in clade E, AtExo70F1/At5g50380/ArathF1_Exo70 in clade F, AtExo70G1/At4g31540/ArathG1_Exo70 and AtExo70G2/At1g51640/ArathG2_Exo70 in clade G, and eight paralogs – AtExo70H1/At3g55150/ArathH1_Exo70, AtExo70H2/At2g39380/ArathH2_Exo70, AtExo70H3/At3g09530/ArathH3_Exo70, AtExo70H4/At3g09520/ArathH4_Exo70, AtExo70H5/At2g28640/ArathH5_Exo70, AtExo70H6/At1g07725/ArathH6_Exo70, AtExo70H7/At5g59730/ArathH7_Exo70, and AtExo70H8/At2g28650/ArathH8_Exo70 – in clade H. In other studied plants, the number ranges from eight in *Selaginella* to 47 in rice (**Table 2**; see Supplementary Material for a full list of genes), albeit the final count might still change in the genomes whose annotation is still under development (especially *Solanum* sp.).

Unlike the other seven subunits, Exo70 paralogs are rather diverse and their N-terminal part of up to 300 amino acids could not be aligned reliably throughout all the 238 studied sequences. We have used only the well-aligned portion to construct a phylogram (**Figure 3**) that essentially corroborates the previous reports but brings some additional new insights. Our analysis confirms the existence of three major Exo70 lineages Exo70.1, Exo70.2, and Exo70.3 that contain both angiosperm and "lower plant" sequences, as well as the nine clades (A–I) with members of both monocot and dicot origin (Synek et al., 2006). The clade I, restricted only to some angiosperms (it is, e.g., missing in both *Arabidopsis* species), clusters within a branch that includes the compact angiosperm G clade and a group of moss sequences, but none from *Selaginella*, suggesting loss in the lycophyte lineage. We will refer to this wider branch, corresponding to the previously proposed Exo70.3 lineage, as the G/I clade.

Remarkable is the major expansion of a monocot- or grass-specific branch of the F family, the FX clade. Apparently, a single family of Exo70 subunits underwent major expansion in both monocots and dicots. Reverse transcription might have contributed to gene amplification in case of the abundant dicot H clade with a large proportion of single-exon genes (Synek et al., 2006; Chong et al., 2010), but not in case of the monocot FX with a large proportion of multi-exon genes (Chong et al., 2010). Somewhat surprisingly, a very distant paralog OrysaFX8_Exo84, which clusters within the F branch but outside the genuine FX clade,

Table 2 | Numbers of Exo70 paralogs encoded by the studied genomes (in total and in the individual clades).

	All	A	B	C	D	E	F (FX)	G/I	H	BNG[1]
A. thaliana	23	3	2	2	3	2	1(0)	2	8	–
A. lyrata	23	3	2	2	3	2	1(0)	2	8	–
P. trichocarpa	29	4	2	3	2	6	2(0)	5	5	–
S. lycopersicon	22	3	1	3	2	2	1(0)	4	6	–
V. vinifera	15	2	1	1	1	2	1(0)	4	3	–
O. sativa	47	4	3	3	2	1	26 (19)	3	5	–
S. bicolor	31	3	3	2	2	1	16 (12)	3	1	–
B. distachyon	27	5	2	2	2	1	11(6)	3	1	–
S. moellendorffi	8	4	–	–	–	–	–	–	–	4
P. patens	13	3	–	–	–	–	–	4	–	6

[1] *Basal non-angiosperm group.*

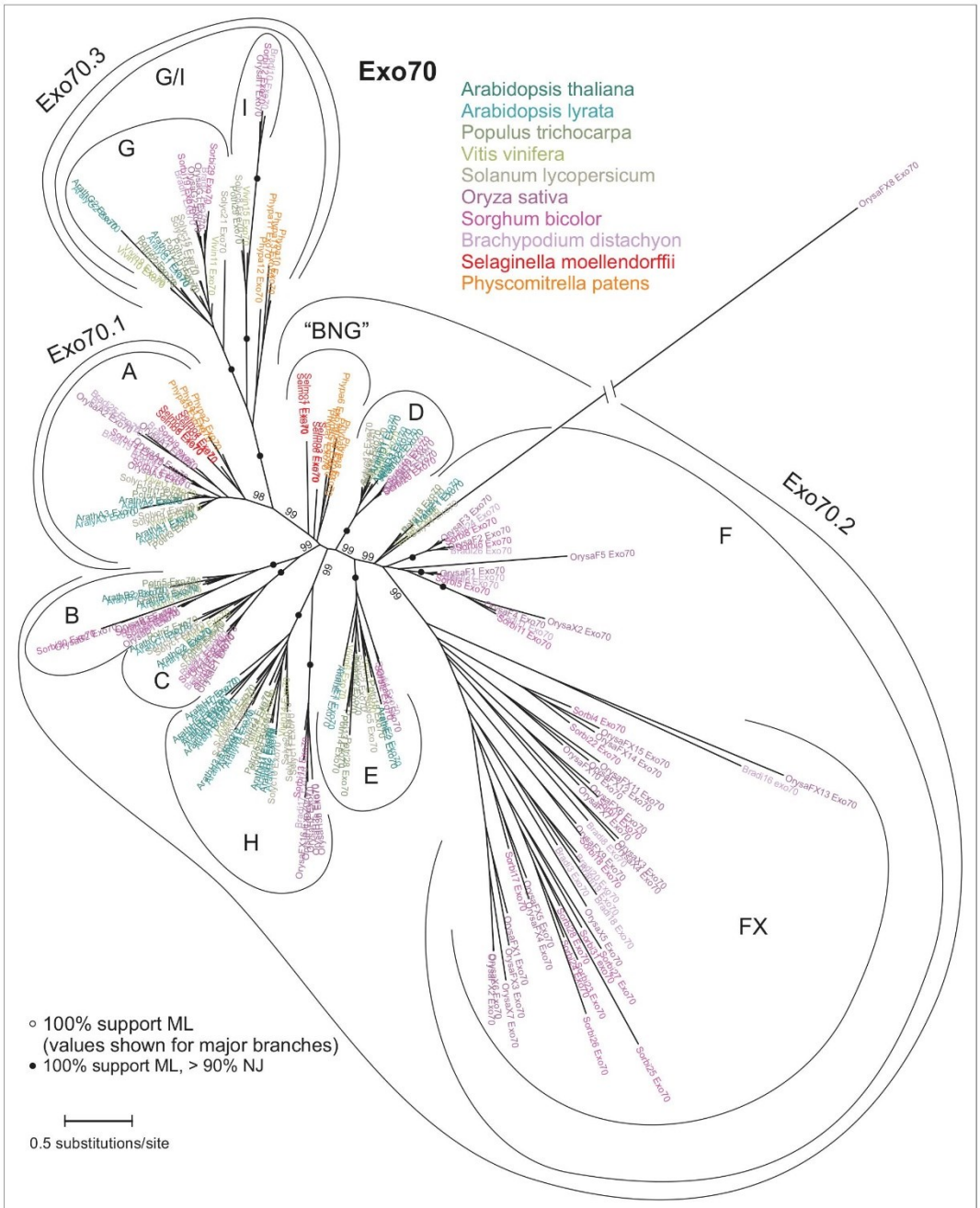

FIGURE 3 | Unrooted maximum likelihood (ML) phylogram of Exo70. SH-like support values above 50% are shown only for major branches for the sake of legibility. A tree obtained using the neighbor-joining (NJ) method was consistent with the ML one except of placing the FX branch outside the F clade; nodes with high support by both ML and NJ algorithms are marked by black dots. "BNG" denotes the basal non-angiosperm group of Exo70 paralogs.

is supported by a full-length cDNA (GenBank AK109785.1) and there are even two closely related ESTs from *Lolium perenne* (GenBank GR511301.1) and *L. temulentum* (GenBank DT673816.1), indicating that this outlier is functional and possibly specific for some grasses.

Duplicated genes tend to be rapidly eliminated by natural selection if they bring no advantage in terms of fitness. Question thus arises why there are so many Exo70 varieties maintained across large evolutionary distances. One possibility would be sub- or neofunctionalization of the conserved Exo70 domain itself. We have thus examined representative *A. thaliana* Exo70 sequences for traces of positive (diversifying) selection by estimation of the residue-specific ratio of non-synonymous to synonymous mutation rates (K_a/K_s). For this analysis, we chose two sequence collection – eight representatives of the main clades (AtExo70A1, AtExo70B1, AtExo70C1, AtExo70D1, AtExo70E1, AtExo70F1, AtExo70G1, and AtExo70H1) to identify markers of selection generating or enhancing between-clade differences, and eight representatives of the H clade (AtExo70H1, AtExo70H2, AtExo70H3, AtExo70H4, AtExo70H5, AtExo70H6, AtExo70H7, and AtExo70H8) to find traces of selection favoring within-clade differences. However, in both cases there was only evidence of purifying selection throughout the length of the sequence, but no positive selection, and we thus conclude that differences within the conserved part of the Exo70 subunits are not likely to play a decisive part in determining the function of the individual paralogs.

Functional diversification, however, may be due to the variable N-terminal sequences. We thus examined these regions in more detail and uncovered two sequence motifs conserved in many, but not all, Exo70 paralogs (**Figure 4**). Distribution of these motifs (see Supplementary Material) suggests that they are ancestral, and that they have been lost or eroded in some of the sequences. Motif 2 is present in most, if not all members of all stable Exo70 clades with exception of FX, and also in the members of the "basal non-angiosperm group," i.e., in the sequences of lower plant origin with unclear mutual relationships that belong to the Exo70.2 supergroup. The more N-terminally located motif 1 was found in most members of the basal non-angiosperm group and of the A, E, and G/I clades. It is present also in members of the F branch except FX, and also except the distant F outlier OrysaFX8_Exo70. This suggests that Motif 1 is also ancestral but was lost in some angiosperm clades within the Exo70.2 supergroup. The presence of the conserved motifs indicates that the variable Exo70 N-termini have largely evolved through a process of mutations and selection rather than domain-shuffling, although this does not have to be the rule in all cases (especially the origin of the diverse and mutually largely unrelated N-termini of the FX proteins remains unclear).

DISCUSSION

The present study provides the first attempt to reconstruct evolution of the land plant, especially angiosperm, exocyst complex in the broader context of higher plant evolution. Our previous works (Eliáš et al., 2003; Synek et al., 2006) have focused only on the most abundant subunit, Exo70, and the only previous phylogenetic study addressing all the eight canonical exocyst subunits in plants (Chong et al., 2010) was based on only four species – *Arabidopsis*, rice and poplar as the representatives of angiosperms, and the moss *P. patens*, allowing only a limited possibility of generalization. We have included a broader and more representative collection of genomes, including a moss (*P. patens*), a lycophyte, i.e., a non-seed vascular plant (*S. moellendorffii*), and eight angiosperms (unfortunately, there is, to date, no sufficiently well-covered gymnosperm genome for an exhaustive search). The angiosperms are represented by five dicotyledonous and three grass species covering a

FIGURE 4 | Alignment of representative examples of the N-terminal conserved motifs found within the variable N-terminal part of Exo70 sequences. Motif 1 is located no more than 70 amino acids from the N terminus and always upstream of motif 2; motif 2 begins less than 250 amino acids from the N terminus. Residues conserved among 75% or more of the sequences containing the motif are shown on a gray background (residue conservation was determined using the Dayhoff matrix). Numbers in brackets indicate the length of variable insertions removed for clarity.

rather broad range of diversity (see the simplified scheme of plant evolution in **Figure 5**). Among dicots, the closest are the two *Arabidopsis* species (*A. thaliana* and *A. lyrata*) that have separated approximately five millions of years ago (Koch et al., 2000). Poplar (*P. trichocarpa*) is included as somewhat more distant representative of the rosid clade, grapevine (*V. vinifera*) as a basal rosid, and several members of the genus *Solanum* (where, unfortunately, no genome is annotated well enough to provide data for all subunits) are representing the asterids. The coverage of the monocot clade is narrower, as all the available genomes belong to grasses. Thus, although we propose some possible monocot-specific features of the exocyst family in this paper on the basis of data from three grass species (*O. sativa*, *S. bicolor*, and *B. distachyon*), we do not know at present if such features are present also in non-grass monocots.

In total, we have analyzed nearly 400 exocyst subunit sequences. Our list, however, may not be complete especially in case of the *Solanum* sp. sequences, where genomic annotation is still under development, and some loci may have been missed. It is not surprising that our inventory yielded novel genes especially in the Exo70 family in addition to those reported previously for *P. trichocarpa* and *O. sativa* (Chong et al., 2010). On the other hand, in the absence of gene expression data and experimental observations, distinction between functional genes and pseudogenes may be somewhat blurry, especially in case of the extensive Exo70 family, containing numerous single-exon members that apparently underwent reverse transcription at some point in the course of their evolution (Synek et al., 2006). Thus, the determined numbers of subunits might still somewhat change in the future, even in well-characterized models (see the possible undocumented duplication of the *Arabidopsis* Sec10 locus). Also allelic diversity in heterozygous diploids may have resulted in identification of extraneous loci in particular in the case of *S. moellendorffii*, where most genes appear to have two closely related paralogs, albeit this species is believed to be one of the few plants without a recent history of whole-genome duplications (Jiao et al., 2011).

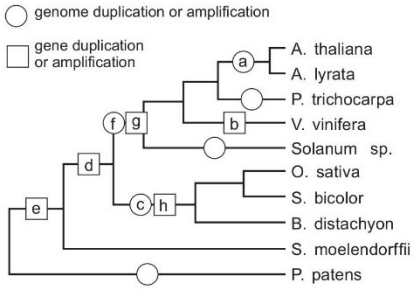

FIGURE 5 | A possible scenario of exocyst evolution in the context of land plant evolution and the history of genome duplications. Selected genome duplication and gene amplification events that may have founded specific subfamilies of exocyst subunits are denoted by letters. (a) Duplication of *Arabidopsis* sp. Sec5; (b) Duplication of grapevine Sec6; (c) Origin of two Sec3 clades (monocot1 and monocot2), and of the Sec15 clades A1 and A2; (d) Origin of Sec15 clades A and B; (e) Origin of Exo84 clades A/B and C/CX; (f) Separation of the Exo84 clades A and B, as well as C and CX, the later subsequently lost in some descendants; (g) Amplification of dicot Exo70 clade H; (h) Amplification of the monocot Exo70 clade FX.

We have found that a subgroup of exocyst subunits, corresponding to the previously proposed core of the complex (Munson and Novick, 2006; Croteau et al., 2009), underwent little or no amplification in the vascular plants, though even these subunits have amplified to a some extent in non-seed plants. These low copy subunits, in particular Sec6, Sec8, and Sec10, but to a somewhat lesser extent also Sec5 and Sec3, exhibit evolutionary trees that are not only topologically similar but also obviously correlated in terms of branch length, which is consistent with co-evolution driven by the requirement of maintaining mutual compatibility of closely interacting complex subunits (Juan et al., 2008; Lovell and Robertson, 2010). The remaining subunits Sec15, Exo84, and in particular Exo70, exhibit greater diversity consistent with their function on the periphery of the complex, providing an interface to a variety of interactors that may be specific to particular lineages or even to particular paralogs.

Whole-genome duplications have played an important part in the evolution of land plants (Van de Peer et al., 2009; Jiao et al., 2011). They also provided an obvious source of "raw materials" for evolution of divergent paralog families of the exocyst subunits. We were able to pinpoint several of the proposed ancient genome duplication or polyploidization events in a widely accepted scenario of land plant evolution (Soltis et al., 2008; Van de Peer et al., 2009; Jiao et al., 2011; Woodhouse et al., 2011) as possible sources of distinct exocyst subunit clades especially in the Sec15 and Exo84 families (**Figure 5**). However, it has to be stressed that not every gene duplication coincident with a genome duplication must be a result of that duplication. For instance, the tandem duplication of *A. thaliana* Sec3 appears to be a local event, while equally distant *A. thaliana* Sec5 paralogs are obviously a product of a whole-genome duplication (see data from Woodhouse et al., 2011).

The greatest part of the putative exocyst diversity is due to the extremely amplified Exo70 subunit that apparently existed in at least three paralogs already in the common ancestor of land plants including Rhyniophytes, and diversified into seven clades prior to the separation of the monocot and dicot lineages (Synek et al., 2006). Reverse transcription may have contributed to early amplification of some clades, which contain mostly single-exon genes, among them also the dicot clade H that has expanded into an extensive family of paralogs. No such expansion, however, took place in the monocots, which have only a few H-type Exo70s. Instead, a branch of the multi-exon F family has amplified and diversified substantially, producing the monocot-specific FX clade.

While there is considerable sequence divergence among the Exo70 paralogs, we found no evidence of positive selection operating across their conserved part. An obvious source of functional diversity, however, would be the variable sequences at both ends of the Exo70 subunits. A possible participation of C-terminal motifs in differential binding to membrane phosphoinositides has been already proposed (Žárský et al., 2009). Here we have uncovered two obviously ancestral N-terminal motifs that document that the N-terminal segments, though highly diversified, have evolved from a common ancestor at least in most of the sequences, without contribution of major domain-shuffling events. Nevertheless,

they have possibly built up enough diversity to mediate interactions with a variety of cellular components, ensuring thus the apparently required functional diversification.

Assuming that the alternative paralogs of exocyst subunits are co-expressed, and that they can freely combine into complexes (which is by no means guaranteed), literally hundreds of distinct exocysts may exist within plant cells. Were the subunit combinations unrestricted (i.e., each Sec15 paralog working with each Exo84 and each Exo70), *Arabidopsis* would be capable of producing 552 distinct exocyst variants, and rice stunning 1128 variants. Alternative splicing may provide an additional source of exocyst diversity. Even in metazoans, an array of Exo70 splicing variants was uncovered, dependent on cell type and age of the tissue (Dellago et al., 2011). It is therefore possible that also in animals hidden multiplicity of exocysts may exist depending on the splice-isoforms of Exo70 (and possibly also other subunits). On the other hand, the actual numbers of plant exocyst varieties are undoubtedly much lower than the numbers of possible subunit combinations, since not all paralogs are co-expressed, and some may be expressed only under special circumstances or not at all. Nevertheless, we cannot avoid asking what is the biological relevance (or selective advantage) of such a profusion of exocyst varieties.

One possible reason may be the need to maintain and manage a variety of qualitatively distinct membranes – not only of intracellular compartments, but also within the cell cortex whose lateral mobility is restricted by the cell wall. Distinct exocyst variants in the same cell, defined especially by different "landmarking" Exo70 subunits, may participate in delimiting specific plasmalemma domains ("activated cortical domains") engaging in distinctly regulated membrane turnover. Together with the underlying cytoplasm (in particular the connected recycling endosomes defined by distinct Rab11 paralogs), the activated cortical domains form larger functional units (recycling domains) that may play a central part in the control of different cortical or endomembrane domains of the many-sided plant cells (see detailed discussion in Žárský et al., 2009; Žárský and Potocký, 2010). Another possibility is functional separation of the diverse complexes in time and/or in tissue or organ space through controlled gene expression of subunit variants optimized for a particular set of circumstances (e.g., specific cell differentiation stages, tissues, or environmental conditions). Participation of Exo84B in the establishment of mycorrhiza (Genre et al., 2012) and, in particular, of distinct Exo70 variants in pathogen response (Pečenková et al., 2011) shows that this indeed appears to be the case. Remarkably, one of the *Arabidopsis* Exo70 paralogs involved in pathogen response is member of the H clade, expanded specifically in the dicots, and it is thus tempting to speculate about a possible analogous role of the even more diversified monocot FX clade.

In summary, both our data and recent experimental observations show that plants do not have "an exocyst complex," but an enormous variety of diverse exocyst complexes, and that this feature is at least as old as the land plants. Unraveling its functional significance will continue to provide interesting challenges for the plant cell biology of the near future.

ACKNOWLEDGMENTS

This work has been supported by the European Community 7th Framework Programme (FP7/2007–2013) Grant No. 238640 PLANTORIGINS, the Grant Agency of the Czech Republic (P305/11/1629), the Ministry of Education of the Czech Republic (MSM 0021620858), and the Charles University in Prague (SVV 265203/2012).

SUPPLEMENTARY MATERIAL

The Supplementary Material for this article can be found online at http://www.frontiersin.org/Plant_Traffic_and_Transport/abstract/31437

Cvrckova_S1.xls | List of the 392 exocyst subunit sequences analyzed, including database accession numbers, phylogenetic classification and domain composition (Microsoft Excel file).

Cvrckova_S2.zip | Protein sequences and alignments used for phylogenetic analyses (compressed Zip file containing protein sequences in text format – ∗.txt and alignment sequences in FASTA format – ∗.fst).

REFERENCES

Anisimova, M., and Gascuel, O. (2006). Approximate likelihood ratio test for branchs: a fast, accurate and powerful alternative. *Syst. Biol.* 55, 539–552.

Awashi, S., Palmer, R., Castro, M., Mobarak, C. D., and Ruby, S. W. (2001). New roles for the Snp1 and Exo84 proteins in yeast pre-mRNA splicing. *J. Biol. Chem.* 276, 31004–31015.

Benson, D. A., Karsch-Mizrachi, I., Clark, K., Lipman, D. J., Ostell, J., and Sayers, E. W. (2012). GenBank. *Nucleic Acids Res.* 40, D48–D53.

Bombarely, A., Menda, N., Buels, R. M., Strickler, S., Fischer-York, T., Pujar, A., Leto, J., Gosselin, J., and Mueller, L. A. (2011). The sol genomics network (solgenomics.net): growing tomatoes using perl. *Nucleic Acids Res.* 39, D1149–D1155.

Chong, Y. T., Gidda, S. K., Sanford, C., Parkinson, J., Mullen, R. T., and Goring, D. R. (2010). Characterization of the *Arabidopsis thaliana* exocyst complex gene families by phylogenetic, expression profiling, and subcellular localization studies. *New Phytol.* 185, 401–419.

Cole, R. A., Synek, L., Žárský, V., and Fowler, J. E. (2005). SEC8, a subunit of the putative *Arabidopsis* exocyst complex, facilitates pollen germination and competitive pollen tube growth. *Plant Physiol.* 138, 2005–2018.

Croteau, N. J., Furgason, M. L. M., Devos, D., and Munson, M. (2009). Conservation of helical bundle structure between the exocyst subunits. *PLoS ONE* 4, e4443. doi:10.1371/journal.pone.0004443

Dellago, H., Löscher, M., Ajuh, P., Ryder, U., Kaisermayer, C., Grillari-Voglauer, R., Fortschegger, K., Gross, S., Gstraunthaler, A., Borth, N., Eisenhaber, F., Lamond, A. I., and Grillari, J. (2011). Exo70, a subunit of the exocyst complex, interacts with SNEV(hPrp19/hPso4) and is involved in pre-mRNA splicing. *Biochem. J.* 438, 81–91.

Dereeper, A., Guignon, V., Blanc, G., Audic, S., Buffet, S., Chevenet, F., Dufayard, J. F., Guindon, S., Lefort, V., Lescot, M., Claverie, J. M., and Gascuel, O. (2008). Phylogeny.fr: robust phylogenetic analysis for the non-specialist. *Nucleic Acids Res.* 36, W465–W469.

Eliáš, M., Drdová, E., Žiak, D., Bavlnka, B., Hála, M., Cvrčková, F., Soukupová, H., and Žárský, V. (2003). The exocyst complex in plants. *Cell Biol. Int.* 27, 199–201.

Fendrych, M., Synek, L., Pečenková, T., Toupalová, H., Cole, N., Drdová, E., Nebesářová, J., Šedinová, M., Hála, M., Fowler, J. E., and Žárský, V. (2010). The *Arabidopsis* exocyst complex is involved in cytokinesis and cell plate maturation. *Plant Cell* 22, 3053–3065.

Genre, A., Ivanov, S., Fendrych, M., Faccio, A., Žárský, V., Bisseling, T., and Bonfante, P. (2012). Multiple exocytotic markers accumulate at the sites of perifungal membrane biogenesis in arbuscular mycorrhizas. *Plant Cell Physiol.* 53, 244–255.

Goodstein, D. M., Shu, S., Howson, R., Neupane, R., Hayes, R. D., Fazo, J., Mitros, T., Dirks, W., Hellsten,

U., Putnam, N., and Rokshar, D. S. (2012). Phytozome: a comparative platform for green plant genomics. *Nucleic Acids Res.* 40, D1178–D1186.

Grunt, M., Žárský, V., and Cvrčková, F. (2008). Roots of angiosperm formins: the evolutionary history of plant FH2 domain-containing proteins. *BMC Evol. Biol.* 8, 115. doi:10.1186/1471-2148-8-115

Guindon, S., and Gascuel, O. (2003). A simple, fast an accurate algorithm to estimate large phylogenies by maximum likelihood. *Syst. Biol.* 52, 696–704.

Guo, W., Grant, A., and Novick, P. (1999). Exo84p is an exocyst protein essential for secretion. *J. Biol. Chem.* 274, 23558–23564.

Guo, W., Roth, D., Gatti, E., and Novick, P. (1997). Identification and characterization of homologues of the exocyst component Sec10p. *FEBS Lett.* 404, 135–139.

Hála, M., Cole, R. A., Synek, L., Drdová, E., Pečenková, T., Nordheim, A., Lamkemeyer, T., Madlung, J., Hochholdinger, F., Fowler, J. E., and Žárský, V. (2008). An exocyst complex functions in plant cell growth in *Arabidopsis* and tobacco. *Plant Cell* 20, 1330–1345.

Hall, T. A. (1999). BioEdit: a user-friendly biological sequence alignment editor and analysis program for Windows 95/98/NT. *Nucl. Acids Symp. Ser.* 41, 95–98.

He, B., and Guo, W. (2009). The exocyst complex in polarized exocytosis. *Curr. Opin. Cell Biol.* 21, 537–542.

He, B., Xi, F., Zhang, X., Zhang, J., and Guo, W. (2007). Exo70 interacts with phospholipids and mediates the targeting of the exocyst to the plasma membrane. *EMBO J.* 26, 4053–4065.

Heider, M. R., and Munson, M. (2012). Exorcising the exocyst complex. *Traffic* 13, 898–907.

Hertzog, M., and Chavrier, P. (2011). Cell polarity during motile processes: keeping on track with the exocyst complex. *Biochem. J.* 433, 403–409.

Jiao, Y., Wickett, N. J., Ayyampalayam, S., Chanderbali, A. S., Landherr, L., Ralph, P. E., Tomsho, L. P., Hu, Y., Liang, H., Soltis, P. S., Soltis, D. E., Clifton, S. W., Schlarbaum, S. E., Schuster, S. C., Ma, H., Leebens-Mack, J., and de Pamphilis, C. W. (2011). Ancestral polyploidy in seed plants and angiosperms. *Nature* 473, 97–100.

Juan, D., Pazos, F., and Valencia, A. (2008). Co-evolution and co-adaptation in protein networks. *FEBS Lett.* 582, 1225–1230.

Kee, Y., Yoo, J. S., Hazuka, C. D., Peterson, K. E., Hsu, S. C., and Scheller, R. H. (1997). Subunit structure of the mammalian exocyst complex. *Proc. Natl. Acad. Sci. U.S.A.* 94, 14438–14443.

Kitashiba, H., Liu, P., Nishio, T., Nasrallah, J. B., and Nasrallah, M. E. (2011). Functional test of *Brassica* self-incompatibility modifiers in *Arabidopsis thaliana*. *Proc. Natl. Acad. Sci. U.S.A.* 108, 18173–18178.

Koch, M. A., Haubold, B., and Mitchell-Olds, T. (2000). Comparative evolutionary analysis of chalcone synthase and alcohol dehydrogenase loci in *Arabidopsis, Arabis,* and related genera (Brassicaceae). *Mol. Biol. Evol.* 17, 1483–1498.

Koumandou, V. L., Dacks, J. B., Coulson, R. M., and Field, M. C. (2007). Control systems for membrane fusion in the ancestral eukaryote; evolution of tethering complexes and SM proteins. *BMC Evol. Biol.* 7, 29. doi:10.1186/1471-2148-7-29

Kulich, I., Cole, R. A., Drdová, E., Cvrčková, F., Soukup, A., Fowler, J. E., and Žárský, V. (2010). Arabidopsis exocyst subunits SEC8 and EXO70A1 and exocyst interactor ROH1 are involved in the localized deposition of seed coat pectin. *New Phytol.* 188, 615–625.

Lamesch, P., Berardini, T. Z., Li, D., Swarbreck, D., Wilks, C., Sasidharan, R., Muller, R., Dreher, K., Alexander, D. L., Garcia-Hernandez, M., Karthikeyan, A. S., Lee, C. H., Nelson, W. D., Ploetz, L., Singh, S., Wensel, A., and Huala, E. (2012). The *Arabidopsis* information resource (TAIR): improved gene annotation and new tools. *Nucleic Acids Res.* 40, D1202–D1210.

Lang, D., Eisinger, J., Reski, R., and Rensing, S. (2005). Representation and high-quality annotation of the *Physcomitrella patens* transcriptome demonstrates a high proportion of proteins involved in metabolism among mosses. *Plant Biol.* 7, 238–250.

Lassmann, T., and Sonnhammer, E. L. (2006). Kalign, Kalignvu and Mumsa: web servers for multiple sequence alignment. *Nucleic Acids Res.* 34, W596–W599.

Lawrence, C. E., Altschul, S. F., Boguski, M. S., Liu, J. S., Neuwald, A. F., and Wootton, J. C. (1993). Detecting subtle sequence signals: a Gibbs sampling strategy for multiple alignment. *Science* 262, 208–214.

Lovell, S. C., and Robertson, D. L. (2010). An integrated view of molecular co-evolution in protein-protein interactions. *Mol. Biol. Evol.* 27, 2567–2575.

McGinnis, S., and Madden, T. L. (2004). BLAST: at the core of a powerful and diverse set of sequence analysis tools. *Nucleic Acids Res.* 32, W20–W25.

Munson, M., and Novick, P. (2006). The exocyst defrocked, a framework of rods revealed. *Nat. Struct. Mol. Biol.* 13, 577–581.

Pečenková, T., Hála, M., Kulich, I., Kocourková, D., Drdová, E., Fendrych, M., Toupalová, H., and Žárský, V. (2011). The role for the exocyst complex subunits Exo70B2 and Exo70H1 in the plant-pathogen interaction. *J. Exp. Bot.* 62, 2107–2116.

Potato Genome Sequencing Consortium. (2011). Genome sequence and analysis of the tuber crop potato. *Nature* 475, 189–195.

Samuel, M. A., Chong, Y. T., Haasen, K. E., Aldea-Brydges, M. G., Stone, S. L., and Goring, D. R. (2009). Cellular pathways regulating responses to compatible and self-incompatible pollen in *Brassica* and *Arabidopsis* stigmas intersect at Exo70A1, a putative component of the exocyst complex. *Plant Cell* 21, 2655–2671.

Schuler, G. D., Altschul, S. F., and Lipman, D. J. (1991). A workbench for multiple alignment construction analysis. *Proteins* 9, 180–190.

Seguí-Simmaro, J. M., Austin, J. R., White, E. A., and Staehelin, L. A. (2004). Electron tomographic analysis of somatic cell plate formation in meristematic cells of *Arabidopsis* preserved by high-pressure freezing. *Plant Cell* 16, 836–856.

Sklarczyk, D., Franceschini, A., Kuhn, M., Simonovic, M., Roth, A., Minguez, P., Doerks, T., Stark, M., Muller, J., Bork, P., Jensen, L. J., and von Mering, C. (2011). The STRING database in 2011: functional interaction networks of proteins, globally integrated and scored. *Nucleic Acids Res.* 39, D561–D568.

Soltis, D. E., Bell, C. D., Kim, S., and Soltis, P. S. (2008). Origin and early evolution of angiosperms. *Ann. N. Y. Acad. Sci.* 1133, 3–25.

Songer, J. A., and Munson, M. (2009). Sec6p anchors the assembled exocyst aomplex at sites of secretion. *Mol. Biol. Cell* 20, 973–982.

Stern, A., Doron-Faigenboim, A., Erez, E., Martz, E., Bacharach, E., and Pupko, T. (2007). Selecton 2007: advanced models for detecting positive and purifying selection using a Bayesian inference approach. *Nucleic Acids Res.* 35, W506–W511.

Synek, L., Schlager, N., Eliáš, M., Quentin, M., Hauser, M. T., and Žárský, V. (2006). AtEXO70A1, a member of a family of putative exocyst subunits specifically expanded in land plants, is important for polar growth and plant development. *Plant J.* 48, 54–72.

Tamura, K., Peterson, D., Peterson, N., Stecher, G., Nei, M., and Kumar, S. (2011). MEGA5: molecular evolutionary genetics analysis using maximum likelihood, evolutionary distance, and maximum parsimony methods. *Mol. Biol. Evol.* 28, 2731–2739.

TerBush, D. R., Maurice, T., Roth, D., and Novick, P. (1996). The exocyst is a multiprotein complex required for exocytosis in *Saccharomyces cerevisiae*. *EMBO J.* 15, 6483–6494.

The Uniprot Consortium. (2012). Reorganizing the protein space at the Universal Protein Resource (UniProt). *Nucleic Acids Res.* 40, D71–D75.

Thompson, J. D., Gibson, T. J., Plewniak, F., Jeanmougin, F., and Higgins, D. G. (1997). The ClustalX windows interface: flexible strategies for multiple sequence alignment aided by quality analysis tools. *Nucleic Acids Res.* 24, 4876–4882.

Van de Peer, Y., Maere, S., and Meyer, A. (2009). The evolutionary significance of ancient genome duplications. *Nat. Rev. Genet.* 10, 725–732.

Wang, J., Ding, Y., Wang, J., Hillmer, S., Miao, Y., Lo, S. W., Wang, X., Robinson, D. G., and Jiang, L. (2010). EXPO, an exocyst-positive organelle distinct from multivesicular endosomes and autophagosomes, mediates cytosol to cell wall exocytosis in *Arabidopsis* and tobacco cells. *Plant Cell* 22, 4009–4030.

Wen, T. J., Hochholdinger, F., Sauer, M., Bruce, W., and Schnable, P. S. (2005). The roothairless1 gene of maize encodes a homolog of sec3, which is involved in polar exocytosis. *Plant Physiol.* 138, 1637–1643.

Whyte, J. R., and Munro, S. (2002). Vesicle tethering complexes in membrane traffic. *J. Cell Sci.* 115, 2627–2657.

Woodhouse, M. R., Tang, H., and Freeling, M. (2011). Different gene families in *Arabidopsis thaliana* transposed in different epochs and at different frequencies throughout the rosids. *Plant Cell* 23, 4241–4253.

Žárský, V., Cvrčková, F., Potocký, M., and Hála, M. (2009). Exocytosis and cell polarity in plants – exocyst and recycling domains. *New Phytol.* 183, 255–272.

Žárský, V., and Potocký, M. (2010). Recycling domains in plant cell

morphogenesis: small GTPase effectors, plasma membrane signalling and the exocyst. *Biochem. Soc. Trans.* 38, 723–728.

Zhang, X., Zajac, A., Zhang, J., Wang, P., Li, M., Murray, J., TerBush, D. R., and Guo, W. (2005). The critical role of Exo84p in the organization and polarized localization of the exocyst complex. *J. Biol. Chem.* 280, 20356–20364.

Zhang, Y., Liu, C. M., Emons, A. M. C., and Ketelaar, T. (2010). The plant exocyst. *J. Integr. Plant Biol.* 52, 138–146.

Conflict of Interest Statement: The authors declare that the research was conducted in the absence of any commercial or financial relationships that could be construed as a potential conflict of interest.

Received: 13 June 2012; paper pending published: 25 June 2012; accepted: 29 June 2012; published online: 18 July 2012.
*Citation: Cvrčková F, Grunt M, Bezvoda R, Hála M, Kulich I, Rawat A and Žárský V (2012) Evolution of the land plant exocyst complexes. Front. Plant Sci. **3**:159. doi: 10.3389/fpls.2012.00159*
This article was submitted to Frontiers in Plant Traffic and Transport, a specialty of Frontiers in Plant Science.

Paper 2:

New Phytologist

Research

The *Physcomitrella patens* exocyst subunit EXO70.3d has distinct roles in growth and development, and is essential for completion of the moss life cycle

Anamika Rawat[1,2], Lucie Brejšková[1,2], Michal Hála[1,2], Fatima Cvrčková[1] and Viktor Žárský[1,2]

[1]Laboratory of Cell Morphogenesis, Department of Experimental Plant Biology, Faculty of Science, Charles University, Viničná 5, 128 44, Prague 2, Czech Republic; [2]Institute of Experimental Botany, Academy of Sciences of the Czech Republic, 165 02, Prague 6, Czech Republic

Author for correspondence:
Viktor Žárský
Tel: +420 221951683
Email: zarsky@ueb.cas.cz

Received: *3 February 2017*
Accepted: *24 February 2017*

New Phytologist (2017)
doi: 10.1111/nph.14548

Key words: auxin, cytokinesis, egg cell development, EXO70, exocyst, phylogeny, *Physcomitrella patens*, secretory pathway.

Summary

• The exocyst, an evolutionarily conserved secretory vesicle-tethering complex, spatially controls exocytosis and membrane turnover in fungi, metazoans and plants. The exocyst subunit EXO70 exists in multiple paralogs in land plants, forming three conserved clades with assumed distinct roles. Here we report functional analysis of the first moss exocyst subunit to be studied, *Physcomitrella patens PpEXO70.3d* (Pp1s97_91V6), from the, as yet, poorly characterized EXO70.3 clade.

• Following phylogenetic analysis to confirm the presence of three ancestral land plant EXO70 clades outside angiosperms, we prepared and phenotypically characterized loss-of-function *Ppexo70.3d* mutants and localized PpEXO70.3d *in vivo* using green fluorescent protein-tagged protein expression.

• Disruption of *PpEXO70.3d* caused pleiotropic cell elongation and differentiation defects in protonemata, altered response towards exogenous auxin, increased endogenous IAA concentrations, along with defects in bud and gametophore development. During mid-archegonia development, an abnormal egg cell is formed and subsequently collapses, resulting in mutant sterility. Mutants exhibited altered cell wall and cuticle deposition, as well as compromised cytokinesis, consistent with the protein localization to the cell plate.

• Despite some functional redundancy allowing survival of moss lacking *PpEXO70.3d*, this subunit has an essential role in the moss life cycle, indicating sub-functionalization within the moss EXO70 family.

Introduction

Spatially and temporally regulated exocytosis, controlled by synchronized action of many factors including small GTPases of the RAB and RHO clades, SNARE complexes, signaling lipids and the vesicle-tethering complex exocyst (Koumandou *et al.*, 2007; see Žárský *et al.*, 2009), is central to multiple aspects of land plant life.

Cell wall biogenesis depends on precisely controlled delivery of secretory vesicles, carrying membrane-localized and exocellular proteins engaged in wall biosynthesis and organization, as well as materials to be incorporated into the cell wall such as pectins and hemicelluloses.

Spatially regulated exocytosis is also essential for deposition of hydrophobic cuticle on air-facing surfaces to avoid water loss, a characteristic adaptation of land plant epidermal cell walls, present already in mosses such as *Physcomitrella patens* and *Funaria hygrometrica* (Budke *et al.*, 2011, 2013; Buda *et al.*, 2013), proving that land plants acquired this feature very early in their evolution (Lang *et al.*, 2008).

Polar auxin transport (PAT), regulated by membrane-localized proteins such as the PIN family efflux carriers, is an important mechanism controlling plant morphogenesis that also depends upon the targeted exocytosis (see Luschnig & Vert, 2014). Auxin-based regulation of developmental processes (Fujita & Hasebe, 2009; Eklund *et al.*, 2010; Jang & Dolan, 2011; Viaene *et al.*, 2014; Mittag *et al.*, 2015), as well as PIN-mediated auxin transport, is conserved also in mosses (Bennett *et al.*, 2014), although in *P. patens* it differs from seed plants by being possibly both uni- as well as bi-directional depending on the developmental context (Viaene *et al.*, 2014; Coudert *et al.*, 2015).

All the above-mentioned processes share the participation of exocyst, an evolutionarily conserved hetero-octameric protein complex comprising SEC3, SEC5, SEC6, SEC8, SEC10, SEC15, EXO70 and EXO84 subunits (see Heider & Munson, 2012; Wu & Guo, 2015), acting upstream of the SNARE complex to aid fusion of vesicles to the target membrane (see Bröcker *et al.*, 2010). In yeast and metazoan cells, exocyst is well known to be localized at the sites of active secretion. All exocyst subunits have been found in every plant species studied to date, including

P. patens; surprisingly, most plant exocyst subunits are encoded by more than one paralogous gene. An extreme is EXO70, with up to dozens of paralogs in angiosperms (Cvrčková *et al.*, 2001, 2012; Eliáš *et al.*, 2003; Synek *et al.*, 2006). An initial diversification of EXO70 isoforms occurred very early in plant evolution; the three EXO70 clades known from angiosperms may perhaps be traced back to the origin of land plants (Eliáš *et al.*, 2003; Cvrčková *et al.*, 2012). The importance of angiosperm exocyst in secretion, cell division, polar cell growth and development, as well as involvement of EXO70 isoforms in functional diversification of the host of existing or hypothetical exocyst complex variants, is well established (Hála *et al.*, 2008; Fendrych *et al.*, 2010; see Žárský *et al.*, 2013; Kulich *et al.*, 2015). At least one of the EXO70 isoforms, EXO70A1, is involved in PIN recycling and auxin transport in Arabidopsis (Drdová *et al.*, 2013).

Here we examine the function of *PpEXO70.3d* (Pp1s97_91V6), one of the 13 EXO70 paralogs from the moss *P. patens*, representing the evolutionarily well-conserved but experimentally poorly characterized EXO70.3 clade. We show that the knock-out mutant of *PpEXO70.3d* displays pleiotropic defects and that this exocyst subunit is necessary for female gametogenesis and therefore for completion of the *P. patens* life cycle. Despite the presence of multiple *EXO70* genes, *PpEXO70.3d* is thus crucial for *P. patens* development and morphogenesis.

Materials and Methods

Phylogenetic analyses

A subset of the previously published collection of plant EXO70 sequences (Cvrčková *et al.*, 2012) containing all annotated paralogs from *P. patens* and *Selaginella moellendorffii* and representatives of all previously characterized angiosperm clades from *Arabidopsis thaliana* and *Oryza sativa* var. *japonica* has been used as a 'seed' dataset for identifying EXO70 sequences from additional species by BLAST searches as described by Cvrčková *et al.* (2012). GenBank and additional species-specific resources were searched, namely PHYTOZOME (Goodstein *et al.*, 2012) for *Sphagnum fallax*, http://marchantia.info for *Marchantia polymorpha*, and CONGENIE (Nystedt *et al.*, 2013) for *Picea abies* and *Pinus taeda*. If needed, predicted protein sequences were revised, taking into account homologous sequences and alternative splicing predictions (Grunt *et al.*, 2008). The complete list of sequences, together with revised protein sequence predictions, are provided in Supporting Information Table S1. Multiple alignments were performed using KALIGN (Lassmann *et al.*, 2009) with manual optimization in BIOEDIT (Hall, 1999). After removal of all gap-containing positions, phylogenetic trees were calculated using the maximum-likelihood method and evaluated by bootstrapping with 500 replicates in MEGA (Tamura *et al.*, 2013). Root position was inferred from a tree from a *de novo* alignment of a subset of plant sequences representing all major clades with inclusion of human Exo70 (identified by a keyword search of GenBank) as an outgroup (see Fig. S1).

Plant material and growth conditions

The 'Gransden' strain of *Physcomitrella patens* (Hedw.) Bruch & Schimp. was used as a wild-type (WT) in this study. Unless stated otherwise, 1-wk-old tissues were homogenized and grown on BCD agar medium containing 1 mM $CaCl_2$ and 5 mM ammonium tartrate (BCDAT) overlaid with cellophane (Cove *et al.*, 2009), at 25°C with 16 h : 8 h, light : dark regime, with or without additives as indicated. For imaging, 7-d-old protonemal colonies (*c.* 2 mm in diameter) were grown on BCDAT and photographed at the indicated time points.

Construction and molecular characterization of knock-out mutants

The knock-out construct was generated by cloning a 930 bp *Bam*HI–*Xho*I 5′ fragment, encompassing a part of the 1st exon and 5′ untranslated region (UTR) (primers PpExo70.3d 5F and PpExo70.3d 5R; Table S2), and a 920 bp *Spe*I–*Hpa*I 3′ fragment, including part of the last exon with 3′UTR (primers PpExo70.3d 3F and PpExo70.3d 3R; Table S2), amplified by PCR using Phusion polymerase (New England Biolabs, Ipswich, MA, USA) and total genomic DNA as a template, into the plasmid pMCS5-LOX-NptIIr-LOX (kindly provided by Fabien Nogué, INRA, Versailles, France). The *nptII* selection cassette flanked by targeting fragments was then PCR amplified from purified plasmid DNA using PpExo70.3d 5F and PpExo70.3d 3R primers (Table S2). The product was purified using a PCR purification Kit (Qiagen) and introduced into WT protoplasts by polyethylene glycol-mediated transformation (Kamisugi *et al.*, 2005). Transformants were selected on BCDAT supplemented with 30 mg l^{-1} G418. Stable lines were analysed by PCR using primer set P1 + P3 and P2 + P4 (Fig. S2a; Table S2).

Construction of green fluorescent protein (GFP) fusion construct

Full-length *PpEXO70.3d* was amplified from WT cDNA using Phusion polymerase and primers pENTR_EXO70.3d_F and pENTR_EXO70.3d_R (Table S2), cloned into *Sal*I–*Not*I sites of pENTR3C and introduced by Gateway recombination in pUBN-GFP-Dest, thus creating the *Ubi:GFP:PpEXO70.3d* expression construct. For stable expression, the *GFP:PpEXO70.3d* fragment was amplified from *Ubi:GFP:PpEXO70.3d* using Phusion polymerase and primers GFP_pUBN_FW and pENTR_EXO70.3d_R (Table S2), re-cloned in pENTR3C and transferred into the destination vector pTHUBi-GATE (Vidali *et al.*, 2007). The resulting *pTHUbi:GFP:PpEXO70.3d* construct was biolistically transformed into WT moss protonemata and stable lines were selected on 25 mg l^{-1} hygromycin.

Reverse transcription PCR (RT-PCR)

Total RNA was isolated from 100 mg of 7-d-old protonemata using an RNeasy Plant Mini kit (Qiagen). cDNA was prepared using a Transcriptor High Fidelity cDNA Synthesis Kit (Roche).

Semi-quantitative PCR was performed with equivalent amounts of cDNA template using DreamTaq polymerase (Thermo Scientific) and primers P7 + P8 (Table S2) for amplification of *PpEXO70.3d* and Pptub_FW+Pptub_RV (Table S2) for tubulin, as a housekeeping gene control.

Southern blot analysis

Genomic DNA was extracted from 7-d-old protonemata using Plant DNAzol (Invitrogen) and 5 μg DNA was digested overnight with *Bgl*II (ThermoFisher Scientific), run on the 0.7% agarose gel and transferred onto a positively charged nylon membrane (Amersham Pharmacia Biotech). The DNA was crosslinked in UV crosslinker (UV Stratalinker) and hybridized with digoxigenin (DIG)-labeled *nptII* probe, synthesized from plasmid PMCS5-LOX-NptIIr-LOX using PCR DIG Probe Synthesis Kit (Roche) following the manual for the kit. The membrane was blocked, incubated with 1 : 10 000 diluted anti-digoxigenin-AP antibody (DIG Luminescent Detection Kit, Roche), CDP-Star (Roche) was then added and detection was carried out using an Amersham ECL Prime Western Blotting detection kit.

Phenotypic analysis

Protonemata and gametophores were photographed using a Canon Powershot S70 attached to a Leica S6D stereomicroscope. To measure individual filament growth rates, edges of protonemal colonies were photographed every 5 min using a Leica DFC310 FX camera mounted on a Leica M165 FC stereomicroscope. For colony growth rate measurements, photographs were taken at 5 d intervals over 30 d. Close-ups of filaments and individual phyllids were imaged under an Olympus BX-51 microscope equipped with an Olympus DP50 camera. All image analyses were performed using ImageJ (Abràmoff *et al.*, 2004). To study the effect of low temperature, 7-d-old protonemata were inoculated on BCDAT overlaid with cellophane, grown for a further 5 d under standard conditions, covered with aluminum foil and placed at 8°C for 3 wk. For imaging, a droplet of water was pipetted on the filaments to lay them flat on media. The plates were then transferred to normal growth conditions for 1 wk and photographed using a Nikon DS-5M digital camera attached to a Nikon SMZ 1500 stereomicroscope.

For protoplast regeneration, protoplasts from 7-d-old tissues were isolated in 0.7% driselase solution for 45 min to 1 h and washed twice with 8% mannitol. Suspension density was adjusted to 3.2×10^6 ml^{-1} before mixing with top medium (BCDAT, 6% mannitol, 1 M $CaCl_2$ and 0.4% agar) and plating on medium overlaid with cellophane (BCDAT, 6% mannitol, 1 M $CaCl_2$ and 0.6% agar). Growing protoplasts were photographed using a Nikon DS-5M digital camera attached to a Nikon SMZ 1500 stereomicroscope.

Developing buds from 10-d-old tissues were removed and stained with 10 μg ml^{-1} propidium iodide for 10 min, washed once with sterile liquid BCDAT and observed under a Zeiss LSM5 DUO confocal laser microscope with 514/590 nm wavelength for excitation/emission. The images are presented as Z-stack projections.

Cell plates were observed under a spinning disc confocal microscope (Yokogawa CSU-X1 on a Nikon Ti-E platform, laser box Agilent MLC400, sCMOS camera Andor Zyla) after staining protonemata with 5 μM FM4-64 for 10 min in chambered cover glass slides.

For gravitropism assays, 7-d-old protonemata were transferred to fresh media supplemented with 2% sucrose. After 5 d the plates were covered with aluminum foil and placed vertically at 25 or 8°C for 3 wk.

For sporophyte induction, gametophores were first induced from fresh protonemata on sterile Jiffy pellets (www.jiffypot.com) in magenta boxes at 25°C and long day (16 h : 8 h, light : dark) regime. After 4 wk, the boxes were filled with sterile water leaving 1 cm from the top of gametophores and transferred to 15°C, short day conditions.

Chl measurement

Total Chl content was determined as described previously (Frank *et al.*, 2005). Briefly, *c.* 200 mg of 7-d-old tissue homogenized in liquid nitrogen was extracted with 80% acetone, centrifuged and absorbance of the supernatant was measured at 645 and 663 nm. The whole volume was then dried to determine the dry matter weight (DW). Total Chl was calculated as: mg Chl (g DW^{-1}) = $[(A_{663})\ (0.00802) + (A_{645})\ (0.0202)] \times$ ml acetone DW^{-1}.

Electron microscopy

For scanning electron microscopy (SEM), samples were fixed in 2.5% (v/v) glutaraldehyde in 0.1 M phosphate buffer at 4°C, post-fixed in 2% (w/v) OsO_4 in the same buffer, dehydrated in ascending ethanol and acetone series, mounted in holders, coated with gold and examined under a JEOL JSM-6380 LV scanning electron microscope. For transmission electron microscopy (TEM), samples were prepared similarly except of using 0.1 M cacodylate buffer (pH 7.2) and embedding in Epon-Araldite. Ultra-thin sections were stained with uranyl acetate and lead citrate and examined using a Morgagni 268D microscope (FEI, Hillsboro, OR, USA).

Auxin sensitivity assay

Seven-day-old moss protonemata were plated on solid media containing 1, 5 or 10 μM NAA (1-naphthaleneacetic acid; Sigma-Aldrich), 5, 10 or 50 μM NPA (*N*-1-naphthylphthalamic acid; Sigma-Aldrich) or their combinations, and incubated for 1 month. The experiment was repeated three times, with three plates containing five individual colonies of each line, for each concentration.

Determination of endogenous auxin

Endogenous auxin was determined by LC/MS as described previously (Dobrev & Kamínek, 2002). Briefly, *c.* 100 mg of 7-d-old

protonemata were homogenized in liquid nitrogen. Cold extraction buffer (methanol : water : formic acid, 15 : 10 : 5, v/v/v, −20°C; 500 µl) along with the internal standards (10 pmol) was added, incubated for 30 min at −20°C and centrifuged at 16 215 *g* to collect the supernatants. Extraction was repeated and supernatants were pooled and evaporated under a speed-vac (Alpha RVC, Christ). Samples were dissolved in 0.1 M formic acid and applied to SPE columns (Oasis-MCX, Waters, Milford, MA, USA). The acidic hormone fraction from the columns was eluted with 100% methanol, dried in the speed-vac at 40°C, dissolved in 30 µl 15% acetonitrile and analyzed by high-performance liquid chromatography (Ultimate 3000, Dionex, Bannockburn, IL, USA) coupled to a 3200 Q TRAP hybrid triple quadrupole/linear ion trap mass spectrometer (MS; Applied Biosystems, Foster City, CA, USA).

Results

PpEXO70.3d represents an ancient clade of plant EXO70s

Previous phylogenetic analysis of plant EXO70 sequences with limited sequence and species coverage has identified PpEXO70.3d as one of the four *P. patens* members of the EXO70.3 clade, one of three ancestral land plant EXO70 clades (Synek *et al.*, 2006) that also contains angiosperm EXO70G and EXO70I (Cvrčková *et al.*, 2012). Using newly available sequence resources, namely the transcriptome of the moss *Sphagnum fallax* from the Phytozome database (Goodstein *et al.*, 2012), the pre-release of the liverwort *Marchantia polymorpha* genome sequence available at its author's website and the draft genome sequence of the charophyte *Klebsormidium flaccidum* (Hori *et al.*, 2014), as well as an incomplete collection of conifer protein sequences collected from several databases, we re-examined the relationships among angiosperm EXO70 paralogs and their gymnosperm, basal land plant and charophyte relatives.

The resulting phylogenetic tree (Fig. 1) confirms our original hypothesis that three major EXO70 clades (EXO70.1, EXO70.2 and EXO70.3) existed already in early land plants (Synek *et al.*, 2006), although EXO70.3 appears to have been lost in *S. moellendorffii* (Cvrčková *et al.*, 2012). However, only a single EXO70 homolog, belonging to the possibly ancestral EXO70.1 clade, was found in *K. flaccidum*. The root of the phylogenetic tree separates EXO70.3 from the rest of the family, suggesting that initial gene duplication of the *EXO70.1/EXO70.2*-like gene gave rise to an ancestor of the EXO70.3 clade, followed by the second duplication that separated the EXO70.1 and EXO70.2 clades.

The *PpEXO70.3d* gene experimentally characterized here therefore represents an ancient, and hitherto largely uncharacterized, branch of the land plant *EXO70* gene family.

Ppexo70.3d knock-out mutants show pleiotropic developmental deviations

Using homologous recombination, we generated two independent knock-out mutant lines in *PpEXO70.3d*. The presence of the gene-targeting construct within the *EXO70.3d* locus and absence of transcript was verified for both lines (Fig. S2). During initial phenotypic characterization both lines behaved similarly under all conditions tested (representative data from only one line are shown for some experiments); line *Ppexo70.3d#6* was chosen for subsequent in-depth characterization.

Both *Ppexo70.3d* lines exhibited reduced growth of protonema and gametophores (Figs 2a–e, S3). One-month-old mutant colonies were much smaller and more compact than WT, with several densely packed small gametophores (Figs 2a, S3a). Mutant colonies were also greener than WT in appearance, although measurements surprisingly revealed decreased total Chl content (Table S3), suggesting altered tissue optical properties or Chl extractability, possibly due to changed cell wall composition.

Rapidly growing caulonemata developed at the edge of WT colonies by day 10 after inoculation (Figs 2b, S3b, arrow), whereas in mutants only chloronemata protruded from the edge of compact growth (Figs 2b, S3b, arrowhead). Differentiation of caulonemata in *Ppexo70.3d* is thus suppressed or substantially impaired under standard growth conditions.

Mutant protonemata were more branched than WT protonemata, which usually develop a side branch from the 3rd subapical cell (Wu *et al.*, 2011). The branch initials in 14-d-old mutant protonemata developed mostly from the 2nd subapical cell, and rarely from the 1st or 3rd subapical cell, while in WT it was mostly from the 3rd subapical cell, and sometimes from 2nd subapical cells (Fig. 2c; Table 1).

While older (14 d) WT produced distinct chloronemal and caulonemal filaments, mutants only produced short chloronemata. Upon closer inspection short and morphologically abnormal filaments, often containing caulonema-like oblique cell walls but with shorter and greener cells than normal caulonemata, were observed (Figs 2d, S3c). These filaments with transitional morphology are here termed 'caulonema-like'.

Mature gametophores in *Ppexo70.3d* are much smaller than WT gametophores, with shorter rhizoids and substantially reduced internode size (Figs 2e, S3d). However, the stunted mutant gametophores exhibited normal phyllotaxy and carried reproductive organs (see below). Since published transcriptome data (Beike *et al.*, 2015) document induction of another EXO70.3 paralog, *PpEXO70.3b* (Pp1s6_436V6) by prolonged cold stress, and since we fortuitously observed a partial suppression of the mutant phenotype during gravitropism tests (see below), we have also followed mutant growth at low temperature (8°C) in the dark, and found that the mutant phenotype was partially rescued under these conditions (Fig. 2f). Upon return to the normal growth conditions, all the induced caulonemata in WT differentiated into secondary chloronemata and caulonemata, while no further caulonemata were produced in mutant plants, and the previously induced caulonemata reverted to the mutant phenotype (Fig. 2f).

Unlike WT, mutant phyllids often had bifurcated tips and sometimes a short appendage or ectopic phyllid at the base (Fig. 2g,h). Such aberrations were found in at least one phyllid of each mutant gametophore. While the WT phyllid is formed by single cell layer with a central midrib, bifurcating mutant phyllids showed secondary midribs (Fig. 2i, arrows).

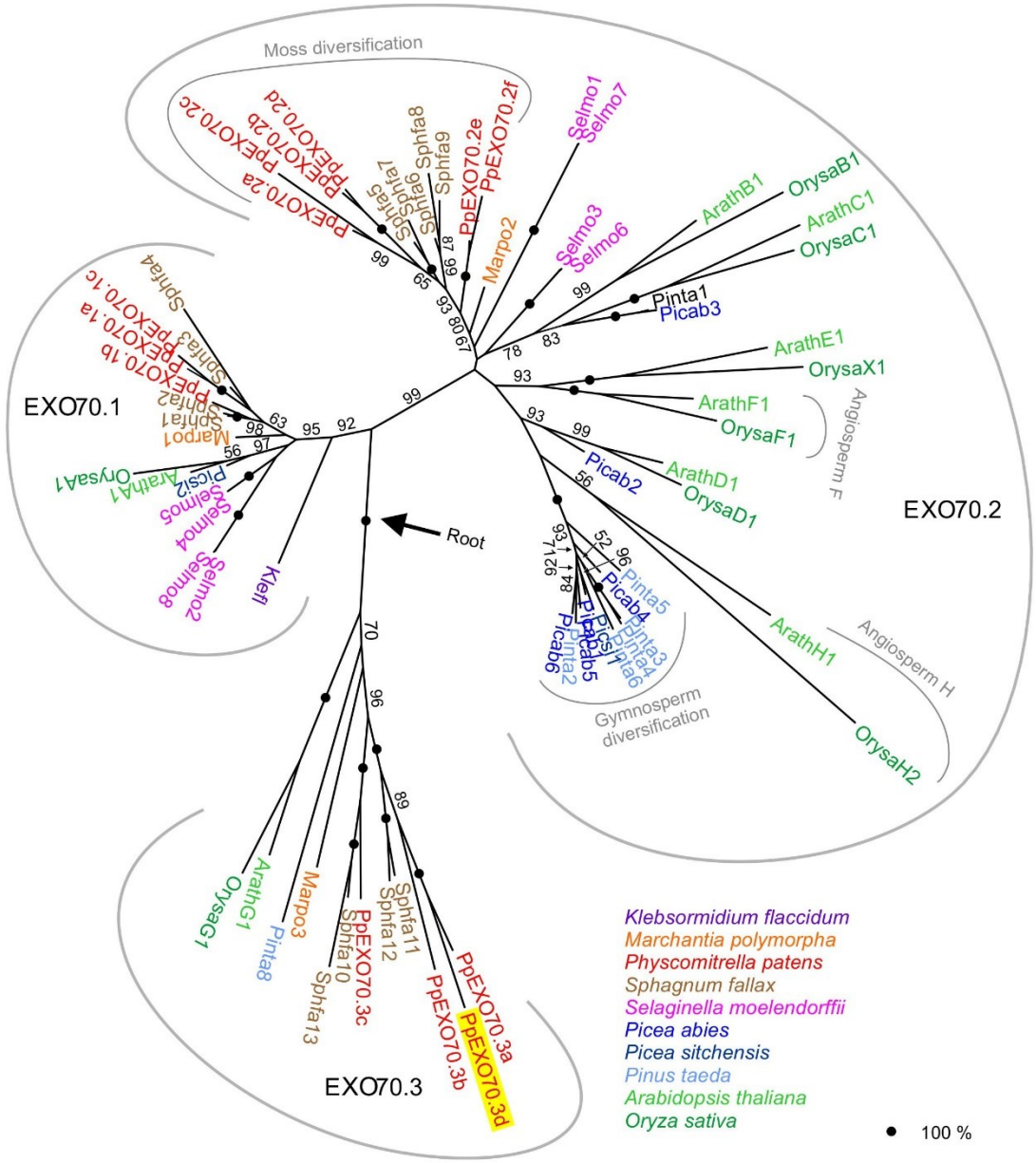

Fig. 1 A maximum-likelihood phylogenetic tree of plant EXO70 protein sequences, including *Physcomitrella patens*. The set of gymnosperm sequences is currently incomplete (some short additional fragments were recovered from genome or transcriptome data of *Picea abies* and *Pinus taeda*), and only one protein from each previously described angiosperm clade was included for Arabidopsis and rice. For a full list of sequences see Supporting Information Table S1. Numbers and symbols at branches represent percentage bootstrap support (from 500 samples). Bootstrap values below 50% are not shown.

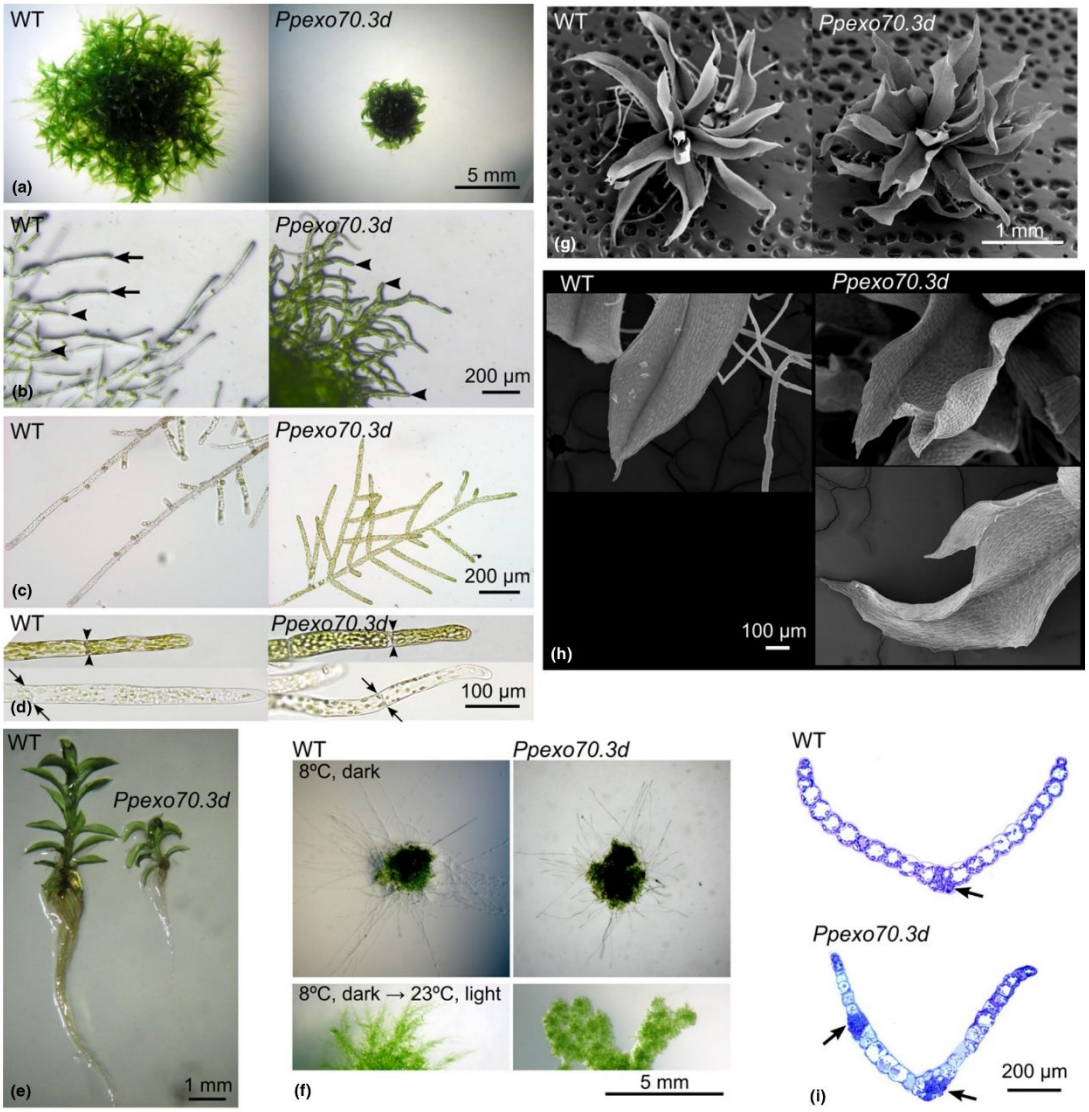

Fig. 2 *Ppexo70.3d* displays pleiotropic morphological deviations. (a) *Physcomitrella patens* wild-type (WT) and *Ppexo70.3d#6*, 1 month after inoculation. (b) Close-up of the edge of 10-d-old colony showing typical caulonema (arrow) and chloronema (arrowhead) growth in WT, while only filaments of chloronemal appearance (arrowhead) protrude beyond the colony edge in *Ppexo70.3d#6*. (c) Branching pattern of filaments originating from the edge of 14-d-old plants showing *Ppexo70.3d#6* forming more side branches than WT. (d) Types of filaments present in 14-d-old WT and *Ppexo70.3d#6* plants. Arrows show oblique cell walls typical for caulonemata, and arrowheads indicate transverse cell walls in chloronemata. (e) Comparison of 4-wk-old gametophores of WT and *Ppexo70.3d#6*. (f) WT and *Ppexo70.3d#6* after growth in the dark at 8°C for 3 wk and then 10 d of transfer to normal growth conditions. (g) Scanning electron micrographs showing structure of gametophores of WT and *Ppexo70.3d#6*. (h) Scanning electron micrographs of phyllid apices of WT and *Ppexo70.3d#6*. (i) Transverse sections of WT and *Ppexo70.3d#6* phyllids showing ectopic midrib formation in the mutant. Arrows indicate midribs.

Table 1 Pattern of side branch initiation on protonemal filaments of *Physcomitrella patens* wild-type (WT) and *Ppexo70.3d* mutants shows a significant shift from the 3rd to 2nd subapical cell in mutant

	1st subapical cell	2nd subapical cell	3rd subapical cell
WT	0	19%	81%
Ppexo70.3d#6	18%	59%	23%

$n = 115$, $P < 0.001$ (chi-square test).

PpEXO70.3d functions in egg cell differentiation and sporophyte formation

Although *Ppexo70.3d* did develop gametophores, initiation of reproductive organs (antheridia and archegonia) was delayed, and mutants never produced a sporophyte, while WT plants completed their life cycle under the inducing conditions. Antheridia of mutant plants were indistinguishable from WT, matured and were able to release spermatozoids (not shown). Also, archegonia were morphologically similar to those of the WT, developed in clusters and produced neck canal cells that degenerated to make openings for spermatozoids to swim into (Fig. 3a,b). However, abnormalities were observed in egg cell development. WT egg precursor cells undergo an asymmetric division producing a small apical cell that becomes degraded and a large basal egg cell that matures and after fertilization forms a sporophyte. Multicellular embryos are usually found at *c.* 4 wk after the induction of gametangia (Landberg *et al.*, 2013; Sakakibara *et al.*, 2014). While we observed various stages of this process in WT plants, we never saw expanded zygotes in *Ppexo70.3d* mutants (Fig. 3a–c). Instead, we often found a collapsed abnormal egg cell, leaving an empty archegonial cavity (Fig. 3b), and sporophytes never formed in the mutant (Fig. 3c). Thus, the mutant is sterile because of an egg cell differentiation defect.

PpEXO70.3d is required for the rapid elongation of chloronemata and for cell expansion by both tip growth and diffuse growth

One-month-old WT colonies were much larger than *Ppexo70.3d* mutant colonies (Fig. 4a). Time-lapse imaging revealed lower growth rates in the mutants (Fig. 4b). To test whether the reduced growth of *Ppexo70.3d* is due to the lack of rapidly growing true caulonemata, we measured the growth rate of individual filament types in 10-d-old protonemata. While WT caulonemal and chloronemal growth rates were in the range described in the literature (Schmiedel & Schnepf, 1980; Menand *et al.*, 2007), mutant chloronemata grew much more slowly (Table 2; Videos S1 and S2, respectively). Thus, the slow growth of *Ppexo70.3d* colonies is not only due to the defect in caulonemata differentiation but also due to slow chloronema growth. Slower growth of mutant chloronemata may be due to reduced cell expansion, cell division or both. We thus measured cell length and width in WT and mutant chloronemata. The length of apical and subapical chloronemal cells in *Ppexo70.3d* was significantly shorter than in WT (Fig. 4c), while cell width was not significantly affected (Fig. 4d), suggesting a tip growth defect. Reduced cell length without much difference in width was also observed in mutant phyllids, which consist of cells expanding in a diffuse manner (Fig. 4e,f). Despite the smaller size and slower growth, *Ppexo70.3d* does not possess fewer cells per unit area (Table S4), making a cell division defect unlikely.

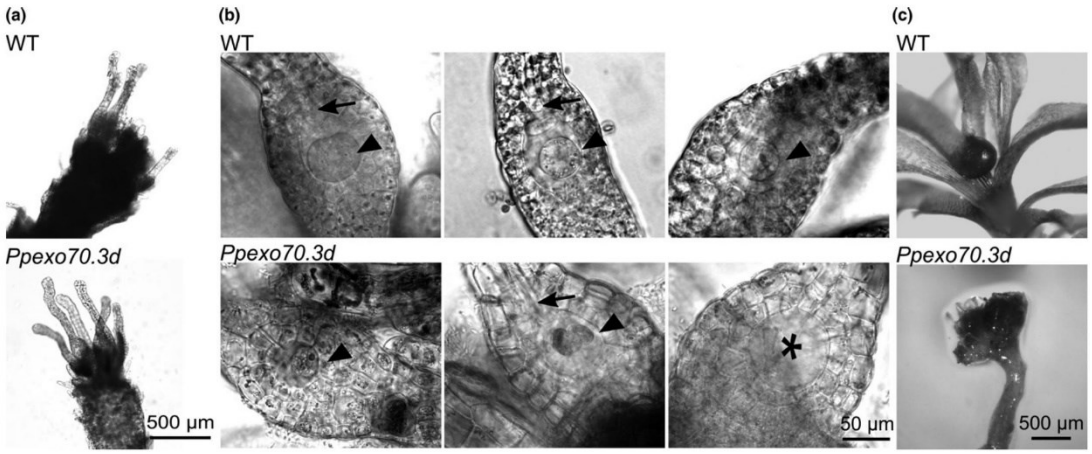

Fig. 3 Egg cell development and sporophyte formation defects of *Ppexo70.3d*. (a) Archegonia of 45-d-old *Physcomitrella patens* wild-type (WT) and *Ppexo70.3d#6* plants have a practically normal appearance. (b) Close-up of representative archegonia of WT and *Ppexo70.3d#6* plants showing normal egg cell development in the WT but degenerating or absent egg cells in the mutant. Arrowheads, egg cells; arrows, visible borders of the apical neck canal cells; asterisk, an empty archegonial cavity. Images were subjected to uniform contrast enhancement. (c) Sporophyte formation is defective in 45-d-old *Ppexo70.3d#6* plants compared to the control.

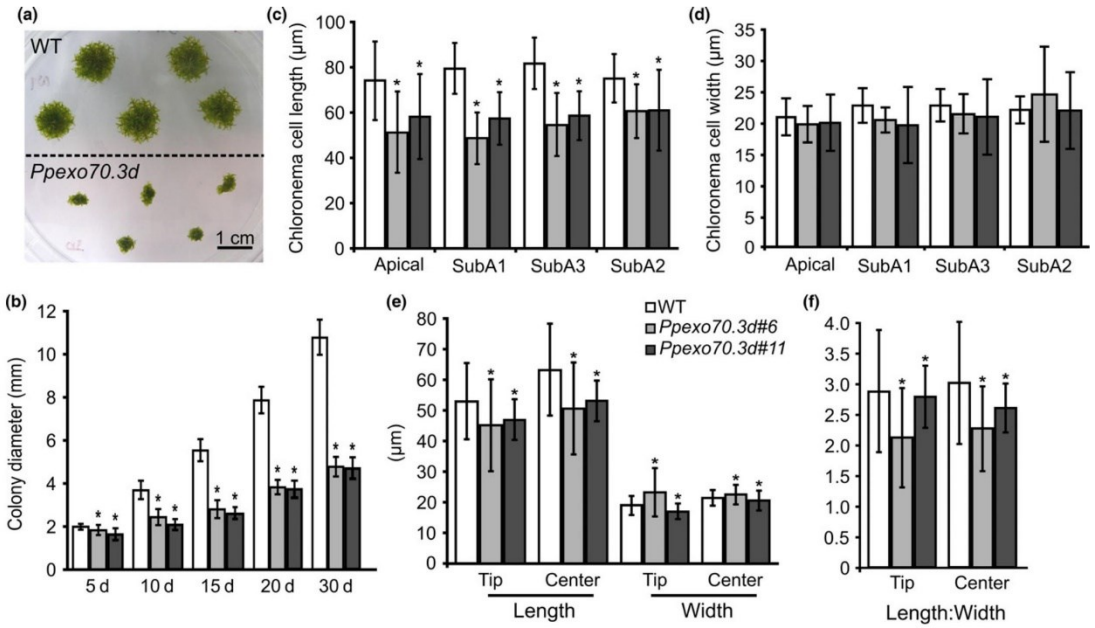

Fig. 4 PpEXO70.3d is required for rapid protonema growth and apical cell elongation in *Physcomitrella patens*. (a) Wild-type (WT) and *Ppexo70.3d#6* after 1 month on BCDAT media. (b) Quantification of growth of WT, *Ppexo70.3d#6* and *Ppexo70.3d#11*. (c, d) Histograms showing the mean ± SD values of length and width of apical cell and subapical cells 1, 2 and 3 (SubA1, SubA2, SubA3) in WT, *Ppexo70.3d#6* and *Ppexo70.3d#11* chloronemata. (e, f) Histograms showing the mean ± SD values of length, width and length : width ratio of cells near the tip and central region of phyllids in WT, *Ppexo70.3d#6* and *Ppexo70.3d#11*. Statistically significant difference from WT (one-way ANOVA): *, $P < 0.05$; $n = 10$ (b); $n \geq 25$ (c, d); $n \geq 50$ (e, f).

Table 2 The growth rate of individual chloronemata in *Physcomitrella patens* mutant *Ppexo70.3d* is reduced compared to the wild-type (WT)

	Caulonema	Chloronema
WT (µm h^{-1})	20.36 ± 5.06	6.45 ± 2.32
Ppexo70.3d#6 (µm h^{-1})	(–)	2.81 ± 1.52

Values are mean ± SD, $n \geq 15$, $P < 0.05$ for chloronema growth rate (*t*-test).

PpEXO70.3d is required for protoplast regeneration

Protoplasts of *P. patens* can re-establish the cell wall, divide and give rise to chloronemata. Typically, this process is non-synchronous, with polar expansion observable in some cells by day 2 and first asymmetric cell division by day 4 (Wang *et al.*, 2014). We observed establishment of polarity and asymmetric cell divisions in WT protoplasts on day 3 after isolation, and on day 4, most protoplasts initiated chloronema formation. Branching of chloronemata and formation of differentiated protonemal tissue usually took place by day 10. By contrast, *Ppexo70.3d* protoplasts showed significantly delayed filament outgrowth, with most of them dying by the 2nd day. Although some mutant protoplasts underwent first asymmetric division on day 3, they did not progress beyond this stage even after 10 d (Fig. 5a). While the majority of WT protoplasts that survived plating remained alive and many grew into filaments, mutant protoplasts exhibited overall low survival rates with progressive loss of viability during the course of observation (Fig. 5b).

Altered early development of *Ppexo70.3d* buds

Ppexo70.3d mutants can initiate buds on chloronemata and form gametophores (Fig. 6). The first cell division in both WT and mutant nascent buds was oblique, producing apical and basal cells as described previously (Harrison *et al.*, 2009). In the WT, the second and third division plane was then oriented perpendicularly to the first division. However, in mutant buds the later cell division planes were oriented aberrantly, and some buds formed a rhizoid-like filament from the basal cell (Fig. 6, arrows). In mutant buds with a normal 2nd division, the plane of subsequent apical cell division was often disoriented. However, regardless of these aberrations, most mutant buds later gave rise to stunted gametophores. Interestingly, a fraction of mutant buds terminated after second division of the basal cell (Fig. 6, arrowheads). In some cases bud initials even dedifferentiated back into filaments, indicating an unstable cell fate regulation (Fig. 6, asterisks).

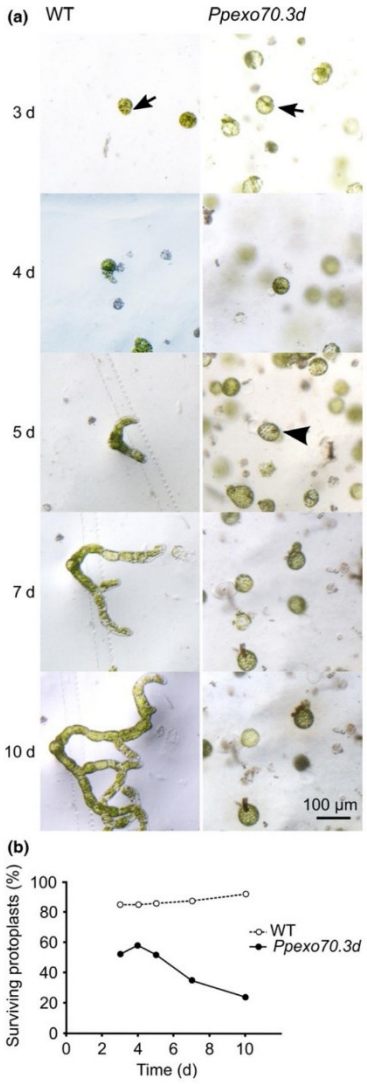

Fig. 5 PpEXO70.3d is required for protoplast regeneration in *Physcomitrella patens*. (a) Representative micrographs of regenerating protoplasts of wild-type (WT) and *Ppexo70.3d*#6 are shown at indicated time points (days after protoplast isolation). The same field is shown for WT from day 5 and for the mutant from day 7. Arrow, first asymmetric division; arrowhead, abnormal cell wall. (b) Data from representative experiments showing that fraction of surviving protoplasts remains almost constant for WT (with apparent slight increase possibly due to disintegration of some dead protoplasts) but rapidly decreases in *Ppexo70.3d*#6; $n \geq 75$. The difference between WT and the mutant is statistically significant for each time point (chi-square test with Bonferroni correction for multiplicity, $P < 0.001$).

PpEXO70.3d is not required for gravity perception

Caulonemata and gametophores, but not chloronemata, exhibit negative gravitropism in the dark (Cove *et al.*, 1978; Jenkins *et al.*, 1986). We exploited this feature to examine if the caulonema-like filaments of *Ppexo70.3d* can still respond to gravistimulation. After 3 wk under the inducing conditions, WT produced long, negatively gravitropic caulonemata. However, *Ppexo70.3d* formed very few extremely short negatively gravitropic filaments (Fig. 7a). Interestingly, at low temperature (see also above) the mutant phenotype was partially rescued and mutant colonies gave rise to many short but typical caulonemata. While WT exhibited reduced caulonema growth at low temperature, it nevertheless still produced more caulonemata than the partially rescued mutant (Fig. 7b).

Ppexo70.3d mutants show altered response towards exogenously applied auxin and increased auxin accumulation

Auxin induces chloronema to caulonema transition in *P. patens* and stimulates the production of caulonemata (Johri & Desai, 1973; Ashton *et al.*, 1979; Jang & Dolan, 2011). We thus examined if exogenous auxin can induce true caulonemata in *Ppexo70.3d*. As expected, treatment with varying concentrations of NAA resulted in enhanced caulonema development in WT compared to non-treated controls, while no such effect was observed in *Ppexo70.3d* (Figs 8a, S4). While 1 and 5 µM NAA stimulated growth of WT colonies compared to mock-treated colonies, at 10 µM NAA colony size started to decrease, suggesting that growth or caulonema production is inhibited at higher NAA concentrations. By contrast, NAA-treated *Ppexo70.3d* colonies were smaller than untreated colonies at all but the lowest tested concentrations, and growth stimulation never occurred. While treatment with the auxin transport inhibitor NPA very slightly but significantly reduced the diameter of mutant colonies at all concentrations tested, the WT was inhibited only at the highest NPA concentration (Fig. 8b, Table S5). Interestingly, NPA-treated WT produced only chloronemata, thus resembling the mutant phenotype (Figs 8a, S4). Combined treatment with both NAA and NPA inhibited growth at all concentrations tested in *Ppexo70.3d* while the WT was not significantly affected by lower concentrations (Figs 8b, S4; Table S5), indicating altered perception of, or response to, these compounds in the mutant. Analysis of endogenous IAA levels showed a substantial increase in the content of this auxin in *Ppexo70.3d* (Fig. 8c).

Bi-directional auxin transport is required for initiation and regulation of side branching in *P. patens* gametophores; increased concentrations of auxin inhibit branching (Coudert *et al.*, 2015). In our hands, the branching of WT gametophores took place along the gametophore axis, with an apical branch-free zone taking approximately the top third of the gametophore. However, in

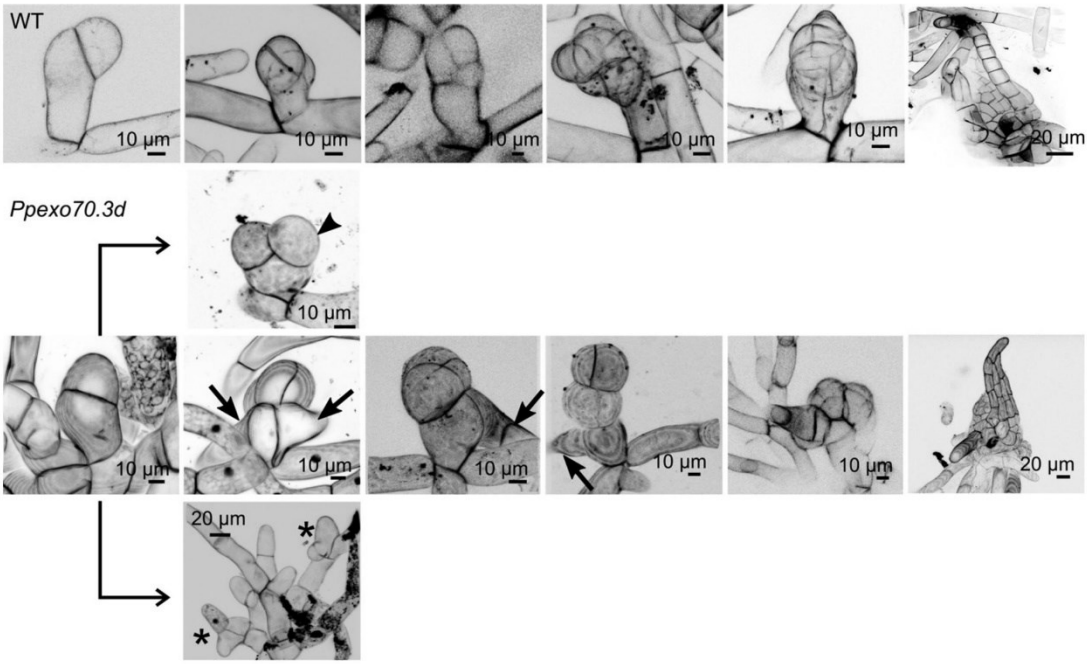

Fig. 6 PpEXO70.3d participates in bud and early gametophore development. Early stages of bud development in *Physcomitrella patens* wild-type (WT) and *Ppexo70.3d#6*. Some aberrations in mutant bud development include defective cell division pattern and early initiation of rhizoids from basal domain (arrows), terminating buds (arrowhead) or dedifferentiation into protonema (asterisk).

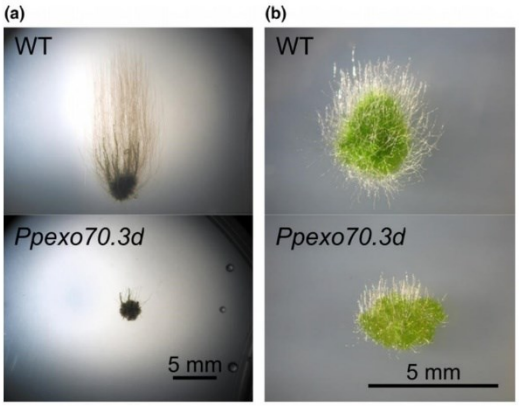

Fig. 7 Comparison of caulonemal growth in *Physcomitrella patens* wild-type (WT) and *Ppexo70.3d#6* after 3 wk in gravistimulating conditions. (a) WT and *Ppexo70.3d#6* grown at standard temperature. (b) WT and *Ppexo70.3d#6* grown at low temperature (8°C), showing partial rescue of the mutant phenotype. The contrast was uniformly enhanced to make the filaments protruding beyond the colony edge clearer.

mutants the branch-free zone extended usually at least to the top half of the gametophore, with some gametophores devoid of side branch initials (Fig. 8d).

PpEXO70.3d functions in moss cuticle deposition

Electron microscopy revealed that deposition of cuticle and epicuticular waxes is compromised in *Ppexo70.3d* mutants. While the epicuticular wax layer usually covers most of the surface of WT phyllid cells (some remnant at the edges of the cell were probably an artefact of sample preparation), in *Ppexo70.3d* this layer was very thin, and in most samples was almost removed from the entire cell surface (Fig. 9a). TEM observations of ultrathin phyllid sections showed that the cuticle layer in *Ppexo70.3d* was less electron dense and also the cell wall appeared to be more fibrous and less homogeneous than in the WT (Fig. 9b). These results show that PpEXO70.3d participates in cuticle deposition on the epidermal cell surface.

GFP:PpEXO70.3d localization suggests a role during cytokinesis

The observed defect of protoplast division alerted us to the possibility of a cytokinetic defect in *Ppexo70.3d*. Close observation of cell plate development by time-lapse microscopy of FM4-64-labeled cells revealed that while most WT and some *Ppexo70.3d* cells complete cytokinesis (from emergence of the cell plate until its insertion into the mother cell wall) within 20–25 min (Fig. 10a; Videos S3, S4), mutants sometimes exhibited delayed or incomplete cell wall formation. In these

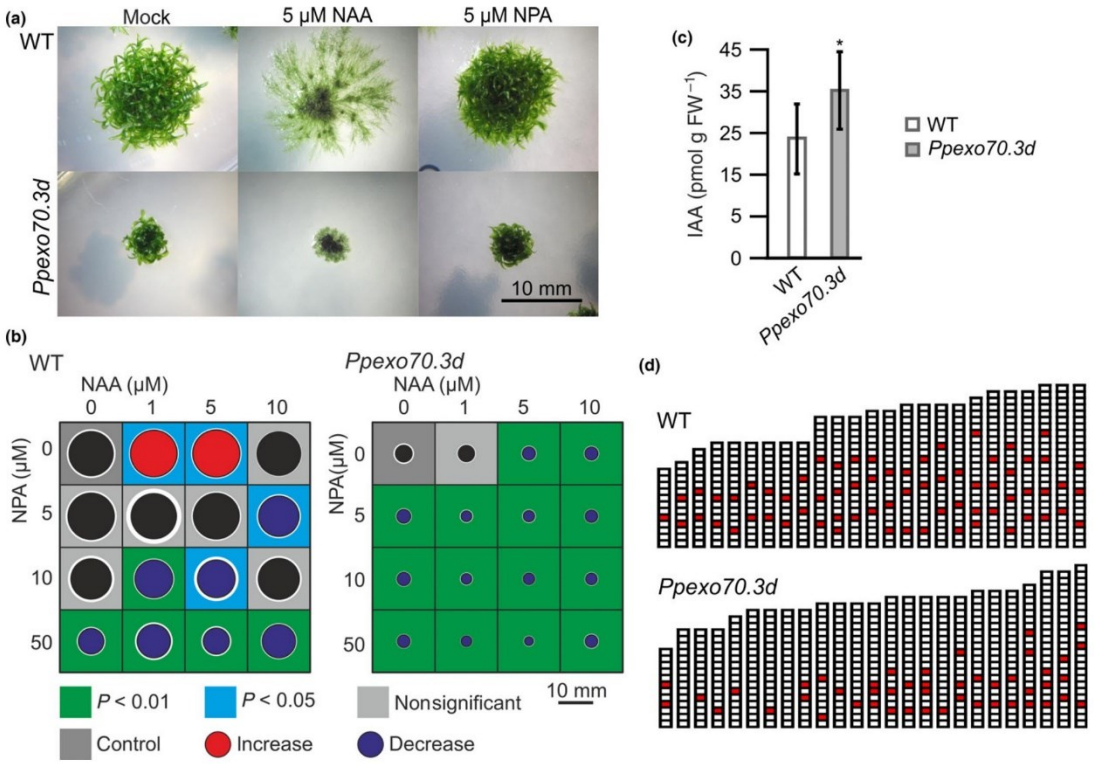

Fig. 8 Response of *Physcomitrella patens* wild-type (WT) and *PpEXO70.3d#6* towards exogenously applied auxin (NAA) and its inhibitor (NPA). (a) Qualitative effects of hormonal treatments on gametophyte development after 1 month on BCDAT media supplied with 5 μM NAA or NPA (see Supporting Information Fig. S4 for effects of a full concentration scale). (b) Effects of treatment with NAA, NPA or both on WT and *Ppexo70.3d#6* colony size after 1 month on BCDAT media supplied with the indicated hormone concentrations. Circle size corresponds to average colony size, and size of the white margin reflects the SD. Background colour reflects statistical significance of differences from untreated control of the same genotype as determined by multifactorial ANOVA with genotype, NAA concentration and NPA concentration treated as factors; circle colour represents the direction of the observed differences (for numerical values see Table S5). The difference between WT and *Ppexo70.3d* was significant ($P < 0.01$) for each treatment. Ten colonies were evaluated for each combination of parameters. (c) *Ppexo70.3d* shows increased concentrations of endogenous IAA as compared to WT. Error bars indicate ± SD. Statistically significant difference from WT by single factor ANOVA; *, $P < 0.05$, $n = 12$. (d) Positioning of gametophore side branches in WT and *Ppexo70.3d*. Each box represents an internode ending at phyllid, and red box indicates phyllid with side branch, $n = 25$.

cases cell plate formation took > 30 min after the nascent cell plate was first observed (which was not necessarily at the time it was formed), and some mutant cells did not finish division at all (Table 3; Fig. 10b,c; Videos S5, S6). By contrast, we never observed such deviations in the WT. Mutant cells with incomplete cell walls were capable of further growth and division (Fig. 10d).

To investigate the subcellular localization of PpEXO70.3d in protonemata, we prepared stable transgenic lines expressing N-terminally GFP-tagged PpEXO70.3d which grew indistinguishably from WT. At sub-cellular levels, the PpEXO70.3d signal was predominantly cytoplasmic with enrichment at the growing tip, and exhibited distinct re-localization during the cell cycle. After nuclear breakdown, the GFP signal formed a cloud in the spindle/phragmoplast area, and later focused to the nascent cell plate, where it intensified and persisted until completion of cytokinesis (Fig. 10e; Video S7). The signal maximum remained at the post-cytokinetic maturing cell wall for 20–30 min after its insertion and then slowly re-localized to the cytoplasm.

Discussion

We present the first experimental study of the exocyst complex in the moss *P. patens*, focusing on one of the 13 paralogs of the EXO70 subunit, *PpEXO70.3d*.

Previous phylogenetic analyses revealed three EXO70 clades, EXO70.1, EXO70.2 and EXO70.3, in *P. patens* and all angiosperms examined (Synek *et al.*, 2006). A subsequent study suggested loss of EXO70.3 in *S. moellendorffii* (Cvrčková *et al.*, 2012), but included very few non-angiosperm species, leaving some doubts regarding early EXO70 evolution. We thus re-examined the phylogeny of plant EXO70 paralogs, including

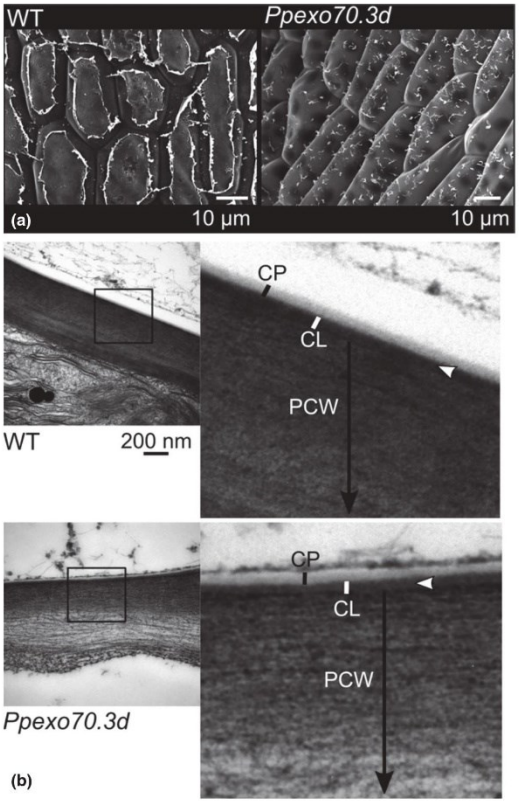

Fig. 9 Cuticle deposition is altered in *Ppexo70.3d*#6. (a) Scanning electron micrographs showing remnants of epicuticular waxes on phyllids of *Physcomitrella patens* wild-type (WT) and *Ppexo70.3d*. (b) Transmission electron micrographs of WT and *Ppexo70.3d* phyllid, showing ultrastructural details of cell wall and cuticle deposition (right side image is a scaled up square field of 500 × 500 nm highlighted in the left side one). Osmophilic layer, cuticle proper (CP); electron-lucent layer, cuticle (CL), indicated by white arrowheads and polysaccharide cell wall (PCW).

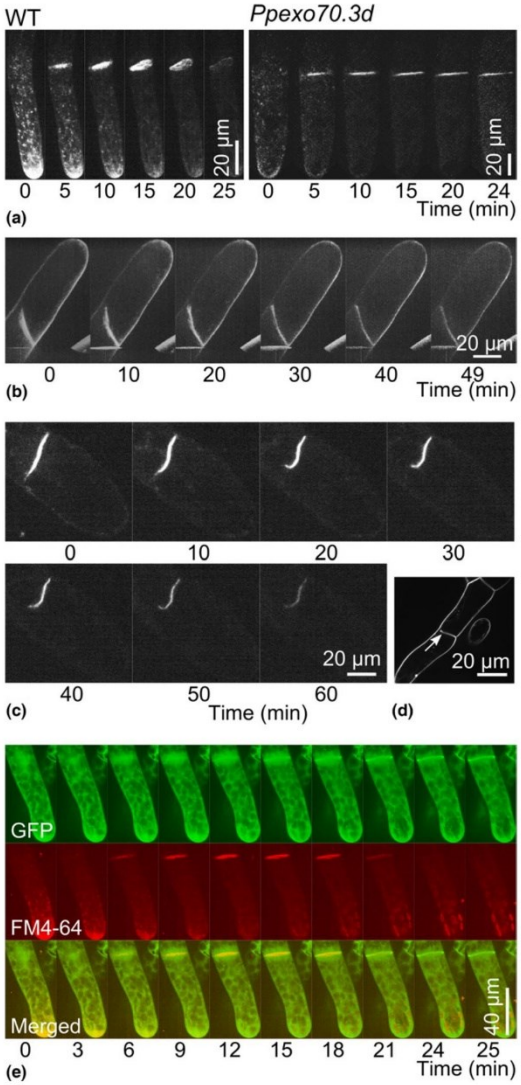

Fig. 10 Cytokinetic defects in *Ppexo70.3d*#6 protonema and subcellular localization of the PpEXO70.3d protein during cell plate formation in *Physcomitrella patens*. (a) FM 4-64-stained wild-type (WT) and *Ppexo70.3d*#6 dividing protonemal tip cell. (b, c) Delayed and unfinished cell plate formation in *Ppexo70.3d* cells. (d) The cell with unfinished cell wall after cytokinesis from (c) has later re-entered mitosis and grown as a normal filament. (e) Dynamics of GFP:PpEXO70.3d localization during cytokinesis and cell plate formation. The filament was stained with FM 4-64 to visualize the nascent cell plate.

additional sequence resources, and confirmed the existence of the three previously described clades in all land plants except *S. moellendorffii*, which apparently lacks EXO70.3. However, our previous study (Synek *et al.*, 2006) detected an *S. moellendorffii* EXO70.3 paralog present in a pre-publication version of the genome, but absent from the published version (Banks *et al.*, 2011). Thus, EXO70.3 might be present in lycophytes but missed during *S. moellendorffii* genome sequencing and annotation. Only one gene, clustering at the base of the EXO70.1 branch, was found in the charophyte *K. flaccidum*.

The three major land plant EXO70 clades were obviously established in two gene duplication events around the time of the separation of the charophyte and land plant lineages, generating in the latter first an ancestor of EXO70.3 and a common ancestor of EXO70.1 and EXO70.2. Subsequently, a series of lineage-specific gene duplications took place. From the species studied, *M. polymorpha* has a single EXO70 in each clade, reflecting either lack of gene duplications or paralog loss. The

Table 3 Cytokinetic defect in *Physcomitrella patens* mutant *Ppexo70.3d*

	< 30 min	> 30 min	> 60 min
Wild-type (WT)	15	0	0
Ppexo70.3d#6	20	7	3

Values are the number of dividing cells observed. Time is shown as duration from observation of the cell plate to insertion into the mother cell. $P = 0.0380$ (Fisher's exact test).

propensity for gene duplications is especially high in the EXO70.2 clade, where distinct subfamilies proliferated in monocots and dicots (Chong *et al.*, 2010; Cvrčková *et al.*, 2012). Yet another EXO70.2 subfamily proliferated in conifers, and even in mosses EXO70.2 is the clade with the most paralogs. The extent of within-clade divergence varies among the three families, with EXO70.1 being the least diverged, possibly due to strong purifying selection, consistent with the severe phenotypic consequences of loss of highly expressed EXO70.1 paralogs in *A. thaliana* (Synek *et al.*, 2006; Li *et al.*, 2013) and rice (Tu *et al.*, 2015).

Most experimental work on plant EXO70 reported so far has concentrated on EXO70.1 and EXO70.2, except one study describing the role of a *Medicago truncatula* EXO70.3 in mycorrhiza (Zhang *et al.*, 2015). We thus focused on *P. patens* EXO70.3, hoping to gain insight into the function of this so far uncharacterized clade, and specifically on *PpEXO70.3d*, whose knockout mutants exhibit conspicuous phenotypic defects described here.

Transcriptomic data show that *PpEXO70.3d* is the most expressed EXO70.3 paralog in protonemata and some parts of the gametophore (Hiss *et al.*, 2014; Ortiz-Ramírez *et al.*, 2016; Fig. S5). Thus, phenotypic deviations can be expected in these tissues, where its absence may not be fully compensated for by other paralogs. Indeed, *Ppexo70.3d* mutants exhibit impaired protonema growth, attributable to reduced chloronema cell elongation and failure to fully differentiate fast-growing caulonemata. Similar phenotypes were reported for mutants defective in tip growth (Finka *et al.*, 2008; Perroud & Quatrano, 2008; Vidali *et al.*, 2009, 2010).

The *Ppexo70.3d* mutants produce caulonema-like filaments with noticeably oblique cell walls, consisting of shorter cells containing sometimes more chloroplasts than normal caulonemata, suggesting incomplete or suppressed caulonema differentiation. Similar apical cell elongation and caulonema differentiation defects were reported for *arp3a*, *arpc1*, *arpc4* and *brick1* mutants affecting actin organization (Harries *et al.*, 2005; Perroud & Quatrano, 2006, 2008; Finka *et al.*, 2008) as well as for mutants lacking transcription factors PpLRL1 and PpLRL2 (Tam *et al.*, 2015). Interestingly, the *Ppexo70.3d* defect was partly and reversibly rescued at low temperature. This might be caused by increased expression of other paralogs at low temperature. Indeed, *PpEXO70.3b* (Pp1s6_436V6) is induced by prolonged cold stress (Beike *et al.*, 2015).

Mutants with altered cell elongation and caulonema differentiation often exhibit modified filament branching. Our *Ppexo70.3d* mutants have more branched protonemata, with multiple branches sometimes originating from a single cell, similar to the myosin mutant Δ*myo8ABCDE*, *arpc1* mutants and strigolactone-deficient *ccd8* mutants (Harries *et al.*, 2005; Proust *et al.*, 2011; Wu *et al.*, 2011), but unlike *brick1* mutants which produce few, if any, branches (Perroud & Quatrano, 2008). Multiple branching might result from defective cell plate positioning. Consistent with previously reported localization of exocyst subunits to the cell plate (Fendrych *et al.*, 2010; Zhang *et al.*, 2013), PpEXO70.3d localizes to the cell plate and post-cytokinetic cell wall in freshly divided cells, while the protein was cytoplasmic in non-dividing cells, with enrichment at the tip, where massive exocytosis takes place. This is consistent with the existence of multiple membrane trafficking domains within a cell, suggested by, for example, a recent study documenting distinct function and diverse localization of tobacco EXO70 isoforms in growing pollen tubes, which also elongate by tip growth (Sekereš *et al.*, 2017). The multiple branching phenotype in *Ppexo70.3d* mutants may also be due to compromised auxin action (Ashton *et al.*, 1979).

We observed delayed or defective cytokinesis in *Ppexo70.3d* protonemata, reminiscent of Arabidopsis exocyst mutants (Fendrych *et al.*, 2010). Similar defects, together with a mitotic delay, were also described in *P. patens NACK* kinesin-defective lines (Naito & Goshima, 2015). Defective mutant protoplast regeneration and outgrowth is consistent with the reported high expression level of PpEXO70.3d in protoplasts (Fig. S5) and suggests problems in cell wall construction and establishment of the polar axis, which is a prerequisite for first asymmetric cell division and elongation. A similar phenotype was reported in protoplasts impaired in actin organization due to an *arpc1* mutation or latrunculin B treatment (Harries *et al.*, 2005) or in the function of PpWOX13L transcription factors that control the expression of cell wall-remodeling enzymes (Sakakibara *et al.*, 2014).

Consistent with *PpEXO70.3d* participating in cell wall construction, our mutants are impaired in the deposition of cuticle, a waxy layer that protects aerial organs from water loss, present already in mosses (Budke *et al.*, 2011; Buda *et al.*, 2013). Deposition of angiosperm cuticular wax involves the secretory pathway (McFarlane *et al.*, 2014). Membrane-localized ABC transporters (whose function also depends on exocytosis) participate in both seed plants and *P. patens* (Pighin *et al.*, 2004; Luo *et al.*, 2007; Buda *et al.*, 2013). The apparently greener appearance of *Ppexo70.3d* plants compared to the WT, despite a decreased amount of Chl, is reminiscent of cuticle-defective *cer* mutants in Arabidopsis (Koornneef *et al.*, 1989). Interestingly, in moss GH3 knock-out mutants with disturbed IAA to amino acid conjugation, the accumulation of IAA is associated with a higher Chl concentration in the dark (Mittag *et al.*, 2015).

Buds and gametophores were assumed to develop only on caulonemata (Ashton *et al.*, 1979; Cove *et al.*, 2006). However, some caulonema-less mutants can produce gametophores (Tam *et al.*, 2015). Likewise, *Ppexo70.3d* forms buds and gametophores, albeit aberrant. Altered cell plate positioning in some mutant buds resembles *dek1* calpain mutants, which, however, do not form gametophores (Perroud *et al.*, 2014). Dedifferentiation of bud initials into filaments was occasionally observed in

Ppexo70.3d mutants. Since both bud initial and secondary filament initials may differentiate from the same parent cell depending on local signals (Harrison *et al.*, 2009), *Ppexo70.3d* mutants might have difficulties in responding to, or keeping memory of, these cues.

Gametophores of *Ppexo70.3d* plants are smaller than WT gametophores and often contain bifurcated or fused phyllids, as well as those with secondary midribs, consistent with the high expression level of this gene in phyllids (Fig. S5). Organ fusion was reported in other mutants with impaired cuticular wax deposition (Koornneef *et al.*, 1989; Luo *et al.*, 2007) or auxin signaling (Okada *et al.*, 1991; Mattsson *et al.*, 1999).

Some aspects of the *Ppexo70.3d* phenotype may be related to altered PAT or auxin signaling. PAT depends on exocyst function in seed plants, since Arabidopsis EXO70A1, a EXO70.1 clade member, is involved in recycling the plasmalemma localized PIN auxin efflux carriers (Drdová *et al.*, 2013). PAT is required for *P. patens* protoplast regeneration (Bhatla *et al.*, 2002) and sporophyte formation, although its role in gametophyte development is disputed (Fujita *et al.*, 2008; Bennett *et al.*, 2014; Viaene *et al.*, 2014). Disruption of PAT by inhibitors results in formation of multiple sporangia (Fujita & Hasebe, 2009). The *pin* mutants in *P. patens* have branched sporophytes similar to some fossil mosses (Bennett *et al.*, 2014).

Unfortunately, we could not study sporophytic phenotypes of *Ppexo70.3d* mutants, which did not form sporophytes due to a pre-zygotic defect – a failure to differentiate functional egg cells. While auxin-defective *SHI/STY* mutants of *P. patens* exhibit developmental defects in both antheridia and archegonia (Landberg *et al.*, 2013), so far the only moss mutants with a similar female sterility phenotype as a part of a more complex defect are those impaired in the function or regulation of the dicer-like protein *DCL4* and the receptor-like kinase mutant *Pp*Δ*cr4* (Arif *et al.*, 2012; Demko *et al.*, 2016).

Auxin enhances caulonema induction in *P. patens* (Ashton *et al.*, 1979; Cove *et al.*, 2006; Jang & Dolan, 2011). Remarkably, in our *Ppexo70.3d* mutant caulonemata could not be induced by exogenously applied auxin, suggesting reduced sensitivity or impaired response towards auxin. Mutants also showed increased levels of IAA, suggesting either a defect in auxin transport, or a compensatory increase of auxin concentration by cells with impaired auxin response. Similar results were reported for Δ*PpGH3-1* and Δ*PpGH3-2* mutants, which are more sensitive to IAA treatments and have increased IAA contents at elevated temperatures and in dark conditions (Ludwig-Müller *et al.*, 2009; Mittag *et al.*, 2015). Interestingly, treatment with NPA, an inhibitor of plasmalemma-localized PINs, partly mimics the mutant phenotype in WT plants. Thus, *Ppexo70.3d* might be resistant toward exogenous auxin due to adaptation to an increased endogenous auxin content.

Auxin induces expression of *PpRSL1* and *PpRSL2* transcription factors in chloronemata, a prerequisite of caulonema differentiation. Double *rsl1 rsl2* mutants are resistant to the auxin treatment and do not produce caulonemata (Jang & Dolan, 2011). It would thus be interesting to examine the status of *PpRSL1* and *PpRSL2* expression in *Ppexo70.3d* mutants.

Auxin also causes stem and leaf elongation in moss gametophores (Decker *et al.*, 2006) and controls the gametophore branching pattern. While in flowering plants initiation of new branches requires basipetal PIN-dependent auxin transport, *P. patens* branching involves bi-directional auxin transport (Coudert *et al.*, 2015). The auxin biosynthesis mutants *shi1* or *shi2* have shorter internodes (Eklund *et al.*, 2010). The observed shift of branching in *Ppexo70.3d* towards the lower part of gametophores might thus be due to increased concentration of auxin in mutant tissues, resulting in auxin content dropping below the threshold permissive for branch initiation at the lower parts of gametophore than in the WT. Compromised auxin transport or signaling may also contribute to this phenotype.

The interaction between Sec3 and Exo70 exocyst subunits and PIP2 is well documented in yeast and/or Arabidopsis (He *et al.*, 2007; Zhang *et al.*, 2008; Pleskot *et al.*, 2015; Bloch *et al.*, 2016). It is thus remarkable that some aspects of *Ppexo70.3d* phenotype resemble PIPK-defective plants exhibiting altered caulonema and rhizoid development, reduction in both protonema and rhizoid growth, and shorter individual cell length compared to WT. While these defects are to some extent present already in single *pipk1* mutants, *pipk1 pipk2* double mutants also do not produce sporophytes. Remarkably, moss *pipk1* and *pipk1 pipk2* double mutants also have increased Chl content (Saavedra *et al.*, 2011). Thus, the function of *PpEXO70.3d* might be linked to phosphoinositide signaling.

In summary, we show that loss of *PpEXO70.3d*, an EXO70.3 paralog expressed throughout the moss life cycle, but especially in protonemata, results in defects in cell elongation and differentiation, altered auxin signaling, a partial cytokinesis and cell wall structure defect, and pre-zygotic female sterility. However, *PpEXO70.3d* is not essential for cell viability and bud and gametophore development, indicating functional redundancy and subfunctionalization of distinct *P. patens* EXO70 paralogs.

Acknowledgements

We thank Hana Soukupová for reading the manuscript; Miroslav Hyliš and Tomáš Moravec for help with electron microscopy; Petre Dobrev for phytohormone analyses; Liam Dolan and Thomas Tam for help with time-lapse imaging; and Fabien Nogué, Louis Vidali and Helena Štorchová for sharing vectors and protocols. This work was supported by grants from CSF/GACR (15-14886S), EU Marie Curie Network (no. 238640 PLANTORIGINS) and MSMT (NPUI LO1417).

Author contributions

A.R., L.B. and V.Z. planned and designed the research; A.R. performed the experiments; F.C. performed the bioinformatic analyses; A.R., L.B., M.H., F.C. and V.Z. analysed and interpreted the data and wrote the manuscript. All authors approved the final version of the manuscript.

References

Abràmoff MD, Magalhães PJ, Ram SJ. 2004. Image processing with ImageJ. *Biophotonics International* **11**: 36–42.

Arif MA, Fattash I, Ma Z, Cho SH, Beike AK, Reski R, Axtell MJ, Frank W. 2012. DICER-LIKE3 activity in *Physcomitrella patens* DICER-LIKE4 mutants causes severe developmental dysfunction and sterility. *Molecular Plant* **5**: 1281–1294.

Ashton NW, Grimsley NH, Cove DJ. 1979. Analysis of gametophytic development in the moss, *Physcomitrella patens*, using auxin and cytokinin resistant mutants. *Planta* **144**: 427–435.

Banks JA, Nishiyama T, Hasebe M, Bowman JL, Gribskov M, dePamphilis C, Albert VA, Aono N, Aoyama T, Ambrose BA *et al.* 2011. The *Selaginella* genome identifies genetic changes associated with the evolution of vascular plants. *Science* **332**: 960–963.

Beike AK, Lang D, Zimmer AD, Wüst F, Trautmann D, Wiedemann G, Beyer P, Decker EL, Reski R. 2015. Insights from the cold transcriptome of *Physcomitrella patens*: global specialization pattern of conserved transcriptional regulators and identification of orphan genes involved in cold acclimation. *New Phytologist* **205**: 869–881.

Bennett TA, Liu MM, Aoyama T, Bierfreund NM, Braun M, Coudert Y, Dennis RJ, O'Connor D, Wang XY, White CD *et al.* 2014. Plasma membrane-targeted PIN proteins drive shoot development in a moss. *Current Biology* **24**: 2776–2785.

Bhatla SC, Kiessling J, Reski R. 2002. Observation of polarity induction by cytochemical localization of phenylalkylamine-binding sites in regenerating protoplasts of the moss *Physcomitrella patens*. *Protoplasma* **219**: 99–105.

Bloch D, Pleskot R, Pejchar P, Potocký M, Trpkošová P, Cwiklik L, Vukašinović N, Sternberg H, Yalovsky S, Žárský V. 2016. Exocyst SEC3 and phosphoinositides define sites of exocytosis in pollen tube initiation and growth. *Plant Physiology* **172**: 980–1002.

Bröcker C, Engelbrecht-Vandré S, Ungermann C. 2010. Multisubunit tethering complexes and their role in membrane fusion. *Current Biology* **20**: R943–R952.

Buda GJ, Barnes WJ, Fich EA, Park S, Yeats TH, Zhao L, Domozych DS, Rose JKC. 2013. An ATP binding cassette transporter is required for cuticular wax deposition and desiccation tolerance in the moss *Physcomitrella patens*. *Plant Cell* **25**: 4000–4013.

Budke JM, Goffinet B, Jones CS. 2011. A hundred-year-old question: is the moss calyptra covered by a cuticle? A case study of *Funaria hygrometrica*. *Annals of Botany* **107**: 1279–1286.

Budke JM, Goffinet B, Jones CS. 2013. Dehydration protection provided by a maternal cuticle improves offspring fitness in the moss *Funaria hygrometrica*. *Annals of Botany* **111**: 781–789.

Chong YT, Gidda SK, Sanford C, Parkinson J, Mullen RT, Goring DR. 2010. Characterization of the *Arabidopsis thaliana* exocyst complex gene families by phylogenetic, expression profiling, and subcellular localization studies. *New Phytologist* **185**: 401–419.

Coudert Y, Palubicki W, Ljung K, Novak O, Leyser O, Harrison CJ. 2015. Three ancient hormonal cues co-ordinate shoot branching in a moss. *eLife* **4**: e06808.

Cove DJ, Bezanilla M, Harries P, Quatrano R. 2006. Mosses as model systems for the study of metabolism and development. *Annual Review of Plant Biology* **57**: 497–520.

Cove DJ, Perroud P-F, Charron AJ, McDaniel SF, Khandelwal A, Quatrano RS. 2009. The moss *Physcomitrella patens*: a novel model system for plant development and genomic studies. In: Crotty DA, Gann A, eds. *Emerging model organisms, a laboratory manual*. New York, NY, USA: Cold Spring Harbor Laboratory Press, 69–104.

Cove DJ, Schild A, Ashton NW, Hartmann E. 1978. Genetic and physiological studies of the effect of light on the development of the moss, *Physcomitrella patens*. *Photochemistry and Photobiology* **27**: 249–254.

Cvrčková F, Eliáš M, Hála M, Obermeyer G, Žárský V. 2001. Small GTPases and conserved signalling pathways in plant cell morphogenesis: from exocytosis to the exocyst. In: Geitmann A, Cresti M, Heath IB, eds. *Cell biology of plant and fungal tip growth*. Amsterdam, the Netherlands: IOS Press, 105–122.

Cvrčková F, Grunt M, Bezvoda R, Hála M, Kulich I, Rawat A, Žárský V. 2012. Evolution of the land plant exocyst complexes. *Frontiers in Plant Science* **3**: 159.

Decker EL, Frank W, Sarnighausen E, Reski R. 2006. Moss systems biology en route: phytohormones in *Physcomitrella* development. *Plant Biology* **8**: 397–406.

Demko V, Ako E, Perroud PF, Quatrano R, Olsen OA. 2016. The phenotype of the CRINKLY4 deletion mutant of *Physcomitrella patens* suggests a broad role in developmental regulation in early land plants. *Planta* **244**: 275–284.

Dobrev PI, Kamínek M. 2002. Fast and efficient separation of cytokinins from auxin and abscisic acid and their purification using mixed-mode solid-phase extraction. *Journal of Chromatography A* **950**: 21–29.

Drdová EJ, Synek L, Pečenková T, Hála M, Kulich I, Fowler JE, Murphy AS, Žárský V. 2013. The exocyst complex contributes to PIN auxin efflux carrier recycling and polar auxin transport in Arabidopsis. *Plant Journal* **73**: 709–719.

Eklund DM, Thelander M, Landberg K, Ståldal V, Nilsson A, Johansson M, Valsecchi I, Pederson ER, Kowalczyk M, Ljung K *et al.* 2010. Homologues of the *Arabidopsis thaliana* SHI/STY/LRP1 genes control auxin biosynthesis and affect growth and development in the moss *Physcomitrella patens*. *Development* **137**: 1275–1284.

Eliáš M, Drdová E, Žiak D, Bavlnka B, Hála M, Cvrčková F, Soukupová H, Žárský V. 2003. The exocyst complex in plants. *Cell Biology International* **27**: 199–201.

Fendrych M, Synek L, Pečenková T, Toupalová H, Cole R, Drdová E, Nebesářová J, Šedinová M, Hála M, Fowler JE *et al.* 2010. The Arabidopsis exocyst complex is involved in cytokinesis and cell plate maturation. *Plant Cell* **22**: 3053–3065.

Finka A, Saidi Y, Goloubinoff P, Neuhaus J-M, Zrÿd J-P, Schaefer DG. 2008. The knock-out of *ARP3a* gene affects F-actin cytoskeleton organization altering cellular tip growth, morphology and development in moss *Physcomitrella patens*. *Cell Motility and the Cytoskeleton* **65**: 769–784.

Frank W, Ratnadewi D, Reski R. 2005. *Physcomitrella patens* is highly tolerant against drought, salt and osmotic stress. *Planta* **220**: 384–394.

Fujita T, Hasebe M. 2009. Convergences and divergences in polar auxin transport and shoot development in land plant evolution. *Plant Signaling and Behavior* **4**: 313–315.

Fujita T, Sakaguchi H, Hiwatashi Y, Wagstaff SJ, Ito M, Deguchi H, Sato T, Hasebe M. 2008. Convergent evolution of shoots in land plants: lack of auxin polar transport in moss shoots. *Evolution & Development* **10**: 176–186.

Goodstein DM, Shu S, Howson R, Neupane R, Hayes RD, Fazo J, Mitros T, Dirks W, Hellsten U, Putnam N *et al.* 2012. Phytozome: a comparative platform for green plant genomics. *Nucleic Acids Research* **40**: D1178–D1186.

Grunt M, Žárský V, Cvrčková F. 2008. Roots of angiosperm formins: the evolutionary history of plant FH2 domain-containing proteins. *BMC Evolutionary Biology* **8**: 115.

Hála M, Cole R, Synek L, Drdová E, Pečenková T, Nordheim A, Lamkemeyer T, Madlung J, Hochholdinger F, Fowler JE *et al.* 2008. An exocyst complex functions in plant cell growth in Arabidopsis and tobacco. *Plant Cell* **20**: 1330–1345.

Hall TA. 1999. BioEdit: a user-friendly biological sequence alignment editor and analysis program for Windows 95/98/NT. *Nucleic Acids Symposium Series* **41**: 95–98.

Harries PA, Pan A, Quatrano RS. 2005. Actin-related protein2/3 complex component ARPC1 is required for proper cell morphogenesis and polarized cell growth in *Physcomitrella patens*. *Plant Cell* **17**: 2327–2339.

Harrison CJ, Roeder AH, Meyerowitz EM, Langdale JA. 2009. Local cues and asymmetric cell divisions underpin body plan transitions in the moss *Physcomitrella patens*. *Current Biology* **19**: 461–471.

He B, Xi F, Zhang X, Zhang J, Guo W. 2007. Exo70 interacts with phospholipids and mediates the targeting of the exocyst to the plasma membrane. *EMBO Journal* **26**: 4053–4065.

Heider MR, Munson M. 2012. Exorcising the exocyst complex. *Traffic* **13**: 898–907.

Hiss M, Laule O, Meskauskiene RM, Arif MA, Decker EL, Erxleben A, Frank W, Hanke ST, Lang D, Martin A *et al.* 2014. Large-scale gene expression profiling data for the model moss *Physcomitrella patens* aid understanding of developmental progression, culture and stress conditions. *Plant Journal* **79**: 530–539.

Hori K, Maruyama F, Fujisawa T, Togashi T, Yamamoto N, Seo M, Sato S, Yamada T, Mori H, Tajima N *et al.* 2014. *Klebsormidium flaccidum* genome reveals primary factors for plant terrestrial adaptation. *Nature Communications* **5**: 3978.

Jang G, Dolan L. 2011. Auxin promotes the transition from chloronema to caulonema in moss protonema by positively regulating *PpRSL1* and *PpRSL2* in *Physcomitrella patens*. *New Phytologist* **192**: 319–327.

Jenkins GI, Courtice GRM, Cove DJ. 1986. Gravitropic responses of wild-type and mutant strains of the moss *Physcomitrella patens*. *Plant, Cell & Environment* **9**: 637–644.

Johri MM, Desai S. 1973. Auxin regulation of caulonema formation in moss protonema. *Nature – New Biology* **245**: 223–224.

Kamisugi Y, Cuming AC, Cove DJ. 2005. Parameters determining the efficiency of gene targeting in the moss the *Physcomitrella patens*. *Nucleic Acids Research* **33**: e173.

Koornneef M, Hanhart CJ, Thiel F. 1989. A genetic and phenotypic description of *eceriferum* (*cer*) mutants in *Arabidopsis thaliana*. *Journal of Heredity* **80**: 118–122.

Koumandou VL, Dacks JB, Coulson RM, Field MC. 2007. Control systems for membrane fusion in the ancestral eukaryote; evolution of tethering complexes and SM proteins. *BMC Evolutionary Biology* **7**: 29.

Kulich I, Vojtíková Z, Glanc M, Ortmannová J, Rasmann S, Žárský V. 2015. Cell wall maturation of Arabidopsis trichomes is dependent on exocyst subunit EXO70H4 and involves callose deposition. *Plant Physiology* **168**: 120–131.

Landberg K, Pederson ERA, Viaene T, Bozorg B, Friml J, Jönsson H, Thelander M, Sundberg E. 2013. The moss *Physcomitrella patens* reproductive organ development is highly organized, affected by the two *SHI/STY* genes and by the level of active auxin in the *SHI/STY* expression domain. *Plant Physiology* **162**: 1406–1419.

Lang D, Zimmer AD, Rensing SA, Reski R. 2008. Exploring plant biodiversity: the *Physcomitrella* genome and beyond. *Trends in Plant Sciences* **13**: 542–549.

Lassmann T, Frings O, Sonnhammer ELL. 2009. Kalign2: high-performance multiple alignment of protein and nucleotide sequences allowing external features. *Nucleic Acids Research* **37**: 858–865.

Li S, Chen M, Yu D, Ren S, Sun S, Liu L, Ketelaar T, Emons AM, Liu CM. 2013. EXO70A1-mediated vesicle trafficking is critical for tracheary element development in Arabidopsis. *Plant Cell* **25**: 1774–1786.

Ludwig-Müller J, Jülke S, Bierfreund NM, Decker EL, Reski R. 2009. Moss (*Physcomitrella patens*) GH3 proteins act in auxin homeostasis. *New Phytologist* **181**: 323–338.

Luo B, Xue XY, Hu WL, Wang LJ, Chen XY. 2007. An ABC transporter gene of *Arabidopsis thaliana*, *AtWBC11*, is involved in cuticle development and prevention of organ fusion. *Plant and Cell Physiology* **48**: 1790–1802.

Luschnig C, Vert G. 2014. The dynamics of plant plasma membrane proteins: PINs and beyond. *Development* **141**: 2924–2938.

Mattsson J, Sung ZR, Berleth T. 1999. Responses of plant vascular systems to auxin transport inhibition. *Development* **126**: 2979–2991.

McFarlane HE, Watanabe Y, Yang W, Huang Y, Ohlrogge J, Samuels AL. 2014. Golgi- and trans-Golgi network-mediated vesicle trafficking is required for wax secretion from epidermal cells. *Plant Physiology* **164**: 1250–1260.

Menand B, Calder G, Dolan L. 2007. Both chloronemal and caulonemal cells expand by tip growth in the moss *Physcomitrella patens*. *Journal of Experimental Botany* **58**: 1843–1849.

Mittag J, Gabrielyan A, Ludwig-Müller J. 2015. Knockout of GH3 genes in the moss *Physcomitrella patens* leads to increased IAA levels at elevated temperature and in darkness. *Plant Physiology and Biochemistry* **97**: 339–349.

Naito H, Goshima G. 2015. NACK kinesin is required for metaphase chromosome alignment and cytokinesis in the moss *Physcomitrella patens*. *Cell Structure and Function* **40**: 31–41.

Nystedt B, Street NR, Wetterbom A, Zuccolo A, Lin Y-C, Scofield DG, Vezzi F, Delhomme N, Giacomello S, Alexeyenko A *et al.* 2013. The Norway spruce genome sequence and conifer genome evolution. *Nature* **497**: 579–584.

Okada K, Ueda J, Komaki MK, Bell CJ, Shimura Y. 1991. Requirement of the auxin polar transport system in early stages of Arabidopsis floral bud formation. *Plant Cell* **3**: 677–684.

Ortiz-Ramírez C, Hernandez-Coronado M, Thamm A, Catarino B, Wang M, Dolan L, Feijó JA, Becker JD. 2016. A transcriptome atlas of *Physcomitrella patens* provides insights into the evolution and development of land plants. *Molecular Plant* **9**: 205–220.

Perroud P-F, Demko V, Johansen W, Wilson RC, Olsen OA, Quatrano RS. 2014. Defective Kernel 1 (DEK1) is required for three-dimensional growth in *Physcomitrella patens*. *New Phytologist* **203**: 794–804.

Perroud P-F, Quatrano RS. 2006. The role of ARPC4 in tip growth and alignment of the polar axis in filaments of *Physcomitrella patens*. *Cell Motility and the Cytoskeleton* **63**: 162–171.

Perroud P-F, Quatrano RS. 2008. BRICK1 is required for apical cell growth in filaments of the moss *Physcomitrella patens* but not for gametophore morphology. *Plant Cell* **20**: 411–422.

Pighin JA, Zheng H, Balakshin LJ, Goodman IP, Western TL, Jetter R, Kunst L, Samuels AL. 2004. Plant cuticular lipid export requires an ABC transporter. *Science* **306**: 702–704.

Pleskot R, Cwiklik L, Jungwirth P, Žárský V, Potocký M. 2015. Membrane targeting of the yeast exocyst complex. *Biochimica et Biophysica Acta – Biomembranes* **1848**: 1481–1489.

Proust H, Hoffmann B, Xie X, Yoneyama K, Schaefer DG, Yoneyama K, Nogué F, Rameau C. 2011. Strigolactones regulate protonema branching and act as a quorum sensing-like signal in the moss *Physcomitrella patens*. *Development* **138**: 1531–1539.

Saavedra L, Balbi V, Lerche J, Mikami K, Heilmann I, Sommarin M. 2011. PIPKs are essential for rhizoid elongation and caulonemal cell development in the moss *Physcomitrella patens*. *Plant Journal* **67**: 635–647.

Sakakibara K, Reisewitz P, Aoyama T, Friedrich T, Ando S, Sato Y, Tamada Y, Nishiyama T, Hiwatashi Y, Kurata T *et al.* 2014. WOX13-like genes are required for reprogramming of leaf and protoplast cells into stem cells in the moss *Physcomitrella patens*. *Development* **141**: 1660–1670.

Schmiedel G, Schnepf E. 1980. Polarity and growth of caulonema tip cells of the moss *Funaria hygrometrica*. *Planta* **147**: 405–413.

Sekereš J, Pejchar P, Šantrůček J, Vukašinović N, Žárský V, Potocký P. 2017. Analysis of exocyst subunit EXO70 family reveals distinct membrane polar domains in tobacco pollen tubes. *Plant Physiology* **173**: 1659–1675.

Synek L, Schlager N, Eliáš M, Quentin M, Hauser MT, Žárský V. 2006. ATEXO70A1, a member of a family of putative exocyst subunits specifically expanded in land plants, is important for polar growth and plant development. *Plant Journal* **48**: 54–72.

Tam THY, Catarino B, Dolan L. 2015. Conserved regulatory mechanism controls the development of cells with rooting functions in land plants. *Proceedings of the National Academy of Sciences, USA* **112**: E3959–E3968.

Tamura K, Stecher G, Peterson D, Filipski A, Kumar S. 2013. MEGA6: molecular evolutionary genetics analysis version 6.0. *Molecular Biology and Evolution* **30**: 2725–2729.

Tu B, Hu L, Chen W, Li T, Hu B, Zheng L, Lv Z, You S, Wang Y, Ma B *et al.* 2015. Disruption of *OsEXO70A1* causes irregular vascular bundles and perturbs mineral nutrient assimilation in rice. *Scientific Reports* **5**: 18609.

Viaene T, Landberg K, Thelander M, Medvecka E, Pederson E, Feraru E, Cooper ED, Karimi M, Delwiche CF, Ljung K *et al.* 2014. Directional auxin transport mechanisms in early diverging land plants. *Current Biology* **24**: 2786–2791.

Vidali L, Augustine RC, Kleinman KP, Bezanilla M. 2007. Profilin is essential for tip growth in the moss *Physcomitrella patens*. *Plant Cell* **19**: 3705–3722.

Vidali L, Burkart GM, Augustine RC, Kerdavid E, Tüzel E, Bezanilla M. 2010. Myosin XI is essential for tip growth in *Physcomitrella patens*. *Plant Cell* **22**: 1868–1882.

Vidali L, van Gisbergen PAC, Guérin C, Franco P, Li M, Burkart GM, Augustine RC, Blanchoin L, Bezanilla M. 2009. Rapid formin-mediated actin-filament elongation is essential for polarized plant cell growth. *Proceedings of the National Academy of Sciences, USA* **106**: 13341–13346.

Wang X, Qi M, Li J, Ji Z, Hu Y, Bao F, Mahalingam R, He Y. 2014. The phosphoproteome in regenerating protoplasts from *Physcomitrella patens* protonemata shows changes paralleling postembryonic development in higher plants. *Journal of Experimental Biology* **65**: 2093–2106.

Wu B, Guo W. 2015. The exocyst at a glance. *Journal of Cell Science* **128**: 2957–2964.

Wu SZ, Ritchie JA, Pan AH, Quatrano RS, Bezanilla M. 2011. Myosin VIII regulates protonemal patterning and developmental timing in the moss *Physcomitrella patens*. *Molecular Plant* **4**: 909–921.

Žárský V, Cvrčková F, Potocký M, Hála M. 2009. Exocytosis and cell polarity in plants – exocyst and recycling domains. *New Phytologist* **183**: 255–272.

Žárský V, Kulich I, Fendrych M, Pečenková T. 2013. Exocyst complexes multiple functions in plant cells secretory pathways. *Current Opinion in Plant Biology* **16**: 726–733.

Zhang Y, Immink R, Liu CM, Emons AM, Ketelaar T. 2013. The Arabidopsis exocyst subunit SEC3A is essential for embryo development and accumulates in transient puncta at the plasma membrane. *New Phytologist* **199**: 74–88.

Zhang X, Orlando K, He B, Xi F, Zhang J, Zajac A, Guo W. 2008. Membrane association and functional regulation of Sec3 by phospholipids and Cdc42. *Journal of Cell Biology* **180**: 145–158.

Zhang X, Pumplin N, Ivanov S, Harrison MJ. 2015. EXO70I is required for development of a sub-domain of the periarbuscular membrane during arbuscular mycorrhizal symbiosis. *Current Biology* **25**: 2189–2195.

Supporting Information

Additional Supporting Information may be found online in the Supporting Information tab for this article:

Fig. S1 Maximum-likelihood phylogenetic tree of selected plant EXO70 protein sequences, including human EXO70 as an outgroup.

Fig. S2 Generation of *Ppexo70.3d* knockout mutants.

Fig. S3 Phenotypic deviations in *Ppexo70.3d#11*.

Fig. S4 Effect of exogenous NAA and NPA supply on WT and *Ppexo70.3d#6*.

Fig. S5 Relative expression of *Physcomitrella patens* EXO70.3 paralogs in moss tissues, as documented by published transcriptome data.

Table S1 Protein sequences included in phylogenetic analyses

Table S2 List of primers

Table S3 Quantification of amount of total Chl in WT and *Ppexo70.3d*

Table S4 Quantification of cell numbers in WT and *Ppexo70.3d* phyllids

Table S5 Quantification of NAA and NPA effect on WT and *Ppexo70.3d* colony growth

Video S1 Time-lapse of WT protonemata growth.

Video S2 Time-lapse of *Ppexo70.3d* protonemata growth.

Video S3 Cell division in WT protonemal apical cell.

Video S4 Normal cell division in *Ppexo70.3d* protonemal apical cell.

Video S5 Delayed cytokinesis in *Ppexo70.3d* protonemal apical cell.

Video S6 Aberrant cytokinesis in *Ppexo70.3d* protonemal apical cell.

Video S7 Localization of GFP:PpEXO70.3d during cytokinesis.

Please note: Wiley Blackwell are not responsible for the content or functionality of any Supporting Information supplied by the authors. Any queries (other than missing material) should be directed to the *New Phytologist* Central Office.

Manuscript 3: Moss SEC6 exocyst subunit is essential for growth and development

Lucie Brejšková[1,2], Michal Hála[1,2], Anamika Rawat[1,2], Hana Soukupová[1], Fatima Cvrčková[2], Fabien Nogué[3] and Viktor Žárský[2,*]

1- Institute of Experimental Botany, Academy of Sciences of the Czech Republic, Rozvojová 263, 165 02 Prague 6, Czech Republic,
2- Department of Experimental Plant Biology, Faculty of Science, Charles University, Viničná 5, 128 44 Prague 2, Czech Republic, and
3- INRA Centre de Versailles-Grignon, Route de St-Cyr (RD10) 78026 Versailles Cedex France

*For correspondence (tel. +420-221951683, e-mail zarsky@ueb.cas.cz).

Running title (max. 50 characters) Exocyst SEC6 subunit in moss.

Significance statement Exocyst mutants with truncated SEC6 subunit display pleiotropic growth and developmental deviations.

SUMMARY

Cell polarity regulation during cell division and cell expansion plays important roles in plant growth and morphogenesis and relies on the cooperation between cytoskeleton and secretory pathways. Octameric complex exocyst is a phylogenetically conserved exocytotic vesicles tethering factor, functioning as an effector of Rho and Rab GTPases at the plasma membrane. In contrast to most other land plants exocyst subunits, the *SEC6*, a core exocyst subunit, is encoded by only one paralogue in genomes of *Physcomitrella patens* and *Arabidopsis thaliana*. Arabidopsis SEC6 loss-of-function mutation causes male gametophytic lethality.

Here we show that attempts to produce the full disruption of *PpSEC6* by targeted gene replacement did not result in any moss plant regenerated. However accidentally we generated two independent mutant strains with only partial deletion at the C´-terminus of the *PpSEC6* coding locus displaying pleiotropic developmental deviations. Mutants display diminished rate of caulonema filaments elongation - in contrast to normally growing chloronema cells which were however resistant in respect to auxin induced transition to caulonema. Gametophore buds were initiated mostly from chloronema cells exhibited disordered cell file organization with cross wall perforations and were arrested in the 8-10-cell stage of development. Complementation of both mutant lines with *PpSEC6* and *AtSEC6* cDNA succesfully

rescued WT gametophore development. Induction of reproduction resulted in sexual organs differentiation; however sporophyte formation and production of viable spores was achieved only in lines complemented by moss SEC6. This indicates a partial functional conservation of SEC6 exocyst subunit between land plant lineages with possible specific moss SEC6 molecular features necessary to successfully finish the whole moss life cycle. Our results demonstrate an essential role of the moss SEC6 exocyst subunit in growth and development of *P. patens*.

Key words: exocyst, SEC6, *Physcomitrella patens,* secretion/exocytosis, polarity, three-dimensional division planes, tip growth, axillary hair, cytokinesis, land plants

INTRODUCTION

Exocytosis, a fundamental process required for the growth and differentiation of any eukaryotic organism, involves several distinct steps: delivery, tethering, docking and fusion of secretory vesicles derived from TGN to the specific sites at the plasma membrane. Tethering of exocytotic vesicles is facilitated by the exocyst CATCHR type tethering complex (Hsu *et al.*, 1990; He and Guo, 2009; Koumandou *et al.*, 2007). Most of exocyst subunits were discovered originally in budding yeast in a paradigmatic *sec* screen as temperature sensitive mutants of the secretory pathway (Novick *et al.*, 1980). Exocyst is a multiprotein complex with 8 subunits (SEC3, SEC5, SEC6, SEC8, SEC10, SEC15, EXO70 and EXO84) evolutionary conserved also in plants and most other eukaryote lineages (Eliáš *et al.*, 2003; Koumandou *et al.*, 2007; Hála *et al.*, 2008; Cvrčková *et al.*, 2012) and shown to be preferentially located at the sites of polarized secretion (e.g. TerBush and Novick, 1995; Guo *et al.*, 1999; TerBush *et al.*, 1999; Hála et al., 2008; Fendrych et al. 2013; Sekereš et al. 2017; Hsu *et al.*, 1996). Directed by activated RAB and Rho GTPases it acts prior to SNARE complex (soluble N-ethylmaleimide–sensitive attachment protein receptors) formation, which facilitates complete fusion of the vesicle to the PM and thus the cargo delivery, see review (Munson and Novick 2006). Exocyst mutants in plants display various morphological and cell polarity establishment defects, as retarded growth in pollen tubes and root hairs, abberant seed-coat deposition, cell plate formation defects during cytokinesis and compromised hypocotyl elongation (Cole *et al.*, 2005; Synek *et al*., 2006; Hála *et al*., 2008; Fendrych *et al*., 2010; Kulich *et al.,* 2010; Rawat *et al*., 2017). Exocyst subunit EXO70B2 and EXO70H1 are involved in plant-pathogen response (Pečenková *et al*., 2011; for review see Žárský *et al.* 2013).

SEC6 together with SEC8 are considered to be the core subunits of the exocyst complex (in mammalian cell biology therefore sometimes called Sec6/8 complex), and both have only one or two paralogues during the land plant evolution, indicating possibly active selection for stechiometry already on the level of gene copies after known several rounds of whole genome duplications in land plants (Eliáš

et al., 2003; Cvrčková *et al*., 2012). Loss-of-function (LOF) *sec6* mutants are inviable in *S. cerevisiae,* indicating that the protein is essential (Novick *et al.*, 1980, 1981; Lamping *et al.*, 2005). Interactions of Sec6 with t-SNARE Sec9, and also with SNARE regulator Sec1 are important for SNARE complex regulation (Sivaram *et al.*, 2005; Morgera *et al*., 2012; Hong and Lev 2014) and the interaction of SEC6/exocyst with SNARE complexes is necessary for the proper operation of exocytotic pathway (Dubuke *et al.*, 2015). In yeast, Sec6p is required not only for the whole complex assembly, but surprisingly also to anchor exocyst complexes to the membrane domains of secretion (Songer and Munson, 2009). Recently the SEC6 subunit in Chlamydomonas was shown to be essential for the contractile vacuole function (Comsic-Buchmann *et al*., 2012). In Drosophila *SEC6* mutations result in cell growth disruption in developing photoreceptors cells and cell lethality (Beronja *et al*., 2006) and at the hyphal apex of the Neurospora *crassa* SEC6 together with SEC5, SEC8 and SEC15 were localized as a plasma membrane crescent at the hyphal dome (Riquelme *et al*., 1014).

In Arabidopsis SEC6 (along with SEC8, SEC15b, EXO70A1 and EXO84b exocyst subunits; and possibly whole exocyst as other subunits were not visualized), is present at the developing cell plate (Fendrych *et al.*, 2010). Wu *et al*., (2013) showed that of all the exocyst subunits, only SEC6 interacts directly with KEULE SM (Sec1/Munc 18-like) protein and in tobacco cell culture *At*SEC6 along with KEULE is co-localized on the developing cell plate in Arabidopsis. SEC6, along with EXO70A1, SEC3 and SEC8 was localized in regions of growing root hairs and pollen tube tips (Cole *et al*., 2005; Synek et *al.*, 2006; Hála *et al.*, 2008; Žárský *et al.*, 2009). In Arabidopsis root epidermal cells, exocyst subunits localize to secretory-active regions at the outer plasma membrane (and the dynamics of the exocyst complex visualised in this region by variable angle epifluorescence microscopy revealed that subunits colocalize in defined foci at the plasma membrane (Fendrych *et al.*, 2013). Subcellular localization of ectopically over-expressed Arabidopsis SEC6 was reported in BY-2 cells being predominantly cytoplasmic (Chong *et al.,* 2010).

Physcomitrella patens represents a well-established model for Bryophyta land plant lineage with basal position in the evolutionary Embryophyta tree, and was the first non-flowering plant with fully sequenced genome (Rensing *et al.,* 2008). It is now widely used for cell biological, developmental and evolutionary studies in plants (Prigge and Bezanilla, 2010) and also for comparative studies between higher and lower land plants (Medina-Andrés *et al.*, 2015). Well-established homologous recombination (HR) procedure makes it suitable model for targeted knock-out mutation and subsequent characterization (Schaefer and Zrÿd, 1997; Kamisugi *et al.,* 2006). Our recent report on mutants in one of moss EXO70 subunits, *Ppexo70.3d,* identified pleiotropic defects, namely cell elongation and differentiation of protonema, defective bud development, female sterility due to abnormal egg cell, impaired cell wall and cuticle deposition, defects in cytokinesis and altered response towards exogenous auxin (Rawat *et al.*, 2017). In

this report we use moss *Physcomitrella patens* as a model organism to characterize the role of core exocyst subunit in basal land plants. Unlike other exocyst subunits, *P. patens* genome harbours only single copy of *SEC6* gene. Here we show an essential role of SEC6 in moss growth and morphogenesis. While no full KO was recoverd, insertion partially disrupting the C´-terminus of SEC6 subunit in *P. patens* resulted in mutants arrested in protonema stage with very early gametophore buds aborted

Our data indicate an essential role of moss SEC6 subunit in growth and development of *P. patens* and exocyst´s contribution to the transition from filamentous to the three-dimensional body plan of basal land plants.

RESULTS

SEC6 gene targeting in *Physcomitrella* - only partial knock-out lines generated

Both Physcomitrella and Arabidopsis genomes harbour only one paralogue encoding exocyst subunit SEC6 (Pp1s35_276V6.1), sharing 60% identity on protein level (Eliáš *et al.*, 2003, Synek *et al.*, 2006, Cvrčková *et al*., 2012). The genomic sequence of the *PpSEC6* gene was identified from JGI portal http: genome.jgi.doe.gov/Phypa1_1/Phypa1_1.home.html using Arabidopsis SEC6 homologue. It comprises 25 exons resulting in total length of 2.2 kb cDNA (Figure S1). The replacement construct was designed to delete the 0.8 kb genomic sequence between 7th and 10th exons and to be replaced by 1.860 kb of *nptII* selection cassette.

After repeated series of independent PEG-mediated transformations and preselection of resistant lines, we were finally left with two moss strains (diploid ones and line comprising ectopic insertion were excluded) confirmed by PCR and Southern hybridization (Figure S1). PCR analysis revealed in both lines targeted insertion at the 3´-end retaining original 5´-part of *SEC6* locus sequence unaffected. Full length *SEC6* cDNA, using primers amplifying 2.2 kbp was obtained in WT, but in none of the transformed strains. Western blot analysis showed absence of intact full length SEC6 signal in transformants, however weak band of lower molecular weight indicates truncated *Pp*SEC6 protein presence in transformation surviving lines (Figure S1d). Two independent stable transformed lines producing truncated protein lacking C-terminus displayed similar phenotypic deviations. Despite repeated attempts we failed to get full *Pp*SEC6 knock-out, and therefore we conclude, that full-gene replacement is gametophytically lethal, as is the case in *Arabidopsis* (Hála *et al*., 2008). Here we report that the compromised function of SEC6 causes pleiotropic defects in moss blocked at the protonemal stage of development.

Ppsec6 do not form gametophores and protonemata consist mostly of chloronema cell type.

Ppsec6 mutants produced mostly chloronema, always without gametophores (Figure 1). Strongly diminished number of the caulonema filaments differentiated later than in WT and apical caulonemal

cells in *Ppsec6* mutants were significantly shorter as compared to WT (Fig. 1d). The only difference between the two mutant strains was the modified filament branching in chloronema (Figure 1b); in contrast to WT and *sec6#6,* the *sec6#8* mutant displayed more branched chloronema with multiple short branches emerging from single cell. Cell width was significantly enhanced in both mutant strains on BCD and BCDAT media. Interestingly, chloronema filaments of *Ppsec6* were significantly longer and wider as compared to WT on the both media tested (Figure 1d). The apical caulonemal cell growth velocity in WT was higher in comparison to chloronema in accordance with published data (Menand *et al*. 2007), but also as compared to fewer caulonema of both *Ppsec6* mutant lines. Interestingly however apical cells of chloronema in both *Ppsec6* mutants grew to our surprise significantly faster than WT (Figure 1e). Lack of gametophores formation is not based on lack of gametophores bud initiation. On the contrary - overbudding phenotype was observed in *sec6,* however only section of bud initials continued dividing for few rounds of cell division before arrest/abortion (Figure 1f; see further).

Occasionally, we observed occurrence of cross wall defects (Figure S2) in *sec6* protonemal filaments (1-2 cells/mm^2). Some cells in filaments displayed incomplete stub-shaped septa. However, neighbouring cells were always intact and these deviations do not affect growth of protonemal filaments.

Gametophore initiations in *Ppsec6* mutants are arrested in early stage due to defective/incomplete cell divisions

The most severe phenotypic deviation observed in *Ppsec6* mutants was early abortion of gametophore development. The buds were initiated mostly on the mutant chloronema, later rarely also on caulonema (buds are initiated at caulonema in WT). Number of initiated buds in mutant was distinctly higher than in WT (Figure 1f). The first asymmetric division of bulbous-shaped single cell side branch resulted in the establishment of the apical and basal domains cells (Harrison *et al.*, 2009). This stage and subsequent 4-cell stage derived from division of both apical and basal cells did not display difference between *Ppsec6* mutant lines and WT. Deviations in cell division plane of apical cell occured in following divisions of mutant *Ppsec6* gametophore bud initials. The apical cell in mutants divided frequently perpendicular to basal-apical axis and produced equal sized cells in contrast to WT cells where newly established cell walls were oriented parallely to basal-apical axis and size of daughter cells is not equal. This implies disordered cell division organization resulting probably in compromised cell identity within *Ppsec6* buds. The cells of mutant buds finally divided once or twice again to form apical part consisting of equal sized cells which stopped further divisions and aborted (Figure 2h,i,m,n). The basal cells continued dividing and formed rhizoid-like initials on the lateral cells before the bud abortion. In most cases, bud aborted in 8-10 cell stage. Single tetrahedral shaped meristematic apical cell which initiates regular phyllids formation in WT (Harrison *et al*., 2009), never formed in *sec6* mutants. General feature of *Ppsec6* buds is

also the expansion of daughter cells in the apical part – they are significantly bigger when compared to WT. When buds of mutant lines reached the stage of about 8-10 cells (including some multinucleated cells due to incomplete cross walls — Figure 3g) they stopped dividing, or necrosis started to spread from the apex (Figure 2j,o). Occasionally, (esp. upon the increased humidity some apical cells continued dividing in perpendicular manner to original bud growth axes direction resulting in the formation of a new ectopic chloronema filament – i.e. reversion back to protonema cell identity. Mispositioned divisions and abnormal cell expansion were however not the only reason for buds' collapses in *Ppsec6* mutants. By detailed 3D analysis of cross walls within these buds, we found incomplete cell walls in *Ppsec6* mutant strains — feature never observed in WT. Confocal micrographs of propidium iodide stained mutant buds, in various bud areas and developmental stages revealed severe damage of the mutant cell walls, especially in abnormally shaped apical-dome cells. The first oblique cell wall was always intact in *Ppsec6* mutants, thus the first bud cytokinesis gave rise to two correctly separated apical and basal cells. The first incomplete cross walls perforations appeared in the subsequent division as an irregular ring of tiny gaps attached to the maternal cell wall. The size of the 4-celled buds was still similar to WT in both mutant lines (see above). However newly formed cross walls after the following divisions in mutant cells were often disrupted by variable sized gaps, mostly bigger as compared to those observed after the second division described above. The size of cell wall gaps thus increased progressively with the bud development (Figure 3f,h). These aberrant cross wall stuctures resembled spider-web anchored by narrow strips of cell wall material to the maternal cell wall – clearly indicating incomplete cell plate fusion with the parental cell wall. We observed sometimes unseparated multiple nuclei accumulated in one expanded cell of apical dome (Figure 3g). The apical domain cells of collapsing mutant buds displayed an extensive lack of the cell wall material - gap size ranged from one third to more than one half of complete cross wall (Figure 3f,h). This aberrant cell divisons finally resulted in cell collapse and necrosis of the mutant bud primordia.

Complementation of the *Ppsec6* deviations by the moss and Arabidopsis cDNA orthologs

To verify specifity of phenotypic deviations related to the partial deletion of SEC6 exocyst subunit and to assess its evolutionary conserved function between non-vascular plants and angiosperms, two complementation experiments were performed. Firstly, *Ppsec6* mutants were complemented with *PpSEC6* cDNA driven by maize ubiquitin promoter from neutral/silent locus. We recovered both complemented strains *UBQ:SEC6/sec6#6* and *UBQ:SEC6/sec6#8* displaying fully restored gametophore development (Figure 4b,c,d,g,h). Also both *Ppsec6* mutant lines were complemented by Arabidopsis *AtSEC6* cDNA resulting in *UBQ:AtSEC6/sec6#6* and *UBQ:AtSEC6/sec6#8* complementants (Figure 4e,f,h). Insertion of full length cDNAs was verified by PCR, RT-PCR and immunologically in case of

moss mutants complemented by Arabidopsis cDNA, using αAtSEC6 antibodies. In all the complemented lines, the triangular meristematic cell was established in the buds and these buds showed normal development into gametophores (Figure 5). Complemented plants showed variable small deviations in shape of some phyllids and in early leafy shoot growth compared to WT. Fully developed gametophores of complemented lines displayed proportion of narrow phyllids with multiple tips (Figure S4). All complemented lines were also subjected to sporophyte inductive conditions. Despite of the well-developed antheridia and archegonia in all of tested strains, only *UBQ:PpSEC6/sec6#6* formed sporophyte capsules containing viable spores (Figure 4d,g).

GFP-SEC6 and SEC6-mRUBY2 tagged lines indicate a role of SEC6 in cytokinesis

To investigate the localization of SEC6 the overexpressions of *Pp*SEC6-GFP and *Pp*SEC6-mRUBY2 in WT and *Ppsec6* mutants under the UBQ promoter were performed (problems with Sec6-GFP complementation are discussed further). Transformed lines displayed fluorescence in cytoplasm, nuclear envelope and cross walls. Cytoplasmic signal showed diffused distribution within protonema with disticnctly enhanced fluorescence domainsobserved at growing tips and in rhizoid initials. Fluorescence was not increased within gametophores bud cells except for rapidly growing basal rhizoids and especially axillary hairs emerging from adaxial side of phyllids, which showed extraordinary strong GFP signal (Figure 6a,b). During the cytokinesis, we observed distinct fluorescent area 'cloud' around the expanding cell plate (Figure 6d). The spindle shape of fluorescent signal with nuclei in polar position resembled the microtubule array (Doonan *et al*., 1985) (Figure 6d; Movie S1). Changes of the GFP/mRUBY cloud localization and intensity were visualized during more than 1h after the first detection of the cell plate (Movie S1). In contrast to WT and tagged strains, where the cell plate formation (monitored by FM4-64 stainig) was finished within approx. 20 min (Movies S1,S2) both *sec6* lines were surprisingly unable to finish intact cell plate under the same observation conditions. Nascent cell plate of *Ppsec6* mutants stalled and subsequently disintegrated into separated spots (Movies S3,S4).

Partial *Pp*SEC6 membrane localization after the cell extracts fractions separation

In order to estimate the proportion of association of *Pp*SEC6 protein with membranes we used the Optiprep density gradient ultracentrifugation of cell extracts from moss complementants expressing *At*SEC6 (as we could use Arabidopsis spec. Sec6 antibody; and WT as another control). To establish fraction identity, we used P-H+ATPase and SPS (sucrose phosphate synthase) antibodies in Western blot analysis. Plasma membrane fraction P-H+ATPase signal was detected in the two upper fractions of the gradient and SPS cytoplasm marker was found in fractions III. to V. The maxima of *At*SEC6 signal corresponded to III-V cytoplasmic fractions, however weak yet distinct signal was also localized to P-

H+ATPase positive PM I-II fractions. Alternatively, the results of fractionation by two-step 100,000 x g microsomes isolation also indicate that minor part of SEC6 is associated with the microsomal fraction (Figures S5,S6).

DISCUSSION

Here we report function of exocyst subunit SEC6 in moss *Physcomitrella patens* using targeted gene knock-out approach. Generally, gene targeting might result in variety of outcomes for example either correct gene replacement by HR, or one-sided integration of donor fragment on one end while non-homology integration occurs at the other. Integrated DNA can be highly rearranged. Original sequence might be excised by homologous recombination and re-integrated to the genome non-homologously (Kamisugi *et al.,* 2006 Wendeler *et al.*, 2015). Despite an extensive effort to create a full *Pp*SEC6 knock-out, we obtained two strains with partial deletions at N´-terminal part. This clearly indicates that the full-gene replacement is gametophytically lethal, as seen for Arabidopsis *sec6-1* and *sec6-2* mutants (Hála *et al.*, 2008). Two independent mutant strains expressing the partial SEC6 fragment, enable us to study SEC6 role in moss growth and development. These two lines display minor differences in growth rate and ratio chloronema/caulonema, and behave similarly in crucial processes, as in the gametophore failure and the complementation rescue. The expression of SEC6 profile is ubiquitous in Physcomitrella, slightly increased in caulonema and within certain sporophytic stages (Ortiz-Ramírez *et al.*, 2016).

Plants defective in SEC6 function display severe developmental changes, as expected. Based on characterization of mutant phenotypic deviations, we can conclude that also moss SEC6 subunit is involved in secretion, as affecting protonema cell elongation. The pollen tube growth arrest was described previously in exocyst core subunits mutants (*sec6, sec8*, *sec10*) and in *sec5a/sec5b* single and double mutants (Cole *et al*., 2005; Hála *et al*., 2008; Bloch *et al*., 2016). The caulonemal cell length is reduced in mutant strains, which is consistent with increased expression of SEC6 in caulonema (Ortiz-Ramírez *et al.*, 2016) and with enhanced demand for cell wall components in the rapidly growing filaments. Caulonema requires 7 hours compared to 24 hours of chloronemal cell cycle to produce new daughter cell (Menand *et al*., 2007; Schween *et al.,* 2003). Different role of both protonema types in moss was shown by distinct organelle distribution. In caulonema, it was estimated 1.2 to 2.7 more Golgi dictyosomes to be present compare to chloronema, which indicates increased trafficking and secretion activity in caulonema (Furt *et al*., 2012). We speculate that both diminished caulonemal apical cell length and decreased growth rate in moss *sec6* are related to restricted exocyst functions. This is reminiscent of the *PpEXO70.3d* mutants, where caulonema differentiation was completely arrested under the normal conditions (Rawat *et al*., 2017). Dominant chloronemal cells in *sec6* are less affected which might be consistent with lower SEC6 expression in chloronema (Ortiz-Ramírez *et al.*, 2016). In slowly growing protonema (i.e. chloronema),

demand for the cargo delivery at the tip is well covered even in cells with compromised SEC6 function, the cell wall in bud initiating cells is not sufficiently supplied by cell wall constituents. Chloronemal apical cells were longer and wider in *sec6.* Under the unfavourable environmental conditions, chloronema cells might convert into brachycytes, which is induced by abscisic acid (Schnepf and Reinhard, 1997). The wider chloronema cell phenotype is reminiscent of the exogenous ABA treated protonema (Sakata *et al.,* 2009) which triggered brood cells formation. Increased cell width observed in *sec6* protonema and intercalary divided chloronema cells with incomplete septa (Figure 2a, Figure S2) indicates sensitivity to stress.

Direct consequence of insufficient cell wall material delivery in developing buds were incomplete septa in all of them. Origin the three-planned body form derived from the proper sequence of assymetrical cell divisions (Harrisson *et al.,* 2009) is disturbed in *sec6*. Defective cell walls, together with origin of multinucleated cells disrupted normal cell division plane. Moss *sec6* mutants display two strong defects within bud development – firstly changes in the division plane resulting in the loss of polarity and secondly during new cross wall maturation often lesions are present, resulting in gaps in cell wall. It is known that transition from protonemal to gametophore growth is regulated by cytokinins, (Hahn and Bopp, 1968, von Schwartzenberg *et al*., 2007). Leafy shoots in *Ppsec6* were never formed despite applying exogenous BAP, thus we speculate that *Ppsec6* have low response or resistancy to cytokinins (data not shown/or supplementary data).

Bud initials in moss exocyst mutant *Ppexo70.3d* emerged from chloronema, because true caulonema is not developed. The third cell division in apical dome displays altered orientation. Most of those mutant buds developed later in stunted gametophores. Few of mutant buds stopped differentiation after the second division of basal cell. Not frequent de-differentiation back into filaments was also observed similarly as in *sec6* buds (Rawat *et al.*, 2017).

In flowering plants, DEK1 plays an important role in perception and response to positonal cues involved in formation and function of the epidermal layer in developing seeds. In moss, DEK1 is involved in precise positioning of cell divisions in emerging buds, Δ*dek1* display abnormal orientation in cell division resulting in a developmental bud arrest and inability for further three dimensional growth. Interestingly filament growth was not affected (Perroud, *et al.* 2014). Single codon (Cys for Ser) replacement mutant *dek1°* displays normal early stage divisions in bud; however tetrahedral stem cells and lateral cells are not established. Those phenotypic deviations are almost identical to the ones observed in *Ppsec6* mutant lines; initial divisions (up to third) seem to be completed correctly in *sec6*, Δ*dek1* and *dek1°*. Differentiation of meristematic apical cell, which give rise initial of WT phyllids, fails in all cases. Complementation of Δ*dek1* by *PpDEK1 cDNA* or only moss calpain domain restored formation of gamethophores, expression of *A. thaliana* or *Z. mays* calpain domain did not complement Δ*dek1* (Perroud

et al., 2014). DEK LG3 domain mutant phenotype was rescued by complementation of moss and *Marchantia polymorpha LG3* construct. The same approach used with Arabidopsis DEK1 LG3 did not produce phenotypically rescued plants (Johanssen *et al*., 2016). Gametophore-less plants were also reported in mutants lacking ARPC1 subunit of the Arp2/3 complex (Harries, *et al*. 2005). Furthermore, *arpc1* mutants were unable to form caulonema, defective chloronema consists of short, irregularly shaped cells displaying abnormal division pattern. Arp2/3 complex controls polarized growth and cell division patterning through its regulation of actin (Harries, *et al*. 2005). This indicates that the differentiation of gametophores relies on correct polarity establishment as well as cell identity determination.

Ppton1 loss-of-function mutants also display severe alterations in bud initials as abnormal division plane of the apical cell. Despite impaired division plane, the strongly distorted gametophores still eventually developed. TON1 is related to function, formation and dynamics of preprophase band in gametophores, but not in protonemata (Spinner, *et al.* 2010). AP2 (APETALA)-type transcription factor, also directly regulates bud development. Quadruple disruption of APB genes in Physcomitrella blocked completely gametophore formation (Aoyama *et al*., 2012). Rescue of gametophores in all complemented *sec6* strains and sporophyte recovery in one of them, corroborates an essential role of SEC6 subunit in all stages of moss life cycle.

Abberant initial phases of cell plate development was shown by Fendrych *et al*., 2010, in Arabidopsis *exo70A1* homozygous plants, where newly initiated cell plate was transiently donut-shaped in contrast to solid initial cell plate in WT, gap might be caused by inability of vesicles to fuse efficiently which we presume in *sec6* buds in moss. Moreover, in *Atexo84b* mutant incomplete cell divisions and cell wall stubs were reported (Fendrych *et al*., 2010). Both *Atexo84* and *Atsec6* show lesser defect in leaf epidermal pavement cells and severe impairment in the guard cells, both resulting from the collapse of immature post-cytokinetic cell walls (Fendrych *et al*., 2010). We observed that GFP-tagged SEC6 were associated closely with cell plate during cytokinesis which enable us explain cross wall defects in mutant buds. The moss mutant *Ppexo70.3d* displays defects in protoplast division, and exhibits delayed or incomplete cell plate formation in protonema similarly to cytokinesis defects in *sec6* (Rawat *et al.*, 2017). Arabidopsis VAMP721 and VAMP722 are R-SNAREs involved in cell plate formation during the cytokinesis. Homozygous double mutant *vamp721vamp722* display lethal dwarf phenotype and defective cytokinesis resulting frequently in the cell wall stubs formation (Zhang *et al*., 2011).

Likewise, mutations of two key subunits of TRAPPII tethering complex (regulator of post-Golgi trafficking) AtTRS120 and AtTRS130, result in defects in cytokinesis, cell polarity and often cause incomplete cell walls in Arabidopsis root tip and cotyledon cells (Qi *at al*., 2011). Described defects in Arabidopsis (Qi *at al*., 2011) are similar to ones observed in *Ppsec6* mutants implying that cell wall defects are associated with disordered vesicle trafficking machinery. The best studied Arabidopsis *knolle*

(kn) syntaxin secretory mutant phenotype resembles also cross wall defect in *Ppsec6, knolle* embryo displays enlarged cells with polyploid nuclei incompletely divided with cross wall fragments (Lukowitz *et al.*, 1996). The embryo in Arabidopsis mutant *keule,* shows large multinucleate cells with distinct gaps in cell walls or incomplete cell walls (Assad *et al.*, 1996).

Observed collapses of nascent cell plates during cytokinesis in *sec6* mutants denote higher sensitivity to the shock associated with tissue transfer and FM4-64 treatment, and this observation indicates defective cell wall (Movie S1,S2,S3).

It has been suggested that axillary hair cells in mosses (and all Bryophyta) function in protection and water retaining by secreting mucilage to defend newly formed tissues from desiccation as they are located in the axils of young leaves (Ligrone, 1986; Medina *et al.,* 2011). Axillary hair in Physcomitrella typically consists of two cells (or three comprising epidermal cell), apical=distal cell and basal cell=stalk (Piatkowski, unpublished). We detected strong GFP-SEC6 and SEC6-mRUBY fluorescence in distal cells of axillary hair of newly formed gamethophores. Signal intensity in the stalk cell is weak, comparable to other phyllids cells. SEC6-GFP localization in distal cells differs according to phyllid development stages, in young phyllids we observed more intensive fluorescence, which gives us evidence of the intensive secretion here, whereas clearly weaker and diffused signal occures in post-secretory cells of mature phyllids (Figure 7). Observed SEC6 localization pattern resembles PpCeSA6-GFP expression which is found to be localized in axillary hairs and in the basal rhizoid initials (Wise *et al*. 2011). Occurence of both proteins in axillary hairs is consistent with demands for increased exocytosis - secretion of mucilage through cell wall ruptures (Piatkowski, unpublished). Our results suggest that SEC6 is highly expressed in certain developmental stages, and tissues where indicates increased exocytotic activity.

Cross complementation verified the assumption that SEC6 exocyst is highly conserved core exocyst subunit between basal land plants Bryophyta and Angiosperms. Arabidopsis SEC6 from the sporophytic tissue only partially complemented haploid moss tissue, sporophyte was not observed. The *P. patens* Sec6 protein shares 66 % sequence identity and 86 % similarity with its *A. thaliana* counterpart throughout the whole protein length of 749 amino acids, and the two proteins are thus likely to share overall shape. However, 50 out of the 259 differences affect positions that are absolutely or near-absolutely conserved among monocots and dicots but occupied by an amino acid of substantially different chemical properties in the moss, and many of these positions are clustered in portions of the protein molecule predicted to fold into helices (Figure S7). Albeit Sec6 structure was only partially determined so far, all exocyst subunits are believed to conform to the general CATCHR complex structure with helical bundles exposed to the surface (see Chen et al 2017). At least some of the differences between moss Sec6 and the angiosperm consensus may thus result in altered protein surface properties. The incomplete complementation of our

moss mutants by the *A. thaliana* protein might therefore reflect differences in the ability of moss and angiosperm Sec6 to bind some endogenous protein(s).

Complementation of moss mutant phenotypes by homologous genes from Arabidopsis suggesting a functional conservation throughout evolution of land plants, which bridges period ca. 450 million years (Pires and Dolan, 2012), was reported in several different genes and gene functional groups. *Ppton1* mutant displaying impaired division plane specification and cell elongation defect due involvement in preprophase band function was also successfully rescued by Arabidopsis homologue TON1 (Spinner *et al.*, 2010). Gametophore and sporophyte developmental defects in *Ppxlg* and *Ppgβ2* moss LOFs were also complemented by Arabidopsis G-protein components *XLG2* and *AGB1* genes important for cell cycle completion (Hackenberg *et al.,* 2016). Knock-out of *Pp*ARP3a locus caused severe defects in caulonema, rhizoids and gametophore differentiation, and changes in size and shape of chloronemal cells; complementation with both, moss or Arabidopsis orthologs *ARP3* cDNA restored normal overall morphology and development (Finka *et al.,* 2008).

The results of the immunological localization between cytosolic and microsomal fractions were consistent with microscopic observations of GFP or mRUBY tagged *Pp*SEC6 transformed lines where signal was present throughout the protonema cells, mostly in cytoplasm. The most of the signal was associated with the cytosolic fractions, whereas in microsomal fractions was weak. Signal was enriched around the nuclear envelope, cross walls and apical region of rapidly growing cells and particularly associated with cell plate.

In Arabidopsis, predominant tip-focused localization of SEC6 was found in pollen tubes, much weaker signal forming small spots was distributed in the cytoplasm as well (Hála et al., 2008).

Taken together, these data on *Pp*SEC6 distribution between the cytoplasm and membranes demonstrate similarity of our results from the moss with published data from Arabidopsis and Drosophila (Hála *et al*., 2008; Beronja *et al*., 2006). Just as in Angiosperms, exocyst subunit SEC6 is essential for the lifecycle and development in moss as well.

MATERIALS AND METHODS

Plant material and growth conditions

The *Physcomitrella patens* Gransden strain (kindly provided by Fabien Nogué, INRA) was routinely propagated in vitro on BCD medium supplemented with ammonium tartrate dibasic (BCDAT) according to Cove *et al.,* (2009) in a climate chamber under photoperiod 16h day/8h dark at 25°C, illuminated by fluorescent tubes (40-50 μmol $m^{-2}s^{-1}$. For the sporophyte induction mosses were grown on the solid BCD medium or on autoclaved Jiffy pellets in Magenta jars under the 8h light/16h dark regime at 16°C in growth chamber equipped with LED strips (30 μmol m^{-2} s^{-1}).

DNA/RNA extraction

Extraction of DNA for PCR amplification was performed according to the modified protocol of Doyle and Doyle (1990), high-quality DNA for Southern hybridization was purified with DNAzol® Reagent (Invitrogen) following the manufacturer´s instructions.

Total RNA was isolated from 100 mg of partially dry-squeezed one-week-old protonemal tissue using RNeasy Plant Kit (Quiagen) according to manufacturer´s instructions. Reverse transcription was performed using Fidelity cDNA Synthesis Kit (Roche Applied Science). Moss tubulin fragment (GenBank AB0967 18.1) was used as a control for RT-PCR. Concentration of nucleic acids was measured by Spectrofotometer NanoDrop® ND-1000 Thermo Scientific.

Vector cloning, transformation and analysis of the targeting outcomes

The construct was designed to delete 0.8 kb sequence between 7th and 10th exons and replace it by 1,860 kb of *nptII* selection cassette. PCR amplified 5´end homology arm (1342 bp) and 3´end arm (1621 bp) of *PpSEC6* genomic sequence were cloned into vector PMCS5-LOX-NptIIr-LOX comprising kanamycine resistence (1621 bp) under the 35S. Linearized vector was used for PEG mediated transformation as described in (Schaefer *et al.*, 1991). Two selections on BCDAT medium supplemented with G418 (30 mg/l) were interrupted by two weeks on antibiotic-free medium.

PCR analyses of gene targeting events in mutant lines used three pairs of primers. The 5´end and 3´end specific primers pointing inward come out of sequences located outside of targeting place in combination with outward pointing primers specific to the selection cassette revealed insertion of *NPTII* by homologous recombination on 3´end combined with non-homology end joining on 5´end. Pair of primers derived from the sequence between *Xho*I and *Spe*I amplified 0.7 kb and confirmed persisting of the original 0.8 kb sequence. PCR using pair of primers positioned outside of the targeted sequence was used for full-length amplification.

Protein Gel Blot analysis

In this work we used two different antibodies directed SEC6: A) Polyclonal α-*At*SEC6 antibody was prepared against truncated *At*SEC6 protein, *At*SEC6 cDNA was cleaved by *Bam*HI and religated (Hála *et al*., 2008); B) Polyclonal α-*At*SEC6 antibody was raised against the synthetic peptide (Ac-)NPPKTGFVFPRVKC(-$CONH_2$); this antibody was used for complemented moss lines. Total protein was extracted from 100-150 mg freshly harvested protonemal tissue with 250 µL of modified Sec6/8 homogenization buffer (Hsu *et al*., 1996) (20mM HEPES, pH 6.8, 150mM NaCl, 1mM EDTA, 1mM DTT and 0.5% Tween 20), supplemented with 1x protease inhibitor coctail (Sigma-Aldrich), centrifuged 10 min at 14,000 x g. Supernatants were incubated with 6x loading buffer for 10 min at 98°C and loaded

on 10% SDS-PAGE. Proteins were electroblotted to the nitrocellulose membrane (WHATMANN Optitran BA-S-83) and stained by Ponceau Red (2% Ponceau S in 30% trichloracetic acid and 30% sulfosalicylic acid). Membranes were blocked overnight with 5% non-fat dry milk in PBST (10 mM sodium phosphate, pH 7.2, 0.9% (w/v) NaCl, 0.5% Tween- 20) at 4°C. Blots were incubated with primary antibody (1:10,000) dissolved in blocking solution for 3 h at room temperature, then for 50 min with secondary antibody (conjugated horseradish peroxidase; Anti-mouse IgG Promega) dissolved in blocking solution (1:10,000). Chemiluminiscent ECL detection (Amersham) was carried out and signal exposed to the photosensitive material (Medix XBU FOMA).

Southern hybridization

The DIG labeled probe was synthetized with PCR DIG Probe Synthesis Kit (Roche) from pMCS5-LOX-NptIIr-LOX using primers designed to amplify 0.7 kb fragment of *NPTII*. Moss DNA was extracted from 8-days-old protomema subcultured on BCDAT. Harvested tissue was gently squeezed beween sheets of paper towels, grinded with mortar and pestle in liquid nitrogene and powderized plant material was transfered into Plant DNAzol Reagent (Invitrogen). DNA purification was performed according to the manufacturer´s protocol.

Digestion of DNA (5 µg of each) was done overnight. Samples (40 µl) were mixed with µl 5x bromphenol loading dye and loaded along with the Digoxigenin labeled DNA Molecular Weight Marker III (Roche) on the EtBr-free gel (0.8% agarose in TBE). Gel was run at 0.1-0.2 V cm^{-1} overnight. The gel was then subjected depurination and denaturation followed by neutralization, all steps were done according to Roche´s kit protocols. Genomic DNA fragments were transferred onto the nylon membrane (Hybond Amersham) by overnight capillary blotting and then crosslinked to the wet membrane using UV crosslinker (1200 µJ for 30 s; UV Stratalinker). The membrane was washed by water, incubated in pre-warmed Dig Easy Hyb solution (Roche) for 1.5 h at 42°C and then hybridized with Dig-labeled probe overnight at 42°C. After hybridization, the membrane was slowly shaked in Blocking solution (Dig Wash and Block Buffer Set Roche) containing α-DIG antibody (1:10,000) for 30 min at room temperature. Dig Luminiscent Detection Kit and CDP Star (Roche) were used for chemiluminiscent detection.

Microscopy analysis

Microscopic analysis was carried out by Olympus BX 51 microscope with an attached epifluorescence unit and DP50 camera. Growth rates were calculated from 20 h time-lapse imaging recorded every 20 min under continuous light using the filament tip position of the first and final images. The analySIS® (Soft Imaging System) software was used for image processing. The measurement of filament growth rate was done with ImageJ software (http://rsb.info.nih.gov./ij/). Life imaging of propidium iodide stained buds

(10-15 µg ml^{-1} PI in liquid BCD) was performed with Zeiss LSM 5 DUO confocal laser scanning microscope equipped with Plan-Apochromat 20x/0.8. Excised buds together with short protonema were stained and mounted into glass slide chambers (Lab-Tek II). PI fluorescence was excited at 514 nm with 18%-24% laser power and detected with BP 575-615 IR filter. Zeiss LSM Image Browser Software was used for image analysis and projections.

Microscopic analysis of cytokinesis was performed using an inverted confocal microscope Nikon Spinning Disc Microscope T2 Eclipse (CSU-X1 Yokogawa, Tokyo, Japan, on a Nikon Ti-E platform, Laser box MLC400 Agilent, Santa Clara CA, USA, Zyla cMOS camera by Andor, Belfast, UK). Nikon APO 40x wi and 60x PFS wi objective lenses were used for live cell imaging of four-day-old moss tissue. Moss was stained with 5µM FM 4-64 (Invitrogen).

Macroscopic images were taken by Nikon 5200 digital camera with Sigma 90 mm/2.8 objective supplemented by the life size +10D secondary lens.

_Pp_SEC6 and _At_SEC6 complementation assay

PpSEC6 and *AtSEC6* cDNA was amplified and cloned via *Eco*RI and *Xho*I restriction sites into pENTR3C. Resulting constructs (pENTR3C+*PpSEC6*, pENTR3C+*AtSEC6*) were verified by sequencing. LR reactions (Gateway LR Clonase II Enzyme Mix, Invitrogen) between Entry clones and pThubi-GATE vector were performed according producer´s instructions. *Swa*I linearized vectors were used for the biolistic transformation of WT, *sec6#6* and *sec6#8*. Particle bombardment was carried out by PDS-100/He Instrument (BioRad). The third day after the transformation, the celophane discs with moss tissue were transferred on BCDAT solid medium supplemented with 30 mg l^{-1} hygromycin. Resistants displaying gametophore growth were picked up after 14 days of selection and kept on antibiotic-free medium for 10 days followed by the second selection. Independent lines were obtained from individually excised phyllids.

Transformation of GFP and mRUBY2 tagged _Pp_SEC6 lines

GFP (from pGWB6 plasmid) sequence was PCR amplified from pGFP-1 with a pair of primers flanking restriction sites 5´*Kpn*I and 3´*EcoR*I. We modified previously prepared Entry clone harbouring *SEC6c*DNA by insertion of the GFP sequence lacking stop-codon between *Kpn*I and *Eco*RI.

The *PpSEC6* coding sequence was cloned into the Gateway® TagRFP-AS- N vector (Evrogen), where original RFP was previously replaced by mRUBY2 sequence from pcDNA3.1-Clover-mRuby2 (Addgene plasmid #49089). LR reactions between Entry clones and pTHUBi-GATE destination vector containing Pp108 neutral site were performed according producer´s instructions.

Preparation of cytoplasmic and microsomal fractions

Moss material (0.8-1 g of WT and *At*-complemented mutant lines) was homogenized in liquid nitrogen with mortar and pestle. Moss tissue powder was resuspended in Sec6/8 buffer with 10µl/1ml of protease inhibitors and homogenates were centrifuged in two steps (15,000 rpm/1 min and 10,000 rpm/10 min) at 4°C. Supernatants (total extract) were collected. Protein concentration in samples was measured, and then equilibrated to the same content. The microsomal and cytosolic fractions were separated by centrifugation at 100,000 x g for 60 min at 4°C. Supernatants were collected and pellets resuspended to the same volume with Sec6/8 buffer supplemented by protease inhibitors. Finally, supernatants and resuspended pellets were centrifuged for the second time at 100,000 x g for 60 min at 4°C. Cytoplasmic proteins from supernatants and microsomal fractions from pellets were separated on 8% SDS–PAGE and electroblotted. Membranes were incubated with primary α-SEC6 (1:10,000), and then with secondary antibody (1:10,000). ECL detection was performed. The same process was done parallelly with α-H+ATPase (Agrisera) as a control.

Optiprep density gradient ultracentrifugation

300 µl of total protein extract (described above) were mixed with the same volume of OptiPrep (Sigma) solution and spun down at 100,000 x g for 120 min. Approximately 100 µl of each fraction were separated and used for protein gel blot analysis. Arabidopsis specific α-SEC6 (1:10,000) was used. α-H+ATPase (1:2,000) and α-SPS (1:4,000) antibodies (both Agrisera) were used for control of fraction identity.

Images were compiled using Adobe Photoshop (Adobe, http://www.adobe.com/).

BIOINFORMATIC SOURCE

Genomic sequence and CDS of *PpSEC*6 were downloaded from:
http://genome.jgi.doe.gov/Phypa1_1/Phypa1_1.home.html.

ACKNOWLEDGEMENTS

We thank to Fabien Nogué, Louis Vidali and Helena Štorchová for providing vectors and protocols. This work was supported by grants from the Marie Curie Network (No. 238640 582 PLANTORIGINS), MSMT (NPUI LO1417) and GACR (15-14886S).

SUPPORTING INFORMATION

Figure S1. Structure of *PpSEC6* gene.

Figure S2. Cell wall defects in *sec6* protonema

Figure S3. Spores of WT and complemented line *UBQ:PpSEC6/sec6#6.*

Figure S4. Leaves series to compare WT and complemented lines in 4 wk.

Figure S5. Protein gel blot analysis of *Pp*SEC6 localization. Cytosolic and microsomal fractions were separated by two-step 100,000 x g ultracentrifugation.

Figure S6. Protein gel blot analysis of *Pp*SEC6 localization. Cytosolic and microsomal fractions were separated by Optiprep fractionation

Figure S7. Alignment of Sec6 orthologs from P. patens, A. thaliana and selected representative species from angiosperm and non-angiosperm lineages.

Movie S1. Cytokinesis in FM4-64 stained GFP-tagged complemented strain.

Movie S2. Cytokinesis in FM4-64 stained WT.

Movie S3. Cytokinesis in FM4-64 stained *sec6#6* strain.

Movie S4. Cytokinesis in FM4-64 stained *sec6#8* strain.

Table S1. List of primers used in this study

REFERENCES

Aoyama T., Hiwatashi Y., Shigyo M., Kofuji R., Kubo M., Ito M. and Hasebe M. (2012) AP2-type transcription factors determine stem cell identity in the moss Physcomitrella patens. *Development*, **139,** 3120-3129.

Assaad, F., Mayer, U., Wanner, G. and Jürgens, G. (1996) The KEULE gene is involved in cytokinesis in Arabidopsis. *Mol Gen Genet*. **253**, 267–277.

Beronja, S., Laprise, P., Papoulas, O., Pellikka, M., Sisson, J. and Tepass, U. (2005) Essential function of Drosophila Sec6 in epithelial cell-type specific basolateral and apical exocytosis. *Journal of Cell Biology,* **169**, 635-646.

Cole, R.A., Synek, L., Žárský. V. and Fowler. J.E. (2005) SEC8, a subunit of the putative Arabidopsis exocyst complex, facilitates pollen germination and competitive pollen tube growth. *Plant Physiol.* **138**, 2005-18.

Cove, D.J. and Knight, C.D. (1993) The Moss Physcomitrella patens, a Model System with Potential for the Study of Plant Reproduction. *The Plant Cell*, **5,** 1483-1488.

Cove, D., Perroud, P.-F., Charron, A., McDaniel, S., Khandelwal, A. and Quatrano, R. (2009) The moss *Physcomitrella patens*: a novel model system for plant development and genomic studies. Emerging Model Organisms. NewYork, NY, USA: Cold Spring Harbor Laboratory Press.

Cvrčková, F., Grunt, M., Bezvoda, R., Hála, M., Kulich, I., Rawat, A. and Žárský, V. (2012) Evolution of the land plant exocyst complexes. *Front. Plant. Sci.* **3**, 159.

Doonan, J.H. and Cove, D.J. (1985) Immunofluorescence microscopy of microtubules in intact cell lineages of the moss, *Physcomitrella patens*. *J. Cell. Sci.* **75**, 131-147.

Doyle, J.J. and Doyle, J.L. (1990) Isolation of plant DNA from fresh tissue. *Focus*. 12, 13–15.
Dubuke, M.L., Maniatis, S., Shaffer, S.A. and Munson, M. (2015) The Exocyst Subunit Sec6 Interacts with Assembled Exocytic SNARE Complexes. *J. Biol. Chem.* **290**, 28245-28256.

Eliáš, M., Drdová, E., Ziak, D., Bavlnka, B., Hála, M., Cvrčková, F., Soukupová H. and Žárský V. (2003) The exocyst complex in plants. *Cell. Biol. Int.* **27**, 199-201.

Fendrych, M., Synek, L., Pečenková, T., Toupalová, H., Cole, R., Drdová, E., Nebesářová, J., Šedinová, M., Hála, M., Fowler, J.E. and Žárský, V. (2010) The *Arabidopsis* Exocyst Complex Is Involved in Cytokinesis and Cell Plate Maturation. *The Plant Cell*, ***22***, 3053–3065.

Fendrych, M., Synek, L., Pečenková, T., Janková Drdová, E., Sekereš, J. de Rycke, R., Nowack, M.K. and Žárský, V. (2013) Vizualization of the exocyst complex dynamics at the plasma membrane of the *Arabidopsis thaliana. Molecular Biology of the cell. **24,*** 510-520.

Finka, A., Saidi, Y., Goloubinoff, P., Neuhaus, J.M., Zrÿd, J.P. and Schaefer, D.G. (2008) The knock-out of ARP3a gene affects F-actin cytoskeleton organization altering cellular tip growth, morphology and development in moss *Physcomitrella patens*. *Cell Motility and the Cytoskeleton,* **65**, 769-784.

Guo, W., Roth, D., Walch-Solimena, C. and Novick, P. (1999) The exocyst is an effector for Sec4p, targeting secretory vesicles to sites of exocytosis. *EMBO J*. **18**, 1071-1080.

Hackenberg, D., Perroud, P. F., Quatrano, R. and Pandey, S. (2016) Sporophyte formation and life cycle completion in moss requires heterotrimeric G proteins. *Plant Physiology*, **172,** 1154-1166.

Hahn, H. and Bopp, M. (1968) A cytokinin test with high specificity. *Planta,* **83**, 115-118.

Hála, M., Cole, R., Synek, L., Drdová, E., Pečenková, T., Nordheim, A., Lamkemeyer, T., Madlung, J., Hochholdinger, F., Fowler, J.E. and Žárský V. (2008) An Exocyst Complex Functions in Plant Cell Growth in *Arabidopsis* and Tobacco. *The Plant Cell*, **20**, 1330-1345.

Harries, P.A., Pan, A. and Quatrano, R.S. (2005) Actin-related protein2/3 complex component ARPC1 is required for proper cell morphogenesis and polarized cell growth in Physcomitrella patens. *The Plant Cell***, 17**, 2327–2339.

Harrison, C.J., Roeder, A.H.K, Meyerowitz, E.M. and Langdale, J.A. (2009) Local cues and asymmertic cell divisions underpin body plan transitions in the Moss *Physcomitrella patens. Current Biology,* **19**, 461-771.

He, B. and Guo, W. (2009) The Exocyst Complex in Polarized Exocytosis. *Current Opinion in Cell Biology*, **21**, 537–542.

Heider, M. R., and Munson, M. (2012) Exorcising the Exocyst Complex. *Traffic,* **13,** 898–907.

Heider, M.R., Gu, M., Duffy, C.M., Mirza, A.M., Marcotte, L.L., Walls, A. C., Farrall, N., Hakhverdian, Z., Field, M.C., Rout, M.P., Frost, A. and Munson, M. (2016) Subunit connectivity, assembly determinants and architecture of the yeast exocyst complex. *Nature Structural and Molecular Biology,* **23**, 59-66.

Hong, W. and Lev, S. (2014) Tethering the assembly of SNARE complexes. *Trends Cell. Biol.* **24**, 35-43.

Hsu, S.C., Ting, A.E., Hazuka, C.D., Davanger S, Kenny, J.W., Kee, Y. and Scheller, R.H. (1996) The mammalian brain rsec6/8 complex. *Neuron,* 17, 1209-19.

Chong, Y.T., Gidda, S.K., Sanford, Ch., Parkinson, J., Mullen, R.T. and Goring, D.T. (2010) Characterization of the *Arabidopsis thaliana* exocyst complex gene families by phylogenetic, expression profiling, and subcellular localization studies. *New Phytologist,* **185**, 401-419.

Finka, A., Saidi, Y., Goloubinoff, P., Neuhaus, J.M., Zrÿd, J.P. and Schaefer, D.G. (2008) The knock-out of ARP3a gene affects F-actin cytoskeleton organization altering cellular tip growth, morphology and development in moss *Physcomitrella patens*. *Cell Motility and the Cytoskeleton,* **65**, 769-784.

Furt, F., Lemoi, K., Tüzel, E. and Vidali, L. (2012) Quantitative analysis of organelle distribution and dynamics in Physcomitrella patens protonemal cells. *BMC Plant Biology,* **12,** 70. http://doi.org/10.1186/1471-2229-12-70.

Johansen, W., Ako, A.E., Demko, V., Perroud, P.-F.,Rensing S.A., Mekhlif, A.K., and Olsen O.-A. (2016) The DEK1 calpain linker functions in three-dimensional body patterning in *Physcomitrella patens*. *Plant Physiology*, **172,** 1089–1104.

Kamisugi, Y., Schlink K., Rensing, S.A, Schween, G., von Stackelberg, M., Cuming, A.C, Reski R. and Cove, D.J. (2006) **The mechanism of gene targeting in Physcomitrella patens: homologous recombination, concatenation and multiple integration.** Nucleic acids research, **34**, 6205-14.

Komsic-Buchmann, K., Stephan, L.M. and Becker, B. (2012) The SEC6 protein is required for contractile vacuole function in *Chlamydomonas reinhardtii. Journal of Cell Science,* **125**, 2885–2895.

Koumandou, V.L., Dacks, J.B., Coulson, Richard M.R., R.M. and Field, M.C. (2007) Control systems for membrane fusion in the ancestral eukaryote; evolution of tethering complexes and SM proteins. *BMC Evol. Biology,* **7**, 29. doi:10.1186/1471-2148-7-29.

Lamping, E., Tanabe, K., Niimi, M., Uehara, Y., Monk, B.C. and Cannon, R.D. (2005) Characterization of the Saccharomyces cerevisiae sec6-4 mutation and tools to create S. cerevisiae strains containing the sec6-4 allele. *Gene,* **361**, 57-66.

Ligrone, R. (1986). Structure, development and cytochemistry of mucilage secreting hairs in the moss Timmiella-barbuloides (Brid) Moenk. *Ann Bot.* **58,** 859–868.

Lukowitz, W., Ulrike Mayer, U. and Jürgens, G. (1996) Cytokinesis in the Arabidopsis Embryo Involves the Syntaxin-Related KNOLLE Gene Product. *Cell,* **84**, 61–71.

Medina, R., Lara, F., Mazimpaka, V., Shevock, J.R., Garilleti, R. (2011) Orthotrichum pilosissimum (Orthotrichaceae), a new moss from arid areas of Nevada with unique axillary hairs. *Bryologist,* **114**, 316–324.

Menand, B., Calder, G, Dolan, L. (2007) Both chloronemal and caulonemal cells expand by tip growth in the moss *Physcomitrella patens*. *Journal of Experimental Botany,* **58**, 1843–1849.

Morgera, F., Sallah, M.R, Dubuke, M.L, Gandhi, P., Brewer, D.N, Carr, C.M. and Munson, M. (2012) Regulation of exocytosis by the exocyst subunit Sec6 and the SM protein Sec1. *Mol. Biol. Cell.* **23**, 337-346.

Munson, M., Novick, P. (2006) The exocyst defrocked, a framework of rods revealed. *Nature Structural & Molecular Biology* **13**, 577 – 581.

Songer, J.A. and Munson, M. (2009) Sec6p anchors the assembled exocyst complex at sites of secretion. *Mol Biol Cell.* **20**, 973-982.

Murthy, M., Garza, D., Scheller R.H., Schwarz T.L. (2003) Mutations in the Exocyst Component Sec5 Disrupt Neuronal Membrane Traffic, but Neurotransmitter Release Persists. *Neuron*, **37**, 433-447.

Novick, P., Field, Ch. and Schekman, R. (1980) Identification of 23 complementation groups required for post-translational events in the yeast secretory pathway. *Cell,* **21**, 205-215.

Ortiz-Ramírez, C., Hernandez-Coronado, M., Thamm, A., Catarino, B., Wang, M., Dolan, L., Feijó, J.A. and Becker, J.D. (2016) A transcriptome atlas of *Physcomitrella patens* provides insights into the evolution and development of land plants. *Mol Plant*, **9**, 205–220.

Pečenková, T., Hála, M., Kulich, I., Kocourková, D. , Drdová, E., Fendrych, M., Toupalová, H., and Žárský, V. (2011) The role for the exocyst complex subunits Exo70B2 and Exo70H1 in the plant–pathogen interaction. *Journal of Experimental Botany*, **62**, 2107–2116.

Pires, N.D., and Dolan, L. (2012**).** Morphological evolution in land plants: new designs with old genes. *Philosophical transactions of the Royal Society of London. Series B, Biological sciences*, **367,** 508-518.

Qi, X., Kaneda, M. , Chen, J., Geitmann, A. and Zheng, H. (2011) A specific role for Arabidopsis TRAPPII in post-Golgi trafficking that is crucial for cytokinesis and cell polarity. *The Plant Journal,* **68,** 234–248.

Rawat, A., Brejšková, L., Hála, M., Cvrčková, F., Žárský, V. (2017) The *Physcomitrella patens* exocyst subunit EXO70.3d has distinct roles in growth and development, and is essential for completion of the moss life cycle. *New Phytologist*

Riquelme, M., Bredeweg, E.L., Callejas-Negrete, O., Roberson, R.W., Ludwig, S., Beltrán-Aguilar, A., Seiler, S., Novick, P., Freitag, M. (2014) The Neurospora crassa exocyst complex tethers Spitzenkörper vesicles to the apical plasma membrane during polarized growth. Mol Biol Cell. **25**, 1312-1326.

Sakata, Y., Komatsu, K., Taji, T., & Tanaka, S. (2009). Role of PP2C-mediated ABA signaling in the moss *Physcomitrella patens*. *Plant Signaling and Behavior*, **4**, 887–889.

Schaefer, D.G. and Zrÿd, J.-P. (1997) Efficient gene targeting in the moss *Physcomitrella patens. Plant J.* **11**, 1195-1206.

Schnepf, E. and Reinhard, C. (1997) Brachycytes in Funaria protonemate: induction by abscisic acid and fine structure. *Journal of Plant Physiol.* **151,** 166 – 175.

von Schwartzenberg, K., Núñez, M., F., Blaschke, H., Dobrev, P. I., Novák, O., Motyka, V., Strnad, M. (2007) Cytokinins in the bryophyte Physcomitrella patens: analyses of activity, distribution, and cytokinin oxidase/dehydrogenase overexpression reveal the role of extracellular cytokinins. *Plant Physiol.* **145**, 786-800.

Schween, G., Gorr G., Hohe, A., Reski, R. (2003) Unique tissue-specific cell cycle in *Physcomitrella*. *Plant Biology* **5,** 50–58.

Sivaram, M.V., Saporita, J.A., Furgason, M.L., Boettcher, A.J. and Munson, M. (2005) Dimerization of the exocyst protein Sec6p and its interaction with the t-SNARE Sec9p. *Biochemistry,* **44**, 6302-6311.
Sivaram, M.V., Furgason, M.L, Brewer, D.N. and Munson, M. (2006) The structure of the exocyst subunit Sec6p defines a conserved architecture with diverse roles. Nat Struct Mol Biol, **13**, 555-566.

Songer, J.A. and Munson, M. (2009) Sec6p anchors the assembled exocyst complex at sites of secretion. *Mol Biol Cell.* **20,** 973-982.

Spinner, L., Pastuglia, M., Belcram, K., Pegoraro, M., Goussot, M., Bouchez, D. and Schaefer, D.G. (2010) The function of TONNEAU1 in moss reveals ancient mechanisms of division plane specification and cell elongation in land plants. *Development*, **137**, 2733-42.

Synek, L., Schlager, N., Eliáš, M., Quentin, M., Hauser, M. and Žárský, V. (2006) AtEXO70A1, a member of a family of putative exocyst subunits specifically expanded in land plants, is important for polar growth and plant development. *Plant J.* **48**, 54-72.

TerBush ,D.R. and Novick, P. (1995) Sec6, Sec8, and Sec15 are components of a multisubunit complex which localizes to small bud tips in Saccharomyces cerevisiae. *J. Cell. Biol.* **130**, 299-312.

Ter Bush, D.R., Maurice, T., Roth, D., Novick, P. (1996) The Exocyst is a multiprotein complex required for exocytosis in Saccharomyces cerevisiae. *EMBO Journal,* **15**, 6483-6494.

Wendeler, E., Zobell, O., Chrost, B. and Reiss, B. (2015) Recombination product suggest the frequent occurence of aberrant gene replacement in the moss *Physcomitrella patens. The Plant Journal,* **81**, 548-558.

Wise, H.Z., Saxena, I.M. and Brown Jr., R.M. (2011) Isolation and characterization of the cellulose synthase genes PpCesA6 and PpCesA7 in *Physcomitrella patens*. *Cellulose* **18**:371–384.

Wu, J., Tan, X., Wu, Ch., Cao, K., Li, Y. and Bao, Y. (2013) Regulation of cytokinesis by exocyst subunit SEC6 and KEULE in *Arabidopsis thaliana. Molecular Plant,* **6**, 1863-1876.

Zhang, L., Zhang, H., Liu, P., Hao, H., Jin, J. B. and Lin, J. (2011) *Arabidopsis* R-SNARE proteins VAMP721 and VAMP722 are required for cell plate formation. *PLoS ONE*, **6**, e26129. http://doi.org/10.1371/journal.pone.0026129.

Žárský, V., Cvrčková, F., Potocký, M. and Hála, M. (2009) Exocytosis and cell polarity in plants - exocyst and recycling domains. *New Phytologist,* **183,** 255-272.

Žárský, V., Kulich, I., Fendrych, M., Pečenková, T. (2013) Exocyst complexes multiple functions in plant cells secretory pathways. Curr Opin Plant Biol. **16**, 726-33.

Figure 1.

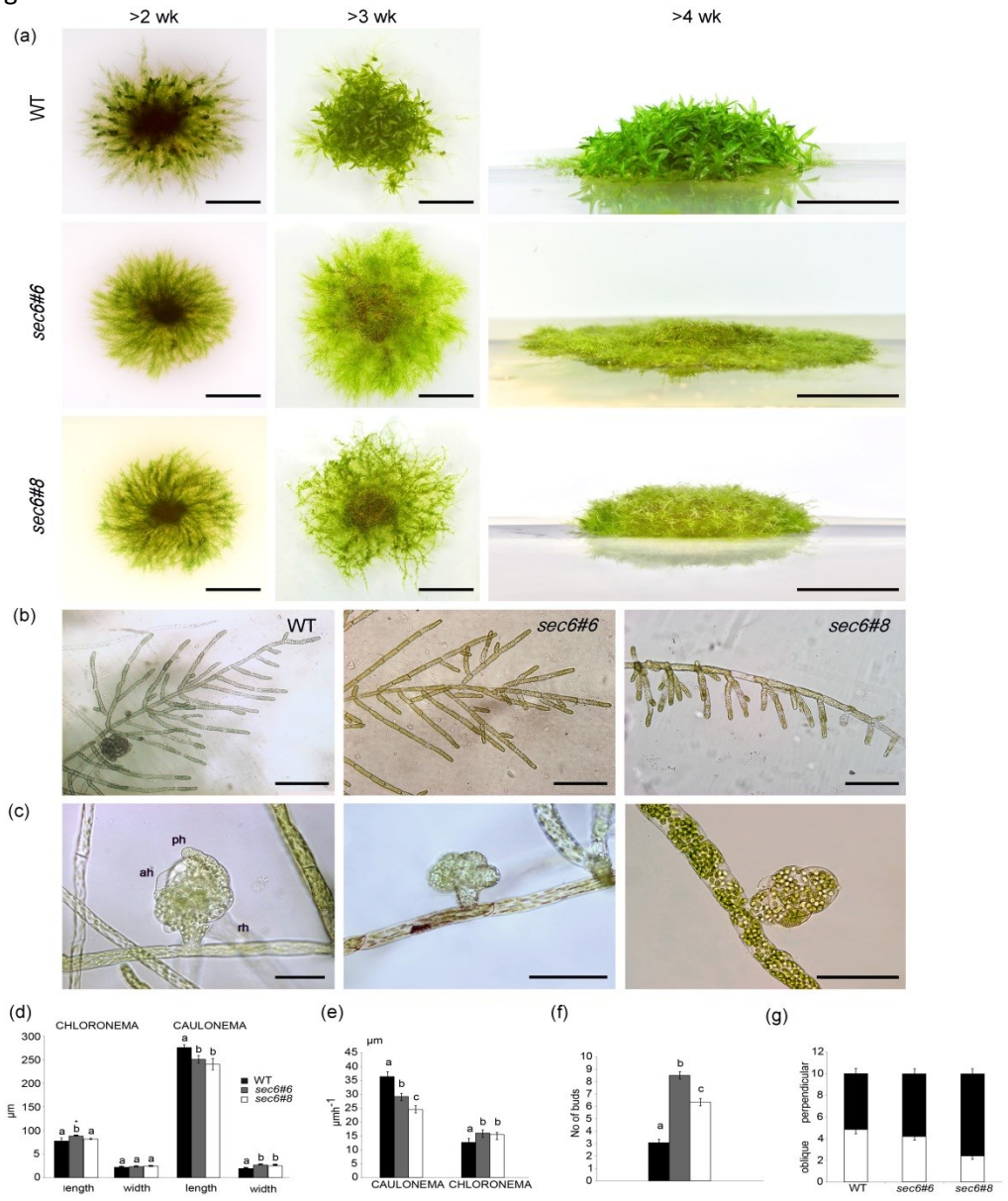

Figure 1. General phenotypes of *sec6* mutants. (a) Development of WT and *sec6* mutants overtime in the vertical and the lateral view. (b) Microscopy images of protonema. (c) Buds in WT and *sec6* mutants. Buds originate mostly on chloronema rarely on caulonema ah axilary hair, ph phyloid, rh rhizoid. (d) The protonemal tip cell length and width in WT and *sec6* mutants on BCD medium. (e) Growth rate of protonemal tip cells. Growth rate was time-lapsed in 15 min intervals for total period of 20 hours. (f) Number of bud initations in 3mm long apical part of filaments. Data were obtained in cells protruding from 3-week-old colonies grown on the thin layer of BCDAT medium. (g) The ratio between oblique and perpendicular cross walls in 10-d-old filaments. n≥30. Number of cells measured in each strain = 30-45. Values marked by various letters represent different significance. $P<0.01$, $P<0.05$ (marked by the asterix) were calculated by One-way Anova, Tukey HSD. Error bars indicate SE of the mean. Scale bars: (a) = 5 mm, (b) = 500 µm, (c) = 100 µm.

Figure 2.

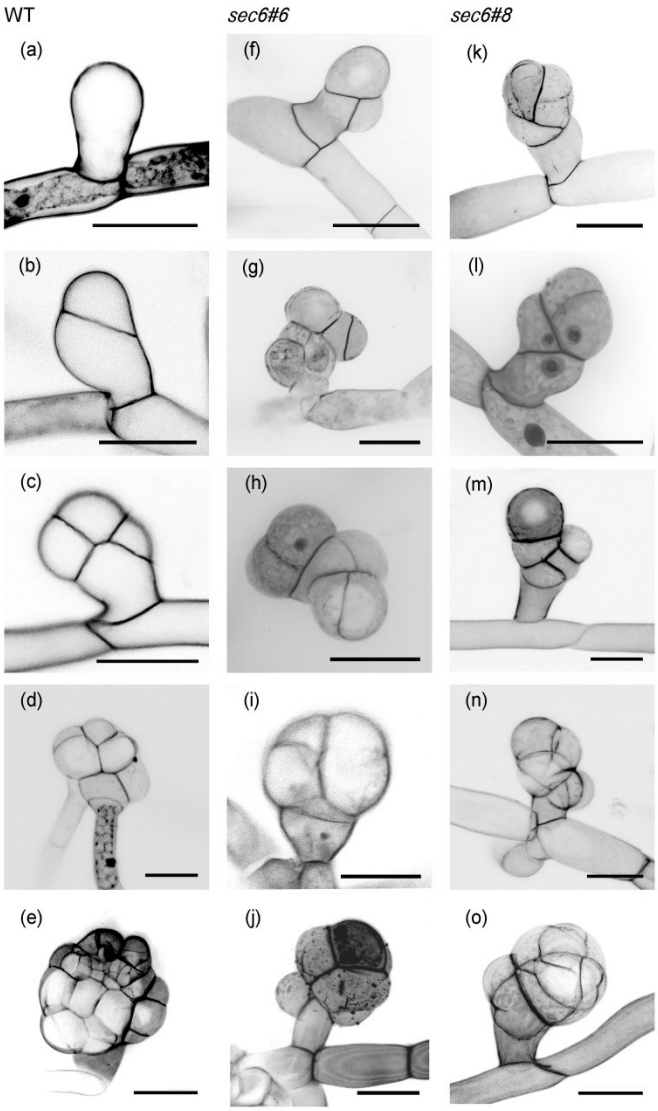

Figure 2. Bud development in *P. patens* WT and *sec6* in 3D reconstructions of confocal Z-stacks. (a-e) WT bud development from one-cell stage to early gametophore with diferentiated phyllids. (d) shows apical meristematic cell surrounded by products of unequal divisions. This stage lacks in *sec6* bud development. Divisions (a-c) resemble the same pattern for WT and *sec6.* (h) Bud differentiation sometimes reverts to the series of symmetrical divisions. (f, k) The first divisions in *sec6* display the correct orientation. Development of mutant buds terminates by expansion of one cell which is unable to continue dividing (i, m, n), stop growing (o) or the apical cell became to be necrotic (j). PI stained live imaging. Scale bars = 50 μm.

Figure 3.

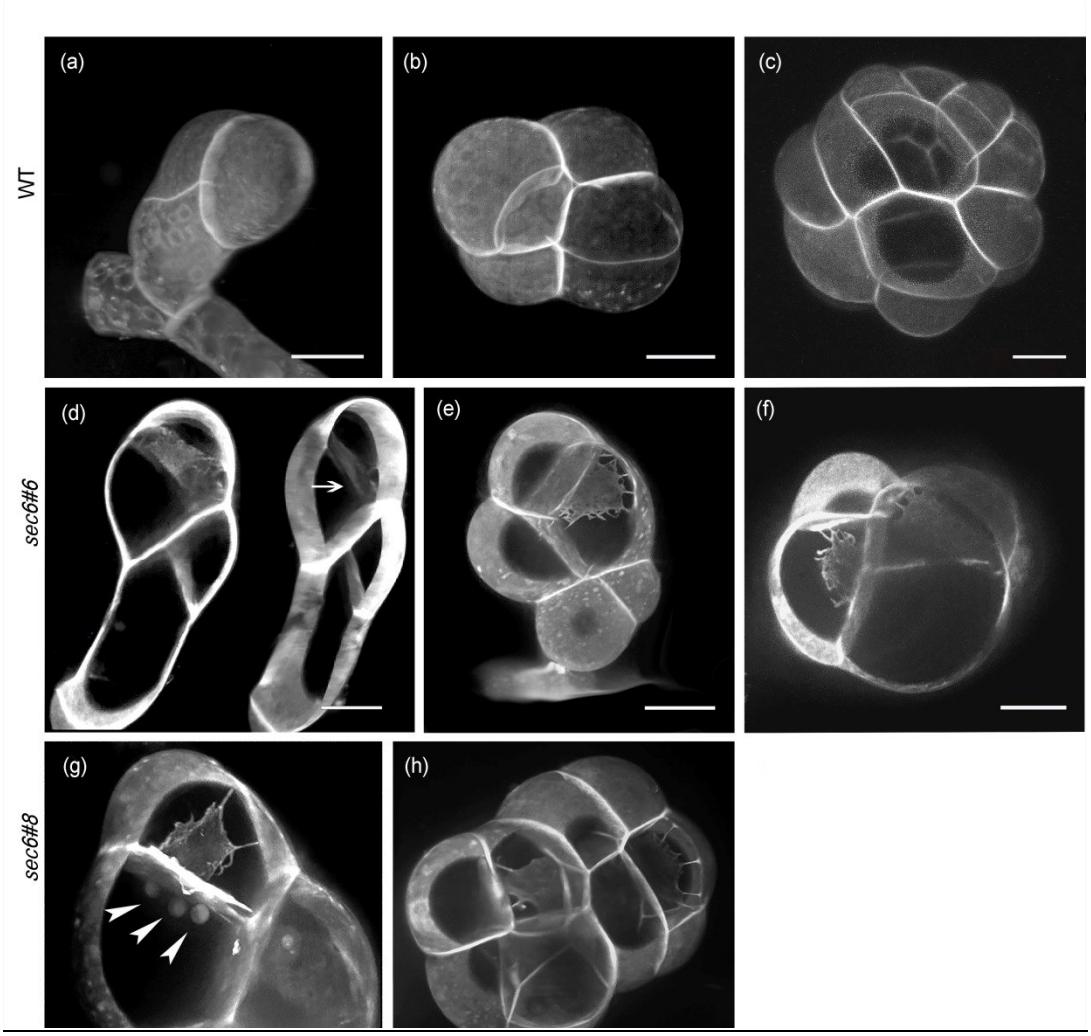

Figure 3. Confocal reconstruction of cross wall integrity in WT and *sec6* buds.
(a, b, c) WT inner cell walls are intact in all stages. (d) The 4-cell stage of bud is rotated to view gap (e) 6-cell mutant bud in 13µm cut-block displays cell wall resembling spider web.. in the cell wall of the apical cell (thickness of cut-block 13 µm in d,e), the first cross wall dividing bud into the apical and basal domain is intact (arrow). (f) Most of subsequent cell walls contains multiple fenestrae in later developmental stages. (g) The bud inner space unseparated by cell walls harbours clustered nuclei (arrowheads). (h) Doubled cells in bud apical dome show incomplete cross walls. PI stained live imaging. Scale bars = 20 µm.

Figure 4.

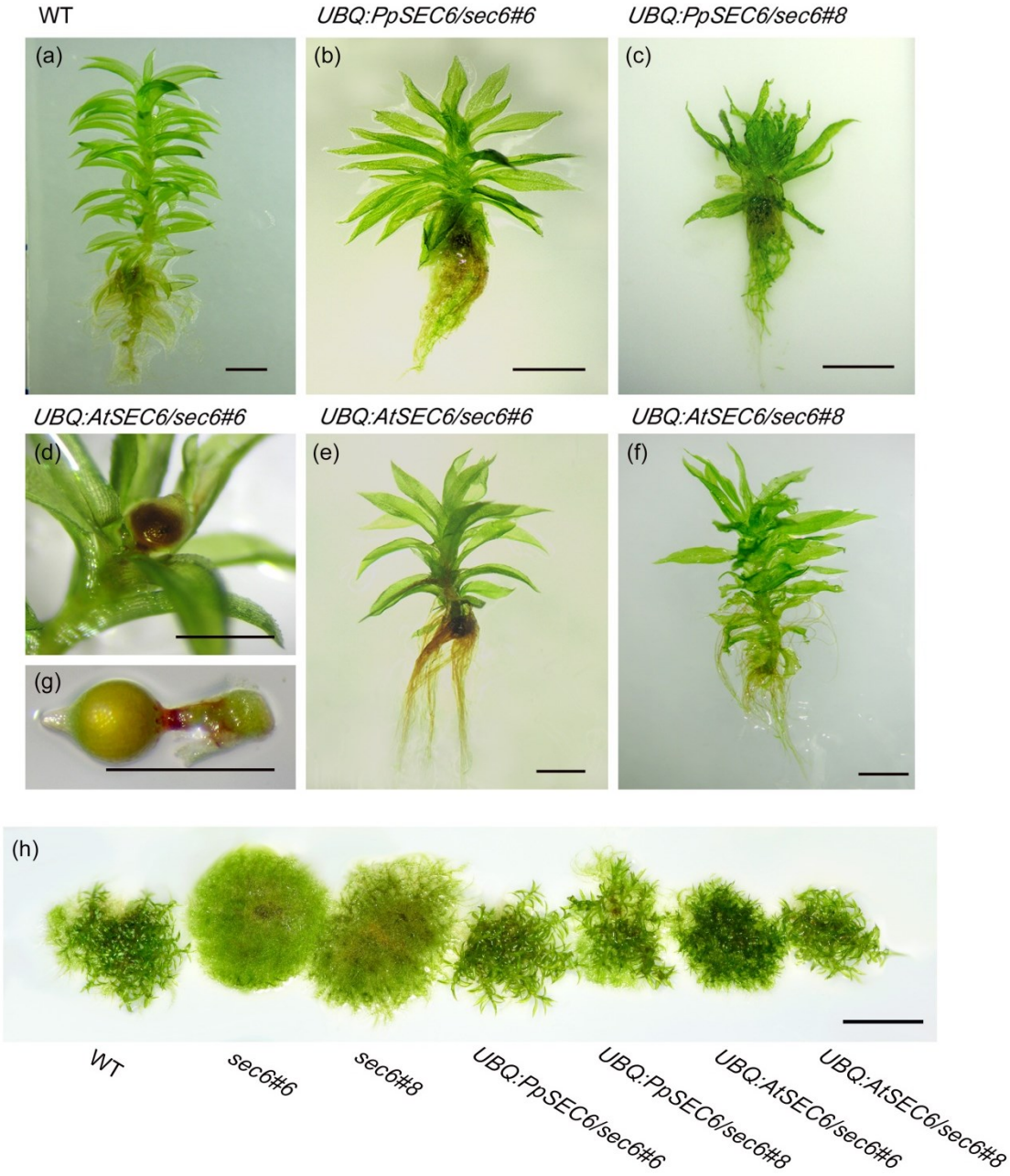

Figure 4. Overall phenotypes of *PpSEC6* and *AtSEC6* complemented strains compared to WT. (a) WT. (b, c) *PpSEC6 cDNA* complemented strains. (d) *UBQ:PpSEC6/sec6#6* comprises fully developed sporophyte. (e, f) *AtSEC6 cDNA* complemented strains. (g) Capsule developed in *UBQ:PpSEC6/sec6#6.* (h) colonies of WT, *sec6#6*, *sec6#8* and rescued mutant strains older than 4 wks. Gametophores were grown on BCD medium for 1 month, sporophytes developed during 3 month under induction conditions (8h light/ 16h dark, 16°C). Scale bars (a-g) = 1mm, (h) = 10 mm.

Figure 5.

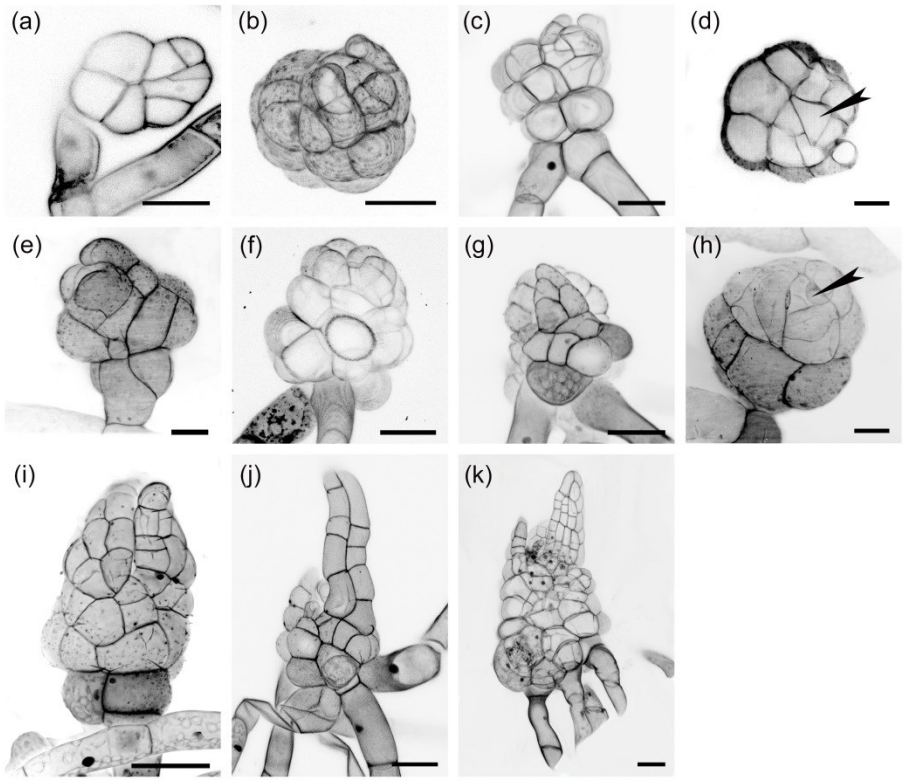

Figure 5. Confocal Z-stack 3D reconstruction of PI stained buds of different stages in complemented lines and WT. (a, b, c, d) show origins of phyllids emerging from early established meristematic apical cell in *UBQ:PpSEC6/sec6#6;* (e, f, g, h) correspond to gametophore development in *UBQ:AtSEC6/sec6#8.* Advanced gametophores of complemented strains (i, j) and in WT (k). Overexpression of *PpSEC6* and *AtSEC6* paralogs in *sec6* mutant strains fully re-established triangular meristematic cells (arrowheads) (d, h). PI stained live imaging. Scale bars = 50 µm.

Figure 6.

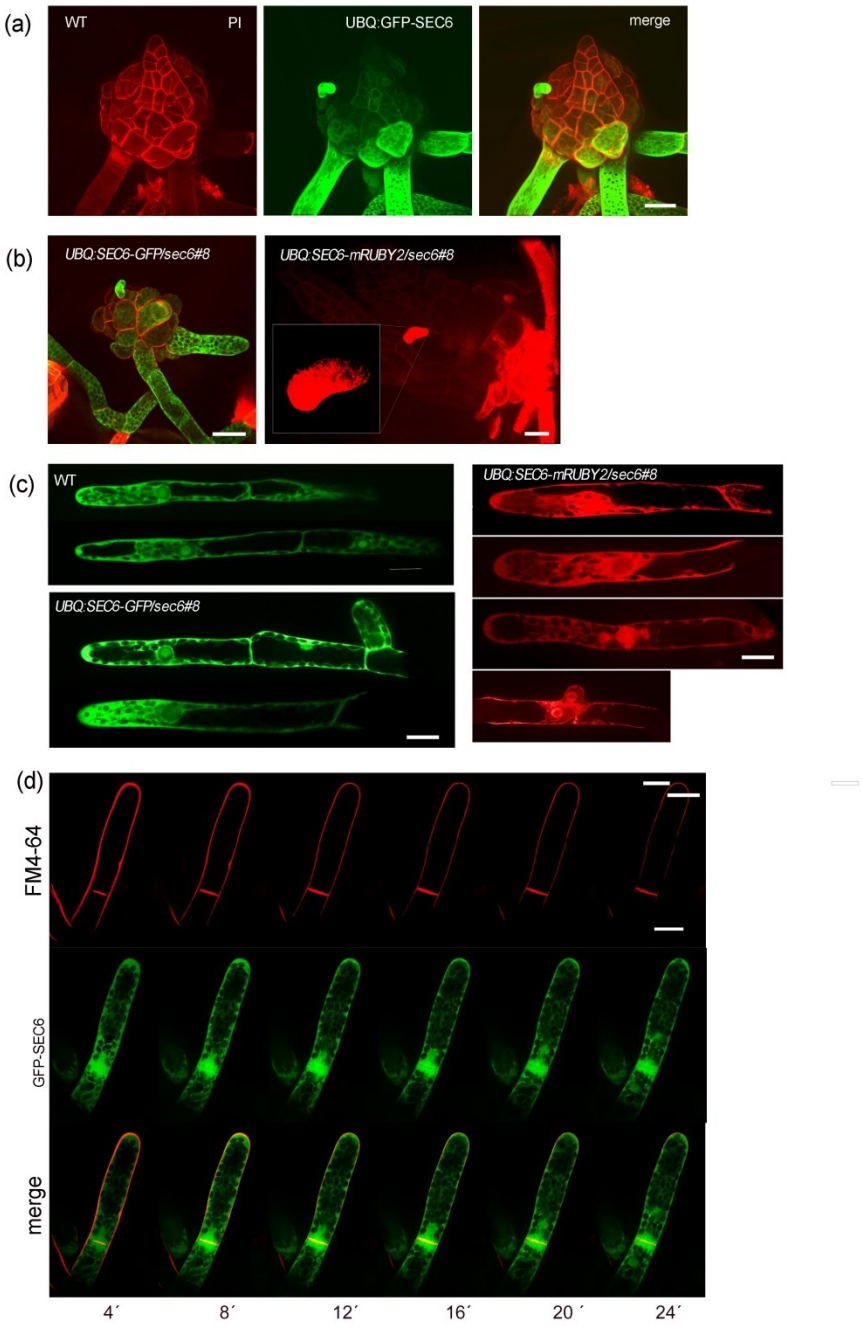

Figure 6. Confocal imaging of subcellular localization of GFP/mRUBY2 tagged SEC6 proteins in buds, protonemal cell and dividing chloronemal apical cell.
(a) Developing gametophore in *UBQ:GFP-SEC6,* GFP signal is increased in axillary hair and basal rhizoids. (b) Bud, chloronema and caulonema in *UBQ:GFP-SEC6/sec6#8.* (c) SEC6-GFP/mRUBY expression in protonema. (d) Cytokinesis in *UBQ:GFP-SEC6/sec6#8.* Total tracking time of cytokinesis was 24 min. Scale bars = 20 μm.

Supporting data

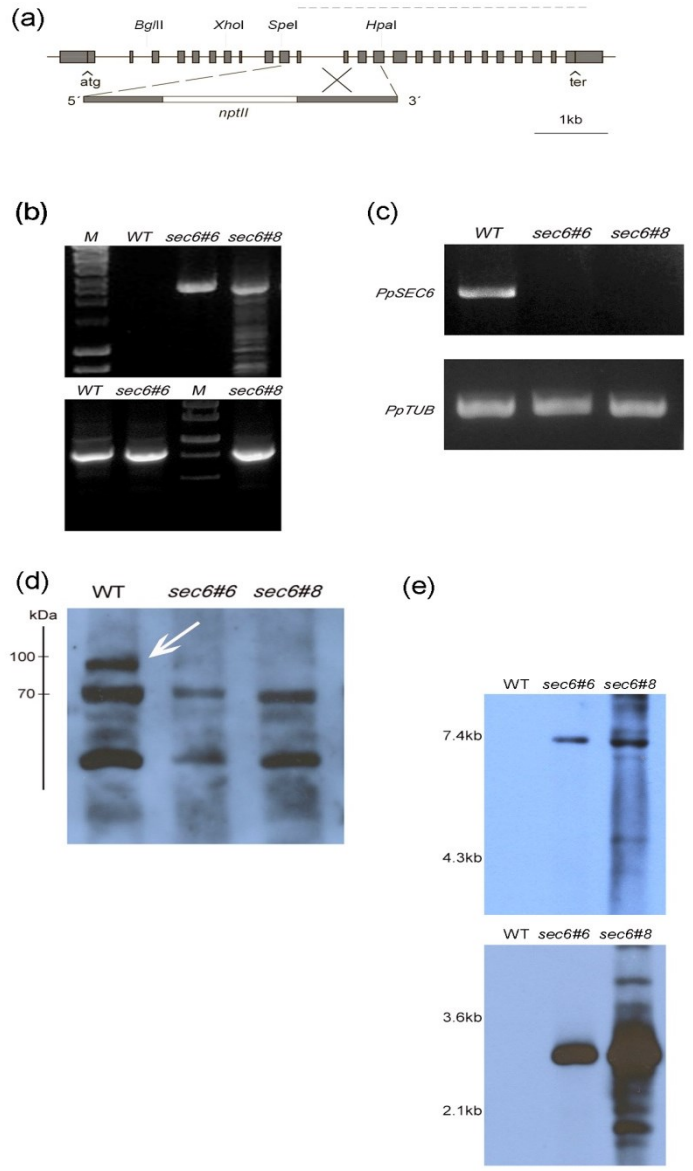

Figure S1. Structure of the *PpSEC6* gene and gene targeting outcomes. (a) Schematic structure of the *PpSEC6* gene. Rectangles represent exons and UTR´s, introns and non-coding sequences were shown as a line. The position of the restriction sites *Bgl*II, *Xho*I, *Spe*I, *Hpa*I which was used to cut out the 788 bp fragment for replacement by the *nptII* cassette is indicated. The construct for disruption *PpSEC6* gene and presumed outcome of gene targeting are displayed below. The grey line indicates truncated mRNA. (b) PCR screen of recombination events. Analysis of gene disruption was performed by set of PCR. Using two pairs of primers always one derived from selection casette and the second one from the corresponding outside segment of the targeting locus displayed successfull homologous recombination on the 3´end only (on the top). Presence of original fragment between *Xho*I and *Spe*I was proved using pair of primers amplifying 762 bp out of the 788 bp (bellow). (c) RT-PCR analyses of the *PpSEC6* in WT and both mutant lines *Ppsec6#8 and Ppsec6#8* (above). The α-tubulin gene fragment was used (bottom) as a template control. (d) Protein gel blot analysis. Total protein fractions of the moss WT and *sec6* mutant lines were loaded on 10% SDS-PAGE and processed by protein gel blot analysis with polyclonal mouse

α-*At*SEC6 mouse antibody prepared against truncated *At*SEC6 protein (Hála *et al*. 2008). The white arrow points at the band corresponding to SEC6. Predicted molecular weight of *Pp*SEC6 is 84.9 kDa. (e) Southern blot analysis of WT and two *Ppsec6* mutant lines. Genomic DNA (4 µg) of 8-day-old protonema was digested with with *BamH*I (a) and *Awa*III (b). The 700bp DIG-labeled sequence of *nptII* resistence cassette was used as a probe. Screen revealed two lines carrying a single copy of selection cassette within the genome. Other strains with more than one copy within the genome were excluded.

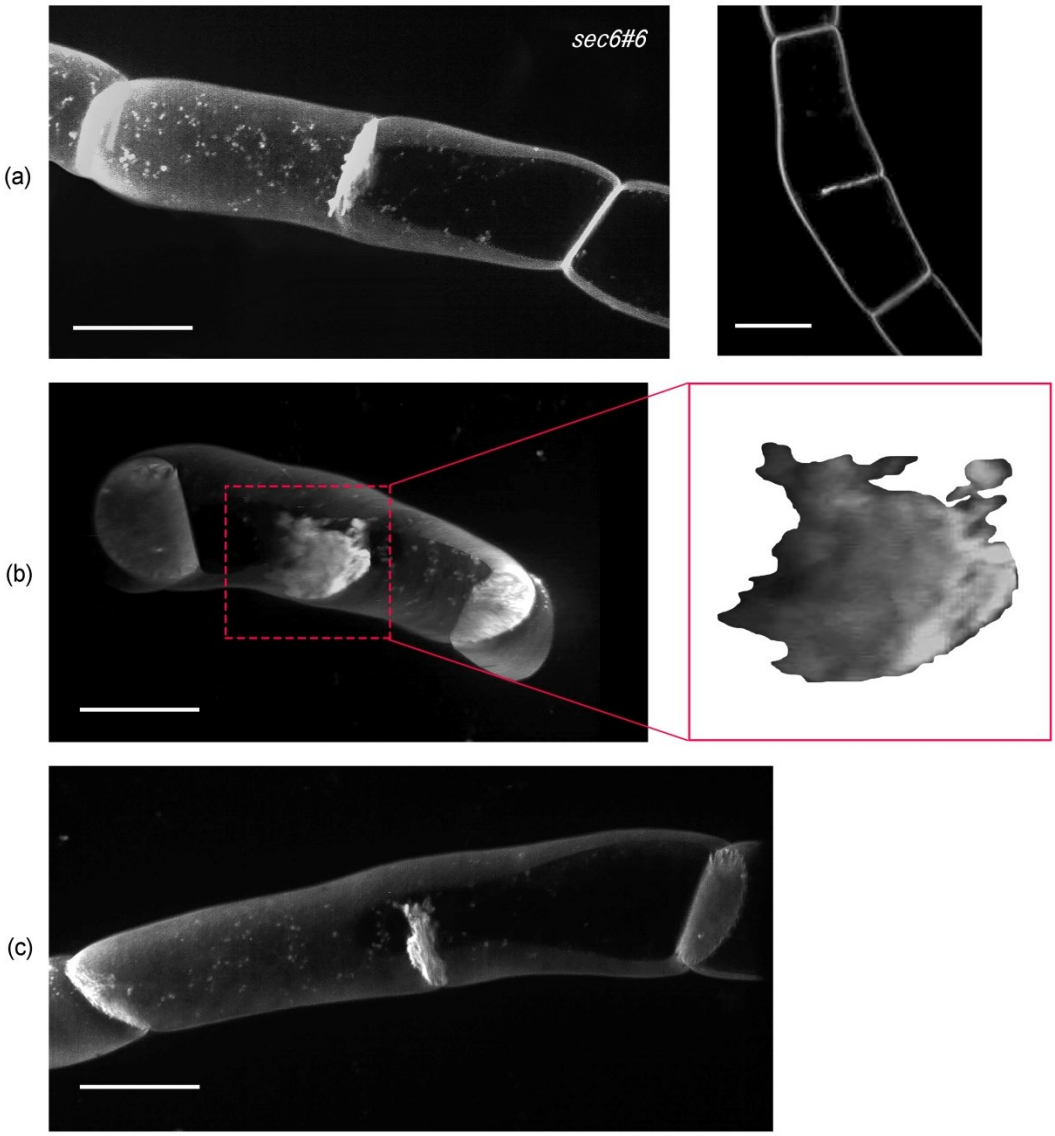

Figure S2. Cell wall defects in *sec6* protonema.
(a) Cell wall defects in *sec6* chloronemal cells. (b) Rotated caulonemal cell with the detail of impaired septa shape is enclosed in the red bordered square. (c) The lateral view to caulonemal cell. Scale bars = 20 µm.

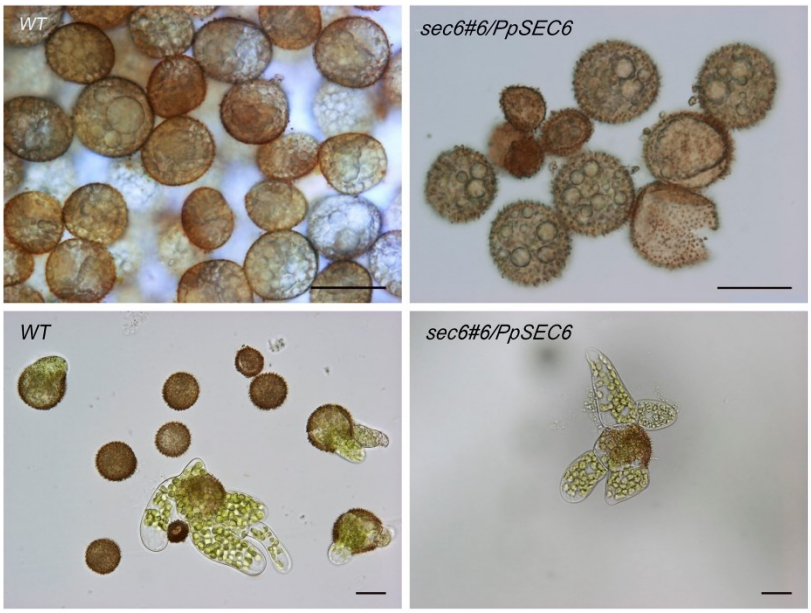

Figure S3. Upper row: Spores of WT and *UBQ:PpSEC6/sec6#6* complemented line. Lower row Germinating spores. Scale bars = 50 µm.

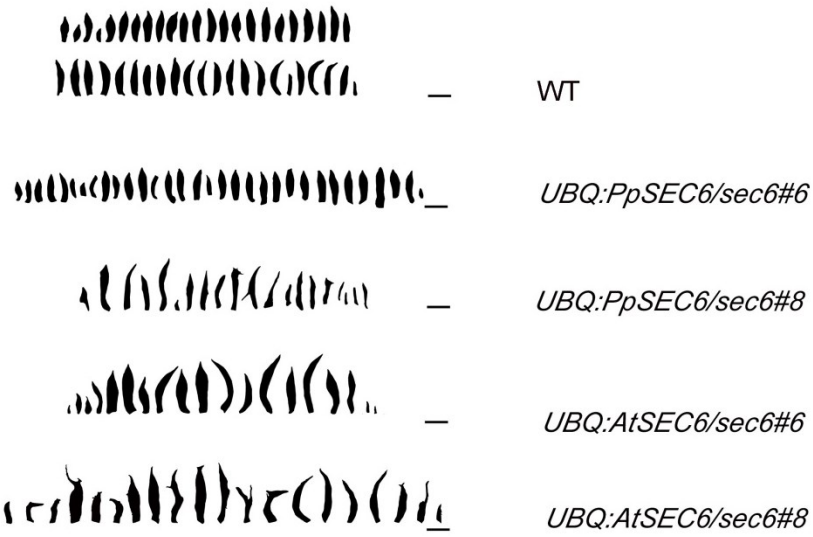

Figure S4. Comparison of leaf series from 4-wk-old gametophores of WT and complemented lines. Scale bars = 1 mm.

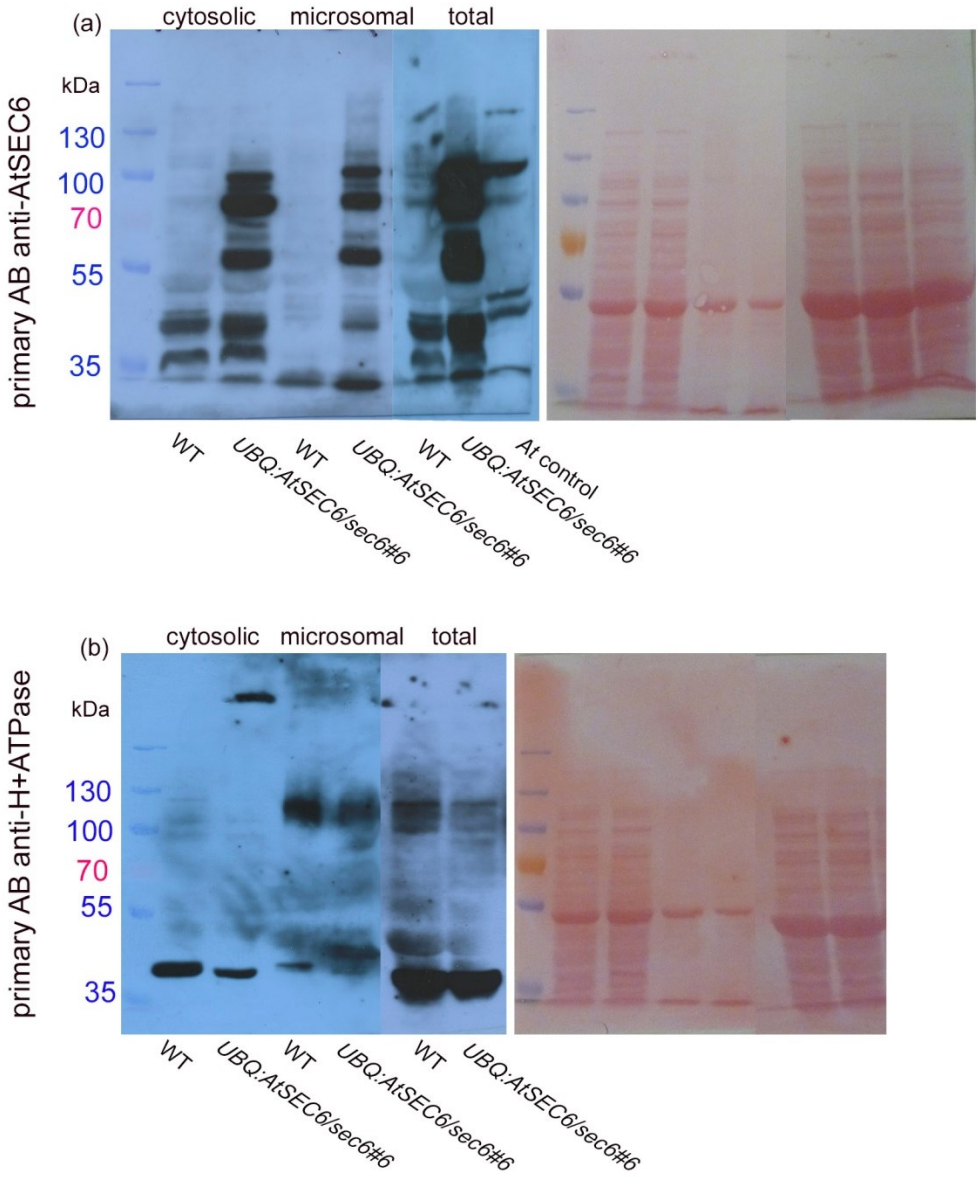

Figure S5. Protein gel blot analysis of *Pp*SEC6 localization. Cytosolic and microsomal fractions were separated by two-step 100,000 x g ultracentrifugation.
(a) Rabbit α-*At*SEC6 antibody was used in cytosolic, microsomal and total protein fractions. Antibody was raised against Arabidopsis SEC6, thus *At*SEC6 complemented strains were used. Moss WT protein extracts were used as a negative control, Arabidopsis total extract as a positive control. (b) Protein gel blot analysis of microsomal, cytosolic and total protein fractions. α-H+ATPase (95 kDa in Arabidopsis) was used as a primary antibody to verify fraction identity. Ponceau S red-stained membrane images are attached.

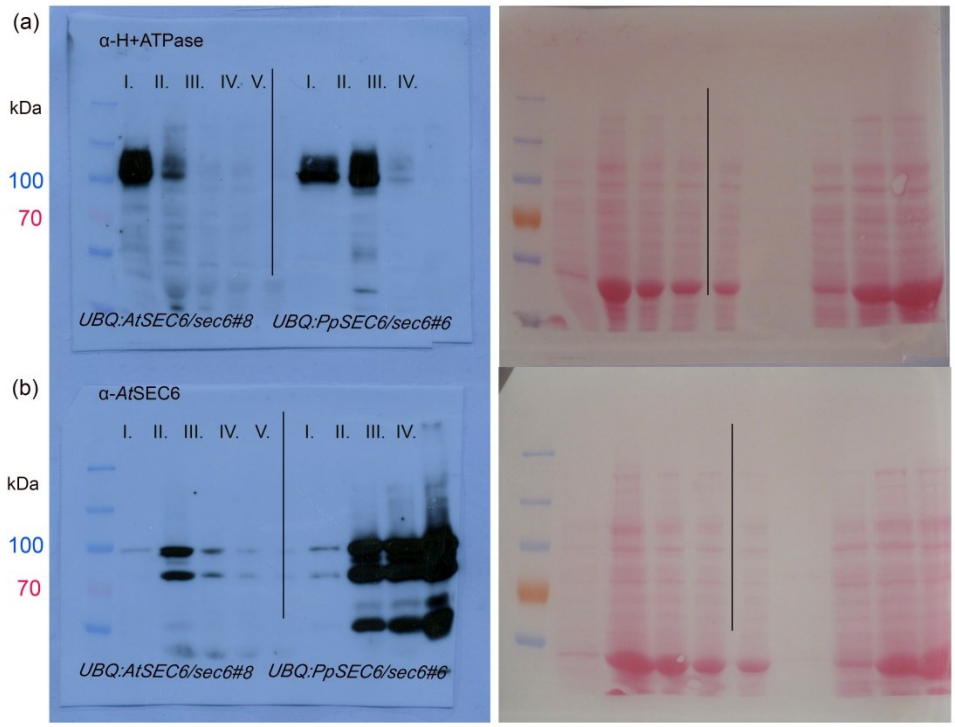

Figure S6. Protein gel blot analysis of *Pp*SEC6 localization. Cytosolic and microsomal fractions were separated by Optiprep fractionation.
(a) α-H+ATPase antibody (95 kDa) was used as a primary antibody to verify fraction identity. (b) α-*At*SEC6 antibody was used to localize SEC6 within 4-5 fractions. Ponceau S red-stained membrane images are attached.

* predicted helical; identical in all species. Only for differences between *A. thaliana* and *P. patens*:
identical in all angiosperms but different in *P. patens* (AA type conserved)
identical in all angiosperms but different in *P. patens* (AA type not conserved).

Figure S7.

Alignment of Sec6 orthologs from *P. patens*, *A. thaliana* and a selection of additional plant species representing both angiosperm and non-amgiosperm lineages. The sequences included are Selmo1 (GenBank XP_002986922.1) and Selmo2 (GenBank XP_002990062.1) for *Selaginella moelendorffii*, Marpo (Phytozome Mapoly0001s0359.1) for *Marchantia polymorpha*, Sphfal (Phytozome Sphfalx0021s0104.1) for *Sphagnum fallax*, Phypa (STRING 3218.JGI179426) for *P. patens*, Arath (STRING 3702.AT1G71820.1-P, At1g71820) for *A. thaliana*, Vivin1 (STRING 29760.GSVIVG00005752001 and Vivin2 (GenBank XP_002268285.2) for *Vitis vinifera*, Potri1 (STRING 3694.estExt_fgenesh4_pm.C_LG_XIX0238) and Potri2 (GenBank XP_002327215.1) for *Populus trichocarpa*, Solyc (Cvrčková et al. 2012) for *Solanum lycopersicon*, OrysaJ (STRING 39947.LOC_Os02g51430.1) for *Oryza sativa* var. *japonica*, Sorbi (STRING 4558.Sb04g027870.1) for *Sorghum bicolor*, and Bradi (STRING 15368.BRADI3G59230.1) for *Brachypodium distachyon*. For database resources, methods of sequence identification and alignment construction see Cvrčková et al 2012. Note that *S. fallax* contains another gene (Phytozome Sphfalx0015s0077.1) with significant similarity to Sec6 in the first N-terminal 165 amino acids followed by an unrelated sequence exhibiting similarity to a splicing factor; this gene was not included in the alignment. Amino acids conserved throughout the whole set are shown on gray background, those where the *P. patens* sequence deviates from an absolute consensus of all included angiosperms (highlighted in green) are highlighted in yellow if amino acid type corresponds to the consensus or in cyan where the amino acid type differs from that of the consensus. Asterisks denote predicted alpha-helical conformation as predicted by a consensus of the MLRC on GOR4, SIMPA96 and SOPMA, DSC and PHD methods as calculated by NPS@ (Combet *et al.,* 2000).

Table S1. List of primers used in this study

Primer name	Sequence
PpSec6-5F	CAGCACAATGATGCTCAGCTCAGC
PpSec6-5R	CTTAGCTCGAGTATTGCTCACATC
PpS6-3F	GAGTTGGTGGACTAGTATATAAGG
PpS6-3R	AAACAGGTTAACTCCTGCCGGAGT
NPT II_Fw	ACGCAGGTTCTCCGGCCGCTT
NPT II_Rv	GAAGCGGTCAGCCCATTCGCC
Ta_S6 EcoRI_Fw	AACGGAATTCATGATGCATGATGCTGG
Ta_S6_XhoI_Rv	AAACTCGAGTCACTTCCTTCCTGGCCCT
PpTubF	TGTGCTGTTGGACAATGAG
PpTubR	ACATCAGATCGAACTTGTG
PpSec6 OFF-Fw	TGAGCAGACTCTTTGGAGCCACAT
PpSec6-OFF-Rv	TGCTTTGTTCCTCTGGAGGTTGAG
S6-out-Fw	TTACATGTGTTGCATCAATTTATC
S6-out-RV	AAGACGCAATATAATTCATGACCT
PpS6-N-gfp-Fw	AAAGGTACCATGAGTAAAGGAGAAGAA
PpS6-N-gfp Rv	AAAGAATTCTTTGTATAGTTCATCCAT
PpS6-GFP EcoRI	AAAGAATTCCTATTTGTATAGTTCATCCAT
Sec6 full Fw	TTCTCGAGATCATGATGATGCATGATGCTGGC
Sec6 full Rv	TTGAATTCTCCTTCCTGGCCTGTATTTTGC
GFP Fw	TTGAATTCCCCGGGTTATGAGTAAAGGAGAAGAAC
GFP Rv	TTTGTCGACCTAGTATAGTTCATCCATGCC

Movie S1. Cytokinesis in FM4-64 stained WT.

Movie S2. Cytokinesis in FM4-64 stained *Ppsec6#6* strain.

Movie S3. Cytokinesis in FM4-64 stained *Ppsec6#8* strain.

Movie S4. Cytokinesis in FM4-64 stained GFP-SEC6-tagged complemented strain, signal relocalization was recorded every 4 min, within 64 min of tracking.

Manuscript 4: The *PpSEC3* genes regulate the sporophyte formation and perispore deposition, giving insight into the spore development in early land plants

Anamika Rawat[1, 2], Klára Aldorfová[1, 2], Lucie Brejšková[1, 2], Juraj Sekereš[1, 2], Fatima Cvrčková[1], Viktor Žárský[1, 2]

[1] Laboratory of Cell Morphogenesis, Department of Experimental Plant Biology, Faculty of Science, Charles University, Viničná 5, 128 44 Prague 2, Czech Republic; [2] Institute of Experimental Botany, Academy of Sciences of the Czech Republic, 165 02 Prague 6, Czech Republic

Author for correspondence: Viktor Žárský

Tel: +420-221-951683; email: zarsky@ueb.cas.cz

ABSTRACT

Polar growth, driven by the controlled exocytosis, is crucial for broad range of biological processes in living organisms. Exocyst, an evolutionary conserved secretory vesicle tethering complex, functions in later stages of exocytosis and targets the secretory vesicle on plasma membrane, just prior to fusion. In yeast the exocyst subunit Sec3 and also Exo70 interacts with the plasma membrane, thus marking the site for vesicle fusion. Here we report the functional role of two SEC3 genes (*PpSEC3A* and *PpSEC3B*) in moss *P. patens.*

Out of three SEC3 paralogs present in *P. patens*, we prepared single as well as double mutants in two of the genes that had interesting expression pattern in the moss tissue, esp. sporophytes. The mutants were phenotypically characterized to understand the role of *SEC3* in moss *P. patens*.

Knock-outs of *SEC3A* and *SEC3B* resulted in unusual protonemal growth when initiated from protoplasts, indicating loss of directional cues during the polar growth in *Ppsec3* mutants. The initiation of cell growth during stem cell formation in phyllids was altered in *Ppsec3a* and *Ppsec3ab*. Mutants also exhibited defective sporophytes and spores. Only a fraction of mutant spores was viable and exhibited compromised perispore layer formation. The N-term PH-domain of *PpSEC3A* showed positive interaction with membrane PI(4,5)P2 under *in vitro* conditions.

Taken together our results show that the role of *SEC3* in regulating the polar growth is conserved, and that it is one of the factor needed for proper construction of spore wall and spore viability in moss *P. patens*.

INTRODUCTION

The transition of plants from water to land that took place *approx*. 470-450 million years ago was the key event in evolution of land plants and life on the earth. This event of changeover from green algae to terrestrial plants led plants to face various challenges. The two most critical ones being 1. exposure to intense UV radiations 2. water loss due to desiccation; causing various morphological, physiological and cellular changes in plants. During the process of evolution, the loss of non-essential characters: like flagella, motile gametes, heterotropism; and rapid gain of new features: like development waxy cuticle, stomata, etc., assisted the plants to encounter the terrestrial habitat. These series of changes helped them to successfully adapt to the dry habitat.

The pollen wall of angiosperms as well as of gymnosperms, is built of: exine (made of tough insoluble polymer called sporopollenin, exceptionally stable and resistant to physical, chemical and biological degradation) and intine (a pectocellulosaic layer). The pollen grains of 'higher' plants and spores of 'lower' spore-bearing plants are homologs, and both have their outer wall made up of sporopollenin. The spores also have similar architecture and composition of the exine and intine. In addition to exine, the early divergent land plants (mosses, hornworts, lycopsids and ferns) often possess an additional layer called perispore (or perine) derived from tapetum. However this layer is absent in liverworts, as they lack tapetum (Wellman, 2004). The complex structure of exine present in recently evolved higher plants groups (gymnosperms and angiosperms) perhaps is the result of incorporation of perispore in exospore/exine layer over evolutionary time.

The exocyst complex is well known for its role in process of exocytosis and polarity establishment or maintenance (Wu & Guo, 2015). The octameric vesicle tethering protein complex first identified in yeast (TerBush *et al*., 1996) is now well described also in plants (Elias *et al*., 2003; Cvrčková *et al*., 2012; reviewed in Žárský *et al*., 2013). Recently we showed the functional importance of exocyst complex in basal land plant *P. patens* (Rawat *et al.,* 2017; Brejsková *et al*., in preparation). The EXO70 and SEC3 subunits, at least in yeast, interact with membrane signaling lipid $PI(4,5)P_2$ and act as site marking subunits on the plasma membrane (PM), thus driving the vesicle fusion (He *et al*., 2007; Zhang *et al*., 2008). A recent report shows that the SEC3 N-terminal PH-domain from tobacco pollen interacts with PIP_2, and that SEC3 is determinant of polarity in growing pollen tubes (Bloch *et al*., 2016).

In the present study we examined the function of SEC3 protein in moss *Physcomitrella patens*. The curling protonemata phenotype of *Ppsec3a*, *Ppsec3b* and *Ppsec3ab* mutants proves that SEC3 in *P. patens* provides direction to the polar growth in protonemata. We show that PpSEC3 is involved in sporophyte and spore development in moss and also speculate that exocyst is responsible for transporting either the sporopollenin precursors or its transporters or both. Our results confirm the presence of conserved N-terminal PIP_2-interacting PH-domain in *P. patens* SEC3 protein.

RESULTS

P. patens SEC3 mutants show mild developmental defects

The *P. patens* genome encodes three *SEC3* genes, here indicated as *PpSEC3A* (*Pp1s31_198V6*), *PpSEC3B* (*Pp1s80_181V6*) and *PpSEC3C* (*Pp1s63_200V6*). According to transcriptomic data from eFP browser (http://bar.utoronto.ca, Fig. S1), the expression of *PpSEC3A* peaks in the young sporophyte stages, followed by spore, archegonia and protoplasts, while the *PpSEC3B* is highly expressed in mature sporophyte, followed by protoplast, chloronema, spore and caulonema. Surprisingly, the transcript of *PpSEC3C* is present at very low levels in moss tissues, except for caulonemata. The interesting and overlapping expression pattern of both *PpSEC3A* and *PpSEC3B*, appealed us to investigate the functional role of these two paralogs in moss *P. patens*.

In order to study the function of *PpSEC3A* and *PpSEC3B* in *P. patens*, we generated both single as well as double knock out (KO) mutants in these two genes. Firstly, using targeted gene disruption by homologous recombination, we created several lines of *Ppsec3a* single KO mutant, of which *Ppsec3a#29* was selected for making double mutant *Ppsec3ab*. Later the *PpSEC3b* KO construct was transformed into WT moss as well as in *Ppsec3a#29* to create single *Ppsec3b* and double *Ppsec3ab* mutants respectively. To confirm the disruption of the gene of interest, all mutant lines were verified by PCR for proper integration in WT locus, and the absence of respective transcript in the mutants was confirmed by reverse transcription (RT)-PCR (Fig. 1). Two independently transformed lines from each mutant were chosen for further characterization.

The overall structure of protonemata and gametophores of *Ppsec3a, Ppsec3b* and *Ppsec3ab*, when grown under standard growth conditions, was not very distinct from WT (Fig. 2a). All three mutant genotypes grew normally producing caulonemata, chloronemata and gametophores similar to WT. From 10-11 days after germination of spore, the young WT protonemal colonies start to initiate the nascent gametophores (Ashton *et al*., 1979). Interestingly, when the number of gametophores were counted in 1 week old colonies (14 day after homogenization in total), the *Ppsec3b* produced significantly more gametophores than the WT (Fig. 2b,c). The colony growth rate showed a minor but significant decrease for both *Ppsec3a* and *Ppsec3ab* mutant lines, while *Ppsec3b* colonies were first indistinguishable from WT and by the 3rd week even slightly but significantly bigger than WT (Fig. 2d). Consistent with this observation, the growth rate of protonemal apical cell revealed a slight increase in growth rate of *Ppsec3b* caulonemata (Table 2), the type of filaments responsible for spread of moss colony. In contrast to *Ppsec3b,* both *Ppsec3a* and *Ppsec3ab* lines not only had smaller colonies but also shorter gametophores with fewer phyllids than the WT (Table 3).

***PpSEC3* is required for accurate cell morphogenesis and polarized cell growth in early stages of protonemata establishment.**

Protoplasts do not encode any polarity or positional information. They first undergo the process of fast cell wall regeneration that always precedes the cell division. In protoplasts, the development of cell wall is a precondition for cell division and establishment of polarity. In our growth conditions the protoplasts, from WT, *Ppsec3a*, *Ppsec3b* and *Ppsec3ab*, showed distinctive regeneration and division patterns (Fig. 3). After 3rd day 36% of WT protoplasts regenerated the cell wall and were either divided or with pear shaped structure indicating the establishment of the polar axis. However, in mutant lines there were more of dead protoplasts and only upto 26% showed initial polar growth (Fig. 3). By 10th day, in WT more than 40% of protoplasts formed small branched colonies of protonemal filaments, whereas in *Ppsec3a* and *Ppsec3b* only upto 25% and 10% respectively were at this stage. Interestingly, in *Ppsec3b* almost 12% of protoplasts underwent non-regulated division pattern, and appeared like a tiny mass of callus. These callus-like divided protoplasts either died, or were able to grow filaments and later formed normal protonemal colonies. As expected, after 10 days *Ppsec3ab* had small number of branched filaments that formed young colonies. Interestingly, the callus-like structures due to nonregulated cell divisions in *Ppsec3ab* were not as prominent as in *Ppsec3b*, although there were protoplasts still in different stages of early division, showing a delay in the process of regeneration and growth in *Ppsec3ab*. Not only the mutants differed in regeneration and division pattern of protoplasts, but also the newly initiated filaments from both single *Ppsec3a*, *Ppsec3b* and double *Ppsec3ab* mutant protoplasts were curled and formed spirals of protonemata in the proximal region (Fig. 4). The curled protonemata phenotype was not observed in older colonies, showing that the phenotype is specific to protonemata derived from regenerating protoplasts and young protonemal colonies only, where the tissues attain initial polar growth.

***Ppsec3* mutants have normal gravitropic response**

The *P. patens* caulonemata and gametophores are the only moss tissue that can perceive the gravity signal and grow against the gravity vector in dark (Jekins *et al*., 1986). We did not observe difference between WT and *Ppsec3* mutants when grown under gravi-stimulation conditions (Fig. 5). The caulonemata in all four genotypes grew against the gravity vector, showing that *PpSEC3* is not required for sensing the gravitational cues in moss *P. patens* or responding to them. Interestingly, the caulonemata in *Ppsec3b* grew slightly longer than WT ones, while those of *Ppsec3a* and *Ppsec3ab* were shorter. These results correspond with the slightly increased *Ppsec3b* caulonemata growth rate as indicated above (Table 2).

The response to wounding is altered in *Ppsec3a* and *Ppsec3ab* mutants

P. patens has unique ability to transform differentiated cells into stem cells upon wounding. When phyllids of *P. patens* are detached from gametophores, the cells at the wound margin are reprogrammed into stem cells, which later form protonemal filaments, and thus can initiate formation of new moss colony upon damage (Prigge & Bezanilla, 2010; Ishikawa *et al.,* 2011). This process requires an extensive exocytosis, and establishment of polar axis in newly initiated stem cells. We observed that upon mechanical wounding by razor, WT phyllids reprogrammed some cells into stem cells that subsequently by asymmetric division initiated filamentous tip growth. In contrast to WT, the double mutant *Ppsec3ab* displayed decreased frequency of newly initiated tip growth (Fig. 6a). Similar phenotype but at low frequency was seen in *Ppsec3a*, whereas no difference from WT was detected for *Ppsec3b* (Fig. 6a). In WT and *Ppsec3b* many of the cells near the cut end of phyllids displayed the deposition of callose after 24 hours of wounding, while *Ppsec3a* and *Ppsec3ab* had reduced number of callose spots in this region (Fig. 6b). This suggests delayed response to mechanical stress, or wounding, in *Ppsec3ab* and up to some extent also in *Ppsec3a* mutant.

Loss of *PpSEC3A* and *PpSEC3B* leads to defective sporophytes and imperfect spore wall development

Both *PpSEC3A* and *PpSEC3B* are highly expressed in different sporophytic stages. The spore wall is made up of multiple components, layers of which are laid down in a regulated manner during spore development. In order to investigate the consequence of *PpSEC3* mutation on sporophyte and spore development, we carried out SEM analysis on WT and *Ppsec3a*, *Ppsec3b* and *Ppsec3ab*, which clearly showed defects in sporophytes and spores of mutant lines (Fig. 7). In mutants a range of sporophytes with aberrant structures were observed (Table 4). In *Ppsec3a* and *Ppsec3b*, there were: 1. WT-like sporophytes with elongated apex 2. rounded sporophytes, with no apical elongation and archegonia shifted to one side of the capsule and 3. aborted sporophytes (Fig. 7a,d). In *Ppsec3ab* we did not observe any sporophytes with WT-like structure, but only rounded and malformed sporophytes, thus *Ppsec3ab* displayed the most severe phenotype. Interestingly, in *Ppsec3b* some of the gametophores bore multi-sporangiate sporophytes (Fig. 7a, Table 4). The sporophytes from all the mutant lines had mixed population of spores: normal large and spherical spores, partially collapsed spores and completely distorted spores (Fig. 7b).

Not only the sphorophyte structure but also the spore wall architecture was defective in all three mutants. The surface of WT spores are decorated with spiny projections composed of perispore elements made of sporopollenin, these projection are pointed and evenly distributed on the whole surface of WT spores (Fig. 7b). However the mutant spores from all sporophyte variants had highly irregular surface with globular to granulose protrusions, and lacked the characteristic perispore layer. The protrusions were

present either as very few short projections or were almost absent, giving smooth appearance to the spore surface (Fig. 7b). Interestingly, there were some spores that were attached to other 2-3 spores, and were not able to separate (Fig. 7c). These fused spores might be due to the defective sporopollenin deposition on the outer wall surface, which is known to release the spores from the tetrads into individual spores. These observations indicate the role of *PpSEC3* in spore viability and wall architecture by regulating sporopollenin deposition in perispore layer.

N-term PH-domain of *PpSEC3A* binds to membrane phospholipids

Yeast and plant *SEC3* has been shown to interact with the membrane lipids by its PH-domain, located at the N-term of the protein (Zhang *et al*., 2008; Bloch *et al*., 2016). *PpSEC3* also encodes N-terminally located PH-domain and may thus participate in similar interactions with membrane lipids. To test this hypothesis, we cloned the 5' fragment of *PpSEC3A* containing PH-domain, and transcribed and translated the protein in in-vitro conditions. As seen in Fig. 8, the *PpSEC3A*, just like the control PH-domain from PLC, showed strong binding with membrane lipid $PI4,5P_2$. However *PpSEC3A* also showed positive interaction with $PI3,4,5P_3$, which probably is due to the non-specific binding of protein, as this is not plant specific phospholipid. This shows that *PpSEC3A* interacts with phospholipids in the membrane though its N-terminally located PH-domain, and that this interaction is conserved in mosses as well.

DISCUSSION

Exocyst is an octameric protein complex implicated in process of tethering secretory vesicles on the PM in yeast, mammalian cells, fungi and also plants (reviewed in Wu & Guo., 2015). Several reports published so far have clearly established the role of exocyst complex in regulated exocytosis and polar growth of plant cells (reviewed in Vukašinović *et al*., 2016). Recently we showed that EXO70 and SEC6 subunit of the exocyst complex are required for performing various cellular processes also in the moss *P. patens* (Rawat *et al*., 2017; Brejsková *et al*., in preparation). Here we show the role of yet another exocyst subunit PpSEC3 in process of exocytosis in moss *P. patens*.

Moss caulonemata and chloronemata grow by the tip growth mechanism (Menand *et al*., 2007). This process requires the secretion of new cell wall materials to the tip in a highly polarized manner. In recent times we showed that mutants in exocyst subunit EXO70.3d are defective in growing true caulonemata and have reduced elongation of chloronemal filaments, thus showing a partial failure in tip growth (Rawat *et al*., 2017). Mutants in yet another exocyst subunit PpSEC6, encoded by just single paralogue in most of the species studied so far (Eliáš *et al*., 2003; Cvrčková *et al*., 2012), cannot transit beyond protonemal stage (Brejsková *et al*., in preparation). Thus, the exocyst complex is involved in controlling the polar growth in *P. patens*.

The moss *Ppsec3a* and *Ppsec3ab* mutants showed slightly but significantly reduced colony size, gametophore number and gametophore size indicating that PpSEC3A, while not required for cell growth and division, contributes to the control of growth and development of moss tissues, Interestingly, the slightly bigger colonies after 3 weeks of inoculation and comparatively fast growing caulonemata of *Ppsec3b* represent the opposite phenotype than *Ppsec3a* and *Ppsec3ab*, which is consistent with such a control function and might suggest specific role of these two isoforms in *P. patens*.

Protoplasts provide excellent model for studying the initiation of polar growth. One of the exocyst subunit EXO70.3d has been shown to be involved in establishment of polar growth in *P. patens* protoplasts (Rawat *et al*., 2017). Unlike *Ppexo70.3d* protoplasts, which are highly affected in regeneration, the isolated protoplasts from *Ppsec3* mutant lines were able to recover and grow the protonemata, however, they exhibited altered early protonemal growth polarity, leading to curled protonemata. SEC3 is involved in directing the site of polar growth in pollen tubes by controlling the location of exocytosis (Bloch *et al*., 2016), and the *Arabidopsis sec3a* mutants have defective pollen germination and lack the polar accumulation of cell wall material during germination (Li *et al*., 2017). Both *PpSEC3A* and *PpSEC3B* are expressed in protoplasts, and the curling phenotype supports the fact that SEC3 protein participates in determining the direction to the growth, and that this phenomenon also exists in *P. patens*. The curling phenotype of protonemata is recovered during later phases of moss growth, which can be also seen in gravitropic assays where all the mutants grew caulonemata just like WT, aligned against gravity. We suspect the presence of 3rd *SEC3* paralog might overtake the loss of *PpSEC3A* and *PpSEC3B* function in later stages, which is consistent with its high expression in caulonemata (Ortiz-Ramírez *et al*., 2016; Fig. S1).

P. patens has the ability to reprogram the cells near a wound into stem cells, which can differentiate into new protonemata (Prigge & Bezanilla, 2010; Ishikawa *et al.,* 2011). In *Ppsec3a* and *Ppsec3ab* mutants the stem cell formation and initiation of tip growth from the detached and cut phyllids is delayed, but not in *Ppsec3b*. This shows the inability of *Ppsec3a* and *Ppsec3ab* to respond properly to wounding. This was also reflected by the reduced callose deposition, which is first line of defense against mechanical damage in plant cell, in these two mutants.

WUS-related homeobox (WOX)13-like genes have been shown to control the reprogramming of moss tissue into stem cells (Sakakibara *et al*., 2014). The double mutant *Δppwox13lab*, unlike WT, shows strong reduction in frequency of divided cells that initiate the tip growth after wounding (Sakakibara *et al*., 2014). It would be interesting to look for the expression of WOX13 in *Ppsec3* mutants, and of SEC3 paralogs in *Δppwox13lab* mutants during wounding response to establish the relationship between SEC3 and WOX13-like genes in the wound-induced reprogramming of *P. patens* stem cells and the later process of protonemal differentiation

Both *PpSEC3A* and *PpSEC3B* are highly expressed during the various sporophytic stages (Ortiz-Ramírez et al., 2016; Fig. S1). Consistently with these data, our observations showing that both single *Ppsec3a* and *Ppsec3b* mutants are defective in producing normal sporophytes and spore wall architecture, with more severe phenotype shown by double mutant *Ppsec3ab* suggest a partial functional overlap, or redundancy, of PpSECA and PpSEC3B.

The biosynthesis of sporopollenin is regulated by several genes and the mutants in the genes involved in this pathway show defects in formation of exine in Arabidopsis as well as in *P. patens* (Morant *et* al., 2007; Wallace *et* al., 2015; Daku *et al*., 2016). The pollen wall development in flowering plants is under the control of Gibberellin (GA), which is under the regulation of GAMYB transcription factors. However in mosses and perhaps also in other basal plants the GA signaling and biosynthesis pathways do not exists, but still GAMYB homologs are conserved and promotes development of outer walls of spores by regulating CYP703 expression (Aya *et al*., 2011).

In plants the export of cuticular lipids from epidermal cells to the surface needs ABC transporters (Pighin *et al*., 2004). The cuticular waxes are deposited onto the PM via secretory pathway, and involve ATP binding cassette (ABC) transporters of G family. The disruption of these transporters leads to wax accumulation in ER (McFarlane *et al*., 2010; McFarlane *et al*., 2014), and the moss Δ*ppabcg7* mutants show reduced cuticular wax deposition both on phyllids and spores (Buda *et al*., 2013). In Arabidopsis the ABCG26 transports sporopollenin precursors across tapetum for polymerization on surface of developing microspores, and the mutants in ABCG26 lacks exine layer formation, suggesting its crucial role in exine development (Quilichini *et al*., 2010). Another membrane protein involved in exine formation in *Arabidopsis* pollen is DEX1. The *dex1* mutants, although synthesize the sporopollenin normally, have alteration in its deposition and thus exine formation is delayed and ultimately reduced (Paxson-Sowders *et al*., 2001). The mutants in moss *Ppexo70.3d*, one of the subunit of exocyst complex, have defective cuticular layer on the phyllids (Rawat *et al*., 2017). Since the exocyst complex is responsible for transporting various membrane proteins from site of synthesis within the cell to the site of functioning on the PM, we suspect the moss exocyst assists in trafficking of either the precursors of cuticle and sporopollenin or their transporters or even both. The defect in perispore formation, as seen in the spores of *Ppsec3* mutants, indicates the crucial involvement of exocyst in cuticle deposition.

The *P. patens pin* mutants have disrupted sporophytes and *pinB* mutants sometimes show branched sporophytes (Bennett *et al*., 2014). The *Ppsec3b* mutant also displayed similar branched sporophytes, however at low frequency (13%, Table 4). The exocyst complex is involved in recycling of PIN proteins in Arabidopsis (Drdová *et al*., 2013), and the *Ppexo70.3d* mutants display phenotype that hints towards interplay of exocyst and auxins in mosses as well (Rawat *et al*., 2017). It would be interesting to see if exocyst participates in PIN recycling also in *P. patens.*

In yeast and mammals, the EXO70 binds to PI(4,5)P_2 through the positively charged residues enriched at C-terminus (He *et* al., 2007; Pleskot *et al.,* 2015), while, SEC3 interacts with membrane lipids by its N-terminally located PH-domain (Zhang *et al*., 2008). Recently Bloch *et al*. (2016) showed this interaction of SEC3 PH-domain with membrane phosphoinositides also occurs in angiosperms, however is not needed for functioning and localization of SEC3. This PIP_2 independent localization pattern of SEC3 has also been shown for *sec3a* mutants in *Arabidopsis* (Li *et al.,* 2017). Our results show that, just like yeast Sec3p and tobacco SEC3, the moss SEC3 also contains N-terminal PH- domains which can interact with PI(4,5)P_2. The N-terminal domain contains a cryptic pleckstrin homology (PH) fold, and all six positively charged lysine and arginine residues in this PH-domain are predicted to bind PIP2 head group. It would be interesting to look for the interacting residues in *PpSEC3A*. Our data thus support the hypothesis proposed by Bloch *et al*., 2016 that plant exocyst might also interact directly, via both SEC3 and EXO70 subunits, with specific membrane phosphoinositide. This interaction is thus conserved and perhaps can be traced back to early plant lineages.

MATERIALS AND METHODS

Plant material and growth conditions

The 'Gransden' strain of *Physcomitrella patens* (Hedw.) B.S.G. was used as a wild type (WT) in this study. Unless stated otherwise, 1wk old tissues were homogenized and grown on BCD agar medium containing 1mM $CaCl_2$ and 5mM ammonium tartrate (BCDAT) overlaid with cellophane (Cove *et al*., 2009), at 25°C with 16 h light : 8 h dark regime, with or without additives as indicated.

Construction and molecular characterization of knock-out mutants

The 5' and 3' flanking regions of both *PpSEC3A* and *PpSEC3B* genes were amplified from *P. patens* genomic DNA by PCR using Phusion polymerase (New England Biolabs) and primers listed in Table 1. The resulting DNA fragments were ligated into the plasmids pMCS5-LOX-NptIIr-LOX and pBHRF to create PpSEC3A and PpSEC3B knock-out construct respectively. The plasmids thus obtained were used as PCR template to amplify the selection cassette flanked by targeting fragments. The product was purified using PCR purification Kit (Qiagen) and introduced into WT protoplasts by PEG-mediated transformation (Kamisugi *et al*., 2005). To create double mutant *Ppsec3ab*, *PpSEC3B*-KO construct was transformed into *Ppsec3a#29*. Transformants were selected on BCDAT supplemented either with 30mgl^{-1} G418 or 50mgl^{-1} hygromycin. Stable lines were analysed by PCR using primer set PpSEC3a_LP + nptII_RV, PpSEC3a_RP.1 + nptII_FW and PpSEC3.B_LP + Hyg_RV, PpSEC3.B_RP + Hyg_FW (Table 1).

Construction of HA-SEC3A-N plasmid and lipid-protein binding assay

The first 183 amino acid of *P. patens SEC3A* were amplified with primer Sec3a-N_FW-1+ Sec3a-N_RV (Table 1). To the N-term of the amplified fragment a HA- tag was added by PCR using primer Mega-HA+ Sec3a-N_RV (Table 1). This fragment was cloned in between *SalI-NotI* site of pTNT plasmid (Promega). This construct was transcribed and used to translate the protein using TNT Quick coupled transcription/translation system kit (Promega). The protein thus obtained was used for protein-lipid overlay assay with membrane lipid strips according to manufacturer's instructions (Echelon Biosciences P-6001, Salt Lake City, UT), and the signals were detected using anti-HA antibody by enhanced chemi-luminescence (Amersham ECL Prime Western Blotting detection kit)

RT-PCR

Total RNA was isolated from 100 mg of 7 d old protonemata using RNeasy Plant Mini kit (Qiagen). cDNA was prepared using Transcriptor High Fidelity cDNA Synthesis Kit (Roche). Semi-quantitative PCR was performed with equivalent amounts of cDNA template using DreamTaq polymerase (Thermo Scientific) and primers Sec3a_RT-FW+Sec3a_RT-RV and Sec3b_RT-FW+Sec3b_RT-RV (Table 1) for amplification of *PpSEC3A* and *PpSEC3B* transcripts respectively. Primer pair Pptub_FW+Pptub_RV (Table 1) was used to amplify tubulin as a housekeeping gene control.

Phenotypic analysis

The closeup of protonemata and gametophores were photographed using Canon Powershot S70 attached to Leica S6D stereomicroscope. To measure individual filament growth rate, edges of protonemal colonies, grown on BCD media, were photographed every 5 min for 2 hours using Zeiss AxioImager. For growth rate measurements the colonies grown on BCDAT were photographed after every 7 days for three weeks by Canon Powershot S70 attached to Leica S6D stereomicroscope. All image analyses were performed using ImageJ (Abramoff *et al*., 2004).

For protoplast regeneration, protoplasts from 7 d old tissues were isolated in 0.7 % driselase solution for 45 min – 1 h and washed twice with 8% mannitol. Suspension density was adjusted to $3.2x10^6$ ml^{-1} prior to mixing with top medium (BCDAT, 6% mannitol, 1% 1M $CaCl_2$ and 0.4% agar) and plating on medium overlaid with cellophane (BCDAT, 6% mannitol, 1% 1M $CaCl_2$ and 0.6% agar). Growing protoplasts were photographed using Nikon DS-5M digital camera attached to Nikon SMZ 1500 stereomicroscope.

For gravitropism assays, 7 d old protonemata were transferred to fresh media supplemented with 2% sucrose. After 5d the plates were covered with aluminium foil and placed vertically at 25°C or 8°C for 3 weeks.

For sporophyte induction, gametophores were first induced from fresh protonemata on sterile Jiffy pellets (www.jiffypot.com) in magenta boxes at 25°C and long day (16 h light : 8 h dark) regime. After 4 weeks, the boxes were filled with sterile water leaving 1 cm from top of gametophores and transferred to 15 °C, short day conditions.

To quantify the regeneration of protonemal filament from phyllid cells in WT and *Ppsec3* mutants, the phyllids were detached from gametophores and cut into two halves with a sharp razor. The upper half of the phyllids were placed on a layer of BCDAT solid media overlaid with cellophane and photographed after 0 and 96 hours using Olympus BX-51 microscope equipped with Olympus DP50 camera.

To stain callose, the phyllids, 24 hours after wounding were fixed and destained overnight in 1:3 acetic acid/ethanol. The phyllids were then placed in 150 mM K_2HPO_4 for 1 hour and later stained with 0.01% aniline blue. The samples were mounted in 50% glycerol and images were recorded with Olympus BX-51 microscope equipped with Olympus DP50 camera.

Electron microscopy

For scanning electron microscopy (SEM), samples were fixed overnight in 2.5 % (v/v) glutaraldehyde in 0.1 M phosphate buffer at 4 °C. The fixed samples were washed briefly with 1X PBS and then dehydrated in ascending ethanol and acetone series. Later the samples were mounted on the holders, coated with gold for 2 minutes and examined under JEOL JSM-6380 LV SEM microscope.

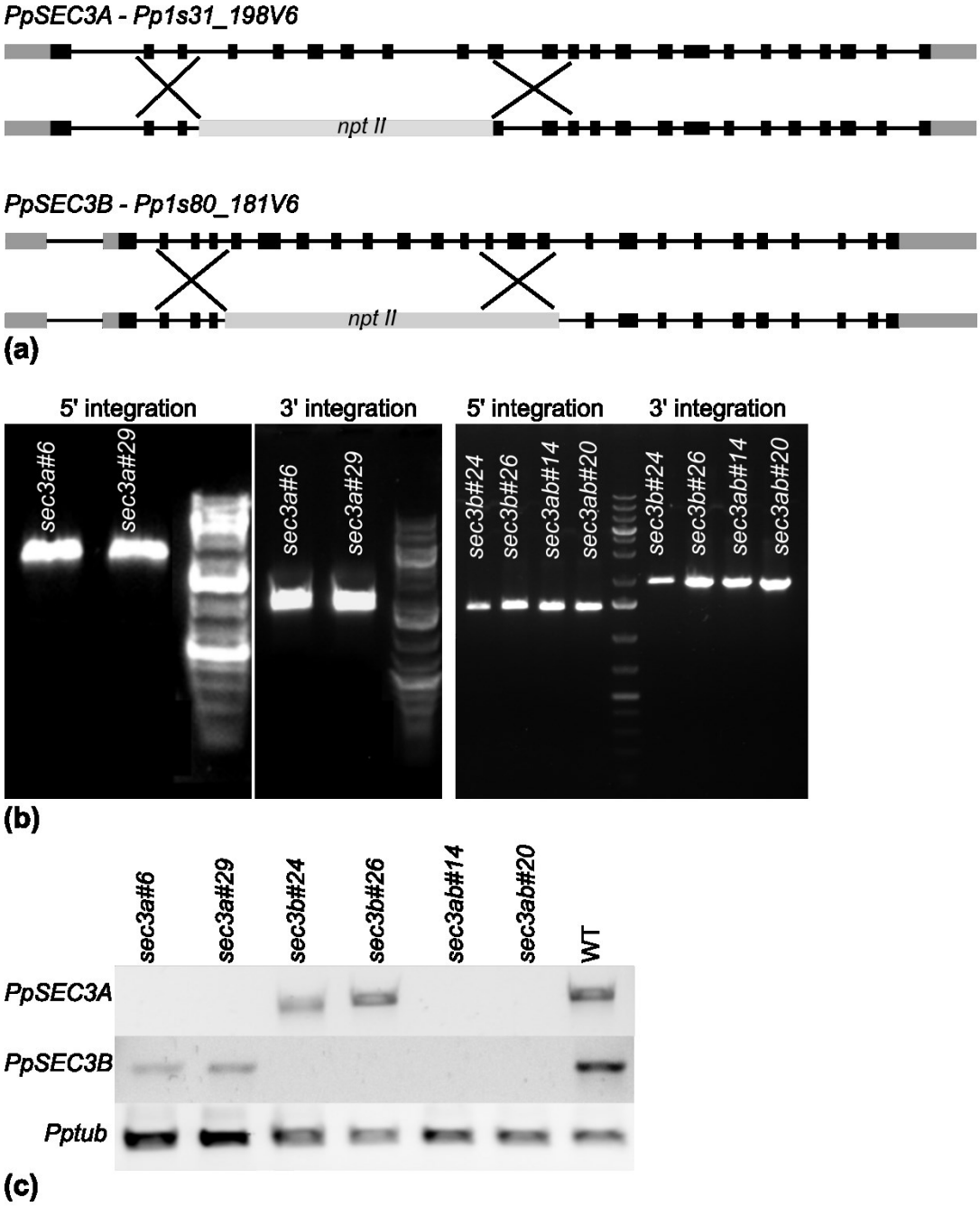

Fig. 1. Generation of *Ppsec3a*, *Ppsec3b* and *Ppsec3ab* mutant lines. (a) Gene structure and strategy for creation of KO mutants. (b) PCR genotyping showing proper 5' and 3' integration of selection cassette in the WT locus. (c) RT-PCR showing the absence of *PpSEC3A* and *PpSEC3B* transcripts in *Ppsec3a*, *Ppsec3b* and *Ppsec3ab* mutants. Lower panel shows reaction with Tubulin, as a house keeping gene control.

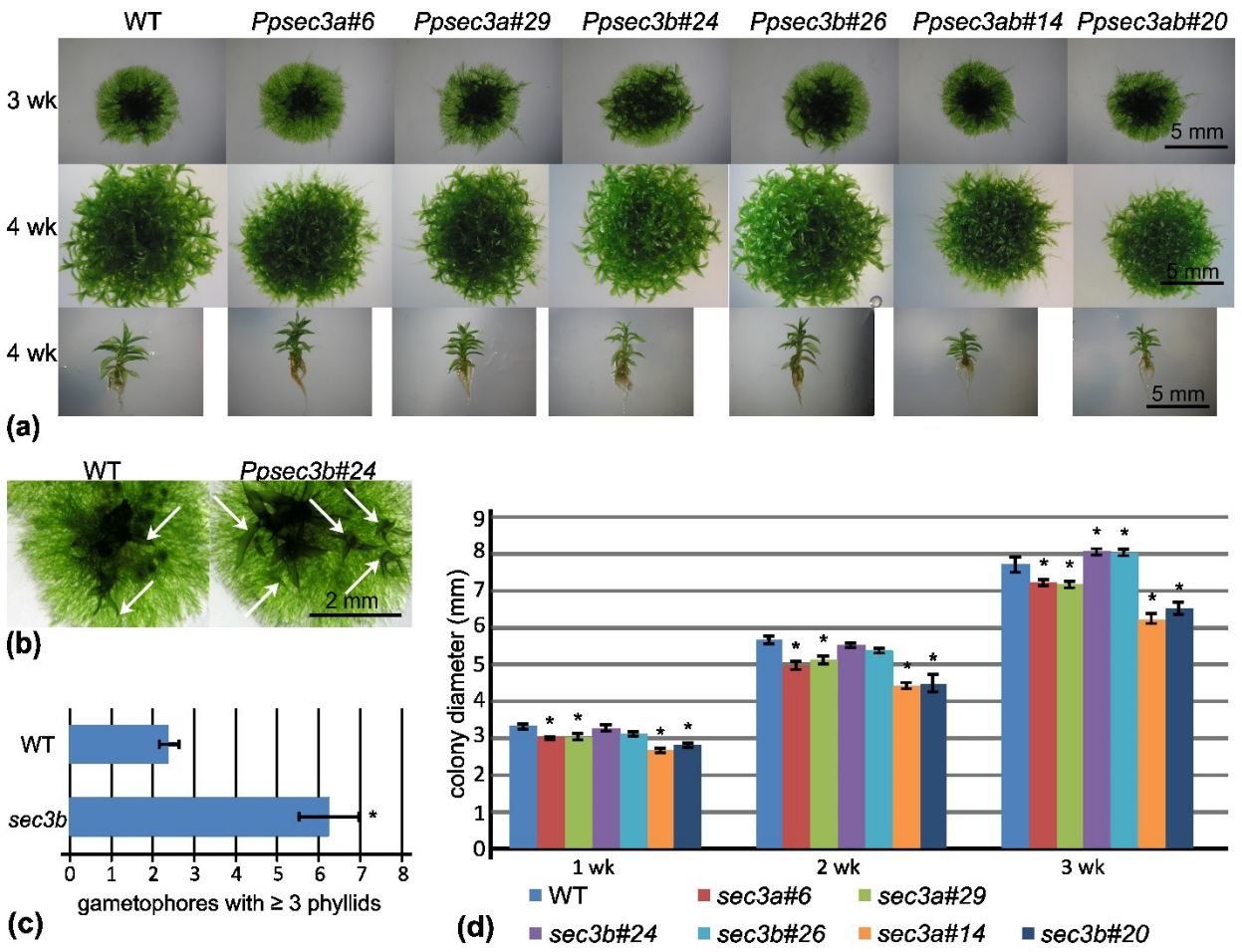

Fig. 2. General phenotype of *Ppsec3a*, *Ppsec3b* and *Ppsec3ab* mutants. (a) Colonies WT and *Ppsec3* mutant lines after 3rd and 4th week on BCDAT. (b) 1 week old WT and *Ppsec3b* colonies showing newly formed gametophores. Arrows indicate gametophores at least with 3 phyllids. (c) Number of gametophores with 3 or more phyllids in 1 week old WT and *Ppsec3b*. (d) Quantification of growth in WT, *Ppsec3a*, *Ppsec3b* and *Ppsec3ab*. * indicates significant difference from WT (Anova, $p<0.05$). Error bars represent standard error, n=25 (c), n=23 (d).

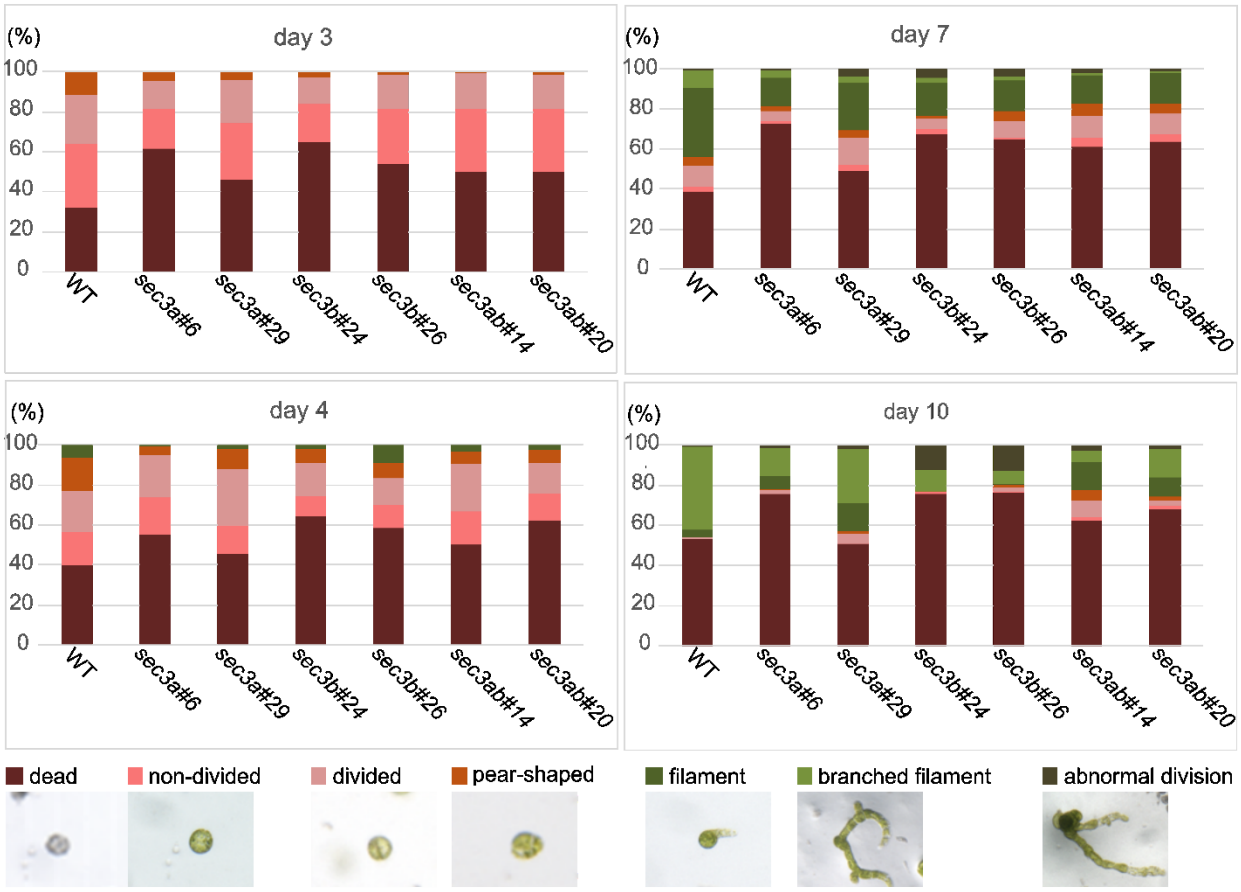

Fig. 3. Developmental stages of WT and *Ppsec3* protoplasts at various time points after plating on protoplast regeneration media. Deletion of moss SEC3 genes perturbs germination of protoplasts. Values indicate percentage of protoplasts in particular developmental stage, n>150. Lower most panel show different stages of regeneration from protoplasts to early protonemal filaments.

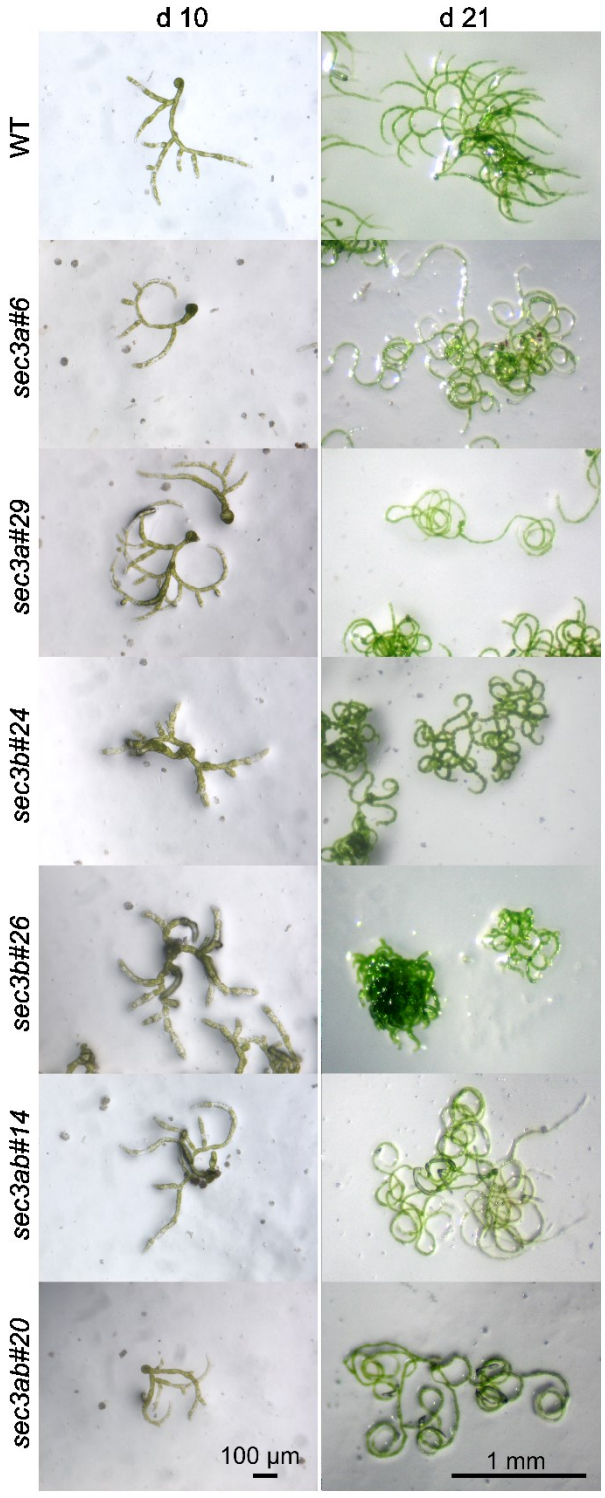

Fig. 4. PpSEC3 is a controlling factor for direction of protonemal growth. WT and *Ppsec3a, Ppsec3b* and *Ppsec3ab* protoplasts at 10 and 21 days after isolation, showing curling of protonemal filaments in later stage of development.

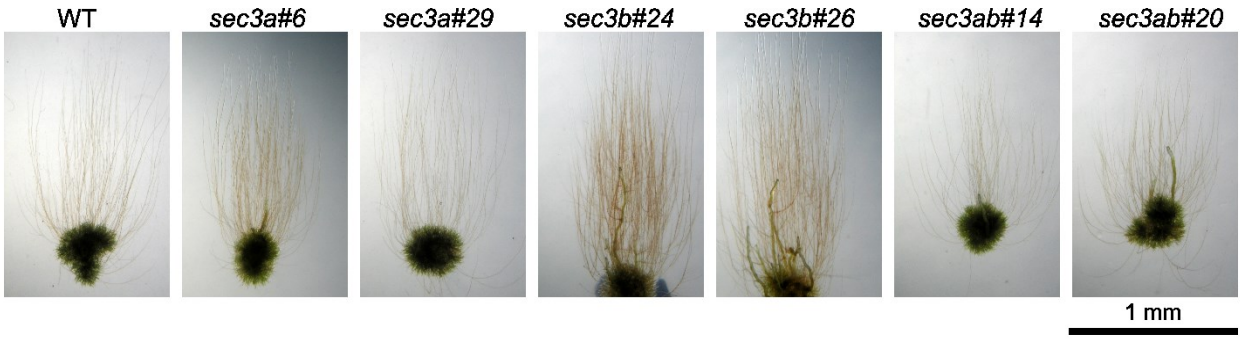

Fig. 5. WT, *Ppsec3a*, *Ppsec3b* and *Ppsec3ab* after 3 weeks under gravi-stimulation conditions. Both *Ppsec3a* and *Ppsec3ab* had shorter caulonemata, while *Ppsec3b* showed no difference than WT.

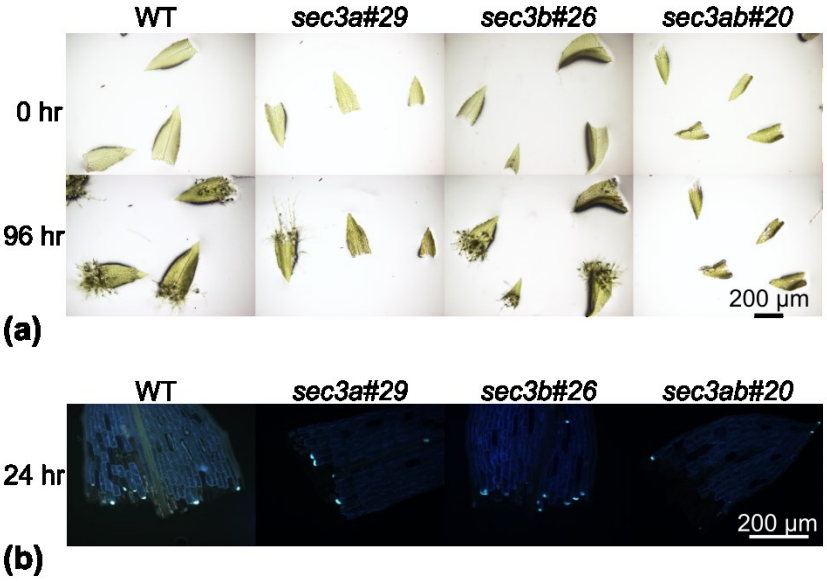

Fig. 6. PpSEC3A is required for wounding-induced protonema formation. (a) WT and *PpSEC3* mutants after 0 hour and 96 hour upon detachment from gametophore showing the reprogrammed cells after wound giving rise to new chloronemal filaments in WT and *Ppsec3b*, while only few to none cells started initiation for protonemata in *Ppsec3a and Ppsec3ab*. (b) Deposition of callose at cut edge of phyllids 24 hour after wounding. *Ppsec3a and Ppsec3ab* showing reduced deposition of callose compared to WT and *Ppsec3b*.

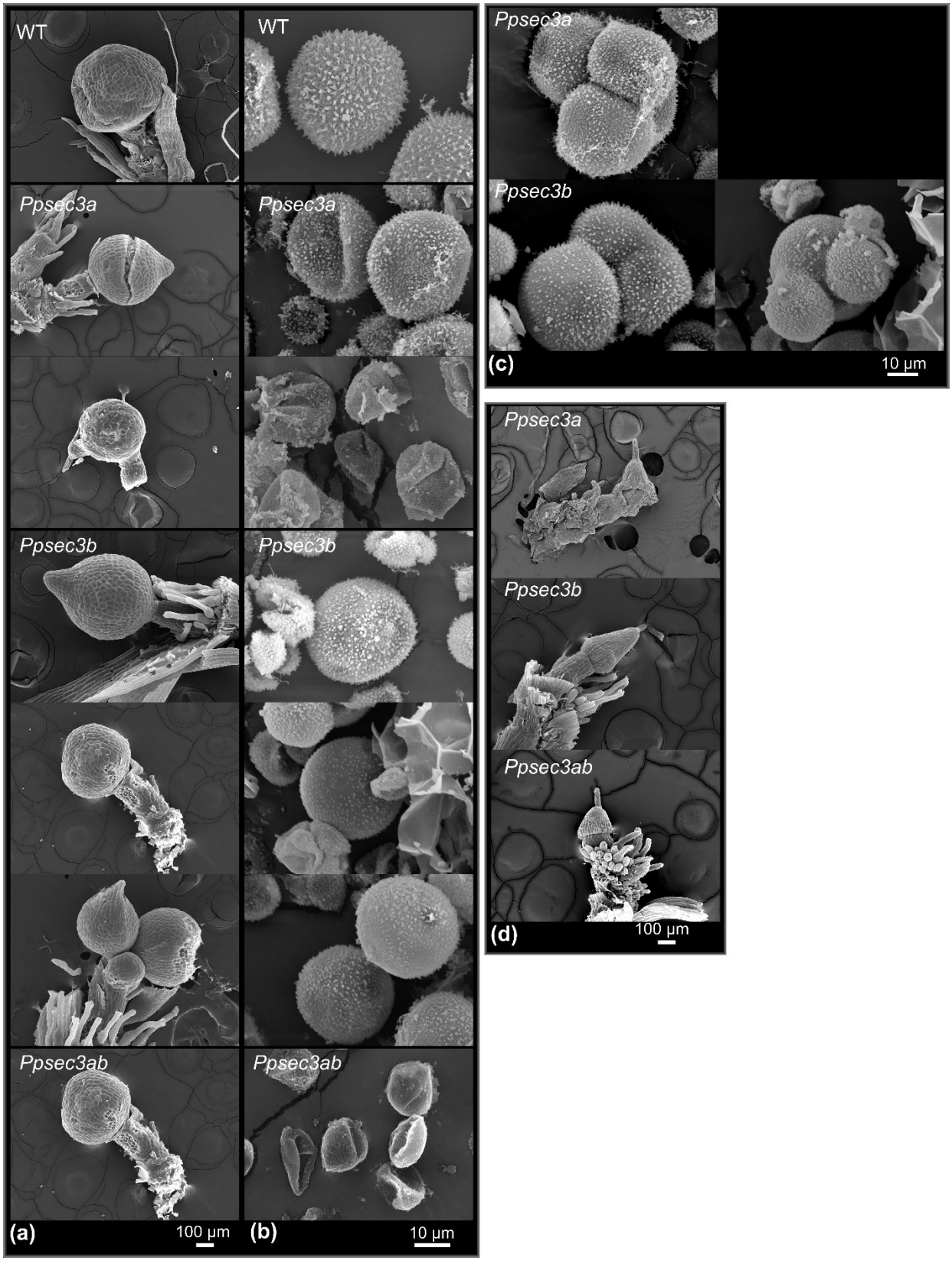
WT
WT
Ppsec3a
Ppsec3a
Ppsec3b
Ppsec3b
Ppsec3ab
Ppsec3ab
(a)
100 µm
(b)
10 µm
Ppsec3a
Ppsec3b
(c)
10 µm
Ppsec3a
Ppsec3b
Ppsec3ab
(d)
100 µm

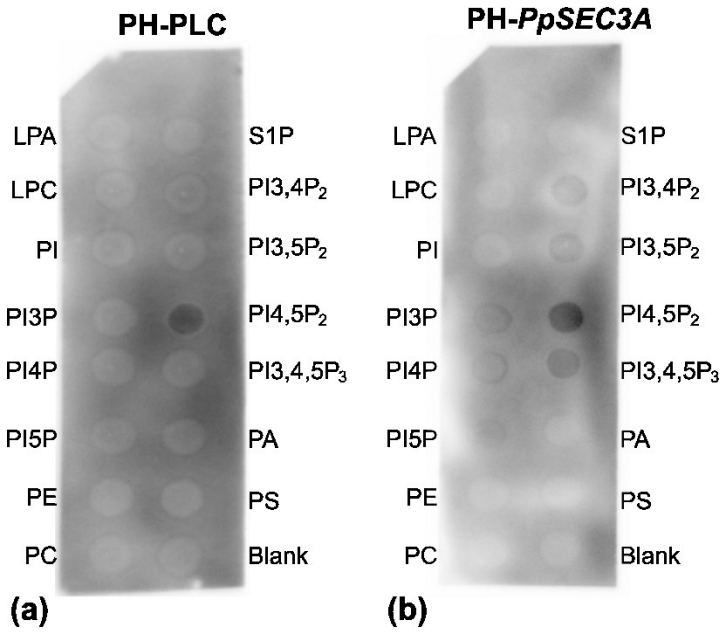

Fig. 8. Lipid binding assay of *PpSEC3A* PH-domain with membrane phospholipids. Binding of PH-domain from (a) PIP_2 generic marker PLC as positive control and (b) PpSEC3A to PIP_2

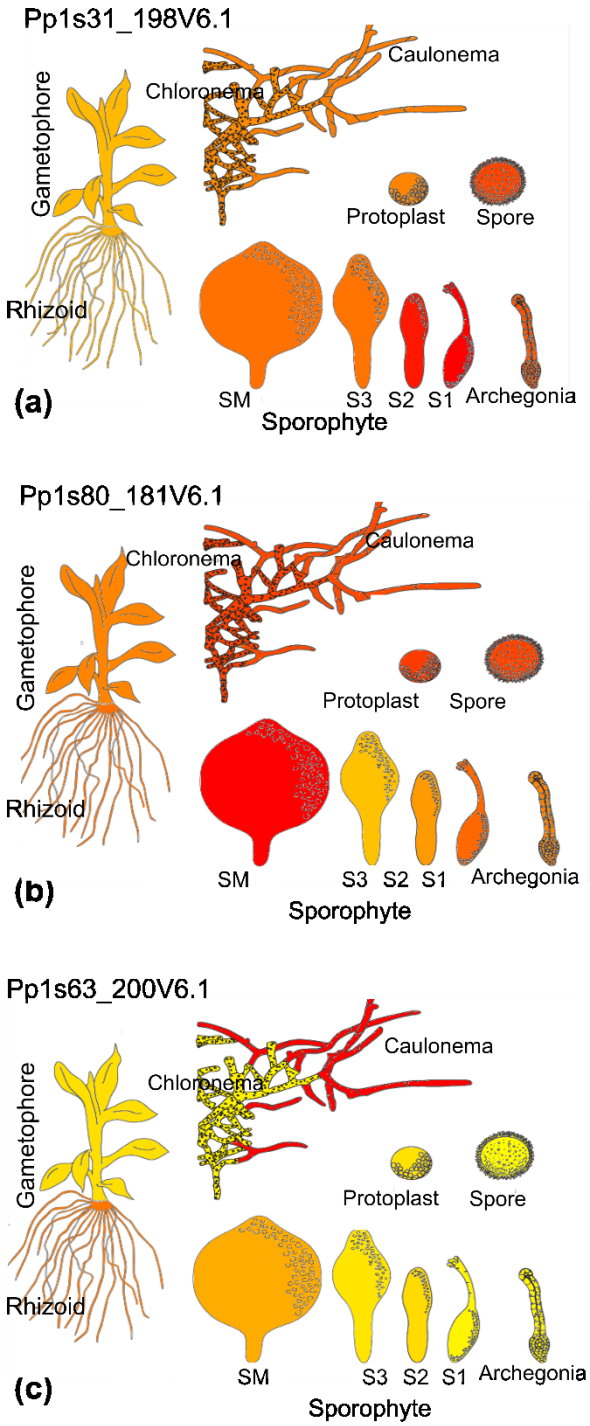

Fig. S1. Expression profile of (a) *PpSEC3A* (b) *PpSEC3B* and (c) *PpSEC3C* transcripts (http://bar.utoronto.ca)

TABLES

Primer	Sequence
PpSEC3A.5F	AGGATCCAATTTGGCAACGTCCAACTC
PpSEC3A.5R	ACTCGAGACTATGCGCTGCGAATTCTT
PpSEC3A.3F	TACTAGTCAGCAGTTCTGCAGAGTGGA
PpSEC3A.3R	AGTTAACATGATCCGGCCGTTTTAACT
PpSEC3B.5F	TAAGCTTCAGTCAAGCCTTCACCAGT
PpSEC3B.5R	TCTCGAGCCCAAACAACCTCTGCTGTC
PpSEC3B.3F	TACTAGTGGGAAGTATCTGTCGCGTT
PpSEC3B.3R	AGTTAACCTCGACAACAGCAATGAGG
Hyg_RV(promo)	CGTGCTCCACCATGTTGACGAAG
Hyg_FW(termi)	GCTGAAATCACCAGTCTCTCTCTAC
nptII_RV	ATATTGCTGAAGAGCTTGGCGGCA
nptII_FW	CTGCCTCGTCTTGGAGTTCATTCA
PpSEC3a_LP	TGGAGGCGTTCTTCTCTGAT
PpSEC3a_RP.1	AGTCTCCGCAGCCAGTAAAA
PpSEC3.B_LP	CCGACCTGAAAATGGAAGAA
PpSEC3.B_RP	CCCAGTCTGCAACAGCATAA
Sec3a_RT-FW	TGGAGGCGTTCTTCTCTGAT
Sec3a_RT-RV	CTGATGAAGGGGTCAGTGGT
Sec3b_RT-FW	CCGACCTGAAAATGGAAGAA
Sec3b_RT-RV	ACTTCTCCAAAGCAGGCGTA
Sec3c_RT-FW	ACGAATTACGGGGTTTTGTG
Sec3c_RT-RV	GGCTCCGTCGATAGCAGTAG
Sec3a-N_FW-1	GTTCCAGATTACGCTATGGCAGCGAATGGTG
Sec3a-N_RV	TTGCGGCCGCTTACTCACTTGGAAGGGTTTTCG
Mega-HA	AAGTCGACGCCGCCACCATGTACCCATACGATGTTCCAGATTACGCTATG
Pptub_FW	TGTGCTGTTGGACAATGAG
Pptub_RV	ACATCAGATCGAACTTGTG

Table 1. List of primers used in this study

	Caulonemata (µm)	Chloronemata (µm)
WT	22 ± 1.3	10.4 ± 1.0
Ppsec3a	20 ± 1.0*	7 ± 0.9*
Ppsec3b	25 ± 0.8*	9 ± 0.9*
Ppsec3ab	20± 0.2*	8 ± 0.8*

Table 2. Growth rate of protonemal filaments in WT, *Ppsec3a, Ppsec3b* and *Ppsec3ab*.
*denotes significant difference (*Anova, $p<0.05$) Values represent average ± SE. $n \geq 27$.

	Gametophore length	Rhizoid length	Number of phyllid
WT	3.6 ± 0.1	3.2 ± 0.1	23.4 ± 0.4
Ppsec3a	2.8 ± 0.1**	2.9 ± 0.1	22.6 ± 0.5
Ppsec3b	3.3 ± 0.1	3.6 ± 0.2	23.1 ± 0.4
Ppsec3ab	2.4 ± 0.1**	3.2 ± 0.1	20.0 ± 0.5**

Table 3. Quantification of length (in mm) of gametophores and rhizoids, and number of phyllids in gametophores of WT and *Ppsec3* mutants**.**

*denotes significant difference from WT (Anova with Bonferroni and Holm test, $p<0.01$) Values represent average ± SE. $n = 25$.

	WT-like	Defective	aborted	Branched sporophyte
WT	85%	0%	15%	0%
Ppsec3a	22%	45%	33%	0%
Ppsec3b	42%	26%	19%	13%
Ppsec3ab	0%	58%	42%	0%

Table 4. Quantification of sporophytes with different morphologies in WT and *Ppsec3* mutants. $n \geq 60$.

4. DISCUSSION

While the role of the evolutionarily conserved exocyst complex in various aspect of seed plant's life is relatively well known, the goal of this project was to study the exocyst complex and its involvement in growth and development of the model moss *P. patens*. Here we studied the functioning of three selected representatives of the moss exocyst subunits, namely EXO70 and SEC3 (considered to be land-marking subunits of the complex, at least in yeast) and the core subunit SEC6. The results obtained were interpreted from the evolutionary point of view to gain insight into a possible role of the exocyst complex in evolutionary process of land plants migration from water onto the land. This project took initial steps to test the functional role of the exocyst complex in *P. patens*, and showed that it controls various cellular and developmental processes and is essential for life cycle of the moss *P. patens.*

4.1.Exocyst is an evolutionary conserved complex

We have reconstructed the evolutionary history of exocyst complex, esp. in angiosperms (8 selected plant species in total, including both dicots and grasses), but also including a bryophyte moss *P. patens*, lycophyte *S. moellendorffii*, as a representative of basal non-vascular land plant lineages from the evolutionary tree (PAPER1). The previous phylogenetic studies of exocyst were focused only on EXO70 subunit of the complex (Eliáš *et al.,* 2003; Synek *et al*., 2006), or if on all subunits, it was focused only on few selected species: *Arabidopsis thaliana*, *Oryza sativa*, *Populus trichocarpa* and moss *P. patens* (Chong *et al*., 2010). We showed that the core subunits of the complex, Sec6, Sec8, Sec10 and also upto some extent Sec5 and Sec3, underwent little or only few amplification in the vascular plants, though a bit amplified in non-seed plants. The subunits Sec15, Exo84 and in particular Exo70, exhibit the highly diversified families, which is consistent with their function and position on the periphery of the complex. The diversity in the function of the exocyst complex can be attributed to the massive number of paralogs in Exo70 family, which existed in at least three paralogs already in common ancestor of land pants, and later diversified into seven clades (Synek *et al*., 2006). Later in PAPER 2, we performed detailed phylogenetic study of EXO70 subunit of the complex by including representatives each from angiosperm, gymnosperm, lycophyte, moss, liverwort and also charophyte algae, and confirmed the presence of previously described three EXO70 clades of in all land plants except for S. *mollendorffii* where, however, we suspect that available genomic data may be incomplete.

Based on the number of paralogs, the exocyst subunits are characterized into following three categories: families with (a) low copy numbers, (b) intermediate copy numbers and (c) intensively diversified families. The core subunits of the exocyst complex, namely SEC3, SEC5, SEC6, SEC8 and

SEC10, underwent no or just few, if any, amplification events in plants and are characterized as families with low copy number of paralogs. These subunits are represented by one to maximum of three paralogs only. The SEC15 and EXO84 are the subunits within the category of intermediate copy numbers of paralogs. These subunits are encoded by two to eight genes in plant genome, except for *S. moellendorffii* where SEC15 is represented by 1 and EXO84 by 2 genes only. The third category consists solely of EXO70 gene family, where the gene number ranges from three (*M. polymorpha*) to several dozen (*O. sativa*). This enormous number of paralogs can be classified into three well-conserved EXO70 lineages: EXO70.1, EXO70.2 and EXO70.3, and presence of these three classes can be seen not only in angiosperms but also in basal land plants. Interestingly, *S. moellendorffii* lacks EXO70.3 class, but this needs more attention, as a *S. moellendorffii* EXO70.3 paralog was found to be present in a pre-publish version of genome (Synek *et al*., 2006), but not in the published version (Banks *et al*., 2011). The presence of only one EXO70 clade (EXO70.1) in *K. flaccidum* shows that the three land plant-specific EXO70 clades were established after green algae divergence but early during the evolution of land plants. These three EXO70 lineages, are formed as result of two gene duplication events, first forming an ancestor of EXO70.3 and a common ancestor of EXO70.1 and EXO70.2, and later giving rise to lineage-specific gene duplication events (see PAPER 2). The EXO70 paralogs being less conserved at sequence levels, esp. at their N- and C- terminal part could be the reason for functional diversity of the exocyst complex.

The phylogenetic analysis shows that the core subunits are less diverse, while the subunits at the periphery of the complex, namely SEC15, EXO84 and EXO70 in particular, are having enormous diversities within the gene families. This diversity could be related to the various functional requirements of the complex, which might also involve communication with different interactors or even to paralogs involved in different cellular pathways.

4.2.Exocyst complex in moss *P. patens* development

Mosses sensu lato (incl. hornworts and liverworts; and some extinct pre-rhyniophytes or rhyniophytes) are considered to be the first plants that colonized the land. Their simple body organization and ease in creating targeted mutants in moss *P. patens* make them suitable model organism to study function of genes. This motivated us to study and deduce the functional roles of vesicle tethering complex exocyst in moss *P. patens*.

There are several reports showing involvement of exocyst in secretion, cell division, polar cell growth and development in angiosperms. Most of the studies showing functional role of exocyst complex focused on Exo70 isoform, and some even showed its involvement in functional diversification of exocyst complex (Hála *et al*., 2008; Fencrych *et al*., 2010; Pečenková, *et al*., 2011; see Žárský *et al*., 2013; Kulich

et al., 2015). Both EXO70 and SEC3 are considered to be the subunits that mark the sites of vesicle fusion onto the PM. Characterization of mutants in both these subunits, namely *PpEXO70.3d* and *Ppsec3a*, *Ppsec3b* and *Ppsec3ab*, along with mutant in PpSEC6 – the core subunit of the complex, show importance of exocyst complex in moss.

4.2.1. Role of EXO70.3d in life cycle of moss *P. patens*

Our report (PAPER 2) shows involvement of EXO70.3d, an isoform from the EXO70.3 clade, in moss development, and documents that this protein is essential for completion of the life cycle in *P. patens*.

The transition from chloronema to caulonema requires several genes to be expressed and function in this process. Published transcriptomic data show high expression of *PpEXO70.3d* in gametophytic tissues, like protonemata, followed by spores, protoplasts and gametophores (Hiss *et al*., 2014; Ortiz-Ramírez *et al*., 2016). The phenotypes that we see in *Ppexo70.3d* mutants nicely correlate with the transcriptomic data (Fig. 4.1). The major phenotypic defect of *Ppexo70.3d* mutant is compromised polarity maintenance, resulting in short stature of gametophores, shorter protonemal colonies lacking proper elongation of apical cell and also nonexistence of true caulonemata. Although mutant gave rise to caulonema-like filaments with noticeable oblique cell walls, such filaments were shorter and sometimes contained more chloroplast than normal caulonema. We suspect these to be differentiating caulonemal filaments, but due to lack of *PpEXO70.3d* this differentiation is obstructed and they cannot reach to their final fate. Similar phenotypes were reported for mutants in Arp2/3 complex, BRICK1, PpLRL1 and PpLRL2, where mutant moss colonies were smaller in size either due to absence of caulonemata or lack of apical cell elongation (Harries *et al*., 2005; Perroud and Quatrano, 2006; Perroud and Quatrano, 2008; Tam *et al*., 2015). The chloronemal filaments in *Ppexo70.3d* are also shorter in length, and grow at 1/3 of the rate of WT chloronemata. The slow growth of mutant colonies could be due to following reasons 1. Lack of fast growing caulonemal filaments. 2. Reduced tip growth in the chloronemal filaments. 3. Failure of cells to elongate in absence of *PpEXO70.3d*. There are many reports showing that *P. patens* mutants defective in tip growing components have similar phenotype (Finka *et al*., 2008; Perroud and Quatrano. 2008). Taken together all these results shows tip growth in moss is controlled by EXO70.3d.

Some moss mutants with altered polarity e.g. Δ*myo8ABCDE*, *Ppccd8*Δ and *Pparpc1*, have highly branched protonemata with multiple branching from a single cell and have smaller caulonemal cells at apex (Harries et al., 2005; Proust et al., 2011; Wu et al., 2011), while Δ*brk1* displays opposing phenotype with either reduced or completely absent filament branching (Perroud and Quatrano, 2008). In *Ppexo70.3d*, lateral branching of protonemata was found to be increased with multiple branches from

single cell. We speculate that the defect in cell plate positioning, as seen also during bud development, could be reason behind multiple branching in *Ppexo70.3d*.

Exocyst's involvement in cell plate formation and maturation in angiosperms is well known (Fendrych *et al*., 2010; Zhang *et al*., 2013). The present study shows that this is the case also in mosses. *Ppexo70.3d* mutants show defective cytokinesis in various stages of life cycle, e.g. in protoplasts, early stages of bud development and also during protonemal apical cell division; mosses thus also need exocyst for completion of cytokinesis. The localization study of the EXO70.3d protein showed that although the protein in present in cytoplasm in non-dividing cells - (similar to Arabidopsis EXO70B2 reported by Pećenková *et al*., 2011), it is enriched in tip of the protonema. After nuclear envelope breakdown, a clear re-localization of signal in the area of future cell plate formation, and later at the nascent cell plate, shows evident role of PpEXO70.3d in cytokinesis.

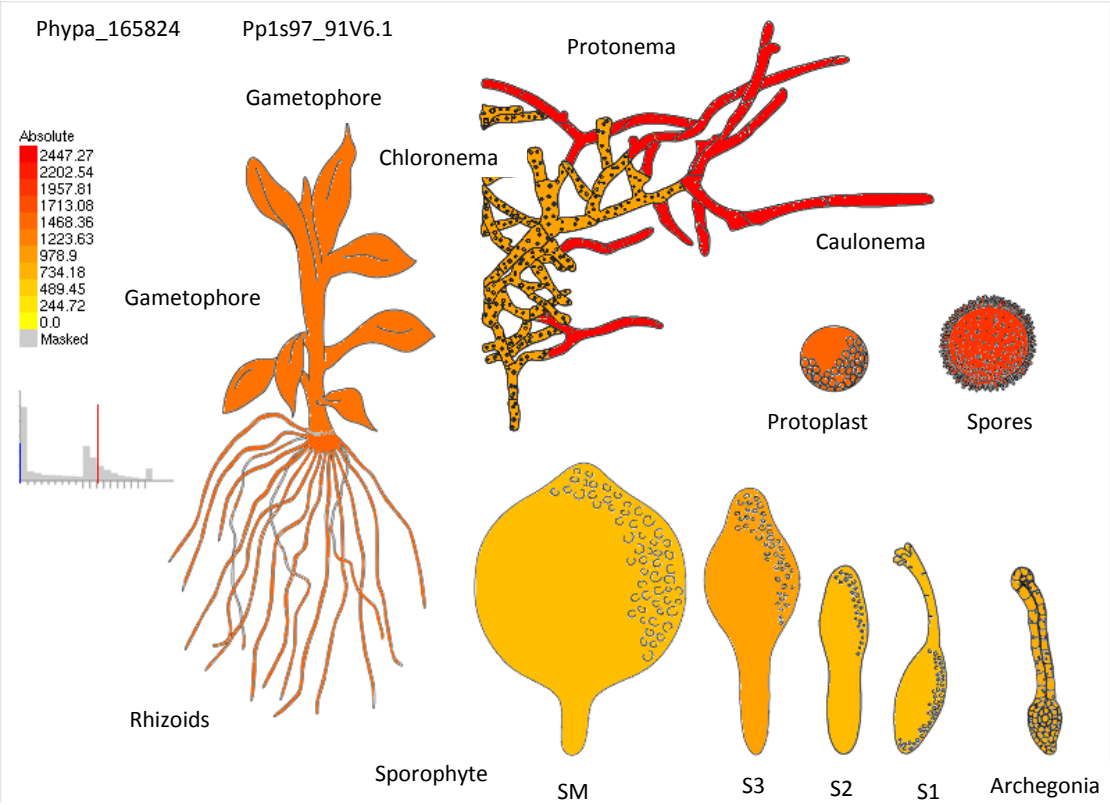

Figure 4.1. *P. patens* eFP Browser at http://bar.utoronto.ca/efp_physcomitrella/cgi-bin/efpWeb.cgi

Transcriptomic data from different tissue types showing highest level of expression of *PpEXO70.3d* in caulonemal filaments, followed by spores protoplasts and gametophores respectively.

Protoplasts and protonemal filaments in moss *P. patens* provide excellent system to study the cell polarity, apical growth and cell wall formation. In moss *P. patens*, the isolated protoplast attains the polarity within 2-3 days. Phosphoproteome analysis of 4day old protoplast shows presence of secretory pathway proteins (Wang *et al.,* 2014). In mosses, the polar auxin transport (PAT) is one of the requirements for protoplast to regenerate and divide (Bhatla *et al*., 2002). Exocyst controls PAT in *Arabidopsis thaliana* by recycling PIN1 (Drdová *et al*., 2013) and Arabidopsis *exo70A1* mutants display defective cell wall formation, showing involvement of exocyst in cytokinesis (Fendrych *et al*., 2010). We suggest similar scenario also exists in moss, explaining for delayed and extremely low germination rate of protoplasts in *Ppexo70.3d*. Some of the *Ppexo70.3d* protoplasts undergo mitosis but did not finish the complete cell wall formation, suggesting problems in cell wall synthesis and establishment of polar axis- a prerequisite for first asymmetric cell division and germination in moss protoplasts.

Another feature of *Ppexo70.3d* mutant was lack of properly formed cuticle on the phyllids of moss. The mutant plants, instead of having less chlorophyll content were greener than WT, and this could be due to the defect in cuticle deposition, which is also displayed by fused or bifurcated phyllids, a feature also seen in cuticle-defective *cer* mutants (Koornneef *et al*., 1989). Presence of cuticle and cuticular waxes, deposited by means of ABC-transporters, has already been shown in mosses (Budke *et al*., 2011; Buda *et al*., 2013). Recently it was shown that in angiosperms the cuticular wax is deposited on plant surfaces by secretory pathway involving TGN (McFarlane *et al*., 2014). The defective cuticle deposition again points to secretory defect in *Ppexo70.3d* mutants.

The most striking feature of the *Ppexo70.3d* mutants was defective egg cell development, which resulted in the mutant sterility. The *P. patens* auxin-defective *SHI/STY* mutants show similar defects in reproductive organs (Landberg *et al*., 2013), and this points towards possible auxin transport defects in *Ppexo70.3d* mutants.

Effect of auxin on caulonema formation is well know (Ashton *et al*., 1979; Cove *et al*., 2006; Jang & Dolan, 2011). The treatment with exogenous auxin did not result in induction of any true caulonemata in *Ppexo70.3d*, and interestingly the WT phenocopied the mutant at higher dosage of NPA. This indicates that the response towards the auxin in altered in *Ppexo70.3d* mutants. The initiation of new side branches on the gametophores of *P. patens* is under tight control of auxin transport (Coudert *et al*., 2015), and the shift of side branches to lower half of gametophore in *Ppexo70.3d* could be due to defective auxin transport in mutants. These results suggest, just like in Arabidopsis, exocyst might have a function in controlling auxin transport in mosses as well.

Taken together, all these results show involvement of PpEXO70.3d in various processes of moss life cycle.

4.2.2. Core subunit SEC6 is an essential part of moss exocyst complex

The partial knock-out mutants in PpSEC6 generated in our lab gave us an excellent opportunity to study the function of this protein in *P. patens*. The two independent mutant *Ppsec6* lines remain only in 2D protonemal stage, and never form 3D structures such as gametophores, and hence no sporophytes. The expression of only partial SEC6 protein in mutant lines, as detected by the Western blot, shows that complete loss of the protein might be lethal and also protein itself is necessary for transition from filamentous protonemata to gametophore formation in moss *P. patens*.

SEC6 is involved in active secretion also in moss *P. patens*. Not only the gametophore formation is inhibited, but also the caulonemal cell length and elongation in *Ppsec6* is diminished, thus clearly showing secretary defects in these mutant lines. Interestingly the longer and wider chloronemal cells of *Ppsec6* mutants sometimes get converted into brachycytes, the type of cells produced in response to ABA. The cytokinins can enhance the transition of protonemal buds into gametophores (von Schwartzenberg *et al*., 2007), but BAP has no such effect on *Ppsec6* mutants, showing the possibility of mutants being resistant towards cytokinins.

The origin of 3-dimensional structure, i.e. gametophores, in moss requires controlled asymmetrical cell division (Harrison *et al*., 2009). DEK1 protein is involved in perception of and response to positional cues for proper cell divisions in both flowering plants (Lid *et al*., 2005) and moss *P. patens*. The moss Δ*dek1* mutants have normal 2D protonemal stage but display disoriented cell division in buds resulting into no further progression of buds into gametophores (Perroud *et al*., 2014). The loss of tetrahedral stem cell in later stages of bud development in *Ppsec6* is reminiscent of phenotype seen in *dek1º* mutant where one of the three calpain active site amino acid residue is replaced (Cys for Ser) (Johansen *et al*., 2016). Interestingly, although the *dek1-Δloop* and *dek1Δloop* mutant produced gametophores; they were aberrant and lacked phyllid due to failed mitotic activity (Demko *et al*., 2014; Johansen *et al*., 2016).

The Arp2/3 complex controls polarized growth and cell division. The *arp1* mutants have defective chloronemata with abnormal cell division patterns (Harries *et al*., 2005). In *Arabidopsis*, the mutants in components of secretory pathway e.g. tethering complexes like exocyst and TRAPII, are defective in cell plate formation and maturation during cytokinesis (Fendrych *et al*., 2010; Qi *et al*., 2011). *Ppsec6* display defects similar to these mutants, thus showing that PpSEC6 is required for execution of proper cell division process in moss *P. patens*. Related to defective cell division and disrupted secretion in *Ppsec6* mutants, the buds often display gaps in cell walls, thus indicating towards compromised cell wall integrity.

4.2.3. The *PpSEC3* is an important factor involved in spore wall architecture and viability in moss *P. patens*

P. patens encodes three *SEC3* genes, two of which are strongly expressed in sporophytes, followed by archegonia and protoplasts. The mutants in two of the *SEC3* genes *(PpSEC3A* and *PpSEC3B)* showed strong deviation in sporophyte and spore formation. The caulonemal filaments of *Ppsec3a* and *Ppsec3ab* mutants have slightly reduced growth, while in *Ppsec3b* they grow slightly faster than WT. The contradictory phenotypes of *Ppsec3a* and *Ppsec3b* lines hint towards the cargo specificity for both *PpSEC3A* and *PpSEC3B*, leading to cell wall alterations. The exocyst data so far, atleast for EXO70 subunit, suggests specific functions for the subunits of the exocyst complex and based on our observations we propose similar specificity also exists for SEC3 in *P. patens*.

SEC3 has been shown to bind the membrane lipids and regulate the exocytosis and polar growth in pollen tubes (Zhang *et al*., 2008; Bloch *et al*., 2016). The N-terminally located PH-domain mediates this interaction with phospholipids. Our results clearly show that SEC3 has similar role of controlling the polar growth in *P. patens*, and that its binding with PIP_2 is conserved as moss pH-domain from SEC3A shows specific binding to membrane $PI4,5,P_2$.

Spores, during the evolution of plants, developed a tough outer wall to protect themselves from various physical, mechanical, biological and chemical damages. The spore wall comprises of two layers, the inner layer known as intine, and the outer layer called exine. The exine is made up of an exceptionally tough bio-polymer known as “Sporopollenin”. Sporopollenin is deposited on the pre-patterned cells surface, which acts like an exine precursors. There are reports showing that the biosynthetic pathway of sporopollenin is conserved in land plant lineages and *P. patens* mutants defective in components of this pathway show defects in exine formation (Aya *et al*., 2011; Wallace *et al*., 2015; Daku *et al*., 2016). The sporopollenin precursors are synthesized within the cell and are transported onto the cell surface, ABCG transporters are one such set of transporters required for cuticular wax deposition and spore wall architecture in mosses (Buda *et al*., 2013). The deposition of waxes is carried out through secretory pathway involving the endomembrane vesicle trafficking in order to reach to plasma membrane localized ABC transporters (McFarlane *et al*., 2014). The *Ppsec3* mutants show highly reduced and granulose protrusion of perispore layer. The collapsed as well as conjoint spores indicate towards the defective perispore layer formation, due to lack of sporopollenin deposition. Thus here we provide additional evidence to the one suggested by McFarlane *et al*., (2014) and show that most probably this trafficking is facilitated by exocyst complex.

To conclude, our results show that exocyst complex subunit SEC3 is involved in perispore layer formation either directly through the deposition of sporopollenin precursors or indirectly by carrying the transporters required for transporting the precursors from within the cell onto the cell surface.

5. CONCLUSIONS

Over the last decade, exocyst, an evolutionary conserved tethering complex, has been studied extensively in plants. These studies so far were focused primarily on Arabidopsis, rice, maize etc. i.e. angiosperms and up to now there are no reports on its function in non-angiosperm plant lineages.

Our phylogenetic analysis of the exocyst complex in land plants indicates that it has undergone immense diversification, due to genome duplication events (not just the only factor!) in the course of plant evolution which has resulted in multiple gene families of exocyst subunits, esp. in case of EXO70 subunit. We confirmed the existence of the exocyst complex subunits not only in angiosperms but also in gymnosperms and other plants from basal groups of plant lineages.

Mosses, due to their position in the phylogeny, present an excellent model for evo-devo studies. Using this system, we are able to show that exocyst complex is an important factor for polar growth, secretion and development in mosses as well. The tip growth, secretion of surface cuticle, cell morphogenesis and transition, cell division etc. are just few of those processes that require intensive polarized exocytosis. Moss exocyst mutants displaying defects in these processes, along with the others, point towards the lack of polarized exocytosis. Based on our results we can say that exocyst truly is a conserved complex which has played an important role during the course of land plant evolution.

6. LITERATURE

- Ashton NW, Grimsley NH, Cove DJ. 1979. Analysis of gametophytic development in the moss, *Physcomitrella patens*, using auxin and cytokinin resistant mutants. *Planta* 144: 427–435.
- Aya K, Hiwatashi Y, Kojima M, Sakakibara H, Ueguchi-Tanaka M, Hasebe M, Matsuoka M. 2011. The Gibberellin perception system evolved to regulate a pre-existing GAMYB-mediated system during land plant evolution. Nature Communications 2: 544.
- Baek K., Knödler A., Lee S. H., Zhang X., Orlando K., Zhang J., Foskett T. J., Guo W., and Dominguez R. (2010). Structure-function study of the N-terminal domain of exocyst subunit Sec3. Journal of Biological Chemistry. 285:10424–10433.
- Banks JA, Nishiyama T, Hasebe M, Bowman JL, Gribskov M, dePamphilis C, Albert VA, Aono N, Aoyama T, Ambrose BA *et al*. 2011. The *Selaginella* genome identifies genetic changes associated with the evolution of vascular plants. *Science* 332: 960-963.
- Beronja S., Laprise P., Papoulas O., Pellikka M., Sisson J., Tepass U. 2005. Essential function of Drosophila Sec6 in epithelial cell-type specific basolateral and apical exocytosis. Journal of Cell Biology. 169:635-646.
- Bezanilla M., Oan A., Quatrano RS. 2003. RNA interference in the moss Physcomitrella patens. Plant Physiology. 133:470-474.
- Bhatla SC, Kiessling J, Reski R. 2002. Observation of polarity induction by cytochemical localization of phenylalkylamine-binding sites in regenerating protoplasts of the moss *Physcomitrella patens*. *Protoplasma* 219: 99–105.
- Bloch D, Pleskot R, Pejchar P, Potocký M, Trpkošová P, Cwiklik L, Vukašinović N, Sternberg H, Yalovsky S, Žárský V. 2016. Exocyst SEC3 and phosphoinositides define sites of exocytosis in pollen tube initiation and growth. Plant Physiology 172: 980-1002.
- Buda GJ, Barnes WJ, Fich EA, Park S, Yeats TH, Zhao L, Domozych DS, Rose JKC. 2013. An ATP binding cassette transporter is required for cuticular wax deposition and desiccation tolerance in the moss *Physcomitrella patens*. Plant Cell 25: 4000-4013.
- Budke JM, Goffinet B, Jones CS. 2011. A hundred-year-old question: Is the moss calyptra covered by a cuticle? A case study of *Funaria hygrometrica*. Annals of Botany 107: 1279-1286.
- Chong YT, Gidda SK, Sanford C, Parkinson J, Mullen RT, Goring DR. 2010. Characterization of the *Arabidopsis thaliana* exocyst complex gene families by phylogenetic, expression profiling, and subcellular localization studies. *New Phytologist* 185: 401-419.
- Clarke JT., Warnock RCM., Donoghue PCJ. 2011. Establishing a time-scale for plant evolution. New Phytologist. 192:266-301.

- Cole RA., Synek L., Žárský V., Fowler JE. 2005. SEC8, a subunit of the putative Ara- bidopsis exocyst complex, facilitates pollen germination and competitive pollen tube growth. Plant Physiology. 138:2005-2018.
- Collonnier C., Epert A., Mara K., Maclot F., Guyon-Debast A., Charlot F., Schaefer DG., Nogué F. 2016. CRISPR-Cas9-mediated efficient directed mutagenesis and RAD51-dependent and RAD51-independent gene targeting in the moss Physcomitrella patens. Plant Biotechnology Journal. 15:122–131.
- Coudert Y, Palubicki W, Ljung K, Novak O, Leyser O, Harrison CJ. 2015. Three ancient hormonal cues co-ordinate shoot branching in a moss. *eLife* 4: e06808.
- Cove DJ, Bezanilla M, Harries P, Quatrano RS. 2006. Mosses as model systems for the study of metabolism and development. *Annual Review of Plant Biology* 57: 497–520.
- Cove DJ, Perroud P-F, Charron AJ, McDaniel SF, Khandelwal A, Quatrano RS. 2009. The moss *Physcomitrella patens*: A novel model system for plant development and genomic studies. In: Crotty DA, Gann A, eds. *Emerging model organisms, a laboratory manual*. New York, NY, USA: Cold Spring Harbor Laboratory Press, 69-104.
- Daku RM., Rabbi F., Buttigieg J., Coulson IM., Horne D., Martens G., Ashton NW., Suh D-Y. 2016. PpASCL, the Physcomitrella patens anther-specific chalcone synthase-like enzyme implicated in sporopollenin biosynthesis, is needed for integrity of the moss spore wall and spore viability. PLoS ONE. 11:e0168174.
- Decker EL, Reski R. 2007. Moss bioreactors producing imporved biopharmaceuticals. Current Opinion in Biotechnology. 18:393-398.
- Decker EL., Frank W., Sarnighausen E., Reski R. 2006. Moss systems biology en route: phytohormones in *Physcomitrella* development. *Plant Biology* 8: 397– 405.
- Demko V., Perroud PF., Johansen W., Delwiche CF., Copper ED., Remme P., Ako AE., Kugler KG., Mayer KFX., Quatrano R., Olsen OA. 2014. Genetic analysis for DEFECTIVE KERNEL 1 loop function in three-dimensional body patterning in Physcomitrella patens. Plant physiology. 166:903-U684.
- Drdová EJ, Synek L, Pečenková T, Hála M, Kulich I, Fowler JE, Murphy AS, Žárský V. 2013. The exocyst complex contributes to PIN auxin efflux carrier recycling and polar auxin transport in *Arabidopsis*. *Plant Journal* 73: 709-719.
- Eliáš M, Drdová E, Žiak D, Bavlnka B, Hála M, Cvrčková F, Soukupova H, Žárský V. 2003. The exocyst complex in plants. *Cell Biology International* 27: 199-201.
- Fendrych M, Synek L, Pečenková T, Toupalová H, Cole RA, Drdová E, Nebesářová J, Šedinová M, Hála M, Fowler JE *et al*. 2010. The *Arabidopsis* exocyst complex is involved in cytokinesis and cell plate maturation. *The Plant Cell* 22: 3053-3065.
- Finka A, Saidi Y, Goloubinoff P, Neuhaus J-M, Zryd J-P, Schaefer DG. 2008. The knock-out of *ARP3a* gene affects F-actin cytoskeleton organization altering cellular tip growth, morphology and development in moss *Physcomitrella patens*. *Cell Motility and the Cytoskeleton* 65: 769-784.

- Furt, F., Liu, Y.C., Bibeau, J.P., Tuzel, E., and Vidali, L. 2013. Apical myosin XI anticipates F-actin during polarized growth of Physcomitrella patens cells. Plant J 73: 417-428.
- Guo W., Grant A., Novick, P. 1999. Exo84p is an exocyst protein essential for secretion. Journal of Biological Chemistry. 274:23558–23564.
- Hála M, Cole RA, Synek L, Drdová E, Pečenková T, Nordheim A, Lamkemeyer T, Madlung J, Hochholdinger F, Fowler JE *et al*. 2008. An exocyst complex functions in plant cell growth in *Arabidopsis* and tobacco. *Plant Cell* 20: 1330-1345.
- Harries PA, Pan A, Quatrano RS. 2005. Actin related protein2/3 complex component ARPC1 is required for proper cell morphogenesis and polarized cell growth in *Physcomitrella patens*. *Plant Cell* 17: 2327–2339.
- Harrison CJ, Roeder AH, Meyerowitz EM, Langdale JA. 2009. Local cues and asymmetric cell divisions underpin body plan transitions in the moss *Physcomitrella patens*. *Current Biology* 19: 461–471.
- He B, Xi F, Zhang X, Zhang J, Guo W. 2007. Exo70 interacts with phospholipids and mediates the targeting of the exocyst to the plasma membrane. *EMBO Journal* 26: 4053-4065.
- Heider M R., Gu M., Duffy CM., Mirza AM., Marcotte LL., Walls AC., Farrall N., Hakhverdyan Z., Field MC., Rout MP., et al. 2016. Subunit connectivity, assembly determinants and architecture of the yeast exocyst complex. Nature structural & molecular biology 23:59–66.
- Heider MR, Munson M. 2012. Exorcising the exocyst complex. *Traffic* 13: 898–907.
- Hiss M, Laule O, Meskauskiene RM, Arif MA, Decker EL, Erxleben A, Frank W, Hanke ST, Lang D, Martin A *et al*. 2014. Large-scale gene expression profiling data for the model moss *Physcomitrella patens* aid understanding of developmental progression, culture and stress conditions. *Plant Journal* 79:530-539.
- Hsu SC., Hazuka CD., Roth R., Foletti DL., Heuser J, Scheller RH. 1998. Subunit composition, protein interactions, and structures of the mammalian brain sec6/8 complex and septin filaments. Neuron 20:1111–1122.
- Jang G, Dolan L. 2011. Auxin promotes the transition from chloronema to caulonema in moss protonema by positively regulating *Pp*RSL1and *Pp*RSL2 in *Physcomitrella patens*. *New Phytologist* 192: 319-327.
- Johansen W, Ako AE, Demko V, Perroud PF, Rensing SA, Mekhlif AK, Olsen OA. 2016. The DEK1 calpain linker functions in three-dimensional body patterning in *Physcomitrella patens*. *Plant Physiology* 172: 1089–1104.
- Johri MM, Desai S. 1973. Auxin regulation of caulonema formation in moss protonema. *Nature – New Biology* 245: 223–224.
- Kalmbach L., Hematy K., Bellis D., Barberon M., Fujita S., Ursache R., Daraspe J., Geldner N. 2017. Transient cell-specific EXO70A1 activity in the CASP domain and casparian stirp localization. Nature Plants. doi:10.1038/nplants.2017.58
- Kamisugi Y, Cuming AC, Cove DJ. 2005. Parameters determining the efficiency of homologous recombination mediated gene targeting in the moss *Physcomitrella patens*. *Nucleic Acids Research* 33: e173.

- Komsic-Buchmann K., Stephan LM., Becker B. 2012. The SEC6 protein is required for contractile vacuole function in *Chlamydomonas reinhardtii*. Journal of Cell Science. 125: 2885–2895.
- Koornneef M, Hanhart CJ, Thiel F. 1989. A genetic and phenotypic description of *eceriferum* (*cer*) mutants in *Arabidopsis thaliana*. *Journal of Heredity* 80: 118–122.
- Kulich I, Vojtíková Z, Glanc M, Ortmannová J, Rasmann S, Žárský V. 2015. Cell wall maturation of *Arabidopsis* trichomes is dependent on exocyst subunit EXO70H4 and involves callose deposition. *Plant Physiology* 168:120-131.
- Kulich I., Cole R., Drdová E., Cvrčková F., Soukup A., Fowler J., Žárský V. 2010. Arabidopsis exocyst subunits SEC8 and EXO70A1 and exocyst interactor ROH1 are involved in the localized deposition of seed coat pectin. New Phytologist 188: 615–625.
- Kulich I., Pečenková T., Sekereš J., Smetana O., Fendrych M., Foissner I., Höftberger M., Žárský V. 2013. Arabidopsis Exocyst Subcomplex Containing Subunit EXO70B1 Is Involved in Autophagy-Related Transport to the Vacuole. Traffic 14: 1155–1165.
- Landberg K, Pederson ERA, Viaene T, Bozorg B, Friml J, Jönsson H, Thelander M, Sundberg E. 2013. The moss *Physcomitrella patens* reproductive organ development is highly organized, affected by the two *SHI/STY* genes and by the level of active auxin in the *SHI/STY* expression domain. *Plant Physiology* 162: 1406–1419.
- Li S, Chen M, Yu D, Ren S, Sun S, Liu L, Ketelaar T, Emons AM, Liu CM. 2013. EXO70A1-mediated vesicle trafficking is critical for tracheary element development in *Arabidopsis*. *Plant Cell* 25: 1774-1786.
- Lid SE, Olsen L, Nestestog R, Aukerman M, Brown RC, Lemmon B, Mucha M, Opsahl-Sorteberg HG, Olsen OA. 2005. Mutation in the Arabidopsis thaliana DEK1 calpain gene perturbs endosperm and embryo development while over-expression affects organ development globally. *Planta* 221: 339– 351.
- Ligrone R, Duckett JG, Renzaglia KS. 2012. Major transitions in the evolution of early land plants: a bryological perspective. Annals of Botany. 109:851–871.
- Liu J, Zhao Y, Sun Y, He B, Yang C, Svitkina T, Goldman YE, Guo W. 2012. Exo70 stimulates the Arp2/3 complex for lamellipodia formation and directional cell migration. *Current Biology* 22:1510–1515.
- Lopez-Obando M, Hoffmann B, Géry C, Guyon-Debast A, Téoulé E, Rameau C, Bonhomme S, Nogué F. 2016. Simple and efficient targeting of multiple genes through CRISPR-Cas9 in physcomitrella patens. *G3* 6:3647-3653.
- Luo B, Xue XY, Hu WL, Wang LJ, Chen XY. 2007. An ABC transporter gene of *Arabidopsis thaliana*, *AtWBC11*, is involved in cuticle development and prevention of organ fusion. *Plant and Cell Physiology* 48: 1790–1802.
- MacAlister CA., Ortiz-Ramírez C., Becker JD., Feijó JA., Lippman ZB. 2016. Hydroxyproline O-arabinosyltransferase mutants oppositely alter tip growth in Arabidopsis thaliana and Physcomitrella patens. Plant Journal 85:193–208.

- McFarlane HE, Watanabe Y, Yang W, Huang Y, Ohlrogge J, Samuels AL. 2014. Golgi- and trans-golgi network-mediated vesicle trafficking is required for wax secretion from epidermal cells. *Plant Physiology* 164: 1250-1260.
- Menand B, Calder G, Dolan L. 2007. Both chloronemal and caulonemal cells expand by tip growth in the moss Physcomitrella patens. *Journal of Experimental Botany* 58: 1843-1849.
- Morant M, Jørgensen K, Schaller H, Pinot F, Møller BL, Werck-Reichhart D, Bak S. 2007. CYP703 is an ancient cytochrome P450 in land plants catalyzing in-chain hydroxylation of lauric acid to provide building blocks for sporopollenin synthesis in pollen. Plant Cell 19: 1473–1487.
- Nishiyama T., Fujita T., Shin T., Seki M., Nishide H., Uchiyama I., Kamiya A., Hasebe M. 2003. Comparative Genomics of Physcomitrella patens Gametophytic Transcriptome and Arabidopsis thaliana: Implication for Land Plant Evolution. Proceedings of the National Academy of Sciences, USA 100:8007-8012.
- Novick P, Field C, Schekman R. 1980. Identification of 23 complementation groups required for post-translational events in the yeast secretory pathway. Cell 21:205–215.
- Novick P., Ferro S., Schekman R. 1981. Order of events in the yeast secretory pathway. Cell. 25:461–469.
- Ortiz-Ramírez C, Hernandez-Coronado M, Thamm A, Catarino B, Wang M, Dolan L, Feijó JA, Becker JD. 2016. A transcriptome atlas of *Physcomitrella patens* provides insights into the evolution and development of land plants. *Molecular Plant* 9: 205-220.
- Pečenková T., Hála M., Kulich I., Kocourková D., Drdová E., Fendrych M., Hana T., and Žárský V. 2011. The role for the exocyst complex subunits Exo70B2 and Exo70H1 in the plant– pathogen interaction. Journal of experimental botany. 62:2107-2016.
- Perroud P-F, Demko V, Johansen W, Wilson BC, Olsen OA, Quatrano RS. 2014. Defective Kernel 1 (DEK1) is required for three-dimensional growth in *Physcomitrella patens*. *New Phytologist* 203: 794–804.
- Perroud P-F, Quatrano RS. 2006. The role of ARPC4 in tip growth and alignment of the polar axis in filaments of *Physcomitrella patens*. *Cell Motility and the Cytoskeleton* 63: 162–171.
- Perroud P-F, Quatrano RS. 2008. BRICK1 is required for apical cell growth in filaments of the moss *Physcomitrella patens* but not for gametophore morphology. *Plant Cell* 20: 411–422.
- Picco A., Irastorza-Azcarate I., Specht T., Böke D., Pazos I., Rivier-Cordey A.-S., Devos D. P., Kaksonen M., and Gallego O. 2017. The In Vivo Architecture of the Exocyst Provides Structural Basis for Exocytosis. Cell 168:400–412.
- Pires ND, Dolan L. 2012. Morphological evolution in land plants: new designs with old genes. *Philosophical Transactions of the Royal Society of London. Series B, Biological Sciences* 367: 508–518.
- Prigge M, and Bezanilla M. 2010. Evolutionary crossroads in developmental biology: *Physcomitrella patens*. *Development* 137:3535–3543.

- Proust H, Hoffmann B, Xie X, Yoneyama K, Schaefer DG, Yoneyama K, Nogué F, Rameau C. 2011. Strigolactones regulate protonema branching and act as a quorum sensing-like signal in the moss *Physcomitrella patens*. *Development* 138: 1531–1539.
- Qi X., Kaneda M., Chen J., Geitmann A., Zheng, H. 2011. Aspecific role for Arabidopsis TRAPPII in post−Golgi trafficking that is crucial for cytokinesis and cell polarity. Plant Journal. 68:234–248.
- Qui YL., Li LB., Wang B., Chen ZD., Knoop V., Groth-Malonek M., Dombrovska O., Lee J., Kent L., Rest J., *et al*. 2006. The deepest divergences in land plants inferred from phylogenomic evidence. Proceedings of the National Academy of Sciences of the USA. 103:15511–15516.
- Rensing SA., Lang D., Zimmer AD., Terry A., Salamov A., Shapiro H., Nishiyama T., Perroud PF., Lindquist EA., Kamisugi Y., *et al.* 2008. The *Physcomitrella* genome reveals evolutionary insights into the conquest of land by plants. Science 319:64-69.
- Ruhfel BR., Gitzendanner MA., Soltis PS., Soltis DE., Burleigh JG. 2014. From algae to angiosperms-inferring the phylogeny of green plants (Viridiplantae) from 360 plastid genomes. BMC Evolutionary Biology 14:23.
- Schaefer D. A new moss genetics: targeted mutagenesis in *Physcomitrella patens*. 2002. *Annual Review in Plant Biology*. 53:477–501.
- Seguí-Simarro JM., Austin II JRII, White EA, Staehelin LA. 2004. Electron tomographic analysis of somatic cell plate formation in meristematic cells of Arabidopsis preserved by high- pressure freezing. *Plant Cell* 16: 36–856.
- Sivaram MVS, Furgason MLM, Brewer DN, Munson M. 2006. The structure of the exocyst subunit Sec6p defines a conserved architecture with diverse roles. Nat. Struct. Mol. Biol. 13:555–556.
- Songer JA, Munson M. 2009. Sec6p anchors the assembled exocyst complex at sites of secretion. Mol. Biol. Cell 20:973–982.
- Synek L, Schlager N, Eliáš M, Quentin M, Hauser MT, Žárský V. 2006. ATEXO70A1, a member of a family of putative exocyst subunits specifically expanded in land plants, is important for polar growth and plant development. *Plant Journal* 48: 54-72.
- Synek L, Vukašinović N., Kulich I., Hála M., Aldorfová K., Fendrych M., Žárský V. 2017. EXO70C2 is a key regulatory factor for optimal tip grwoth of pollen. Plant Physiology. Doi: https://doi.org/10.1104/pp.16.01282.
- Tam THY, Catarino B, Dolan L. 2015. Conserved regulatory mechanism controls the development of cells with rooting functions in land plants. *Proceedings of the National Academy of Sciences, USA* 112: 3959–3968.
- Tan X., Feng Y., Liu Y., and Bao Y. 2016. Mutations in exocyst complex subunit SEC6 gene impaired polar auxin transport and PIN protein recycling in Arabidopsis primary root. Plant Science 250:97–104.
- Ter-Bush D. R., Maurice T., Roth D., and Novick P. 1996. The Exocyst is a multiprotein complex required for exocytosis in *Saccharomyces cerevisiae*. EMBO journal 15:6483-6494.

- Thelander M., Olsson T., Ronne H. 2005. Effect of the energy supply on filamentous growth and development in Physcomitrella patens. Journal of Experimental Botany. 56:653–662.
- Vidali L, Augustine RC, Kleinman KP, Bezanilla M. 2007. Profilin is essential for tip growth in the moss Physcomitrella patens. *Plant Cell* 19: 3705-3722.
- Vidali L, Bezanilla M. 2012. Physcomitrella patens: a model for tip cell growth and differentiation. Current Opinion in Plant Biology. 15:625-631.
- Vidali L, Burkart GM, Augustine RC, Kerdavid E, Tüzel E, Bezanilla M. 2010. Myosin XI is essential for tip growth in *Physcomitrella patens*. *Plant Cell* 22:1868-1882.
- Vukašinović N., Oda Y., Pejchar P., Synek L., Pečenková T., Rawat A., Sekereš J., Potocký M., Žárský V. 2016. Microtubule-dependent targeting of the exocyst complex is necessary for xylem development in Arabidopsis. New Phytologist. 213:1052–1067.
- Vukašinović N., Žárský V. 2016. Tethering complexes in the Arabidopsis endomembrane system. Frontiers in Cell and Developmental Biology. 4:46.
- Žárský V. (2016a). "Microtubule-dependent targeting of the exocyst complex is necessary for xylem development in Arabidopsis". In: New Phytologist.
- von Schwartzenberg K., Núñez MF., Blaschke H., Dobrev PI., Novák O., Motyka V., Strnad M. 2007. Cytokinins in the bryophyte Physcomitrella patens: analyses of activity, distribution, and cytokinin oxidase/dehydrogenase overexpression reveal the role of extracellular cytokinins. Plant Physiology. 145:786-800.
- Wallace S., Chater CC., Kamisugi Y., Cuming AC., Wellman CH., Beerling DJ., Fleming AJ. 2015. Conservation of Male Sterility 2 function during spore and pollen wall development supports an evolutionary early recruitment of a core component in the sporopollenin biosynthetic pathway. New Phytologist. 205:390-401.
- Wang X., Qi M., Li J., Ji Z., Hu Y., Bao F., *et al*. 2014. The phosphoproteome in regenerating protoplasts from *Physcomitrella patens* protonemata shows changes paralleling postembryonic development in higher plants. *Journal of Experimental Botany.* 65:2093–2106.
- Wellman CH. 2004. Origin, function and development of the spore wall in early land plants. In: Hemsley AR, Poole I, eds. Evolution of plant physiology. London, UK: Royal Botanic Gardens, Kew. 43–63.
- Wen TJ, Hochholdinger F, Sauer M, Bruce W, Schnable PS. 2005. The roothairless1 gene of maize encodes a homolog of sec3, which is involved in polar exocytosis. *Plant Physiology.* 138: 1637-1643.
- Wickett NJ, Mirarab S, Nguyen N, Warnow T, Carpenter E, Matasci N, Ayyampalayam S, Barker MS, Burleigh JG, Gitzendanner MA *et al*. 2014. Phylotranscriptomic analysis of the origin and early diversification of land plants. *Proceedings of the National Academy of Sciences, USA* 111: E4859–E4868.
- Wodniok S, Brinkmann H, Glockner G, Heidel AJ, Philippe H, Melkonian M, Becker B. 2011. Origin of land plants: Do conjugating green algae hold the key? *BMC Evolutionary Biology* 11:104.
- Wu B, Guo W. 2015. The exocyst at a glance. *Journal of Cell Science* 128: 2957-2964.

- Wu SZ, Ritchie JA, Pan AH, Quatrano RS, Bezanilla M. 2011. Myosin VIII regulates protonemal patterning and developmental timing in the moss *Physcomitrella patens*. *Molecular Plant* 4: 909–921.
- Žárský V, Cvrčková F, Potocký M, Hála M. 2009. Exocytosis and cell polarity in plants – exocyst and recycling domains. *New Phytologist* 183: 255-272.
- Žárský V, Kulich I, Fendrych M, Pečenková T. 2013. Exocyst complexes multiple functions in plant cells secretory pathways. *Current Opinion in Plant Biology* 16: 726-733.
- Zhang X, Orlando K, He B, Xi F, Zhang J, Zajac A, Guo W. 2008. Membrane association and functional regulation of Sec3 by phospholipids and Cdc42. *Journal of Cell Biology* 180: 145–158.
- Zhang Y, Immink R, Liu CM, Emons AM, Ketelaar T. 2013. The arabidopsis exocyst subunit SEC3A is essential for embryo development and accumulates in transient puncta at the plasma membrane. *New Phytologist* 199: 74-88.